Lentiviral Hematopoietic Stem Cell Gene Therapy for MNGIE

Rana Yadak

2017

Lentiviral Hematopoietic Stem Cell Gene Therapy for MNGIE

Lentivirale hematopoietische stamcelgentherapie voor MNGIE

Rana Mahmoud AbdulRaheem Yadak

Lentiviral Hematopoietic Stem Cell Gene Therapy for MNGIE

Lentivirale hematopoietische stamcelgentherapie voor MNGIE

Proefschrift

ter verkrijging van de graad van doctor aan de
Erasmus Universiteit Rotterdam
op gezag van de
rector magnificus

Prof.dr. H.A.P. Pols

en volgens besluit van het College voor Promoties.
De openbare verdediging zal plaatsvinden op

dinsdag 19 december 2017 om 11:30 uur

door

Rana Mahmoud AbdulRaheem Yadak
geboren te Nablus, de West Bank, Palestina

Erasmus University Rotterdam

Promotiecommissie:

Promotor:

        Prof.dr. P.A.E. Sillevis Smitt

Overige leden:

        Prof.dr. A.G. Vulto
        Prof.dr. J.J. Cornelissen
        Prof.dr. R.C. Hoeben

Copromotoren:

        Dr. N.P. van Til
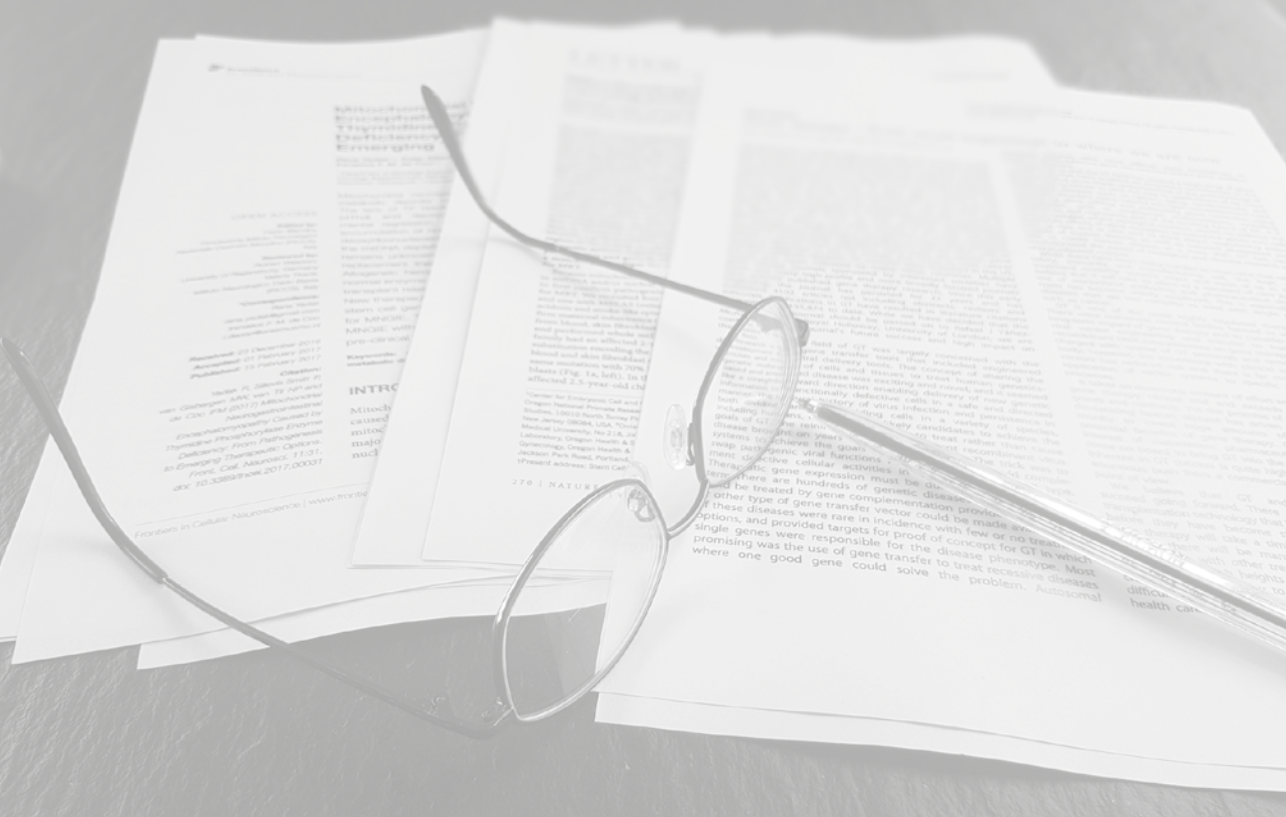   Dr. I.F.M. de Coo

إهداء للوالد و الوالدة

For my father and mother.

|TABLE OF CONTENTS

General introduction

1

|HEMATOPOIETIC STEM CELL GENE THERAPY (HSCGT)

Hematopoietic stem cells (HSCs) are multipotent stem cells with dual functional attributes of self-renewal to retain the stem cell pool and to differentiate into cells of the immune system and blood through hematopoiesis.[1,2] The bone marrow (BM) niche is the microenvironment where quiescent HSCs reside, hematopoiesis occurs, and from which HSCs mobilize into the periphery and home to and engraft after BM transplantation. Primary stromal cells are involved in these processes, in which adhesion molecules, chemokines, and cytokines play a major role (reviewed in Lapidot T *et al.* 2002, 2005).[3,4] This forms the basis of hematopoietic stem cell transplantation (HSCT). HSCT is a common clinical procedure to reconstitute the hematopoietic/immune system after conditioning by radiation or chemotherapeutic regimens. Allogeneic HSCT involves the transplantation of donor matched-BM, mobilized peripheral blood, or umbilical cord blood (UCB)-derived HSCs, and is the therapy of choice for a variety of (non-) malignant hematological and non-hematological conditions.[5] Graft versus host disease, graft failure, and toxicity of the preparative regimens are common complications related to allogeneic HSCT. Autologous hematopoietic stem cell gene therapy (HSCGT), the *ex vivo* transfer of a functional copy of a gene (therapeutic gene) into the patient's own hematopoietic stem/progenitor cells (HSPCs), is another application of HSCT.

The family of retroviruses contains two members that form the basis of viral vectors used in clinical trials: i.e. gammaretrovirus (γ-RV) and lentivirus (LV), which have been successfully used for HSCGT due to their ability to permanently integrate their DNA into the host HSPCs' genomic DNA. LV vectors offer several advantages over γ-RV vectors. First, LVs possess a central polypurine tract (cPPT) element which significantly improves nuclear import of the pre-integration complex,[6] therefore LV vectors can transduce non-dividing quiescent HSCs. The capacity to transduce non-dividing HSCs significantly reduces the need for excessive *ex vivo* HSPCs cytokine stimulation to proliferate compared with γ-RV vectors, which is detrimental for the long term repopulation of gene modified HSCs *in vivo*.[7] Second, insertional oncogenesis has been observed in clinical trials for X-linked SCID, Wiskott-Aldrich syndrome, and chronic granulomatous disease using γ-RV.[8-12] In contrast, animal studies showed that the LV integration profiles are relatively safe compared to γ-RV as demonstrated with adrenoleukodystrophy.[13] Due to these advantages, HSCGT has recently been applied successfully in several hematological, immunological and metabolic disorders.[14] The rationale for using HSCGT to target metabolic diseases relies on the capacity of the gene modified HSPCs and their progeny to act as a factory of the therapeutic proteins. The protein's substrate can be converted in the gene modified cells or the protein excreted and delivered through cross-correction. HSCs' self-renewal capacity and the highly proliferative progenitors mediate the long lasting effects of HSCGT. The rationale for and the clinical procedure of autologous LV-based HSCGT are presented in **Figure 2A, Chapter 2**.

|MITOCHONDRIAL NEUROGASTROINTESTINAL ENCEPHALOMYOPATHY (MNGIE)

MNGIE is a rare metabolic disease caused by mutations in the *TYMP* gene, which results in defective thymidine phosphorylase (TP) enzyme activity and subsequent increase in its nucleoside substrates, deoxyribonucleosides thymidine (dThd) and deoxyuridine (dUrd). This consequently results in altered mitochondrial DNA (mtDNA). Due to the limited therapeutic efficacy of the available treatments and the severe toxicity related to allogeneic HSCT, gene therapy emerged as an attractive alternative for treatment of MNGIE. The experiments performed in this thesis were designed to evaluate the efficiency and safety of LV based HSCGT for MNGIE. Genetic defects, clinical manifestations, diagnosis, pathogenesis, current treatments, pre-clinical studies, and future directions in MNGIE research are discussed in **Chapter 2**.

|SCOPE AND OUTLINE OF THIS THESIS

To cure rare inherited diseases, HSCGT has emerged as a promising platform for numerous hematological, immunological, and metabolic disorders[1] (reviewed in Naldini, 2015).[14] The currently investigated treatment options for MNGIE often only provide temporary restoration of biochemical homeostasis that lacks long-term improvement of clinical phenotypes, such as infusion of platelets and peritoneal dialysis. Allogeneic HSCT could be a potential curative treatment, but is associated with substantial morbidity and mortality (discussed in **Chapter 2**). A recent approach to performing liver transplantation has obvious drawbacks, such as life-long immune suppression and graft failure. Alternative therapies that provide life-long effective biochemical and phenotypic correction with acceptable adverse effects are an urgent medical need. The studies performed in this thesis were designed to evaluate the potential application of LV based HSCGT as a safe and efficient treatment for MNGIE.

(i) Optimization of culture conditions for highly efficient LV transduction of HSPCs without compromising long term repopulation efficiency and gene marking *in vivo.*

Most HSPC transduction protocols use multiple rounds of LV vector incubations with high vector doses, yielding many integrated LV copies per genome, and as a consequence, a relatively high genotoxicity risk. Also,

high concentrations of multiple cytokines are used to induce HSPC proliferation and enhance transduction efficiency. Therefore, the development of highly efficient LV transduction protocols for HSPCs are necessary. Optimizing parameters such as the duration of the transduction, reducing the number of integrations per cell, and restriction of growth factors, would increase the number of patients that could be treated per LV vector stock, thereby reducing the costs substantially. Furthermore, this could potentially also improve long-term therapeutic outcomes. To address these points, the following experiments were designed as described in **Chapter 3**. First, lineage-depleted (Lin-) mouse BM cells, rhesus BM CD34+ cells, and human peripheral blood and BM CD34+ progenitor cells, were transduced overnight at an increasing cell density with a proportional increase of transducing units in order to increase their physical contact. Second, lin- cells and human umbilical cord blood CD34+ cells were transduced overnight under varying concentrations of selected growth factors either singularly or in combinations. The repopulation capacity and stable gene marking *in vivo* was assessed by the transplantation of lin- cells into sublethally irradiated wild type recipient mice.

(ii) Efficiency assessment of LV based HSCGT for MNGIE

Initial attempts demonstrated correction of the biochemical phenotype in a mouse

---

[1] https://clinicaltrials.gov

model of MNGIE following LV based HSCGT,[15] encouraging its further pre-clinical development as a treatment option for MNGIE. We aimed at addressing the efficiency in depth, particularly on neurological and intestinal phenotypes which are otherwise unresponsive to allogeneic HSCT. We tested third generation self-inactivating LV vectors with a backbone similar to those applied in clinical trials with a modified Woodchuck post-transcriptional regulatory element, and the cellular human phosphoglycerate kinase (hPGK) promoter to drive the human (*TYMP*) or codon optimized (*TYMPco*) cDNA sequences (**Figure 1A, Chapter 4**). The efficacy of HSCGT was tested in $Tymp^{-/-}Upp1^{-/-}$ for up to 8 - 11 months. Dose scaling of LV vectors and transplanted gene modified cells was performed to establish the minimum required VCN/cell sufficient for biochemical correction. The evaluation of therapeutic outcomes (**Chapter 4**) involved assessments of *(a)* molecular chimerism and integrated LV vector copies; *(b)* biochemical phenotype in urine, blood, brain, intestine, liver, and muscle tissues; *(c)* neurological phenotypes by performing memory and motor function assessments,

brain MRI and immunohistochemistry; and in **Chapter 5** *(d)* we assessed the pathology of the small intestine of mice receiving HSCGT as well as MNGIE patients treated with allogeneic HSCT.

(iii) Safety assessment of LV based HSCGT for MNGIE

To address any potential side effects related to TP overexpression or LV- related genotoxicity, we performed experiments as described in **Chapters 4 and 6**: *(a)* $Tymp^{-/-}Upp1^{-/-}$ mice transplanted with gene modified HSPCs bearing LV vectors with a strong promoter/ enhancer derived from spleen focus forming virus (LV-SF) were monitored long term. *(b)* Long term follow up was performed on $Tymp^{-/-}Upp1^{-/-}$ mice recipients of HSPCs transduced with a therapeutic vector containing the PGK promoter. Both under *(a)* and *(b)* the discomfort was monitored and hematological analysis was performed to exclude hematological abnormalities. *(c)* Secondary transplantations were performed to assess tumor incidence up to 11 months. *(d)* LV integration sites were retrieved by LAM-PCR on genomic DNA of lin- cells and in BM cells after transplantation.

|REFERENCES

1. Doulatov S, Notta F, Laurenti E, Dick JE. Hematopoiesis: a human perspective. Cell Stem Cell. 2012;10:120-136.

2. Ema H, Kobayashi T, Nakauchi H. Principles of Hematopoietic Stem Cell Biology. In: Kondo M, ed. Hematopoietic Stem Cell Biology. Totowa, NJ: Humana Press; 2010:1-36.

3. Lapidot T, Petit I. Current understanding of stem cell mobilization: the roles of chemokines, proteolytic enzymes, adhesion molecules, cytokines, and stromal cells. Exp Hematol. 2002;30:973-981.

4. Lapidot T, Dar A, Kollet O. How do stem cells find their way home? Blood. 2005;106:1901-1910.

5. Copelan EA. Hematopoietic stem-cell transplantation. N Engl J Med. 2006;354:1813-1826.

6. Follenzi A, Ailles LE, Bakovic S, Geuna M, Naldini L. Gene transfer by lentiviral vectors is limited by nuclear translocation and rescued by HIV-1 pol sequences. Nat Genet. 2000;25:217-222.

7. Miller DG, Adam MA, Miller AD. Gene transfer by retrovirus vectors occurs only in cells that are actively replicating at the time of infection. Mol Cell Biol. 1990;10:4239-4242.

8. Hacein-Bey-Abina S, von Kalle C, Schmidt M, et al. A serious adverse event after successful gene therapy for X-linked severe combined immunodeficiency. N Engl J Med. 2003;348:255-256.

9. Hacein-Bey-Abina S, Von Kalle C, Schmidt M, et al. LMO2-associated clonal T cell proliferation in two patients after gene therapy for SCID-X1. Science. 2003;302:415-419.

10. Hacein-Bey-Abina S, Garrigue A, Wang GP, et al. Insertional oncogenesis in 4 patients after retrovirus-mediated gene therapy of SCID-X1. J Clin Invest. 2008;118:3132-3142.

11. Braun CJ, Boztug K, Paruzynski A, et al. Gene therapy for Wiskott-Aldrich syndrome--long-term efficacy and genotoxicity. Sci Transl Med. 2014;6:227ra233.

12. Stein S, Ott MG, Schultze-Strasser S, et al. Genomic instability and myelodysplasia with monosomy 7 consequent to EVI1 activation after gene therapy for chronic granulomatous disease. Nat Med. 2010;16:198-204.

13. Biffi A, Bartolomae CC, Cesana D, et al. Lentiviral vector common integration sites in preclinical models and a clinical trial reflect a benign integration bias and not oncogenic selection. Blood. 2011;117:5332-5339.

14. Naldini L. Gene therapy returns to centre stage. Nature. 2015;526:351-360.

15. Torres-Torronteras J, Gomez A, Eixarch H, et al. Hematopoietic gene therapy restores thymidine phosphorylase activity in a cell culture and a murine model of MNGIE. Gene Ther. 2011;18:795-806.

Mitochondrial Neurogastrointestinal Encephalomyopathy Caused by Thymidine Phosphorylase Enzyme Deficiency: From Pathogenesis to Emerging Therapeutic Options

Rana Yadak[1], Peter Sillevis Smitt[1], Marike W. van Gisbergen[2], Niek P. van Til[3], Irenaeus F. M. de Coo[1]
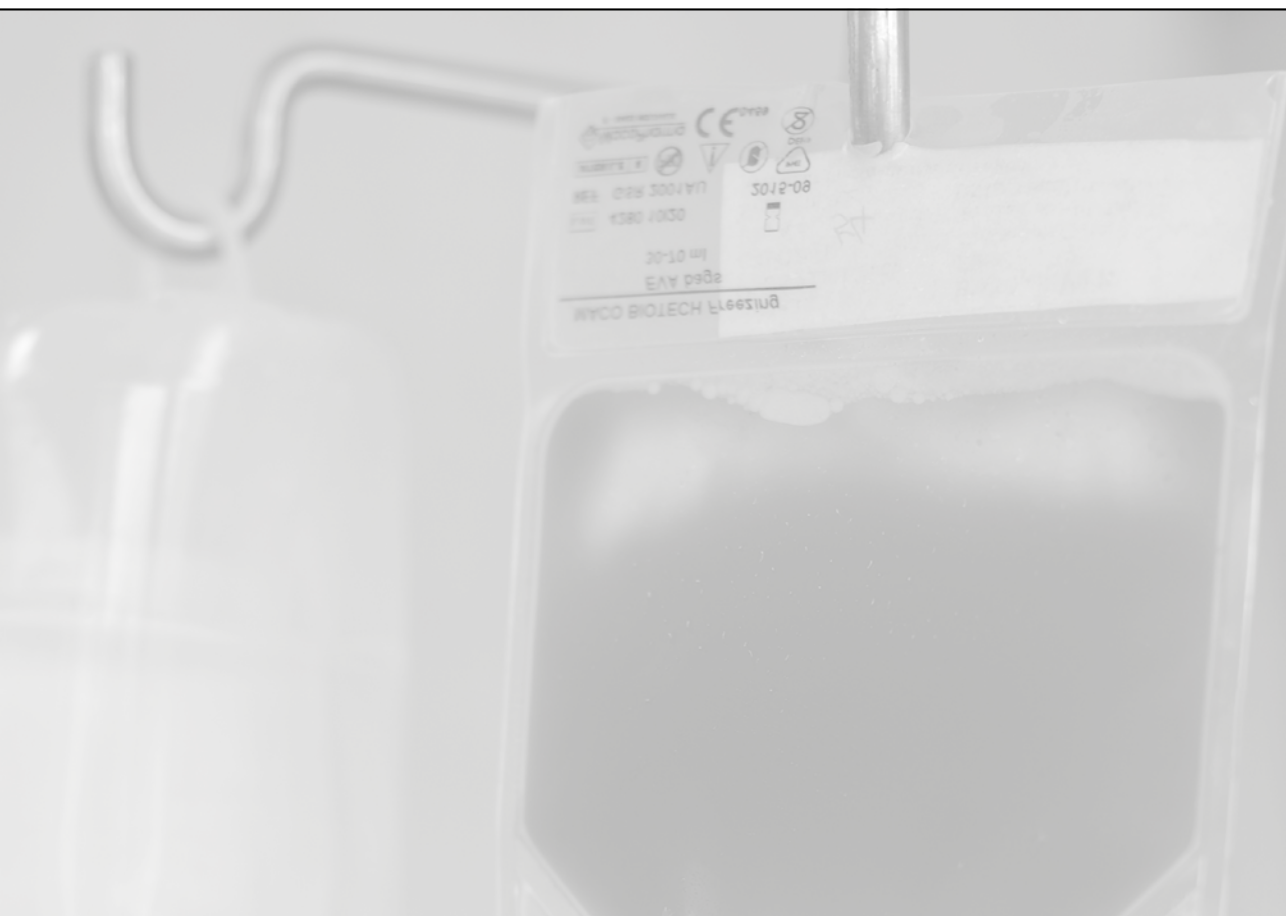
[1]Department of Neurology, Erasmus University Medical Center, Rotterdam, The Netherlands;
[2]Department of Radiation Oncology (MaastRO-Lab), GROW – School for Oncology and Developmental Biology, Maastricht University Medical Centre, Maastricht, The Netherlands;
[3]Laboratory of Tumor Immunology, University Medical Center Utrecht, Utrecht, The Netherlands

|ABSTRACT

Mitochondrial neurogastrointestinal encephalomyopathy (MNGIE) is a progressive metabolic disorder caused by thymidine phosphorylase (TP) enzyme deficiency. The lack of TP results in systemic accumulation of deoxyribonucleosides thymidine (dThd) and deoxyuridine (dUrd). In these patients, clinical features include mental regression, ophthalmoplegia and fatal gastrointestinal complications. The accumulation of nucleosides also causes imbalances in mitochondrial DNA (mtDNA) deoxyribonucleoside triphosphates (dNTPs), which may play a direct or indirect role in the mtDNA depletion/deletion abnormalities, although the exact underlying mechanism remains unknown. The available therapeutic approaches include dialysis and enzyme replacement therapy, both can only transiently reverse the biochemical imbalance. Allogeneic hematopoietic stem cell transplantation (AHSCT) is shown to be able to restore normal enzyme activity and improve clinical manifestations in MNGIE patients. However, transplant related complications and disease progression result in a high mortality rate. New therapeutic approaches, such as adeno-associated viral (AAV) vector and hematopoietic stem cell gene therapy have been tested in $Tymp^{-/-}Upp1^{-/-}$ mice, a murine model for MNGIE.

This review provides background information on disease manifestations of MNGIE with a focus on current management and treatment options. It also outlines the pre-clinical approaches towards future treatment of the disease.

Key words: mitochondrial neurogastrointestinal encephalomyopathy; MNGIE; thymidine phosphorylase; metabolic disease; HSCT; HSCGT; lentiviral vector

INTRODUCTION

Mitochondrial diseases represent a genetically and clinically heterogeneous group of disorders caused by mutations in mitochondrial DNA (mtDNA), that affect synthesis and function of mitochondrial proteins, such as tRNA (in MELAS disease) and ND1, 4, 6 (responsible for the majority of cases in LHON disease) (DiMauro, 2004). Another group is caused by mutations in nuclear DNA (nDNA) that lead to defects in nuclear encoded mitochondrial proteins. Part of these proteins exert their effect on mtDNA maintenance, thus known as nuclear-mitochondrial communication disorders. A subtype of the latter is mitochondrial DNA depletion syndrome (MDS); a group of mainly autosomal recessive disorders caused by defects in nuclear genes involved in mtDNA replication (e.g. *POLG* and *PEO1* causing hepatocerebal MDS), or genes crucial

for maintenance of mtDNA including *TK2* (responsible for myopathic MDS*), RRM2B* (encephalomypathic MDS) and thymidine phosphorylase (*TYMP*) gene mutations associated with MNGIE (El-Hattab and Scaglia, 2013). MNGIE, initially described in 1976 by Okamura (Okamura et al., 1976) is a fatal rare inherited metabolic disorder without genetic or ethnic predisposition (Gamez et al., 2005). The estimated rate of occurrence is 1-9:1,000,000[1], and as of 2011 fewer than 200 cases have been described in the medical literature (Halter et al., 2011). Due to its variable clinical presentations, MNGIE can be easily overlooked or misdiagnosed as Crohn's disease, psychiatric disorder, anorexia nervosa or myasthenia gravis (Rickards et al., 1994;Teitelbaum et al., 2002; Marti et al., 2004).

GENETIC DEFECTS, CLINICAL MANIFESTATIONS AND DIAGNOSIS

Genetic defects

MNGIE is an autosomal recessive inherited disease that is caused by mutations in the nuclear gene *TYMP* (previously known as *ECGF1*). *TYMP* codes for the TP enzyme (EC 2.4.2.4.) and is located on chromosome 22q13.33 (Stenman et al., 1992).TP is a cytoplasmic enzyme expressed in most human tissues, including gastrointestinal tract, central and peripheral nervous system, spleen, liver, bladder, leukocytes and in platelets which account for most of the TP activity in human blood (Fukami

and Salganicoff, 1973;Shaw et al., 1988). In contrast, TP is present at low levels in muscles and is lacking in kidney, aorta and fat tissues (Fox et al., 1995;Valentino et al., 2007). MNGIE is caused by a variety of pathogenic homozygous or compound heterozygous mutations in the exons or flanking regions of the *TYMP* gene. Various mutations are reported to date (Stenson et al., 2014) including deletions, single nucleotide insertions (Nishino et al., 1999), splice site (Kocaefe et al., 2003;Szigeti et al., 2004b) and frameshift mutations (Blazquez et al., 2005)

---

[1] http://www.orpha.net/consor/cgi-bin/index.php

and a homozygous duplication mutation in exon 8 of the *TYMP* gene (Gamez et al., 2005). The majority of these mutations are loss of function mutations. Heterozygous mutation carriers are asymptomatic with approximately 35% residual TP activity, although the plasma nucleoside levels are similar to healthy controls (Marti et al., 2004).

In addition, non-pathogenic polymorphisms have been described in the *TYMP* gene. The A465T polymorphism (c.1393G>A) was reported both in subjects with MNGIE like features and control subjects (Vissing et al., 2002;Martin et al., 2004). In some MNGIE cases there is no or mild clinical involvement of gastrointestinal tract or skeletal muscle, despite the presence of mutations in the *TYMP* gene leading to marked reduction in TP activity, probably indicating that environmental factors contribute to the severity of the clinical symptoms (Martin et al., 2004;Szigeti et al., 2004b). Apart from late-onset forms of the disease (Marti et al., 2005;Massa et al., 2009;Etienne et al., 2012), most patients display typical MNGIE features before the age of 20 years (Nishino et al., 2000;Teitelbaum et al., 2002).

Clinical manifestations

Gastrointestinal and ocular involvement are usually the first complications in this disease, although neuropathy and hearing loss have been reported as primary symptoms in some cases (Garone et al., 2011). Clinical symptoms are summarized in **Table 1**.

Diagnosis

Detailed patient history, thorough clinical examination, particular findings on magnetic resonance imaging (MRI) of the brain (**Figure 1**), genomic DNA screening for mutations in *TYMP* gene and biochemical analysis all contribute to the diagnosis of MNGIE. Biochemical diagnosis of MNGIE includes at least one of the following parameters (Marti et al., 2004): (1) Increased blood plasma levels of dThd and dUrd (>3μmol/L and >5μmol/L respectively). (2) Severely reduced TP enzyme activity in buffy coat leukocytes (<8% of healthy controls; healthy control mean TP activity equivalent to 634 nmol thymine formed /hr/mg protein). Biochemical analysis reduces the risk of missing the diagnosis in case of non-identified mutation sites (Nishino et al., 2000) or in case of unclassified variants (UV). Additionally, biochemical diagnosis contributes to the confirmation or exclusion of the the role of a UV as a cause for MNGIE. Similarly, biochemical assessment is preferred over clinical diagnosis since some of the classical symptoms of MNGIE can be absent. Other frequently observed findings in MNGIE patients include metabolic abnormalities such as lactic acidosis, deficiency of mitochondrial respiratory chain enzymes, mainly complex I and IV (Hirano et al., 1994) (Debouverie et al., 1997), urinary Thd and dUrd accumulation (Fairbanks et al., 2002;Spinazzola et al., 2002;la Marca et al., 2006) and elevated protein levels in CSF (Bedlack et al., 2004). Infrequently, skeletal muscle biopsies may reveal ragged red fibers, and mtDNA analysis may reveal acquired deletions, depletions or point mutations (Teitelbaum et al., 2002;Nishigaki et al., 2003).
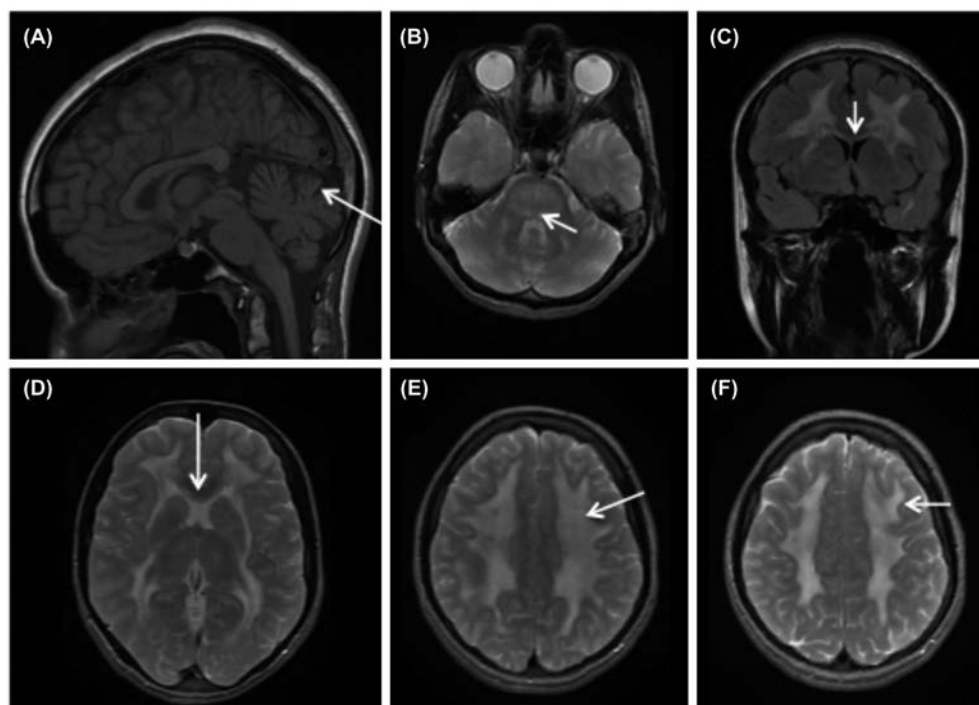
Figure 1. Brain MRI findings in MNGIE. MRI of MNGIE patient at age 16 with " typical" MNGIE phenotype . **(A)** T1 weighted sagital image shows cerebellar vermis atrophy (arrow) and normal gyral pattern. **(B)** Axial T2 with hyperintensities in the dorsal pons and mesencephalon (arrow). (**C** coronal flair image, **D** axial T2) show extensive signal abnormalities in the cerebral white matter. The external capsule is involved as is the inner blade of the corpus callosum (arrow **C**, **D**). **(E**, **F)** Extensive white matter involvement with sparing of the U-fibers (arrow).

|PATHOGENESIS

The TP enzyme converts mitochondrial dThd and dUrd to the nucleotide bases thymine and uridine respectively and 2-deoxy ribose 1-phosphate (Friedkin and Roberts, 1954). This occurs in *de novo* synthesis or via the salvage pathway. dThd and dUrd are homogeneously present in cellular and plasma compartments and they translocate between compartments through nucleoside transporters (NTs). In humans two unrelated protein families have been described (Young et al., 2013), concentrative nucleoside transporters (CNTs), an active transport system, and equilibrative nucleosides transporters (ENTs) responsible for passive facilitated diffusion.

The bidirectional ENTs, mainly ENT1, are ubiquitously present on almost all cell types and mediate the uptake and efflux of nucleosides **(Figure 2B)**. Therefore they are important for cells that rely on the salvage pathway for supply of nucleosides, including bone marrow cells, erythrocytes and leukocytes, brain and muscles (Young et al., 2008). Although TP is not expressed in all tissues, the TP expressed in circulating

21

Table 1. Common and rare clinical symptoms in MNGIE patients.

Complication	Symptoms	Pathophysiology
Gastrointestinal	Appetite loss, satiety Weight loss Digestive features: Chronic diarrhea, abdominal pain, cramps, nausea, colonic distension, dysphagia	Myogenic (visceral smooth muscle): atrophy in the muscularis propria of the stomach and small intestines. Neurogenic (enteric nervous system): loss of the interstitial cells of Cajal. Mixed myo-neurogenic causes
Ocular	External ophthalmoplegia, ptosis, retinal pigmentary changes, glaucoma, optic nerve atrophy	
Auditory	Deafness	Dysfunction of cranial nerve and auditory cortex. Atrophy of the stria vascularis in the cochlea
CNS	Mental changes, subcortical loss of cognitive functions, memory impairment	leukencephalopathy
PNPs	Numbness and paraesthesia	Demyelinating sensorimotor type: reduced sensory motor conduction, loss of myelin sheaths in lumbar and brachial plexus.
Skeletal muscle	Proximal myopathy	mtDNA molecular alterations and abnormal respiratory chain enzymes in skeletal muscles
Others	Endocarditis Spontaneous abdominal esophageal perforation Short stature Cardiomyopathy Psoriasis	

CIPO, Chronic intestinal pseudo obstruction; CPEO, Chronic progressive external ophthalmoplegia; CNS, central nervous system; PNPs, polyneuropathies

| Remarks	Study
A major cause of death and survival is generally related to the severity of these symptoms.	(Granero Castro et al., 2010),(Garone et al., 2011),(Giordano et al., 2008),(Zimmer et al., 2009) ,(Perez-Atayde et al., 1998) ,(Blondon et al., 2005),(Chapman et al., 2014).
Can lead to severe denutrition, anaemia and eventually the necessity for nutritional supportive treatments.	
CIPO in the early disease course is under recognized.	
CPEO phenotype is often present. Recovered upon HSCT transplantation compared to untreated patient.	(Threlkeld et al., 1992),(Barboni et al., 2004),(Vinciguerra et al., 2015)
Hearing loss is common among patients (in 61% of patients).	(Hirano et al., 1994), (Yasumura et al., 2003), (Li et al., 2011), (Mattman et al., 2011)
Satisfactory results were obtained soon following cochlear implantation in MNGIE patients.	
MNGIE is an example of an adult mitochondrial disorder in which leukodystrophy is observed.	(Millar et al., 2004),(Barragan-Campos et al., 2005),(Scaglia et al., 2005) ,(Schupbach et al., 2007),(Schiffmann and van der Knaap, 2009) ,(Scarpelli et al., 2013),(Carod-Artal et al., 2007;Salsano et al., 2013)
Patients presenting the characteristic multisystem symptoms of MNGIE have a unique pattern on brain MRI indicative of vasogenic oedema and glial cell dysfunction.	
To date, it is debatable whether or not the extent of these brain MRI signal alterations, correlates with age, clinical severity, CNS involvement or the biochemical and genetic profiles of MNGIE patients.	
Neuropathy usually is not among the first symptoms of the disease.	(Simon et al., 1990),(Hirano et al., 1994),(Bedlack et al., 2004),(Menezes and Ouvrier, 2012),(Pupe et al., 2012)
Some MNGIE cases are misdiagnosed with chronic inflammatory demyelinating polyneuropathy.	
Two cases with classical clinical presentation of MNGIE, were reported without skeletal muscle involvement.	(Papadimitriou et al., 1998),(Hirano et al., 2004), (Szigeti et al., 2004b;Cardaioli et al., 2010; Bax et al., 2013)
Both cases showed identical homozygous splice-acceptor site mutation in *TYMP* gene (c.215-1G>C), which may suggest a genotype-phenotype correlation.	
Rare complications	(Hirano et al., 1994),(Yolcu et al., 2014),(Kalkan et al., 2015)
Short stature as seen in many mitochondrial diseases and partly as a complication of failure to thrive	

2
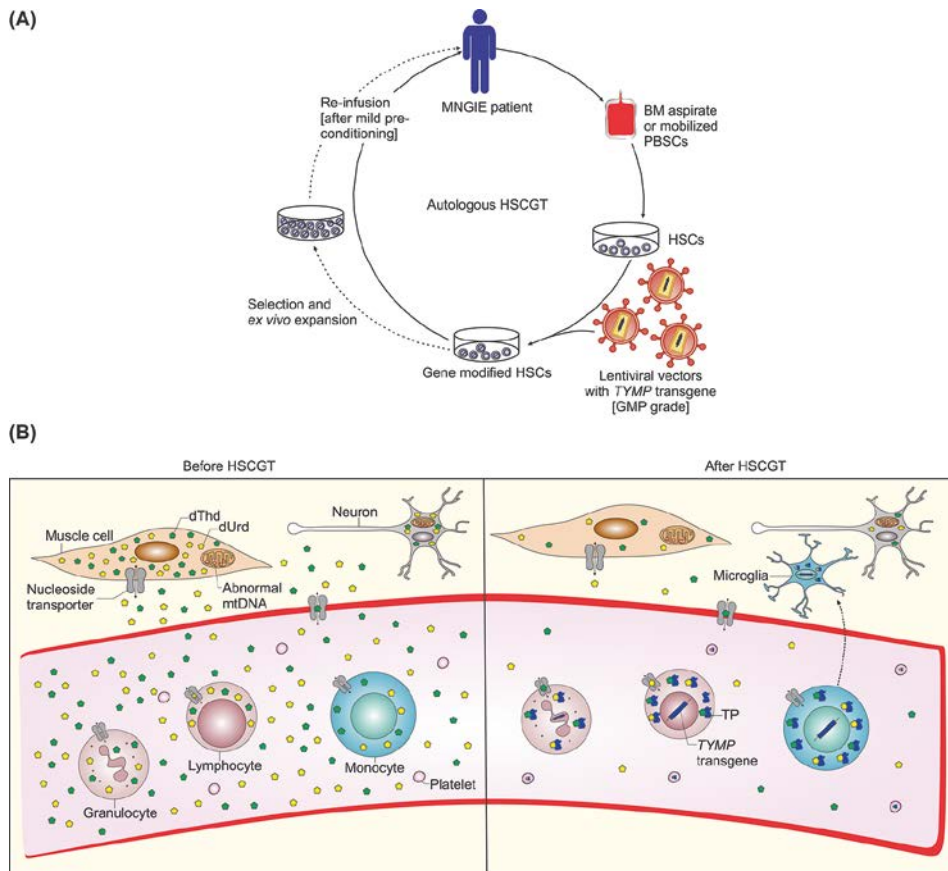
Figure 2. Schematic representation of autologous hematopoietic stem cell based gene therapy for MNGIE and possible mechanism of biochemical correction by gene modified HSCs. (A) Autologous bone marrow (BM) aspirates or apheresis of peripheral blood HSCs (PBSCs) after treatment with rh-G-CSF or plerixafor are collected from MNGIE patient. HSCs are *ex vivo* transduced by GMP grade lentiviral vectors containing the human *TYMP* transgene. Before infusion of the transduced cells, MNGIE patients are pre-treated with non-myeloablative conditioning to allow minimal engraftment of gene modified HSCs. (Selection and *ex vivo* expansion of gene modified HSCs allows for transplantation of large numbers of gene modified HSCs to obviate the need for myeloablative pre-conditioning and allows (to some degree) for assessment of safety of the gene modified HSCs prior to transplantation, for example by lentiviral vector integration analysis (reviewed in (Watts et al., 2011). **(B)** The enzyme thymidine phosphorylase (TP) is deficient in all tissues of MNGIE patients, which leads to accumulation of the nucleoside substrates dThd and dUrd and depletion of the nucleotide dCTP and finally mtDNA depletion and deletion (Gonzalez-Vioque et al., 2011). Following transplantation of gene modified HSCs and homing to bone marrow, these cells differentiate into all types of blood cells, LV genome and human *TYMP* transgene are integrated in leukocyte DNA ensuring stable expression of TP. TP catalyzes the chemical reaction which breaks down the nucleosides. This process eventually leads to reduction of systemic nucleosides accumulation. Nucleoside transporters mediate nucleosides transfer via passive facilitated diffusion (ENTs) and active transport (CNTs), the ubiquitous bidirectional ENTs are depicted (Young et al., 2013). In addition, some gene modified HSCs differentiate into monocytes and may migrate to the brain giving rise to microglia which act as a TP reservoir and cross correct the other cells in CNS.

platelets and leukocytes and some other tissues is essential to degrade the excess amounts of dThd and dUrd nucleosides which are secreted into the blood (Lara et al., 2007).

The molecular pathological mechanism in MNGIE involves imbalanced nucleosides and nucleotide pools. Initially, loss of function mutations in *TYMP* gene were identified resulting in reduced TP activity (Nishino et al., 1999) leading to accumulation of access amounts of the nucleoside substrates in blood plasma, urine and almost all tissues (Spinazzola et al., 2002;Valentino et al., 2007). It has been hypothesized that this biochemical imbalance disturbs the equilibrium of intra-mitochondrial deoxyribonucleoside triphosphates (dNTPs) pools (Spinazzola et al., 2002) and hence is responsible for mtDNA depletion, multiple deletions and point mutations associated with MNGIE (Hirano et al., 1994;Papadimitriou et al., 1998) (Nishino et al., 2000;Nishigaki et al., 2003). Therefore, recent studies have addressed the relationship between biochemical and dNTP pool imbalances and subsequent mtDNA abnormalities in MNGIE. *In vitro*, mtDNA point mutations and deletions, similar to those detected in MNGIE patients were reported in cultured HeLa cells after long time culture in the presence of high levels of thymidine in the culture medium. These mtDNA alterations were attributed to expanded levels of deoxythymidine triphosphate (dTTP) and deoxyguanosine triphosphate (dGTP) and reduced levels of deoxycytidinetriphosphate (dCTP) and deoxyadenosine triphosphate (dATP). However, no mtDNA depletion was observed in these HeLa cells (Song et al., 2003). Further investigation revealed that this increase in dTTP, under similar culture conditions,

was more pronounced in non-cycling skin and lung fibroblasts leading to depletion in mtDNA in a dThd dose and time dependent manner (Pontarin et al., 2006). Interestingly, mtDNA levels were recovered upon removal of the dThd from the culture medium. In order to understand the influence of metabolites accumulation on the creation of mtDNA alterations, an in organelle experimental model was used. Excess amounts of dThd were responsible for the significant increase in mitochondrial levels of dTTP, together leading to secondary TK2 inhibition mediated reduction of dCTP nucleotides (Gonzalez-Vioque et al., 2011). Subsequent studies confirmed these findings in *in vitro* fibroblast cultures and *in vivo* in the *Tymp$^{-/-}$Upp1$^{-/-}$* mouse model and suggest that the inadequate availability of dCTP accounts for the mtDNA depletion observed in MNGIE (Gonzalez-Vioque et al., 2011;Camara et al., 2014;Torres-Torronteras et al., 2014).

Altogether, these studies demonstrate that indeed it is the nucleoside accumulation and subsequent reduction of dCTP nucleotides, rather than the deficiency of TP *per se*, that accounts for the molecular and phenotypic alterations in MNGIE. An excellent illustration of this observation is the fact that TP expression in skeletal muscles is absent, nonetheless, some but not all MNGIE cases were reported with skeletal muscle mtDNA deletions, histological and oxidative phosphorylation abnormalities (Papadimitriou et al., 1998;Hirano et al., 2004).

When available, although limited, analysis of *postmortem* MNGIE samples is relevant and beneficial to gain knowledge about the molecular and pathological basis of the disease. Severe intestinal dysmotility,

also known as chronic intestinal pseudo obstruction (CIPO), and weight loss are principle presentations of MNGIE. Histopathological analysis of MNGIE gastrointestinal samples revealed depletion in mtDNA and mitochondrial proliferation, and consequently cell atrophy in the muscularis propria layer of the stomach and small intestines (Giordano et al., 2006;Giordano et al., 2008). Additionally, loss of interstitial cells of Cajal and morphologically abnormal muscularis propria and ganglion cells have been reported (Zimmer et al., 2009). On the other hand, the study of brain tissues of 2 MNGIE patients revealed no pathological proliferation of glial cells nor neuronal loss. However, the study suggested a role of TP deficiency in impairment of blood brain barrier, which could contribute to the observed hyperintense T2 signals on brain MRI scans (Szigeti et al., 2004a).

Nucleoside accumulation is detrimental probably during the early course of the disease, because nucleoside clearance did not improve mtDNA content per cell or reduce COX deficient fibers after liver transplantation (De Giorgio et al., 2016). Mitochondrial DNA instability is a hallmark for diseases caused by defective nuclear genes essential for mtDNA replication and repair (such as *PEO1*, *POLG1,2*) or maintenance of dNTP pools (such as *ANT1*, *TYMP*) or others involved in mtDNA homeostasis (such as *FBXL4*) (Young and Copeland, 2016). Mutations in *PEO1*, *POLG* and *ANT1* underlie the autosomal dominant form of progressive external ophthalmoplegia (adPEO), a very well characterized mtDNA disorder involving stalling of mtDNA replication (Van Goethem et al., 2001;Goffart et al., 2009). Therefore, stalling of Twinkle helicase or DNA polymerase γ could be a common pathological mechanism underlying mtDNA instability in MNGIE, PEO and mtDNA depletion syndrome (Hirano et al., 2001;Liu et al., 2008).

|CURRENT TREATMENTS FOR MNGIE

In general, treatment of mitochondrial diseases is mainly based on symptom management and supportive care (Pfeffer et al., 2013). Vitamin and amino acid supplements (Tanaka et al., 1997) and exercise therapy (Taivassalo et al., 1998) aiming to improve mitochondrial functions are recommended for mitochondrial myopathies. Symptomatic management of MNGIE consists of nutritional support (Wang et al., 2015), prevention of infections and pain relief including interventions such as celiac plexus neurolysis and blockage of the splenic nerve (Teitelbaum et al., 2002;Celebi et al., 2006). Since the metabolic and mtDNA abnormalities are attributed to the systemic nucleoside imbalances, clinical interventions focus on direct removal of these metabolites to restore the balance or by introducing the deficient enzyme to reduce the metabolites.

Hemodialysis and peritoneal dialysis

The first hemodialysis aiming to remove the excess amounts of nucleosides from the circulation was performed in 2002 (Spinazzola et al., 2002) in two MNGIE patients followed by another in 2006. In the first two patients, significantly reduced thymidine levels were observed shortly after hemodialysis, however this effect was

transient as thymidine levels returned to pre-dialysis levels 3 hours after dialysis (Spinazzola et al., 2002). A progressive reduction in Thd levels below the basal levels was observed after repetitive dialysis treatments in the third case (la Marca et al., 2006). A MNGIE patient who had peritoneal dialysis showed an improvement in gastrointestinal symptoms (such as vomiting, anorexia, abdominal pain and diarrhea) during the continuing peritoneal dialysis for three years with body weight gain, although other major symptoms including ocular and neurological abnormalities and brain MRI signals did not change (Yavuz et al., 2007). Another case report noted improvement of the gastrointestinal and neurological symptoms, mainly the mitigation of numbness in the hands, until nucleoside levels increased again 15 months after continuous ambulatory peritoneal dialysis (Ariaudo et al., 2014).

Enzyme Replacement Therapy (ERT)

Initially, platelet infusions were performed in two MNGIE patients to restore TP enzyme activity in the blood. This approach showed efficient recovery of functional TP enzyme and correction in nucleoside imbalances, however, like dialyses, these improvements were temporary requiring multiple treatment sessions for long-term responses. ERT is a reliable, well-tolerated approach to replace the deficient enzyme in a variety of lysosomal storage disorders including Gaucher, Pompe and Fabry disease and Sly syndrome (Wilcox et al., 2004;Burrow et al., 2007). For MNGIE, approaches were developed to encapsulate TP in order to prolong the half-life of circulatory TP enzyme and reduce the immunogenic reactions. These include polymeric

nanoparticles (De Vocht et al., 2009) and erythrocytes as they are permeable and affect the plasma metabolites, such as in adenosine deaminase deficiency (Bax et al., 2000;Moran et al., 2008). The erythrocyte encapsulated TP (EE-TP) concept is under clinical development as an orphan ERT for MNGIE with the first attempt carried out in a MNGIE patient in 2008 (Moran et al., 2008). In this approach, autologous erythrocytes were isolated from patients and loaded with recombinant *E.Coli* TP enzyme *in vitro* via hypo osmotic dialysis. Significant clinical improvements were observed such as the ability to walk and climb and the recovery of sensation and the mitigation of numbness in hands and feet, even after 23 months after termination of multiple cycles of EE-TP (Bax et al., 2013). When using the EE-TP approach, there is a high risk that an immunological reaction is triggered against the bacterial TP, especially if the infusions are repeated several times, although this has not been observed (Levene et al., 2013).

Orthotopic liver transplantation (OLT)

Liver transplantation is a new ERT strategy for treatment of MNGIE patients. TP protein levels are high in healthy human liver tissues and significantly higher than in bone marrow cells (Boschetti et al., 2014). Recently, OLT was successfully applied in a severely affected, 25-years old MNGIE patient (De Giorgio et al., 2016). Steady state nucleoside balance was observed up to13 months post OLT. Slight improvements in lower limb strength and brain metabolism (reduced lactate levels) and structure (reduced cerebellar mean diffusivity values at diffusion MRI), improved quality of

life scores and nutritional parameters, but not body weight (40 kg), were observed up to six months after OLT. When ileostomy closure was performed, the gastrointestinal (GI) functions and body weight declined at 13 months (37 kg). Therefore, it remains uncertain whether the mild restoration of GI function was due to the decompressive ileostomy, instead of the OLT. In addition, skeletal muscle mtDNA content per cell was slightly increased after OLT. The study suggests that the damage in post mitotic tissues during late stages of the disease is irreversible despite recovery of nucleoside balance. Therefore, biochemical correction should probably be achieved prior to irreversible damage, preferably before the intestinal symptoms appear. Preoperative conditioning for OLT is not required. However, this approach requires matched organ donors (which are limited), involves transplantation related risks and requires long-term immunosuppression which all can further affect the quality of life of the patients.

Hematopoietic stem cell transplantation (HSCT)

Another possibility to restore TP enzyme activity in the circulation is by HSCT. Recently, a retrospective analysis of all HSC transplanted MNGIE patients between 2005-2011 showed that only nine out of 24 patients were alive up to four years after transplantation. All nine survivors had normalized TP activity in their blood while seven of them showed improved body mass index, gastrointestinal symptoms and peripheral neuropathy. On the other hand, nine MNGIE patients died mainly due to transplant-related causes such as GVHD and graft failure, including recipients of HLA-mismatched unrelated cord blood transplants, while the remaining six patients died of disease progression. The recommendations of this study included transplantation of a sufficient number of cells, because in some patients the graft was rejected, and to consider more closely HLA matched donor cells, because of the large number of GVHD observed in this retrospective study, and to transplant at an earlier age before major organ damage has occurred (Halter et al., 2011; Halter et al., 2015).

The poor physical state of MNGIE patients when they enroll HSCT trials increases the risk for transplantation related complications caused by conditioning regimens and immune-suppressants. Other problems may arise from the drugs used in HSCT which are potentially harmful to mitochondria such as cyclophosphamide (Mariana Ponte Cardoso et al., 2015). Therefore, MNGIE patients are treated with Busulfan and fludarabine prior to HSCT, following the recommendations of MNGIE consensus meeting in 2011 (Halter et al., 2011). For MNGIE patients who develop liver cirrhosis, AHSCT should be contraindicated and OLT would be the treatment of choice (Finkenstedt et al., 2013). Pre-existing liver cirrhosis complicates liver failure which may develop after AHSCT due to multiple factors such as viral infections in immunocompromised recipients or due to hepatotoxic conditioning drugs.

|PRE-CLINICAL EXPERIMENTAL APPROACHES TOWARDS THERAPY

Models of MNGIE

In organello experiments and human MNGIE fibroblasts were used for highlighting parts of the molecular mechanism of MNGIE (Gonzalez-Vioque et al., 2011;Camara et al., 2014). To study therapeutic interventions, such as gene therapy, *in vivo* models are required. A mouse model was developed by targeted disruption of exon 4 of the *TYMP* gene to generate *Tp^-/-* mice. In contrast to human TP, murine TP degrades both dThd and dUrd; *Tp^-/-* mice were crossed with *Upp1^-/-* to generate the *Tymp^-/-Upp1^-/-* mice, which are currently the only relevant *in vivo* animal model (Haraguchi et al., 2002;Lopez et al., 2009). *Tymp^-/-Upp1^-/-* mice show increased levels of the purine nucleosides dThd and dUrd in plasma and tissues. Diffuse leukoencephalopathy manifests late during the lifetime of these animals, around the age of 22 months (Lopez et al., 2009). Other symptoms associated with MNGIE, such as decreased motor coordination and gastrointestinal features have not been reported in this mouse model. Brain mtDNA depletion was not consistently found in this mouse model (Lopez et al., 2009;Torres-Torronteras et al., 2011;Camara et al., 2014). Therefore, high doses of exogenous nucleosides were administered to exacerbate the mitochondrial phenotype (Garcia-Diaz et al., 2014), an approach that was rationalized by the lower nucleoside levels in *Tymp^-/-Upp1^-/-* mice compared to MNGIE patients. Mice were on an exogenous dThd and dUrd diet for a long time (24 months) before pronounced mtDNA depletion, diffuse leukoencephalopathy and motor abnormalities were observed.

Experimental approaches have been explored for treatment of MNGIE; among which experiments performed by Camara *et al* which suggest that modulation of dNTP metabolism through increasing the availability of dCTP or inhibition of its catabolism can indeed reverse and prevent, at least, dCtd imbalance. A strategy that can be applied for other similar mitochondrial disorders that are caused by altered nucleosides and dNTP metabolism, for example in disorders caused by mutations in *TK2* or *DGUOK* deficiency (Camara et al., 2014).

Gene Therapy

The *Tymp^-/-Upp1^-/-* mouse model has also been used for testing potential curative treatments. A recently investigated strategy is the use of gene therapy. Both lentiviral (LV) and adeno-associated viral (AAV) vector mediated *TYMP* gene transfer have been evaluated in pre-clinical studies for treatment of MNGIE.

AAV-mediated liver directed gene therapy

AAV vector gene therapy has been explored in clinical trials for a variety of inherited and acquired diseases (Naldini, 2015). The main limitation of this approach is the human immune response to AAV capsid, as demonstrated in hemophilia B trials. In one of the first AAV trials targeting the liver, therapeutic levels of coagulation factor IX (FIX) were achieved at a high vector dose (2×10^{12} vector genomes per kilogram of body weight, vg/kg). Nonetheless, this high vector dose was associated with an early decline of FIX (~8 weeks after treatment)

due to T-cell immunity against AAV capsid antigens eliminating transduced hepatocytes (Manno et al., 2006).

The hybrid vector AAV2/8 with modified molecular configuration (packaged double stranded genome) and improved cassette design (codon optimized hFIX) to enhance transduction and translational efficiency was explored in a hemophilia B trial (Nathwani et al., 2006). Stable FIX expression diminished use of the costly FIX concentrate and importantly, clinical improvement was achieved in a dose dependent manner. The least bleeding episodes were seen in recipients of the highest AAV dose (steady state 5% of normal levels at a single vector peripheral vein infusion of 2×10^{12} vg/kg up to four years) (Nathwani et al., 2014). For MNGIE, an AAV2/8 expressing human *TYMP* under the control of hepatic promoter was used for treatment of *Tymp*^{-/-} *Upp1*^{-/-} mice (Torres-Torronteras et al., 2014). Low AAV doses (2×10^{11} vg/kg) were sufficient to reduce nucleoside imbalances to normal levels in liver, skeletal muscle and brain for up to eight months, while higher doses reduced nucleosides below detection levels. However, only at higher doses ($>2 \times 10^{11}$ vg/kg) TP activity was increased in the liver (but not in skeletal muscle or brain).

In light of the clinical data of the hemophilia B trial which shows that clinical improvement was AAV dose dependent (Nathwani et al., 2014), the question for MNGIE is whether or not the low AAV dose would be sufficient to reverse a clinical phenotype beyond biochemical correction. MNGIE mouse studies failed to report any relevant clinical phenotype in *Tymp*^{-/-}*Upp1*^{-/-} mice, and therefore the potential or required dosage to cure it has not been demonstrated (Torres-Torronteras et al., 2011;Torres-Torronteras et

al., 2014). Importantly, upon AAV treatment nucleosides accumulation was not reduced in the intestine of treated mice at the highest dose (10^{13} vg/kg) administered. Since the intestines are heavily affected in MNGIE patients it is important to obtain evidence of correction in this organ. Preclinical studies in hemophilic dogs and non-human primates could predict the therapeutic dose in human trials (Manno et al., 2006;Nathwani et al., 2014) if that is the case for MNGIE too, biochemical correction in the intestine might require improved expression cassettes to enhance protein production, targeting the expression to major affected organs, or the less favorable option of using higher AAV doses ($>10^{13}$ vg/kg). High doses, for example 7.2×10^{12} vg/mouse were sufficient to transduce 100% of mouse hepatocytes (Nakai et al., 2005). Such high doses might be required for gene therapy of systemic diseases, i.e. when non hepatic tissues are also affected, as in MNGIE. However, these high AAV doses are likely to cause hepatocellular toxicity, biodistribution to other unwanted organs and shedding of the AAV, enhanced risk of eliciting immunity towards the viral capsid and increased costs of virus production. Immunity against ectopic TP might be an additional concern for MNGIE patients, therefore prophylactic immunosuppression might be required. Additional pre-clinical studies have to address the possibility of an immune response against ectopic TP in previously untreated patients. In addition to increased liver TP activity correlating with vector dose, an unexpected increase in liver dGTP of *Tymp*^{-/-}*Upp1*^{-/-} mice was observed in a dose depend manner as well, although the consequences of this increase are unknown. Together these findings suggest

that studies into optimal dosing of AAV may be required for clinical application.

Human AAV trials should be carried out cautiously as they can reveal complications that were not observed during preclinical studies. An example is the early decline in FIX expression (Manno et al., 2006) and hepatotoxicity observed in 4/6 recipients of a high AAV dose (2×10^{12} vg/kg) (Nathwani et al., 2014), due to immunity against AAV capsid. MNGIE patients are often > 12 years and probably have been pre-exposed to AAV and consequently can mount strong immune responses to AAV. Therefore, individuals with neutralizing antibodies to AAV should be excluded from clinical trials to avoid an immune response towards AAV. Another concern is the durability of transgene expression considering the longer lifespan of humans, compared with the animals in preclinical studies, and the potential need for recurrent AAV injections, especially at lower vector doses. In this respect hematopoietic stem cell gene therapy (HSCGT) would provide a preferable option as a single, long lasting intervention method. Additional concerns related to AAV mediated gene therapy include purity of AAV preparations and manufacturing costs (Mingozzi and High, 2013).

LV-mediated hematopoietic stem cell gene therapy (HSCGT)

The encouraging therapeutic outcomes and favorable safety profile renders LV-HSCGT an attractive therapeutic approach for a variety of hereditary metabolic disorders (Wagemaker, 2014), and is potentially advantageous over AHSCT for certain selected diseases (Naldini, 2015). Proof of concept of HSC gene therapy was obtained

in $Tymp^{-/-}Upp1^{-/-}$ mice (Torres-Torronteras et al., 2011) using a phosphoglycerate kinase promoter driving native human $TYMP$ cDNA and a GFP reporter in hematopoietic cells resulting in biochemical correction in peripheral blood (Torres-Torronteras et al., 2011). More recently, we developed clinically applicable LVs that carry human $TYMP$ cDNA, and demonstrated long-term biochemical correction in $Tymp^{-/-}Upp1^{-/-}$ mice at low vector copy number (VCN). Our data demonstrates the feasibility to further develop clinical protocols for HSCGT for MNGIE (Yadak et al., 2015). Similar results in a long-term follow up of 20 months confirms the correction of biochemical imbalances which was maintained at low vector copy number and chimerism (Torres-Torronteras et al., 2016).

In HSCGT for MNGIE, HSCs are isolated from MNGIE patients, transduced *ex vivo* by LV vectors carrying a functional copy of $TYMP$ and infused back into the patient (**Figure 2A**). The newly formed HSCs and its progenitors produce TP which catabolize the excess amounts of nucleosides (**Figure 2B**). Since the patient's own stem cells are used, GVHD is not a concern. However, mild prophylactic immunosuppression maybe required to prevent possible immune reaction against the TP transgene.

Myeloablative pre-conditioning might be necessary for high levels of engraftment in other metabolic disorders, such as metachromatic leukodystrophy (MLD), due to lack of selective advantage of gene modified cells. In particular, busulfan myeloablative conditioning is used in MLD patients for depletion of endogenous microglia and mobility of gene modified monocytes through the blood brain barrier (BBB) (Capotondo et

2

al., 2012). The contribution of gene modified microglia to correct biochemical imbalances has never been explored in MNGIE. However, murine gene therapy studies using LV and AAV vectors implicate reversal of nucleoside imbalance at low or possibly no increase in brain TP activity (Torres-Torronteras et al., 2014;Torres-Torronteras et al., 2016). In liver directed AAV2/8 gene therapy, it is not expected that brain cells will be transduced. In HSCGT, gene modified monocytes are expected to migrate to brain and differentiate into microglia. Nonetheless, the results of the HSCGT MNGIE mouse study do not rule out the potential that gene modified microglia can contribute to correction of brain biochemistry and phenotype, although this might not be necessary if ectopic expression outside the brain is high enough. When transduction efficiency is high enough, significant TP activity can be measured in the brain, indicating that transduced microglia might reside in the brain after long-term follow-up. To that end, two potential mechanisms might act synergistically to normalize the brain nucleoside levels, a systemic ectopic source and one local contribution of gene-modified cells (**Figure 2B**).

Potential options and future research for application in MNGIE patients include alternative conditioning strategies to obviate the cytotoxicity related to myeloablative conditioning and strategies to enhance the quality of infused gene modified HSCs. One approach is to mobilize endogenous HSCs into peripheral blood in order to create (space) in the bone marrow for the infused donor HSCs to engraft (Chen et al., 2006). Human granulocyte colony stimulating factor (G-CSF) was sufficient in

immunocompromised mice (Huston et al., 2014), probably due to the selective advantage of the gene modified cells, however more stringent agents might be required in normal immunocompetent mice. A possibility is G-CSF in combination with the more potent HSCs mobilizer plerixafor (a specific CXCR4 antagonist) or the selectins inhibitor fucoidan. Such regimens probably require additional mild chemotherapeutics, in particular if the gene corrected TP-expressing HSCs lack selective growth advantage to overcome host cells. These HSCs mobilizers act via different mechanisms, therefore parameters such as the optimal dose and time frame for transplantation after mobilization need to be established in relevant pre-clinical models. Alternatively, targeting specific endogenous hematopoietic populations might reduce the off-target toxicity related to the common non-specific conditioning (Aiuti and Naldini, 2016). Examples include inhibiting c-kit, a HSC tyrosine kinase cell surface antigen (Xue et al., 2010) and the recently developed immunotoxin against hematopoietic stem cells (CD45-SAP) (Palchaudhuri et al., 2016).

Strategies such as *ex vivo* expansion of gene modified HSCs can improve the quality of the infused gene modified cells and enhance the outcome of gene therapy (Watts et al., 2011). In particular when combined with additional approaches to enrich for HSCs, preserve stemness of- and enhance homing and engraftment ability of gene modified HSCs (Psatha et al., 2016). Ultimately, this approach combined with improved mild preconditioning protocols, could benefit patients in poor health condition at transplantation, such as in MNGIE patients.

A risk of HSC gene therapy is insertional mutagenesis. The first HSC gene therapy

trials used gammaretrovirus (γ-RV) based vectors for treatment of X-linked severe combined immunodeficiency (SCID-X1) (Gaspar et al., 2004;Hacein-Bey-Abina et al., 2010), adenosine deaminase (ADA-SCID) (Aiuti et al., 2002), chronic granulomatous disease (CGD) (Ott et al., 2006) and Wiskott-Aldrich syndrome (WAS) (Boztug et al., 2010). Although efficient correction of immunodeficiency was achieved in most patients in SCID-X1, CGD and WAS trials, lympho-proliferative disorders (Hacein-Bey-Abina et al., 2003a;Hacein-Bey-Abina et al., 2003b;Hacein-Bey-Abina et al., 2008;Howe et al., 2008;Braun et al., 2014) and myelodysplasia (Stein et al., 2010) developed secondary to γ-RV vector integrations within or nearby proto-oncogenes. In addition to the preferred integration profiles over γ-RV vector (Deichmann et al., 2007;Gabriel et al., 2012;Cattoglio et al., 2007), LV efficiently transduce non-cycling primitive HSCs and under minimum culture conditions (Naldini et al., 1996;Guenechea et al., 2000). Therefore, attention was focused on development of LV as a relatively safer approach, leading eventually to development of third-generation self-inactivating HIV derived-vectors (SIN-LV) (Dull et al., 1998;Zufferey et al., 1998). Several pre-clinical studies indicate the reduced genotoxicity of SIN-LV vectors compared with γ-retroviral vectors, in particular SIN-LV common integration sites (CIS) revealed no preference of integration near proto-oncogenes (Montini et al., 2006;Modlich et al., 2009;Romero et al., 2013;Zhou et al., 2013;Biffi et al., 2011). Since then, SIN-LV vectors have been applied successfully in ongoing clinical trials for a variety of metabolic (Cartier et al., 2009;Biffi et al., 2013) and immunodeficiency disorders

(Aiuti et al., 2013), and no adverse events have yet been reported in these trials. Moreover, the therapeutic benefits without toxicity related to transgene expression and biosafety of SIN-LV vectors has been further validated through a growing body of recent preclinical studies supporting the initiation of clinical trials, for example for β-thalassemia (Negre et al., 2015) and mucopolysaccharidosis I disease (Visigalli et al., 2016).

Furthermore, selective advantage for growth and differentiation conferred by the therapeutic transgene expression increases the potential risk for proliferative disorders, this was reported in some immunodeficiency conditions (Aiuti and Roncarolo, 2009). For metabolic disorders, for instance lysosomal storage disorders , however, most studies show that enzyme positive cells have no selective advantage (Bernardo and Aiuti, 2016), which is most likely the case in MNGIE as well. To improve safety, technologies such as *ex vivo* expansion of gene modified HSCs may permit for safety assessment (to some degree) prior to transplantation, by analysis of LV integration sites (Watts et al., 2011) **(Figure 2A)**.

AAV mediated GT or HSCGT?
Regardless of the type of viral vector used for gene therapy, the chosen strategy should provide long-term expression of the gene of interest without side effects in the host. It is important to apply a well-defined vector dose that is sufficient to reverse the biochemical and nucleotide imbalance without any potential side effects. In particular, abnormal overexpression of the TP enzyme is detected in different tumor types, including non-small cell lung-, colorectal-, breast-, gastrointestinal-, and hepatic cancers (Koukourakis et al.,

1997;Mori et al., 2000;Ikeguchi et al., 2001;Nakayama et al., 2005;Mitselou et al., 2012) and correlates with a worse prognosis in colorectal cancer patients (Takebayashi et al., 1996). Besides, disturbance of dNTP pools can be a trigger for cell cycle arrest and apoptosis (Oliver et al., 1996) (Kumar et al., 2010).

|CONCLUDING REMARKS

The lack of mitochondrial histone protection, the limited repair capacity and oxidized dNTPs contributing to mismatch errors (Alexeyev et al., 2013) all make mitochondria more susceptible than nuclear DNA to mutagenesis. It has become evident that it is the systemic accumulation of nucleosides in MNGIE (Di Meo et al., 2015) that causes imbalances in mitochondrial dNTP pools. However, the mechanism by which it causes mtDNA alterations is still unknown. Although the current treatments focus on restoration of TP enzyme activity and/ or elimination of accumulating metabolites, further understanding of cellular mechanisms involved in maintenance of mtDNA integrity and copy number can provide targets for clinical intervention for MNGIE and possibly other mitochondrial disorders.

Platelet infusions, hemato/peritoneal dialysis and erythrocyte encapsulated TP enzyme replacement therapy could be used to provide biochemical correction. AAV gene therapy and lentiviral HSCGT are potential curative options as evidenced by the promising pre-clinical results in *Tymp$^{-/-}$Upp1$^{-/-}$* mice . OLT is a promising emerging treatment and should currently be the treatment of

The medical condition of the patient can also influence the choice of the vector system for clinical application. For terminally ill patients, the AAV approach could be most suitable to avoid the risks associated with the pre-conditioning for transplantation in autologous HSC gene therapy or if a suitable HSCs donor for AHSCT is lacking.

choice for MNGIE patients with pre-existing liver failure. Allogeneic HSCT has risks of graft failure, GVHD and conditioning-related toxicity. Milder conditioning may be applicable in HSCGT, and treatment should preferably be applied at an early age. Novel strategies are being explored to improve the safety and efficiency of viral based gene therapy, ultimately for MNGIE patients as well. These include strategies to enhance transduction, improve engraftment of gene modified HSCs and limit transplantation related toxicity, and others to overcome the limitation of AAV capsid triggered immunity by means of novel serotypes and improved transcription cassettes.

MNGIE patients should receive suitable treatment promptly before permanent damage occurs, which can be challenging, as MNGIE patients are often diagnosed late during disease progression in a poor health condition. Because TP activity and nucleoside levels can be routinely measured in blood samples, MNGIE should be considered to be included in newborn screening programs, similar to other (neuro) metabolic disorders for early diagnosis and treatment (Carlson, 2004;McHugh et al., 2011).

2

|LIST OF ABBREVIATIONS

AAV: adeno-associated virus; ADA-SCID: adenosine deaminase-severe combined immunodeficiency; AHSCT: allogeneic hematopoietic stem cell transplantation; ANT-1: adenine nucleotide translocase type 1; BBB: blood brain barrier; CGD: chronic granulomatous disease; CIPO: chronic intestinal pseudo obstruction; CIS: common integration site; CNT: concentrative nucleoside transporter; CPEO: chronic progressive external ophthalmoplegia; dATP: deoxyadenosine triphosphate; dCTP: deoxycytidinetriphosphate; dGTP: deoxyguanosine triphosphate; DGUOK: deoxyguanosine kinase; dTTP: deoxythymidine triphosphate; dNTP: deoxyribonucleoside triphosphates; dThd: thymidine;dUrd: deoxyuridine; ECGF1: platelet-derived endothelial cell growth factor; EE-TP: erythrocyte encapsulated TP; ENT: equilibrative nucleosides transport; ERT: enzyme replacement therapy; FBXL4: F-box and leucine-rich repeat protein 4; FIX: coagulation factor IX; G-CSF: granulocyte colony stimulating factor; γ-RV: gammaretrovirus; GVHD: graft versus host disease; HSCT: hematopoietic stem cell transplantation; HSCGT: hematopoietic stem cell gene therapy; LHON: Leber's hereditary optic neuropathy; LV: lentivirus; MDS: mitochondrial DNA depletion syndrome; MNGIE: mitochondrial neurogastrointestinal encephalomyopathy; MELAS: mitochondrial encephalomyopathy, lactic acidosis, and stroke-like episodes; NT: nucleoside transporter; OLT: orthotopic liver transplantation; PEO: progressive external ophthalmoplegia; POLG: DNA polymerase subunit gamma; RRM2B: Ribonucleotide Reductase M2 B; SCID- X1: X-linked severe combined immunodeficiency; SIN-LV: self-inactivating LV; TK2: thymidine kinase 2; TYMP: thymidine phosphorylase; WAS: Wiskott-Aldrich Syndrome.

|CONFLICT OF INTEREST STATEMENT

The authors declare no conflict of interest.

|AUTHOR CONTRIBUTIONS

RY framed the structure of the review, analyzed the literature and wrote the manuscript; PS, MW participated in the literature analysis; NP, IF participated in the literature analysis and supervised the writing. All authors discussed the topic and provided intellectual feedback to the article.
All the authors read and approved the manuscript.

|FUNDING

|REFERENCES

1. Aiuti, A., Biasco, L., Scaramuzza, S., Ferrua, F., Cicalese, M.P., Baricordi, C., Dionisio, F., Calabria, A., Giannelli, S., Castiello, M.C., Bosticardo, M., Evangelio, C., Assanelli, A., Casiraghi, M., Di Nunzio, S., Callegaro, L., Benati, C., Rizzardi, P., Pellin, D., Di Serio, C., Schmidt, M., Von Kalle, C., Gardner, J., Mehta, N., Neduva, V., Dow, D.J., Galy, A., Miniero, R., Finocchi, A., Metin, A., Banerjee, P.P., Orange, J.S., Galimberti, S., Valsecchi, M.G., Biffi, A., Montini, E., Villa, A., Ciceri, F., Roncarolo, M.G., and Naldini, L. (2013). Lentiviral hematopoietic stem cell gene therapy in patients with Wiskott-Aldrich syndrome. *Science* 341, 1233151.

2. Aiuti, A., and Naldini, L. (2016). Safer conditioning for blood stem cell transplants. *Nat Biotechnol* 34, 721-723.

3. Aiuti, A., and Roncarolo, M.G. (2009). Ten years of gene therapy for primary immune deficiencies. *Hematology Am Soc Hematol Educ Program*, 682-689.

4. Aiuti, A., Slavin, S., Aker, M., Ficara, F., Deola, S., Mortellaro, A., Morecki, S., Andolfi, G., Tabucchi, A., Carlucci, F., Marinello, E., Cattaneo, F., Vai, S., Servida, P., Miniero, R., Roncarolo, M.G., and Bordignon, C. (2002). Correction of ADA-SCID by stem cell gene therapy combined with nonmyeloablative conditioning. *Science* 296, 2410-2413.

5. Alexeyev, M., Shokolenko, I., Wilson, G., and LeDoux, S. (2013). The maintenance of mitochondrial DNA integrity--critical analysis and update. *Cold Spring Harb Perspect Biol* 5, a012641.

6. Ariaudo, C., Daidola, G., Ferrero, B., Guarena, C., Burdese, M., Segoloni, G.P., and Biancone, L. (2014). Mitochondrial neurogastrointestinal encephalomyopathy treated with peritoneal dialysis and bone marrow transplantation. *J Nephrol*.

7. Barboni, P., Savini, G., Plazzi, G., Bellan, M., Valentino, M.L., Zanini, M., Montagna, P., Hirano, M., and Carelli, V. (2004). Ocular findings in mitochondrial neurogastrointestinal encephalomyopathy:

a case report. *Graefes Arch Clin Exp Ophthalmol* 242, 878-880.

8. Barragan-Campos, H.M., Vallee, J.N., Lo, D., Barrera-Ramirez, C.F., Argote-Greene, M., Sanchez-Guerrero, J., Estanol, B., Guillevin, R., and Chiras, J. (2005). Brain magnetic resonance imaging findings in patients with mitochondrial cytopathies. *Arch Neurol* 62, 737-742. doi: 10.1001/archneur.62.5.737.

9. Bax, B.E., Bain, M.D., Fairbanks, L.D., Simmonds, H.A., Webster, A.D., and Chalmers, R.A. (2000). Carrier erythrocyte entrapped adenosine deaminase therapy in adenosine deaminase deficiency. *Adv Exp Med Biol* 486, 47-50.

10. Bax, B.E., Bain, M.D., Scarpelli, M., Filosto, M., Tonin, P., and Moran, N. (2013). Clinical and biochemical improvements in a patient with MNGIE following enzyme replacement. *Neurology* 81, 1269-1271.

11. Bedlack, R.S., Vu, T., Hammans, S., Sparr, S.A., Myers, B., Morgenlander, J., and Hirano, M. (2004). MNGIE neuropathy: five cases mimicking chronic inflammatory demyelinating polyneuropathy. *Muscle Nerve* 29, 364-368.

12. Bernardo, M.E., and Aiuti, A. (2016). The role of conditioning in hematopoietic stem cell gene therapy. *Hum Gene Ther*.

13. Biffi, A., Bartolomae, C.C., Cesana, D., Cartier, N., Aubourg, P., Ranzani, M., Cesani, M., Benedicenti, F., Plati, T., Rubagotti, E., Merella, S., Capotondo, A., Sgualdino, J., Zanetti, G., von Kalle, C., Schmidt, M., Naldini, L., and Montini, E. (2011). Lentiviral vector common integration sites in preclinical models and a clinical trial reflect a benign integration bias and not oncogenic selection. *Blood* 117, 5332-5339. doi: 10.1182/blood-2010-09-306761.

14. Biffi, A., Montini, E., Lorioli, L., Cesani, M., Fumagalli, F., Plati, T., Baldoli, C., Martino, S., Calabria, A., Canale, S., Benedicenti, F., Vallanti, G., Biasco, L., Leo, S., Kabbara, N., Zanetti, G., Rizzo, W.B., Mehta, N.A., Cicalese, M.P., Casiraghi, M., Boelens, J.J., Del Carro, U., Dow, D.J., Schmidt, M., Assanelli, A., Neduva,

V., Di Serio, C., Stupka, E., Gardner, J., von Kalle, C., Bordignon, C., Ciceri, F., Rovelli, A., Roncarolo, M.G., Aiuti, A., Sessa, M., and Naldini, L. (2013). Lentiviral hematopoietic stem cell gene therapy benefits metachromatic leukodystrophy. *Science* 341, 1233158.

15. Blazquez, A., Martin, M.A., Lara, M.C., Marti, R., Campos, Y., Cabello, A., Garesse, R., Bautista, J., Andreu, A.L., and Arenas, J. (2005). Increased muscle nucleoside levels associated with a novel frameshift mutation in the thymidine phosphorylase gene in a Spanish patient with MNGIE. *Neuromuscul Disord* 15, 775-778.

16. Blondon, H., Polivka, M., Joly, F., Flourie, B., Mikol, J., and Messing, B. (2005). Digestive smooth muscle mitochondrial myopathy in patients with mitochondrial-neuro-gastro-intestinal encephalomyopathy (MNGIE). *Gastroenterol Clin Biol* 29, 773-778.

17. Boschetti, E., D'Alessandro, R., Bianco, F., Carelli, V., Cenacchi, G., Pinna, A.D., Del Gaudio, M., Rinaldi, R., Stanghellini, V., Pironi, L., Rhoden, K., Tugnoli, V., Casali, C., and De Giorgio, R. (2014). Liver as a source for thymidine phosphorylase replacement in mitochondrial neurogastrointestinal encephalomyopathy. *PLoS One* 9, e96692.

18. Boztug, K., Schmidt, M., Schwarzer, A., Banerjee, P.P., Diez, I.A., Dewey, R.A., Bohm, M., Nowrouzi, A., Ball, C.R., Glimm, H., Naundorf, S., Kuhlcke, K., Blasczyk, R., Kondratenko, I., Marodi, L., Orange, J.S., von Kalle, C., and Klein, C. (2010). Stem-cell gene therapy for the Wiskott-Aldrich syndrome. *N Engl J Med* 363, 1918-1927.

19. Braun, C.J., Boztug, K., Paruzynski, A., Witzel, M., Schwarzer, A., Rothe, M., Modlich, U., Beier, R., Gohring, G., Steinemann, D., Fronza, R., Ball, C.R., Haemmerle, R., Naundorf, S., Kuhlcke, K., Rose, M., Fraser, C., Mathias, L., Ferrari, R., Abboud, M.R., Al-Herz, W., Kondratenko, I., Marodi, L., Glimm, H., Schlegelberger, B., Schambach, A., Albert, M.H., Schmidt, M., von Kalle, C., and Klein, C. (2014). Gene therapy for Wiskott-Aldrich syndrome--long-term efficacy and genotoxicity. *Sci Transl Med* 6,

227ra233. doi: 6/227/227ra33 [pii]10.1126/scitranslmed.3007280.

20. Burrow, T.A., Hopkin, R.J., Leslie, N.D., Tinkle, B.T., and Grabowski, G.A. (2007). Enzyme reconstitution/replacement therapy for lysosomal storage diseases. *Curr Opin Pediatr* 19, 628-635. doi: 10.1097/MOP.0b013e3282f161f2.

21. Camara, Y., Gonzalez-Vioque, E., Scarpelli, M., Torres-Torronteras, J., Caballero, A., Hirano, M., and Marti, R. (2014). Administration of deoxyribonucleosides or inhibition of their catabolism as a pharmacological approach for mitochondrial DNA depletion syndrome. *Hum Mol Genet* 23, 2459-2467.

22. Capotondo, A., Milazzo, R., Politi, L.S., Quattrini, A., Palini, A., Plati, T., Merella, S., Nonis, A., di Serio, C., Montini, E., Naldini, L., and Biffi, A. (2012). Brain conditioning is instrumental for successful microglia reconstitution following hematopoietic stem cell transplantation. *Proc Natl Acad Sci U S A* 109, 15018-15023.

23. Cardaioli, E., Da Pozzo, P., Malfatti, E., Battisti, C., Gallus, G.N., Gaudiano, C., Macucci, M., Malandrini, A., Margollicci, M., Rubegni, A., Dotti, M.T., and Federico, A. (2010). A second MNGIE patient without typical mitochondrial skeletal muscle involvement. *Neurol Sci* 31, 491-494.

24. Carlson, M.D. (2004). Recent advances in newborn screening for neurometabolic disorders. *Curr Opin Neurol* 17, 133-138.

25. Carod-Artal, F.J., Herrero, M.D., Lara, M.C., Lopez-Gallardo, E., Ruiz-Pesini, E., Marti, R., and Montoya, J. (2007). Cognitive dysfunction and hypogonadotrophic hypogonadism in a Brazilian patient with mitochondrial neurogastrointestinal encephalomyopathy and a novel ECGF1 mutation. *Eur J Neurol* 14, 581-585. doi: ENE1720 [pii]10.1111/j.1468-1331.2007.01720.x.

26. Cartier, N., Hacein-Bey-Abina, S., Bartholomae, C.C., Veres, G., Schmidt, M., Kutschera, I., Vidaud, M., Abel, U., Dal-Cortivo, L., Caccavelli, L., Mahlaoui, N., Kiermer, V., Mittelstaedt, D., Bellesme, C., Lahlou, N., Lefrere, F., Blanche, S., Audit, M., Payen, E., Leboulch, P., l'Homme,

B., Bougneres, P., Von Kalle, C., Fischer, A., Cavazzana-Calvo, M., and Aubourg, P. (2009). Hematopoietic stem cell gene therapy with a lentiviral vector in X-linked adrenoleukodystrophy. *Science* 326, 818-823.

27. Cattoglio, C., Facchini, G., Sartori, D., Antonelli, A., Miccio, A., Cassani, B., Schmidt, M., von Kalle, C., Howe, S., Thrasher, A.J., Aiuti, A., Ferrari, G., Recchia, A., and Mavilio, F. (2007). Hot spots of retroviral integration in human CD34+ hematopoietic cells. *Blood* 110, 1770-1778.

28. Celebi, N., Sahin, A., Canbay, O., Uzumcugil, F., and Aypar, U. (2006). Abdominal pain related to mitochondrial neurogastrointestinal encephalomyopathy syndrome may benefit from splanchnic nerve blockade. *Paediatr Anaesth* 16, 1073-1076.

29. Chapman, T.P., Hadley, G., Fratter, C., Cullen, S.N., Bax, B.E., Bain, M.D., Sapsford, R.A., Poulton, J., and Travis, S.P. (2014). Unexplained gastrointestinal symptoms: think mitochondrial disease. *Dig Liver Dis* 46, 1-8.

30. Chen, J., Larochelle, A., Fricker, S., Bridger, G., Dunbar, C.E., and Abkowitz, J.L. (2006). Mobilization as a preparative regimen for hematopoietic stem cell transplantation. *Blood* 107, 3764-3771.

31. De Giorgio, R., Pironi, L., Rinaldi, R., Boschetti, E., Caporali, L., Capristo, M., Casali, C., Cenacchi, G., Contin, M., D'Angelo, R., D'Errico, A., Gramegna, L.L., Lodi, R., Maresca, A., Mohamed, S., Morelli, M.C., Papa, V., Tonon, C., Tugnoli, V., Carelli, V., D'Alessandro, R., and Pinna, A.D. (2016). Liver transplantation for mitochondrial neurogastrointestinal encephalomyopathy. *Ann Neurol* 80, 448-455.

32. De Vocht, C., Ranquin, A., Willaert, R., Van Ginderachter, J.A., Vanhaecke, T., Rogiers, V., Versees, W., Van Gelder, P., and Steyaert, J. (2009). Assessment of stability, toxicity and immunogenicity of new polymeric nanoreactors for use in enzyme replacement therapy of MNGIE. *J Control Release* 137, 246-254.

33. Debouverie, M., Wagner, M., Ducrocq, X., Grignon, Y., Mousson, B., and Weber, M. (1997). [MNGIE syndrome in 2 siblings]

34. Le MNGIE syndrome: deux cas dans une meme fratrie. *Rev Neurol (Paris)* 153, 547-553.

35. Deichmann, A., Hacein-Bey-Abina, S., Schmidt, M., Garrigue, A., Brugman, M.H., Hu, J., Glimm, H., Gyapay, G., Prum, B., Fraser, C.C., Fischer, N., Schwarzwaelder, K., Siegler, M.L., de Ridder, D., Pike-Overzet, K., Howe, S.J., Thrasher, A.J., Wagemaker, G., Abel, U., Staal, F.J., Delabesse, E., Villeval, J.L., Aronow, B., Hue, C., Prinz, C., Wissler, M., Klanke, C., Weissenbach, J., Alexander, I., Fischer, A., von Kalle, C., and Cavazzana-Calvo, M. (2007). Vector integration is nonrandom and clustered and influences the fate of lymphopoiesis in SCID-X1 gene therapy. *J Clin Invest* 117, 2225-2232.

36. Di Meo, I., Lamperti, C., and Tiranti, V. (2015). Mitochondrial diseases caused by toxic compound accumulation: from etiopathology to therapeutic approaches. *EMBO Mol Med* 7, 1257-1266. doi: 10.15252/emmm.201505040emmm.201505040 [pii].

37. DiMauro, S. (2004). Mitochondrial diseases. *Biochim Biophys Acta* 1658, 80-88.

38. Dull, T., Zufferey, R., Kelly, M., Mandel, R.J., Nguyen, M., Trono, D., and Naldini, L. (1998). A third-generation lentivirus vector with a conditional packaging system. *J Virol* 72, 8463-8471.

39. El-Hattab, A.W., and Scaglia, F. (2013). Mitochondrial DNA depletion syndromes: review and updates of genetic basis, manifestations, and therapeutic options. *Neurotherapeutics* 10, 186-198.

40. Etienne, G., Shamseddine, K., Pulley, M., and Milfred, F. (2012). Two new gene mutations for late onset mitochondrial neurogastrointestinal encephalopathy (MNGIE). *Translational Neuroscience* 3, 413-414. doi: 10.2478/s13380-012-0042-9.

41. Fairbanks, L.D., Marinaki, A.M., Carrey, E.A., Hammans, S.R., and Duley, J.A. (2002). Deoxyuridine accumulation in urine in thymidine phosphorylase deficiency (MNGIE). *J Inherit Metab Dis* 25, 603-604.

42. Finkenstedt, A., Schranz, M., Bosch, S., Karall, D., Burgi, S.S., Ensinger, C., Drach,

M., Mayr, J.A., Janecke, A.R., Vogel, W., Nachbaur, D., and Zoller, H. (2013). MNGIE Syndrome: Liver Cirrhosis Should Be Ruled Out Prior to Bone Marrow Transplantation. *JIMD Rep* 10, 41-44.

43. Fox, S.B., Moghaddam, A., Westwood, M., Turley, H., Bicknell, R., Gatter, K.C., and Harris, A.L. (1995). Platelet-derived endothelial cell growth factor/thymidine phosphorylase expression in normal tissues: an immunohistochemical study. *J Pathol* 176, 183-190.

44. Friedkin, M., and Roberts, D. (1954). The enzymatic synthesis of nucleosides. I. Thymidine phosphorylase in mammalian tissue. *J Biol Chem* 207, 245-256.

45. Fukami, M.H., and Salganicoff, L. (1973). Isolation and properties of human platelet mitochondria. *Blood* 42, 913-918.

46. Gabriel, R., Schmidt, M., and von Kalle, C. (2012). Integration of retroviral vectors. *Curr Opin Immunol* 24, 592-597.

47. Gamez, J., Lara, M.C., Mearin, F., Oliveras-Ley, C., Raguer, N., Olive, M., Leist, A.T., Perello, A., Perona, M., Cervera, C., Andreu, A.L., Marti, R., and Hirano, M. (2005). A novel thymidine phosphorylase mutation in a Spanish MNGIE patient. *J Neurol Sci* 228, 35-39.

48. Garcia-Diaz, B., Garone, C., Barca, E., Mojahed, H., Gutierrez, P., Pizzorno, G., Tanji, K., Arias-Mendoza, F., Quinzii, C.M., and Hirano, M. (2014). Deoxynucleoside stress exacerbates the phenotype of a mouse model of mitochondrial neurogastrointestinal encephalopathy. *Brain* 137, 1337-1349.

49. Garone, C., Tadesse, S., and Hirano, M. (2011). Clinical and genetic spectrum of mitochondrial neurogastrointestinal encephalomyopathy. *Brain* 134, 3326-3332.

50. Gaspar, H.B., Parsley, K.L., Howe, S., King, D., Gilmour, K.C., Sinclair, J., Brouns, G., Schmidt, M., Von Kalle, C., Barington, T., Jakobsen, M.A., Christensen, H.O., Al Ghonaium, A., White, H.N., Smith, J.L., Levinsky, R.J., Ali, R.R., Kinnon, C., and Thrasher, A.J. (2004). Gene therapy of X-linked severe combined immunodeficiency by use of a pseudotyped gammaretroviral vector. *Lancet* 364, 2181-2187.

51. Giordano, C., Sebastiani, M., De Giorgio, R., Travaglini, C., Tancredi, A., Valentino, M.L., Bellan, M., Cossarizza, A., Hirano, M., d'Amati, G., and Carelli, V. (2008). Gastrointestinal dysmotility in mitochondrial neurogastrointestinal encephalomyopathy is caused by mitochondrial DNA depletion. *Am J Pathol* 173, 1120-1128.

52. Giordano, C., Sebastiani, M., Plazzi, G., Travaglini, C., Sale, P., Pinti, M., Tancredi, A., Liguori, R., Montagna, P., Bellan, M., Valentino, M.L., Cossarizza, A., Hirano, M., d'Amati, G., and Carelli, V. (2006). Mitochondrial neurogastrointestinal encephalomyopathy: evidence of mitochondrial DNA depletion in the small intestine. *Gastroenterology* 130, 893-901. doi: S0016-5085(06)00005-9 [pii]10.1053/j.gastro.2006.01.004.

53. Goffart, S., Cooper, H.M., Tyynismaa, H., Wanrooij, S., Suomalainen, A., and Spelbrink, J.N. (2009). Twinkle mutations associated with autosomal dominant progressive external ophthalmoplegia lead to impaired helicase function and in vivo mtDNA replication stalling. *Hum Mol Genet* 18, 328-340.

54. Gonzalez-Vioque, E., Torres-Torronteras, J., Andreu, A.L., and Marti, R. (2011). Limited dCTP availability accounts for mitochondrial DNA depletion in mitochondrial neurogastrointestinal encephalomyopathy (MNGIE). *PLoS Genet* 7, e1002035.

55. Granero Castro, P., Fernandez Arias, S., Moreno Gijon, M., Alvarez Martinez, P., Granero Trancon, J., Alvarez Perez, J.A., Lamamie Clairac, E., and Gonzalez Gonzalez, J.J. (2010). Emergency surgery in chronic intestinal pseudo-obstruction due to mitochondrial neurogastrointestinal encephalomyopathy: case reports. *Int Arch Med* 3, 35.

56. Guenechea, G., Gan, O.I., Inamitsu, T., Dorrell, C., Pereira, D.S., Kelly, M., Naldini, L., and Dick, J.E. (2000). Transduction of human CD34+ CD38- bone marrow and

cord blood-derived SCID-repopulating cells with third-generation lentiviral vectors. *Mol Ther* 1, 566-573.

57. Hacein-Bey-Abina, S., Garrigue, A., Wang, G.P., Soulier, J., Lim, A., Morillon, E., Clappier, E., Caccavelli, L., Delabesse, E., Beldjord, K., Asnafi, V., MacIntyre, E., Dal Cortivo, L., Radford, I., Brousse, N., Sigaux, F., Moshous, D., Hauer, J., Borkhardt, A., Belohradsky, B.H., Wintergerst, U., Velez, M.C., Leiva, L., Sorensen, R., Wulffraat, N., Blanche, S., Bushman, F.D., Fischer, A., and Cavazzana-Calvo, M. (2008). Insertional oncogenesis in 4 patients after retrovirus-mediated gene therapy of SCID-X1. *J Clin Invest* 118, 3132-3142. doi: 10.1172/JCI35700.

58. Hacein-Bey-Abina, S., Hauer, J., Lim, A., Picard, C., Wang, G.P., Berry, C.C., Martinache, C., Rieux-Laucat, F., Latour, S., Belohradsky, B.H., Leiva, L., Sorensen, R., Debre, M., Casanova, J.L., Blanche, S., Durandy, A., Bushman, F.D., Fischer, A., and Cavazzana-Calvo, M. (2010). Efficacy of gene therapy for X-linked severe combined immunodeficiency. *N Engl J Med* 363, 355-364.

59. Hacein-Bey-Abina, S., von Kalle, C., Schmidt, M., Le Deist, F., Wulffraat, N., McIntyre, E., Radford, I., Villeval, J.L., Fraser, C.C., Cavazzana-Calvo, M., and Fischer, A. (2003a). A serious adverse event after successful gene therapy for X-linked severe combined immunodeficiency. *N Engl J Med* 348, 255-256. doi: 10.1056/nejm200301163480314.

60. Hacein-Bey-Abina, S., Von Kalle, C., Schmidt, M., McCormack, M.P., Wulffraat, N., Leboulch, P., Lim, A., Osborne, C.S., Pawliuk, R., Morillon, E., Sorensen, R., Forster, A., Fraser, P., Cohen, J.I., de Saint Basile, G., Alexander, I., Wintergerst, U., Frebourg, T., Aurias, A., Stoppa-Lyonnet, D., Romana, S., Radford-Weiss, I., Gross, F., Valensi, F., Delabesse, E., Macintyre, E., Sigaux, F., Soulier, J., Leiva, L.E., Wissler, M., Prinz, C., Rabbitts, T.H., Le Deist, F., Fischer, A., and Cavazzana-Calvo, M. (2003b). LMO2-associated clonal T cell proliferation in two patients after gene therapy for SCID-X1. *Science* 302, 415-419.

61. Halter, J., Schupbach, W.M., Casali, C., Elhasid, R., Fay, K., Hammans, S., Illa, I., Kappeler, L., Krahenbuhl, S., Lehmann, T., Mandel, H., Marti, R., Mattle, H., Orchard, K., Savage, D., Sue, C.M., Valcarcel, D., Gratwohl, A., and Hirano, M. (2011). Allogeneic hematopoietic SCT as treatment option for patients with mitochondrial neurogastrointestinal encephalomyopathy (MNGIE): a consensus conference proposal for a standardized approach. *Bone Marrow Transplant* 46, 330-337.

62. Halter, J.P., Michael, W., Schupbach, M., Mandel, H., Casali, C., Orchard, K., Collin, M., Valcarcel, D., Rovelli, A., Filosto, M., Dotti, M.T., Marotta, G., Pintos, G., Barba, P., Accarino, A., Ferra, C., Illa, I., Beguin, Y., Bakker, J.A., Boelens, J.J., de Coo, I.F., Fay, K., Sue, C.M., Nachbaur, D., Zoller, H., Sobreira, C., Pinto Simoes, B., Hammans, S.R., Savage, D., Marti, R., Chinnery, P.F., Elhasid, R., Gratwohl, A., and Hirano, M. (2015). Allogeneic haematopoietic stem cell transplantation for mitochondrial neurogastrointestinal encephalomyopathy. *Brain* 138, 2847-2858. doi: 10.1093/brain/awv226awv226 [pii].

63. Haraguchi, M., Tsujimoto, H., Fukushima, M., Higuchi, I., Kuribayashi, H., Utsumi, H., Nakayama, A., Hashizume, Y., Hirato, J., Yoshida, H., Hara, H., Hamano, S., Kawaguchi, H., Furukawa, T., Miyazono, K., Ishikawa, F., Toyoshima, H., Kaname, T., Komatsu, M., Chen, Z.S., Gotanda, T., Tachiwada, T., Sumizawa, T., Miyadera, K., Osame, M., Yoshida, H., Noda, T., Yamada, Y., and Akiyama, S. (2002). Targeted deletion of both thymidine phosphorylase and uridine phosphorylase and consequent disorders in mice. *Mol Cell Biol* 22, 5212-5221.

64. Hirano, M., Marti, R., Ferreiro-Barros, C., Vila, M.R., Tadesse, S., Nishigaki, Y., Nishino, I., and Vu, T.H. (2001). Defects of intergenomic communication: autosomal disorders that cause multiple deletions and depletion of mitochondrial DNA. *Semin Cell Dev Biol* 12, 417-427.

65. Hirano, M., Nishigaki, Y., and Marti, R. (2004). Mitochondrial neurogastrointestinal

encephalomyopathy (MNGIE): a disease of two genomes. *Neurologist* 10**,** 8-17.

66. Hirano, M., Silvestri, G., Blake, D.M., Lombes, A., Minetti, C., Bonilla, E., Hays, A.P., Lovelace, R.E., Butler, I., Bertorini, T.E., and et al. (1994). Mitochondrial neurogastrointestinal encephalomyopathy (MNGIE): clinical, biochemical, and genetic features of an autosomal recessive mitochondrial disorder. *Neurology* 44**,** 721-727.

67. Howe, S.J., Mansour, M.R., Schwarzwaelder, K., Bartholomae, C., Hubank, M., Kempski, H., Brugman, M.H., Pike-Overzet, K., Chatters, S.J., de Ridder, D., Gilmour, K.C., Adams, S., Thornhill, S.I., Parsley, K.L., Staal, F.J., Gale, R.E., Linch, D.C., Bayford, J., Brown, L., Quaye, M., Kinnon, C., Ancliff, P., Webb, D.K., Schmidt, M., von Kalle, C., Gaspar, H.B., and Thrasher, A.J. (2008). Insertional mutagenesis combined with acquired somatic mutations causes leukemogenesis following gene therapy of SCID-X1 patients. *J Clin Invest* 118**,** 3143-3150.

68. Huston, M.W., Riegman, A.R., Yadak, R., van Helsdingen, Y., de Boer, H., van Til, N.P., and Wagemaker, G. (2014). Pretransplant mobilization with granulocyte colony-stimulating factor improves B-cell reconstitution by lentiviral vector gene therapy in SCID-X1 mice. *Hum Gene Ther* 25**,** 905-914. doi: 10.1089/hum.2014.101.

69. Ikeguchi, M., Sakatani, T., Ueda, T., Hirooka, Y., and Kaibara, N. (2001). Thymidine phosphorylase activity in liver tissue and its correlation with multifocal occurrence of hepatocellular carcinomas. *In Vivo* 15**,** 265-270.

70. Kalkan, I.H., Koksal, A.S., Evcimen, S., Sapmaz, F., Oztas, E., Onder, F.O., and Guliter, S. (2015). Spontaneous abdominal esophageal perforation in a patient with mitochondrial neurogastrointestinal encephalomyopathy. *Acta Clin Belg* 70**,** 44-45.

71. Kocaefe, Y.C., Erdem, S., Ozguc, M., and Tan, E. (2003). Four novel thymidine phosphorylase gene mutations in mitochondrial neurogastrointestinal encephalomyopathy syndrome (MNGIE) patients. *Eur J Hum Genet* 11**,** 102-104.

72. Koukourakis, M.I., Giatromanolaki, A., O'Byrne, K.J., Comley, M., Whitehouse, R.M., Talbot, D.C., Gatter, K.C., and Harris, A.L. (1997). Platelet-derived endothelial cell growth factor expression correlates with tumour angiogenesis and prognosis in non-small-cell lung cancer. *Br J Cancer* 75**,** 477-481.

73. Kumar, D., Viberg, J., Nilsson, A.K., and Chabes, A. (2010). Highly mutagenic and severely imbalanced dNTP pools can escape detection by the S-phase checkpoint. *Nucleic Acids Res* 38**,** 3975-3983. doi: 10.1093/nar/gkq128.

74. la Marca, G., Malvagia, S., Casetta, B., Pasquini, E., Pela, I., Hirano, M., Donati, M.A., and Zammarchi, E. (2006). Pre- and post-dialysis quantitative dosage of thymidine in urine and plasma of a MNGIE patient by using HPLC-ESI-MS/MS. *J Mass Spectrom* 41**,** 586-592.

75. Lara, M.C., Valentino, M.L., Torres-Torronteras, J., Hirano, M., and Marti, R. (2007). Mitochondrial neurogastrointestinal encephalomyopathy (MNGIE): biochemical features and therapeutic approaches. *Biosci Rep* 27**,** 151-163.

76. Levene, M., Coleman, D.G., Kilpatrick, H.C., Fairbanks, L.D., Gangadharan, B., Gasson, C., and Bax, B.E. (2013). Preclinical toxicity evaluation of erythrocyte-encapsulated thymidine phosphorylase in BALB/c mice and beagle dogs: an enzyme-replacement therapy for mitochondrial neurogastrointestinal encephalomyopathy. *Toxicol Sci* 131**,** 311-324.

77. Li, J.N., Han, D.Y., Ji, F., Chen, A.T., Wu, N., Xi, X., Shen, W.D., and Yang, S.M. (2011). Successful cochlear implantation in a patient with MNGIE syndrome. *Acta Otolaryngol* 131**,** 1012-1016.

78. Liu, Z., Ding, Y., Du, A., Zhang, B., Zhao, G., and Ding, M. (2008). A novel Twinkle (PEO1) gene mutation in a Chinese family with adPEO. *Mol Vis* 14**,** 1995-2001.

79. Lopez, L.C., Akman, H.O., Garcia-Cazorla, A., Dorado, B., Marti, R., Nishino, I., Tadesse, S., Pizzorno, G., Shungu, D., Bonilla, E., Tanji, K., and Hirano, M. (2009). Unbalanced deoxynucleotide pools cause mitochondrial

2

DNA instability in thymidine phosphorylase-deficient mice. *Hum Mol Genet* 18**,** 714-722.

80. Manno, C.S., Pierce, G.F., Arruda, V.R., Glader, B., Ragni, M., Rasko, J.J., Ozelo, M.C., Hoots, K., Blatt, P., Konkle, B., Dake, M., Kaye, R., Razavi, M., Zajko, A., Zehnder, J., Rustagi, P.K., Nakai, H., Chew, A., Leonard, D., Wright, J.F., Lessard, R.R., Sommer, J.M., Tigges, M., Sabatino, D., Luk, A., Jiang, H., Mingozzi, F., Couto, L., Ertl, H.C., High, K.A., and Kay, M.A. (2006). Successful transduction of liver in hemophilia by AAV-Factor IX and limitations imposed by the host immune response. *Nat Med* 12**,** 342-347. doi: nm1358 [pii]10.1038/nm1358.

81. Mariana Ponte Cardoso, R., Armanda Emanuela Castro e, S., and José Barata Antunes, C. (2015). *Mitochondrial Dysfunction on the Toxic Effects of Anticancer Agents— From Lab Bench to Bedside.*

82. Marti, R., Spinazzola, A., Tadesse, S., Nishino, I., Nishigaki, Y., and Hirano, M. (2004). Definitive diagnosis of mitochondrial neurogastrointestinal encephalomyopathy by biochemical assays. *Clin Chem* 50**,** 120-124.

83. Marti, R., Verschuuren, J.J., Buchman, A., Hirano, I., Tadesse, S., van Kuilenburg, A.B., van Gennip, A.H., Poorthuis, B.J., and Hirano, M. (2005). Late-onset MNGIE due to partial loss of thymidine phosphorylase activity. *Ann Neurol* 58**,** 649-652.

84. Martin, M.A., Blazquez, A., Marti, R., Bautista, J., Lara, M.C., Cabello, A., Campos, Y., Belda, O., Andreu, A.L., and Arenas, J. (2004). Lack of gastrointestinal symptoms in a 60-year-old patient with MNGIE. *Neurology* 63**,** 1536-1537.

85. Massa, R., Tessa, A., Margollicci, M., Micheli, V., Romigi, A., Tozzi, G., Terracciano, C., Piemonte, F., Bernardi, G., and Santorelli, F.M. (2009). Late-onset MNGIE without peripheral neuropathy due to incomplete loss of thymidine phosphorylase activity. *Neuromuscul Disord* 19**,** 837-840.

86. Mattman, A., Sirrs, S., Mezei, M.M., Salvarinova-Zivkovic, R., Alfadhel, M., and Lillquist, Y. (2011). Mitochondrial disease clinical manifestations: An overview. *British Columbia Medical Journal* 53.

87. McHugh, D., Cameron, C.A., Abdenur, J.E., Abdulrahman, M., Adair, O., Al Nuaimi, S.A., Ahlman, H., Allen, J.J., Antonozzi, I., Archer, S., Au, S., Auray-Blais, C., Baker, M., Bamforth, F., Beckmann, K., Pino, G.B., Berberich, S.L., Binard, R., Boemer, F., Bonham, J., Breen, N.N., Bryant, S.C., Caggana, M., Caldwell, S.G., Camilot, M., Campbell, C., Carducci, C., Bryant, S.C., Caggana, M., Caldwell, S.G., Camilot, M., Campbell, C., Carducci, C., Cariappa, R., Carlisle, C., Caruso, U., Cassanello, M., Castilla, A.M., Ramos, D.E., Chakraborty, P., Chandrasekar, R., Ramos, A.C., Cheillan, D., Chien, Y.H., Childs, T.A., Chrastina, P., Sica, Y.C., de Juan, J.A., Colandre, M.E., Espinoza, V.C., Corso, G., Currier, R., Cyr, D., Czuczy, N., D'Apolito, O., Davis, T., de Sain-Van der Velden, M.G., Delgado Pecellin, C., Di Gangi, I.M., Di Stefano, C.M., Dotsikas, Y., Downing, M., Downs, S.M., Dy, B., Dymerski, M., Rueda, I., Elvers, B., Eaton, R., Eckerd, B.M., El Mougy, F., Eroh, S., Espada, M., Evans, C., Fawbush, S., Fijolek, K.F., Fisher, L., Franzson, L., Frazier, D.M., Garcia, L.R., Bermejo, M.S., Gavrilov, D., Gerace, R., Giordano, G., Irazabal, Y.G., Greed, L.C., Grier, R., Grycki, E., Gu, X., Gulamali-Majid, F., Hagar, A.F., Han, L., Hannon, W.H., Haslip, C., Hassan, F.A., He, M., Hietala, A., Himstedt, L., Hoffman, G.L., Hoffman, W., Hoggatt, P., et al. (2011). Clinical validation of cutoff target ranges in newborn screening of metabolic disorders by tandem mass spectrometry: a worldwide collaborative project. *Genet Med* 13**,** 230-254.

88. Menezes, M.P., and Ouvrier, R.A. (2012). Peripheral neuropathy associated with mitochondrial disease in children. *Dev Med Child Neurol* 54**,** 407-414.

89. Millar, W.S., Lignelli, A., and Hirano, M. (2004). MRI of five patients with mitochondrial neurogastrointestinal encephalomyopathy. *AJR Am J Roentgenol* 182**,** 1537-1541. doi: 10.2214/ajr.182.6.1821537.

90. Mingozzi, F., and High, K.A. (2013). Immune responses to AAV vectors: overcoming

barriers to successful gene therapy. *Blood* 122, 23-36. doi: blood-2013-01-306647 [pii]10.1182/blood-2013-01-306647.

91. Mitselou, A., Ioachim, E., Skoufi, U., Tsironis, C., Tsimogiannis, K.E., Skoufi, C., Vougiouklakis, T., and Briasoulis, E. (2012). Predictive role of thymidine phosphorylase expression in patients with colorectal cancer and its association with angiogenesis-related proteins and extracellular matrix components. *In Vivo* 26, 1057-1067.

92. Modlich, U., Navarro, S., Zychlinski, D., Maetzig, T., Knoess, S., Brugman, M.H., Schambach, A., Charrier, S., Galy, A., Thrasher, A.J., Bueren, J., and Baum, C. (2009). Insertional transformation of hematopoietic cells by self-inactivating lentiviral and gammaretroviral vectors. *Mol Ther* 17, 1919-1928. doi: 10.1038/mt.2009.179.

93. Montini, E., Cesana, D., Schmidt, M., Sanvito, F., Ponzoni, M., Bartholomae, C., Sergi Sergi, L., Benedicenti, F., Ambrosi, A., Di Serio, C., Doglioni, C., von Kalle, C., and Naldini, L. (2006). Hematopoietic stem cell gene transfer in a tumor-prone mouse model uncovers low genotoxicity of lentiviral vector integration. *Nat Biotechnol* 24, 687-696. doi: 10.1038/nbt1216.

94. Moran, N.F., Bain, M.D., Muqit, M.M., and Bax, B.E. (2008). Carrier erythrocyte entrapped thymidine phosphorylase therapy for MNGIE. *Neurology* 71, 686-688.

95. Mori, K., Hasegawa, M., Nishida, M., Toma, H., Fukuda, M., Kubota, T., Nagasue, N., Yamana, H., Hirakawa, Y.S.C.K., Ikeda, T., Takasaki, K., Oka, M., Kameyama, M., Toi, M., Fujii, H., Kitamura, M., Murai, M., Sasaki, H., Ozono, S., Makuuchi, H., Shimada, Y., Onishi, Y., Aoyagi, S., Mizutani, K., Ogawa, M., Nakao, A., Kinoshita, H., Tono, T., Imamoto, H., Nakashima, Y., and Manabe, T. (2000). Expression levels of thymidine phosphorylase and dihydropyrimidine dehydrogenase in various human tumor tissues. *Int J Oncol* 17, 33-38.

96. Nakai, H., Fuess, S., Storm, T.A., Muramatsu, S., Nara, Y., and Kay, M.A. (2005). Unrestricted hepatocyte transduction with adeno-associated virus serotype 8 vectors in mice. *J Virol* 79, 214-224. doi: 79/1/214 [pii]10.1128/JVI.79.1.214-224.2005.

97. Nakayama, Y., Inoue, Y., Nagashima, N., Katsuki, T., Matsumoto, K., Kadowaki, K., Shibao, K., Tsurudome, Y., Hirata, K., Sako, T., Nagata, N., and Itoh, H. (2005). Expression levels of thymidine phosphorylase (TP) and dihydropyrimidine dehydrogenase (DPD) in patients with gastrointestinal cancer. *Anticancer Res* 25, 3755-3761.

98. Naldini, L. (2015). Gene therapy returns to centre stage. *Nature* 526, 351-360. doi: nature15818 [pii]10.1038/nature15818.

99. Naldini, L., Blomer, U., Gallay, P., Ory, D., Mulligan, R., Gage, F.H., Verma, I.M., and Trono, D. (1996). In vivo gene delivery and stable transduction of nondividing cells by a lentiviral vector. *Science* 272, 263-267.

100. Nathwani, A.C., Gray, J.T., Ng, C.Y., Zhou, J., Spence, Y., Waddington, S.N., Tuddenham, E.G., Kemball-Cook, G., McIntosh, J., Boon-Spijker, M., Mertens, K., and Davidoff, A.M. (2006). Self-complementary adeno-associated virus vectors containing a novel liver-specific human factor IX expression cassette enable highly efficient transduction of murine and nonhuman primate liver. *Blood* 107, 2653-2661. doi: 2005-10-4035 [pii]10.1182/blood-2005-10-4035.

101. Nathwani, A.C., Reiss, U.M., Tuddenham, E.G., Rosales, C., Chowdary, P., McIntosh, J., Della Peruta, M., Lheriteau, E., Patel, N., Raj, D., Riddell, A., Pie, J., Rangarajan, S., Bevan, D., Recht, M., Shen, Y.M., Halka, K.G., Basner-Tschakarjan, E., Mingozzi, F., High, K.A., Allay, J., Kay, M.A., Ng, C.Y., Zhou, J., Cancio, M., Morton, C.L., Gray, J.T., Srivastava, D., Nienhuis, A.W., and Davidoff, A.M. (2014). Long-term safety and efficacy of factor IX gene therapy in hemophilia B. *N Engl J Med* 371, 1994-2004. doi: 10.1056/NEJMoa1407309.

102. Negre, O., Bartholomae, C., Beuzard, Y., Cavazzana, M., Christiansen, L., Courne, C., Deichmann, A., Denaro, M., de Dreuzy, E., Finer, M., Fronza, R., Gillet-Legrand, B., Joubert, C., Kutner, R., Leboulch, P., Maouche, L., Paulard, A., Pierciey, F.J., Rothe, M., Ryu, B.,

2

Schmidt, M., von Kalle, C., Payen, E., and Veres, G. (2015). Preclinical evaluation of efficacy and safety of an improved lentiviral vector for the treatment of beta-thalassemia and sickle cell disease. *Curr Gene Ther* 15**,** 64-81.

103. Nishigaki, Y., Marti, R., Copeland, W.C., and Hirano, M. (2003). Site-specific somatic mitochondrial DNA point mutations in patients with thymidine phosphorylase deficiency. *J Clin Invest* 111**,** 1913-1921.

104. Nishino, I., Spinazzola, A., and Hirano, M. (1999). Thymidine phosphorylase gene mutations in MNGIE, a human mitochondrial disorder. *Science* 283**,** 689-692.

105. Nishino, I., Spinazzola, A., Papadimitriou, A., Hammans, S., Steiner, I., Hahn, C.D., Connolly, A.M., Verloes, A., Guimaraes, J., Maillard, I., Hamano, H., Donati, M.A., Semrad, C.E., Russell, J.A., Andreu, A.L., Hadjigeorgiou, G.M., Vu, T.H., Tadesse, S., Nygaard, T.G., Nonaka, I., Hirano, I., Bonilla, E., Rowland, L.P., DiMauro, S., and Hirano, M. (2000). Mitochondrial neurogastrointestinal encephalomyopathy: an autosomal recessive disorder due to thymidine phosphorylase mutations. *Ann Neurol* 47**,** 792-800.

106. Okamura, K., Santa, T., Nagae, K., and Omae, T. (1976). Congenital oculoskeletal myopathy with abnormal muscle and liver mitochondria. *J Neurol Sci* 27**,** 79-91.

107. Oliver, F.J., Collins, M.K., and Lopez-Rivas, A. (1996). dNTP pools imbalance as a signal to initiate apoptosis. *Experientia* 52**,** 995-1000.

108. Ott, M.G., Schmidt, M., Schwarzwaelder, K., Stein, S., Siler, U., Koehl, U., Glimm, H., Kuhlcke, K., Schilz, A., Kunkel, H., Naundorf, S., Brinkmann, A., Deichmann, A., Fischer, M., Ball, C., Pilz, I., Dunbar, C., Du, Y., Jenkins, N.A., Copeland, N.G., Luthi, U., Hassan, M., Thrasher, A.J., Hoelzer, D., von Kalle, C., Seger, R., and Grez, M. (2006). Correction of X-linked chronic granulomatous disease by gene therapy, augmented by insertional activation of MDS1-EVI1, PRDM16 or SETBP1. *Nat Med* 12**,** 401-409. doi: 10.1038/nm1393.

109. Palchaudhuri, R., Saez, B., Hoggatt, J., Schajnovitz, A., Sykes, D.B., Tate, T.A., Czechowicz, A., Kfoury, Y., Ruchika, F., Rossi, D.J., Verdine, G.L., Mansour, M.K., and Scadden, D.T. (2016). Non-genotoxic conditioning for hematopoietic stem cell transplantation using a hematopoietic-cell-specific internalizing immunotoxin. *Nat Biotechnol* 34**,** 738-745.

110. Papadimitriou, A., Comi, G.P., Hadjigeorgiou, G.M., Bordoni, A., Sciacco, M., Napoli, L., Prelle, A., Moggio, M., Fagiolari, G., Bresolin, N., Salani, S., Anastasopoulos, I., Giassakis, G., Divari, R., and Scarlato, G. (1998). Partial depletion and multiple deletions of muscle mtDNA in familial MNGIE syndrome. *Neurology* 51**,** 1086-1092.

111. Perez-Atayde, A.R., Fox, V., Teitelbaum, J.E., Anthony, D.A., Fadic, R., Kalsner, L., Rivkin, M., Johns, D.R., and Cox, G.F. (1998). Mitochondrial neurogastrointestinal encephalomyopathy: diagnosis by rectal biopsy. *Am J Surg Pathol* 22**,** 1141-1147.

112. Pfeffer, G., Horvath, R., Klopstock, T., Mootha, V.K., Suomalainen, A., Koene, S., Hirano, M., Zeviani, M., Bindoff, L.A., Yu-Wai-Man, P., Hanna, M., Carelli, V., McFarland, R., Majamaa, K., Turnbull, D.M., Smeitink, J., and Chinnery, P.F. (2013). New treatments for mitochondrial disease-no time to drop our standards. *Nat Rev Neurol* 9**,** 474-481. doi: 10.1038/ nrneurol.2013.129nrneurol.2013.129 [pii].

113. Pontarin, G., Ferraro, P., Valentino, M.L., Hirano, M., Reichard, P., and Bianchi, V. (2006). Mitochondrial DNA depletion and thymidine phosphate pool dynamics in a cellular model of mitochondrial neurogastrointestinal encephalomyopathy. *J Biol Chem* 281**,** 22720-22728.

114. Psatha, N., Karponi, G., and Yannaki, E. (2016). Optimizing autologous cell grafts to improve stem cell gene therapy. *Exp Hematol* 44**,** 528-539.

115. Pupe, C., Nascimento, O.J., Quintanilha, G., Freitas, M.R., Uchoa, E., Matta, A.P., Dib, J.G., and Escada, T. (2012). Mitochondrial neurogastrointestinal encephalomyopathy mimicking chronic inflammatory demyelinating polyradiculoneuropathy. *Arq Neuropsiquiatr* 70**,** 228-229.

116. Rickards, H., Prendergast, M., and Booth, I.W. (1994). Psychiatric presentation of Crohn's disease. Diagnostic delay and increased morbidity. *Br J Psychiatry* 164, 256-261.

117. Romero, Z., Urbinati, F., Geiger, S., Cooper, A.R., Wherley, J., Kaufman, M.L., Hollis, R.P., de Assin, R.R., Senadheera, S., Sahagian, A., Jin, X., Gellis, A., Wang, X., Gjertson, D., Deoliveira, S., Kempert, P., Shupien, S., Abdel-Azim, H., Walters, M.C., Meiselman, H.J., Wenby, R.B., Gruber, T., Marder, V., Coates, T.D., and Kohn, D.B. (2013). beta-globin gene transfer to human bone marrow for sickle cell disease. *J Clin Invest*. doi: 10.1172/jci67930.

118. Salsano, E., Farina, L., Lamperti, C., Piscosquito, G., Salerno, F., Morandi, L., Carrara, F., Lamantea, E., Zeviani, M., Uziel, G., Savoiardo, M., and Pareyson, D. (2013). Adult-onset leukodystrophies from respiratory chain disorders: do they exist? *J Neurol* 260, 1617-1623. doi: 10.1007/s00415-013-6844-z.

119. Scaglia, F., Wong, L.J., Vladutiu, G.D., and Hunter, J.V. (2005). Predominant cerebellar volume loss as a neuroradiologic feature of pediatric respiratory chain defects. *AJNR Am J Neuroradiol* 26, 1675-1680. doi: 26/7/1675 [pii].

120. Scarpelli, M., Ricciardi, G.K., Beltramello, A., Zocca, I., Calabria, F., Russignan, A., Zappini, F., Cotelli, M.S., Padovani, A., Tomelleri, G., Filosto, M., and Tonin, P. (2013). The role of brain MRI in mitochondrial neurogastrointestinal encephalomyopathy. *Neuroradiol J* 26, 520-530.

121. Schiffmann, R., and van der Knaap, M.S. (2009). Invited article: an MRI-based approach to the diagnosis of white matter disorders. *Neurology* 72, 750-759. doi: 10.1212/01.wnl.0000343049.00540.c872/8/750 [pii].

122. Schupbach, W.M., Vadday, K.M., Schaller, A., Brekenfeld, C., Kappeler, L., Benoist, J.F., Xuan-Huong, C.N., Burgunder, J.M., Seibold, F., Gallati, S., and Mattle, H.P. (2007). Mitochondrial neurogastrointestinal encephalomyopathy in three siblings: clinical, genetic and neuroradiological features. *J Neurol* 254, 146-153. doi: 10.1007/s00415-006-0255-3.

123. Shaw, T., Smillie, R.H., Miller, A.E., and MacPhee, D.G. (1988). The role of blood platelets in nucleoside metabolism: regulation of platelet thymidine phosphorylase. *Mutat Res* 200, 117-131.

124. Simon, L.T., Horoupian, D.S., Dorfman, L.J., Marks, M., Herrick, M.K., Wasserstein, P., and Smith, M.E. (1990). Polyneuropathy, ophthalmoplegia, leukoencephalopathy, and intestinal pseudo-obstruction: POLIP syndrome. *Ann Neurol* 28, 349-360.

125. Song, S., Wheeler, L.J., and Mathews, C.K. (2003). Deoxyribonucleotide pool imbalance stimulates deletions in HeLa cell mitochondrial DNA. *J Biol Chem* 278, 43893-43896.

126. Spinazzola, A., Marti, R., Nishino, I., Andreu, A.L., Naini, A., Tadesse, S., Pela, I., Zammarchi, E., Donati, M.A., Oliver, J.A., and Hirano, M. (2002). Altered thymidine metabolism due to defects of thymidine phosphorylase. *J Biol Chem* 277, 4128-4133.

127. Stein, S., Ott, M.G., Schultze-Strasser, S., Jauch, A., Burwinkel, B., Kinner, A., Schmidt, M., Kramer, A., Schwable, J., Glimm, H., Koehl, U., Preiss, C., Ball, C., Martin, H., Gohring, G., Schwarzwaelder, K., Hofmann, W.K., Karakaya, K., Tchatchou, S., Yang, R., Reinecke, P., Kuhlcke, K., Schlegelberger, B., Thrasher, A.J., Hoelzer, D., Seger, R., von Kalle, C., and Grez, M. (2010). Genomic instability and myelodysplasia with monosomy 7 consequent to EVI1 activation after gene therapy for chronic granulomatous disease. *Nat Med* 16, 198-204.

128. Stenman, G., Sahlin, P., Dumanski, J.P., Hagiwara, K., Ishikawa, F., Miyazono, K., Collins, V.P., and Heldin, C.H. (1992). Regional localization of the human platelet-derived endothelial cell growth factor (ECGF1) gene to chromosome 22q13. *Cytogenet Cell Genet* 59, 22-23.

129. Stenson, P.D., Mort, M., Ball, E.V., Shaw, K., Phillips, A., and Cooper, D.N. (2014). The Human Gene Mutation Database: building a comprehensive mutation repository for clinical and molecular genetics, diagnostic testing and personalized genomic medicine. *Hum Genet* 133, 1-9.

2

130. Szigeti, K., Sule, N., Adesina, A.M., Armstrong, D.L., Saifi, G.M., Bonilla, E., Hirano, M., and Lupski, J.R. (2004a). Increased blood-brain barrier permeability with thymidine phosphorylase deficiency. *Ann Neurol* 56, 881-886. doi: 10.1002/ana.20302.

131. Szigeti, K., Wong, L.J., Perng, C.L., Saifi, G.M., Eldin, K., Adesina, A.M., Cass, D.L., Hirano, M., Lupski, J.R., and Scaglia, F. (2004b). MNGIE with lack of skeletal muscle involvement and a novel TP splice site mutation. *J Med Genet* 41, 125-129.

132. Taivassalo, T., De Stefano, N., Argov, Z., Matthews, P.M., Chen, J., Genge, A., Karpati, G., and Arnold, D.L. (1998). Effects of aerobic training in patients with mitochondrial myopathies. *Neurology* 50, 1055-1060.

133. Takebayashi, Y., Akiyama, S., Akiba, S., Yamada, K., Miyadera, K., Sumizawa, T., Yamada, Y., Murata, F., and Aikou, T. (1996). Clinicopathologic and prognostic significance of an angiogenic factor, thymidine phosphorylase, in human colorectal carcinoma. *J Natl Cancer Inst* 88, 1110-1117.

134. Tanaka, J., Nagai, T., Arai, H., Inui, K., Yamanouchi, H., Goto, Y., Nonaka, I., and Okada, S. (1997). Treatment of mitochondrial encephalomyopathy with a combination of cytochrome C and vitamins B1 and B2. *Brain Dev* 19, 262-267.

135. Teitelbaum, J.E., Berde, C.B., Nurko, S., Buonomo, C., Perez-Atayde, A.R., and Fox, V.L. (2002). Diagnosis and management of MNGIE syndrome in children: case report and review of the literature. *J Pediatr Gastroenterol Nutr* 35, 377-383.

136. Threlkeld, A.B., Miller, N.R., Golnik, K.C., Griffin, J.W., Kuncl, R.W., Johns, D.R., Lehar, M., and Hurko, O. (1992). Ophthalmic involvement in myo-neuro-gastrointestinal encephalopathy syndrome. *Am J Ophthalmol* 114, 322-328.

137. Torres-Torronteras, J., Cabrera-Perez, R., Barba, I., Costa, C., de Luna, N., Andreu, A.L., Barquinero, J., Hirano, M., Camara, Y., and Marti, R. (2016). Long-Term Restoration of Thymidine Phosphorylase Function and Nucleoside Homeostasis Using Hematopoietic Gene Therapy in a Murine Model of Mitochondrial Neurogastrointestinal Encephalomyopathy. *Hum Gene Ther* 27, 656-667.

138. Torres-Torronteras, J., Gomez, A., Eixarch, H., Palenzuela, L., Pizzorno, G., Hirano, M., Andreu, A.L., Barquinero, J., and Marti, R. (2011). Hematopoietic gene therapy restores thymidine phosphorylase activity in a cell culture and a murine model of MNGIE. *Gene Ther* 18, 795-806.

139. Torres-Torronteras, J., Viscomi, C., Cabrera-Perez, R., Camara, Y., Di Meo, I., Barquinero, J., Auricchio, A., Pizzorno, G., Hirano, M., Zeviani, M., and Marti, R. (2014). Gene therapy using a liver-targeted AAV vector restores nucleoside and nucleotide homeostasis in a murine model of MNGIE. *Mol Ther* 22, 901-907.

140. Valentino, M.L., Marti, R., Tadesse, S., Lopez, L.C., Manes, J.L., Lyzak, J., Hahn, A., Carelli, V., and Hirano, M. (2007). Thymidine and deoxyuridine accumulate in tissues of patients with mitochondrial neurogastrointestinal encephalomyopathy (MNGIE). *FEBS Lett* 581, 3410-3414.

141. Van Goethem, G., Dermaut, B., Lofgren, A., Martin, J.J., and Van Broeckhoven, C. (2001). Mutation of POLG is associated with progressive external ophthalmoplegia characterized by mtDNA deletions. *Nat Genet* 28, 211-212. doi: 10.1038/90034.

142. Vinciguerra, C., Federighi, P., Rosini, F., Pretegiani, E., Cardaioli, E., Dotti, M.T., Sicurelli, F., Federico, A., and Rufa, A. (2015). Eye movement changes in mitochondrial neurogastrointestinal encephalomyopathy (MNGIE). *J Neurol Sci* 350, 107-109.

143. Visigalli, I., Delai, S., Ferro, F., Cecere, F., Vezzoli, M., Sanvito, F., Chanut, F., Benedicenti, F., Spinozzi, G., Wynn, R., Calabria, A., Naldini, L., Montini, E., Cristofori, P., and Biffi, A. (2016). Preclinical testing of the safety and tolerability of LV-mediated above normal alpha-L-iduronidase expression in murine and human hematopoietic cells using toxicology and biodistribution GLP studies. *Hum Gene Ther*.

144. Vissing, J., Ravn, K., Danielsen, E.R., Duno, M., Wibrand, F., Wevers, R.A., and Schwartz, M. (2002). Multiple mtDNA deletions with features of MNGIE. *Neurology* 59**,** 926-929.

145. Wagemaker, G. (2014). Lentiviral hematopoietic stem cell gene therapy in inherited metabolic disorders. *Hum Gene Ther* 25**,** 862-865. doi: 10.1089/hum.2014.102.

146. Wang, J., Chen, W., Wang, F., Wu, D., Qian, J., Kang, J., Li, H., and Ma, E. (2015). Nutrition Therapy for Mitochondrial Neurogastrointestinal Encephalopathy with Homozygous Mutation of the TYMP Gene. *Clin Nutr Res* 4**,** 132-136.

147. Watts, K.L., Adair, J., and Kiem, H.P. (2011). Hematopoietic stem cell expansion and gene therapy. *Cytotherapy* 13**,** 1164-1171.

148. Wilcox, W.R., Banikazemi, M., Guffon, N., Waldek, S., Lee, P., Linthorst, G.E., Desnick, R.J., and Germain, D.P. (2004). Long-term safety and efficacy of enzyme replacement therapy for Fabry disease. *Am J Hum Genet* 75**,** 65-74. doi: 10.1086/422366.

149. Xue, X., Pech, N.K., Shelley, W.C., Srour, E.F., Yoder, M.C., and Dinauer, M.C. (2010). Antibody targeting KIT as pretransplantation conditioning in immunocompetent mice. *Blood* 116**,** 5419-5422.

150. Yadak, R., Torres-Torronteras, J., Bogaerts, E., de Ruijter, G., Barquinero, J., Marti, R., Smeets, H.J., Huston, M.W., van Til, N.P., Wagemaker, G., and de Coo, I.F.M. (2015). OP45 – 3024: Efficient lentiviral vector-mediated hematopoietic stem cell gene therapy in MNGIE mice. *European Journal of Paediatric Neurology* 19, Supplement 1**,** S15. doi: http://dx.doi.org/10.1016/S1090-3798(15)30046-5.

151. Yasumura, S., Aso, S., Fujisaka, M., and Watanabe, Y. (2003). Cochlear implantation in a patient with mitochondrial encephalopathy, lactic acidosis and stroke-like episodes syndrome. *Acta Otolaryngol* 123**,** 55-58.

152. Yavuz, H., Ozel, A., Christensen, M., Christensen, E., Schwartz, M., Elmaci, M., and Vissing, J. (2007). Treatment of mitochondrial neurogastrointestinal encephalomyopathy with dialysis. *Arch Neurol* 64**,** 435-438.

153. Yolcu, M., Yolcu, C., Kaya, Z., Cakmak, E.O., and Sezen, Y. (2014). Endocarditis in Mitochondrial Neurogastrointestinal Encephalomyopathy (MNGIE) Syndrome: The First in the Literature. *J Clin Diagn Res* 8**,** SD01-02.

154. Young, J.D., Yao, S.Y., Baldwin, J.M., Cass, C.E., and Baldwin, S.A. (2013). The human concentrative and equilibrative nucleoside transporter families, SLC28 and SLC29. *Mol Aspects Med* 34**,** 529-547.

155. Young, J.D., Yao, S.Y., Sun, L., Cass, C.E., and Baldwin, S.A. (2008). Human equilibrative nucleoside transporter (ENT) family of nucleoside and nucleobase transporter proteins. *Xenobiotica* 38**,** 995-1021.

156. Young, M.J., and Copeland, W.C. (2016). Human mitochondrial DNA replication machinery and disease. *Curr Opin Genet Dev* 38**,** 52-62.

157. Zhou, S., Ma, Z., Lu, T., Janke, L., Gray, J.T., and Sorrentino, B.P. (2013). Mouse transplant models for evaluating the oncogenic risk of a self-inactivating XSCID lentiviral vector. *PLoS One* 8**,** e62333. doi: 10.1371/journal.pone.0062333.

158. Zimmer, V., Feiden, W., Becker, G., Zimmer, A., Reith, W., Raedle, J., Lammert, F., Zeuzem, S., Hirano, M., and Menges, M. (2009). Absence of the interstitial cell of Cajal network in mitochondrial neurogastrointestinal encephalomyopathy. *Neurogastroenterol Motil* 21**,** 627-631. doi: 10.1111/j.1365-2982.2009.01264.xNMO1264 [pii].

159. Zufferey, R., Dull, T., Mandel, R.J., Bukovsky, A., Quiroz, D., Naldini, L., and Trono, D. (1998). Self-inactivating lentivirus vector for safe and efficient in vivo gene delivery. *J Virol* 72**,** 9873-9880.

2

Development of a highly efficient lentiviral gene transfer protocol for hematopoietic stem cells

Niek P. van Til*,[1,2] Rana Yadak*,[1] Valentina Buffa,[1] Marshall W. Huston,[1]
Fatima Aerts-Kaya,[3] Yvette van Helsdingen,[1] Trudi P. Visser,[1]
Monique M. Verstegen,[1] Chiara Bovolenta,[4] Constanze Radek,[5]
Ian C. D. Johnston,[5] and Gerard Wagemaker[1,3,6]

[1]Department of Hematology, Erasmus University Medical Center, Rotterdam, The Netherlands;
[2]Laboratory of Translational Immunology, University Medical Center Utrecht, Utrecht, The Netherlands;
[3]Center for Stem Cell Research and Development, Graduate School of Health Sciences, Hacettepe
University, Ankara, Turkey; [4]MolMed S.p.A., Milan, Italy; [5]Miltenyi Biotec GmbH, Bergisch Gladbach,
Germany; [6]Raisa Gorbacheva Memorial Research Institute for Pediatric Oncology and Hematology,
Saint Petersburg, Russia; * Authors contributed equally.

|ABSTRACT

Efficient *ex vivo* hematopoietic stem/progenitor cell (HSPC) gene transfer protocols requiring low vector doses would reduce the number of vector particles required per patient and minimize the risk of genotoxicity by keeping vector copy number (VCN) low. With current lentiviral (LV) protocols, a high proportion of gene-modified HSPC requires a high vector dose, which often results in an undesirably high number of transgene copies per cell. To reduce genotoxicity risks and to control transgene expression levels, a single integration per cell is preferred. We observed that overnight transduction of VSV-G packaged LV expressing EGFP of lineage-depleted (Lin-) mouse bone marrow cells (BM), rhesus CD34$^+$ BM and human CD34$^+$ derived progenitor cells is markedly improved by solely increasing the cell density with a proportional increase of transducing units (TU)/mL. The principle also partly abrogates the restriction of rhesus monkey CD34$^+$ cells for HIV-1 vectors. Additionally, we show that overnight transduction with the cytokine TPO is sufficient for efficient transduction of mouse and human HSPC progenitors, while maintaining stem cell properties *in vivo*.

We conclude that highly efficient and short LV HSPC transduction protocols with single cytokine additions results in an optimal number of integrations per cell. It is of note that the method will drastically reduce volumes of virus stocks and transduction reagents required for *ex vivo* LV-mediated gene-transfer.

|INTRODUCTION

Gammaretroviral vector (γRV) hematopoietic stem/progenitor cell (HSPC) gene therapy has been demonstrated to be successful for long-term treatment of X-linked severe combined immunodeficiency (SCID-X1)[1, 2] and adenosine deaminase (ADA)-SCID.[3] Unfortunately, γRV have a risk for insertional oncogenesis and consequently, safer self-inactivating (SIN) RVs with reduced-risk genotoxicity have been developed.[4] Third generation SIN lentiviral vectors (LV)[5, 6] may further decrease genotoxicity risks since they feature a reduced likelihood of upregulating proto-oncogenes due to reduced affinity to integrate near transcription start sites compared to RV. [7] The use of eukaryotic promoters, whether constitutively active or cell type-specific, rather than viral promoters could further improve the vector safety profile.

Furthermore, LVs are more efficient in transducing primary human cells than γRVs. As LV vectors require less transduction time and have no prerequisite for growth stimulation or cell division to integrate into the genome the efficiency is enhanced by addition of cytokine cocktails that stimulate cell cycling.[8] Some recent HSPC-based clinical gene therapy trials have therefore changed to lentiviral vectors, e.g. for X-linked adrenoleukodystrophy,[9] β-thalassemia,[10] metachromatic leukodystrophy[11] and Wiskott-Aldrich syndrome.[12]

In most *ex vivo* LV clinical trials, like the γRV protocols, HSPCs are currently pre-stimulated with a cytokine cocktail that includes interleukin 3 (IL-3), even though this condition results in the partial loss/reduction of their stemness.[13] Furthermore, HSPCs are incubated for multiple rounds with a high vector dose and transduced in dishes pre-coated with the CH296 human fragment of fibronectin (RetroNectin) and/or protamine sulfate [9-12, 14] to reduce the distance between the vector and the target cells.

Previous observations with γRV[15] have demonstrated that one of the major limiting factors in viral transduction is the distance between the virus particle and the target cell. This could be reduced by increasing either the cell density or the viral vector concentration, or both.

We examined whether improvement of the physical LV transduction parameters for HSPCs combined with a minimal stimulation protocol, could lead to a more effective generation of genetically modified HSPCs with intact repopulation and homing potential.

To address this, feasibility of increased mouse, rhesus and human HSPC densities and LV multiplicity of infection (MOI) were titrated *in vitro* to obtain optimal transduction efficiencies. For mouse HSPCs, the long term repopulation capacity of the transduced cells at varying MOIs was tested *in vivo* in primary and secondary recipients, including GLP grade LV vector. Furthermore, to obtain minimal cytokine combinations required for efficient transduction of mouse and human HPSCs, while pertaining *in vitro* progenitors and *in vivo* repopulation capacities. In particular, SCF, TPO, Flt3-L combinations were tested, which are cytokines commonly used in clinical trials,[11, 12] with homemade or commercially improved culture media. This enhanced gene transfer protocol would contribute to reduced risks of genotoxicity,

by using low MOI, and reduced transduction time, by increasing the cell density and the optimal cytokine combinations. Moreover, minimally used cytokine cocktails permitting sufficient HSPC proliferation/ differentiation at low vector copy number, would add commercial value by significantly increasing the number of patients treated per LV batch and reduce the amount of cytokine for transduction protocols.

|MATERIALS AND METHODS

Animals

Normal BALB/c mice were obtained from our own breeding colony, CD45.1 and CD45.2 mice from Jackson Laboratory (Maine, USA). Purpose bred rhesus monkeys (*Macaca mulatta*) were free of intestinal parasites, and seronegative for herpes B, simian T-lymphotropic viruses, simian immunodeficiency virus, Ebola and Hepatitis B viruses. All animal experiments were reviewed and approved by an ethical committee of Erasmus MC, Rotterdam in accordance with legislation in The Netherlands.

Lentiviral vector production

The third generation self-inactivating LV vectors pRRL.PPT.SF.EGFP.bPRE4*.SIN (SF. GFP) containing the spleen focus forming virus (SF) or the phosphoglycerate kinase (PGK) promoter driving EGFP have been described previously.[5, 6, 16, 17]

The lentiviral vectors were produced by standard calcium phosphate transfection of HEK 293T cells with the plasmids pMDL-g/pRRE, pMD2-VSVg and pRSV-Rev.[5, 6] Lentiviral vectors were concentrated by ultracentrifugation for 2 hours at 20,000 r.p.m. at 4°C and stored at -80°C. Titers were determined by serial dilution on HeLa cells and GFP expression was measured by flow cytometry five days post-transduction.[18] The good laboratory practice (GLP) lentiviral vector lots were prepared by MolMed S.p.A.

(Milan, Italy) as previously described[11, 12] with the potency/composition mentioned in supplementary table S2.

Hematopoietic stem cell enrichment and lentiviral transduction

Donor bone marrow was extracted from both femurs and tibias of eight to twelve week-old male mice and hematopoietic progenitors were purified by lineage depletion (Lin-) according to the manufacturer's protocol (BD Biosciences, USA). After enrichment, Lin- cells were transduced by the GFP SIN-LV overnight at different cell densities or different multiplicity of infections (MOIs), as indicated, either in serum free modified Dulbecco's medium with supplements (Standard Lab Medium, SLM).[19] Alternatively, StemMACS HSC Expansion Media XF, human (Miltenyi Biotec, Bergisch Gladbach, Germany) and combinations of growth factors, i.e. murine stem cell factor (mSCF) 100 ng/mL, human FMS-like tyrosine kinase 3-ligand (hFlt3-L) 50 ng/mL and murine thrombopoietin (mTPO) 20 ng/mL (STF) was used.[16] After 18 hours of incubation at 37°C, under normoxia, the cells were washed and expanded in the same culture medium supplemented with the growth factors mentioned above for 7 days under hypoxia conditions (3% O_2), for further assessment of GFP expression, VCN and colony forming assays. For *in vivo* experiments, after the overnight transduction,

a titration of transduced BALB/c or CD45.1 Lin- cells were injected in the tail vein of 6 Gy sub-lethally irradiated eight to twelve week-old female BALB/c or CD45.2 recipients respectively (1.4×10^5 to 3×10^6 Lin- cells).

For rhesus CD34+ cells, bone marrow (BM) aspirates were isolated as previously described.[19] After cell separation, BM suspension was frozen in liquid nitrogen. After thawing, the BM cells were washed with Hank's with HEPES, and CD34+ cells were subsequently isolated by immunomagnetic separation using an IgG2a antibody against CD34 (mAb 561 kindly provided by T. Egeland, University of Oslo, Oslo, Norway), which was non covalently linked to rat-anti-mouse IgG2a beads (Dynal, Oslo, Norway). CD34+ cells devoid of the anti-CD34 antibody were recovered using a polyclonal antibody against the Fab part of the anti-CD34 antibody (Detachabead, Dynal). Recombinant full-length rhesus monkey TPO produced by Chinese hamster ovary cells was supplied by Genentech Inc. (South San Francisco, CA) ,[19] and added to the same concentrations of hSCF and hFlt-3L as mentioned above.

For human umbilical cord blood (UCB) CD34+ cells, UCB samples were obtained from umbilical cords of full-term normal pregnancies after informed consent in conformity with legal regulations in The Netherlands. Mononucleated cells were isolated by Ficoll density gradient centrifugation (1,077 g/cm2; Nycomed Pharma AS, Oslo, Norway), and were cryopreserved in 10% dimethylsulphoxide (DMSO), 20% heat-inactivated fetal calf serum (FCS), and 70% Hanks' Balanced Salt Solution (HBSS; GIBCO, Breda, The Netherlands). After thawing by stepwise dilution in HBSS containing 2% FCS and

DNAse, the cells were washed with HBSS containing 1% FCS and CD34+ cells were purified from mononuclear cells by using the CD34+ MicroBead Kit, human (Miltenyi Biotec) according to manufacturer's instructions, and used for gene transduction experiments. Overnight transductions were performed in SLM, or StemMACS HSC expansion media XF (Miltenyi Biotec) with hSCF 100 ng/mL, hFlt3-L 50 ng/mL and hTPO 20 ng/mL (STF) or 20 ng/mL TPO alone under normoxia conditions. After 18 hours of incubation at 37°C, the cells were washed and expanded in the same culture medium supplemented with human SCF 50 ng/mL, human TPO 20 ng/mL, human FGF-1 10 ng/mL, mouse IGF-2 20 ng/mL, human angiopoietin like protein-3 200 ng/mL and heparin 10 μg/mL (STIF-A3) for 7 days under hypoxia conditions (3% O_2) for further assessment of GFP expression, VCN and colony forming assays.

Buffy coats or apheresis harvests from healthy donors were obtained from the University hospitals in Dortmund and Cologne. Bone marrow samples were purchased from AllCells (Alameda, USA). These studies were performed according to established ethical guidelines, and all blood donors gave informed consent. Peripheral blood mononuclear cells (PBMC) were separated by using Ficoll–Hypaque (GE-Healthcare, Bio-Science) density gradient centrifugation. PBMC obtained from buffy coats were pooled before magnetic enrichment of adult CD34+ cells using the CD34 MicroBead Kit, human (Miltenyi Biotec) according to manufacturer's instructions. CD34+ cells were obtained from apheresis harvests or bone marrow samples using CD34 Reagent and the CliniMACS`plus

or CliniMACS° Prodigy instrument according to manufacturer's instructions. CD34+ cells isolated from buffy coats were immediately taken into culture for 24 hours in 24-well plates at 4×10^5 cells per mL in StemSpan SFEM medium (Stem Cell Technologies, Grenoble, France) supplemented with Flt-3L, SCF, IL-3 and IL-6 (StemSpan CC100 Cocktail, Stem Cell Technologies). After 24-hour pre-activation, the concentration of the CD34+ cells was adjusted to 10^5, 10^6 or 10^7 cells per mL and the cells were transduced with VSV-G pseudotyped 3rd generation LVs encoding a GFP transgene (pRRL.ppt.PGK. GFP.wpre.sin-18), that had been concentrated by low-speed centrifugation, at an MOI of 10 or 100. CD34+ cells isolated from apheresis samples or bone marrow were cultivated in CellGro SCGM medium (Cellgenix, Freiburg, Germany) or StemMACS HSC Expansion Media XF, human (Miltenyi Biotec) supplemented with Flt-3L 300 ng/mL, SCF 300 ng/mL, IL-3 60 ng/mL and TPO 100 ng/mL (Miltenyi Biotec). After 24-hour pre-activation, the concentration of the CD34+ cells was adjusted to $10^5 - 10^7$ cells per mL and the cells were transduced with clinical grade LV containing a GFP expression cassette (details supplementary table S2) at an MOI of 10, 20 or 100. Cells transduced at 10^7 per mL were diluted to 10^6 per mL 24 hours post-transduction. Transduction efficiencies were compared to a standard transduction protocol [11], where pre-activated cells were seeded at 10^6 cells per mL on RetroNectin-coated plates before 2 rounds of transduction for 24 hours at an MOI=100. Cells were rested for 12 hours between the two transduction rounds. Cells were assayed for GFP expression between 5 and 14 days post transduction by flow

cytometry using a MACSQuant° Analyzer (Miltenyi Biotec).

Immunological phenotyping

Murine peripheral blood was collected monthly by retro-orbital puncture under isoflurane anesthesia in EDTA tubes. For FACS analysis, GFP expression in erythrocytes and platelets was measured in peripheral blood suspended in 1 mL 0.6% NaCl buffer. Separately, erythrocytes were removed with lysis buffer (0.15M NH_4Cl, 0.1M EDTA) and leukocytes were washed two times with Hank's balanced salt solution (HBSS, Invitrogen) containing 0.5% bovine serum albumin (BSA) and 0.05% sodium azide (HBN). Leukocytes were incubated for 30 minutes at 4°C in HBN containing 2% heat-inactivated normal mouse serum and antibodies against CD45.1, CD3, CD19, CD11b, directly conjugated respectively to APC-Cy7, APC, PE, PerCP-Cy5.5 (BioLegend, London, UK). Leukocytes were resuspended in 40 µL HBN and measured for GFP expression by flow cytometry.

Colony-forming assay

Semisolid methylcellulose 80% of the total volume (MethoCult M3231,and MethoCult H4230 respectively, Stem cell technologies, France) was seeded with fresh or overnight cultured mouse Lin- cells (2×10^3 /ml) or UCB CD34+ cells (1×10^3 /ml) or an equivalent of 500 culture expanded cells suspended in 10% of the total volume. Total volume was completed with IMDM supplemented with murine SCF 100 ng/mL, murine IL-3 30 ng/mL and murine GM-CSF 30 ng/mL for murine colony forming unit- granulocyte monocyte (CFU-GM) or hu-SCF 100 ng/mL, hu-IL-3 30 ng/mL, hu-GM-CSF 20 ng/

mL and hu-EPO 4U/mL for human CFU-GM and burst forming unit- erythroid (BFU-E). Duplicate cultures were incubated at 37 °C in a humidified atmosphere containing 5% CO2 and colonies were scored 7 or 14 days for mouse and human colonies respectively.

Quantitative PCR of lentiviral integrations

The lentiviral copy number per cell (VCN) following murine engraftment was determined on genomic DNA of bone marrow. Product of quantitative PCR was measured in an ABI PRISM 7900 HT sequence detection system (Applied Biosystems) similarly as previously described.[17, 18] Reactions were performed with 100 ng of genomic DNA with SYBR Green PCR Master Mix (Applied Biosystems) with the following primer set: HIV-U3 forward primer, 5'- CTG GAA GGG CTA ATT CAC TC-3', and HIV reverse primer, 5'- GGT TTC CCT TTC GCT TTC AG-3'. The samples were normalized for mouse *gapdh* with the following primer set: forward primer 5'-CAT CAC TGC CAC CCA GAA GAC-3' and reverse primer 5'-TGA CCT TGC CCA CAG CCT TG-3'. A standard line for the lentiviral vector integrations was determined from sorted mouse 3T3 cells

transduced at MOI of 0.05. Samples were analyzed with SDS2.2.2 software.

To quantify the number of lentiviral integrations in human CD34^{+} cells, genomic DNA was isolated using the QIAamp DNA Mini Kit (Qiagen, Hilden, Germany) before quantitative PCR detection using an ABI PRISM 7900 HT Fast (Applied Biosystems) and qPCR core Kit (Eurogentec) using the following primers: HIV-fwd1, 5'-TAC TGA CGC TCT CGC ACC-3', HIVrev1, 5'-TCT CGA CGC AGG ACT CG-3'. The samples were normalized for human actin with the following primer set: Actin forward 5'-AGC GGG AAA TCG TGC GTG AC-3', Actin reverse 5'-CAA TGG TGA TGA CCT GGC CGT-3' (Metabion AG). For quantitation of the integrated lentiviral VCN, HeLa cells transduced at an MOI of 0.05 and subsequently FACS sorted were used as control.

Statistical analysis

Statistical analysis was performed with Graph Pad Prism (version 5.03). Significant differences were determined by one-way ANOVA on ranks with post hoc testing by Dunn's test or Mann-Whitney U test for comparing two groups. Significant difference was assumed if $p < 0.05$.

|RESULTS

In vitro transduction efficiency by increased cell and vector density

Transduction at higher cell and vector concentrations with a constant MOI improved transduction of mouse Lin-hematopoietic stem cell progenitors cells, human UCB CD34^{+} cells and, to a lesser extent, also rhesus macaque CD34^{+} cells

(Fig. 1A). The total number of transduced cells increased exponentially (Fig.1B). The vector copy number (VCN) of the transduced cells is presented in supplementary table S1.

Increasing the MOI in a fixed volume (increased vector concentration) improved the transduction efficiency of rhesus macaque CD34^{+} cells ~4-fold (Fig. 1C), and mouse
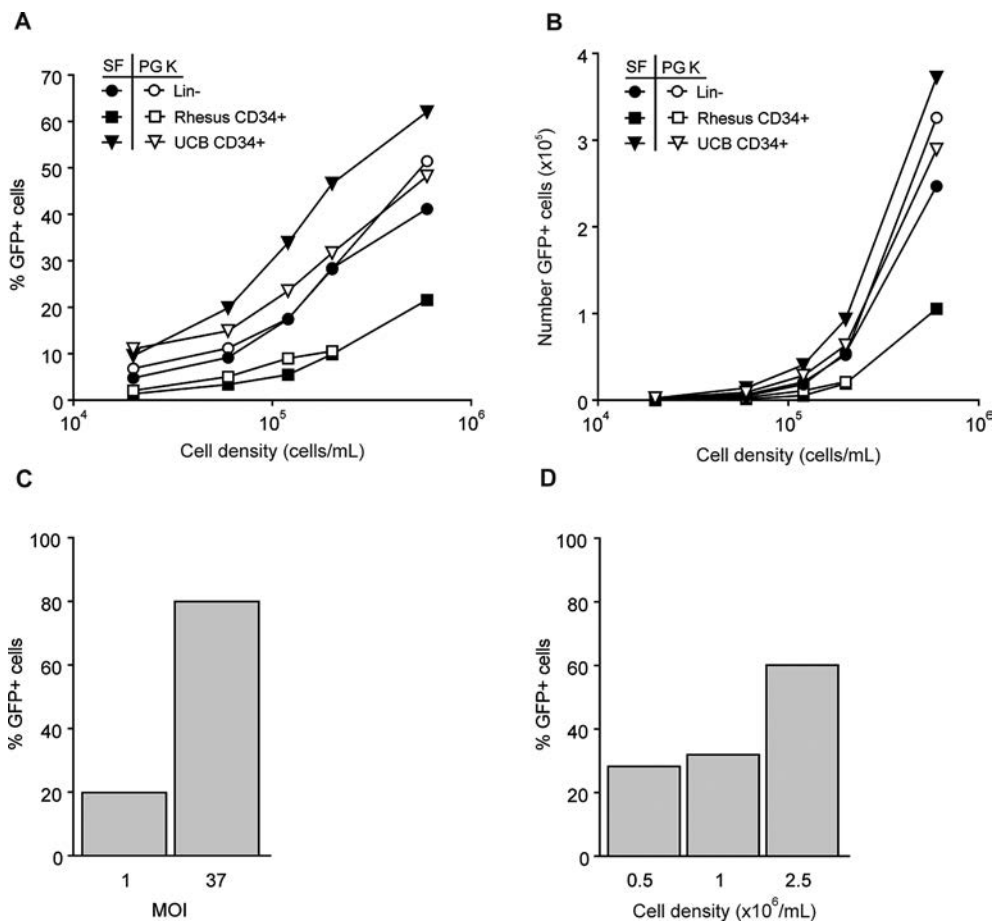
Figure 1. Cell and vector density improves HSC transduction efficiency. (A) Mouse Lin- cells, rhesus BM CD34+ cells and human UCB CD34+ cells transduced at cell densities ranging from 2 × 10^4 – 6 ´ 10^5/mL with an MOI of 1. The mean percentage GFP positive cells is increased at higher cell densities (closed symbols SF.GFP and open symbols PGK.GFP lentiviral vectors, (N=1-3). **(B)** The mean absolute number of transduced cells increases strongly by higher cell densities and larger number of cells (N=1-3). **(C)** The transduction efficiency of rhesus CD34+ cells at 6 ´ 10^5/mL and an MOI 1 compared to MOI 37 (N=1). **(D)** An MOI of 1, but higher cell and vector densities increase the transduction efficiency (N=1-2)

Lin- cells at low cell density (Supplementary Fig. S1A). By keeping the MOI low (MOI 1), but increasing the cell density, transduction efficiencies of rhesus macaque CD34+ cells of ~60% could be obtained (Fig. 1D).

In vivo reconstitution of high cell density transduced hematopoietic progenitors

We next investigated whether Lin- mouse cells transduced under higher densities and transduced at high and low MOI would sufficiently reconstitute sublethally irradiated

mice. High transduction efficiencies were obtained *in vitro* (Supplementary Fig. S2A), and long-term reconstitution was obtained in primary and secondary recipients in erythrocytes, platelets and leukocytes (Supplementary Fig. S2B-G). Lin- cells were also transduced at low MOI ranging from MOI 0.25 to MOI 2. Similar ratios of GFP+ cells were observed in cultured transduced cells and different blood lineages with a 3-fold increase in GFP+ positive percentage between MOI 0.25 and MOI 2 (Fig. S2H-K).

Transduction of human hematopoietic progenitors from peripheral blood, apheresis and bone marrow samples with GLP grade vector.

To further investigate the effect of cell densities on transduction efficiency, human CD34+ cells were subjected to different transduction protocols including protocols similar to those presently used in clinical trials. A good laboratory practice (GLP) lot was used for the experiments (Supplementary table S2).

Pre-stimulated CD34+ hematopoietic progenitors derived from buffy coats (Fig. 2A) were transduced at different cell densities. A standard clinical protocol involving two rounds of transduction at high MOI of 100 on RetroNectin-coated plates at 10^6 cells per mL achieved transduction efficiencies of 89%. A single round of transduction modified 79% of CD34+ cells. Using a lower MOI of 10 at cell densities of 10^7 per mL resulted in GFP positive percentages that approached those of a single MOI 100 and 10^6 cells per mL (Fig. 2A). Further experiments performed on apheresis and bone marrow derived hematopoietic

progenitors showed the same pattern of increasing transduction efficiency when cell and vector density was increased (Fig. 2B). A correlation between vector concentration and transduction efficiency was also noted in the bone marrow and apheresis derived CD34+ cells (Fig. 2C). Finally, the VCN of the transduced hematopoietic progenitors also correlated with cell density and varied between 0.5 and 1.5 VCN per cell (Fig. 2D).

Cytokine combinations for efficient transduction

Strong activation of HSPCs improves transduction efficiency but leads to progenitor cell differentiation and loss of long-term repopulating cells. To investigate which culture parameters are important for efficient transduction and reconstitution under relatively high cell density, different media (home-made SLM medium and StemMACS medium) and varied minimal cytokine combinations were compared. After overnight transduction of Lin- cells and 7 days *in vitro* culture, similar transduction efficiencies were observed when using SLM or StemMACS medium, and a similar trend could be observed in the MFI and VCN values (Fig. 3A-C). The combination of SCF, TPO and Flt3-L (STF) resulted in the most optimal transduction efficiencies, but single cytokine additions resulted (SCF or TPO) in high transduction efficiencies (Fig. 3A-C). If transductions were performed with no cytokines, or Flt3-L alone this resulted in very poor transduction (Fig. 3A-C). Colony assays of Lin- cells seeded at day 1 were similar between SLM and StemMACS, but 7 days culture increased the number of CFU-GMs specifically when cultured in StemMACS
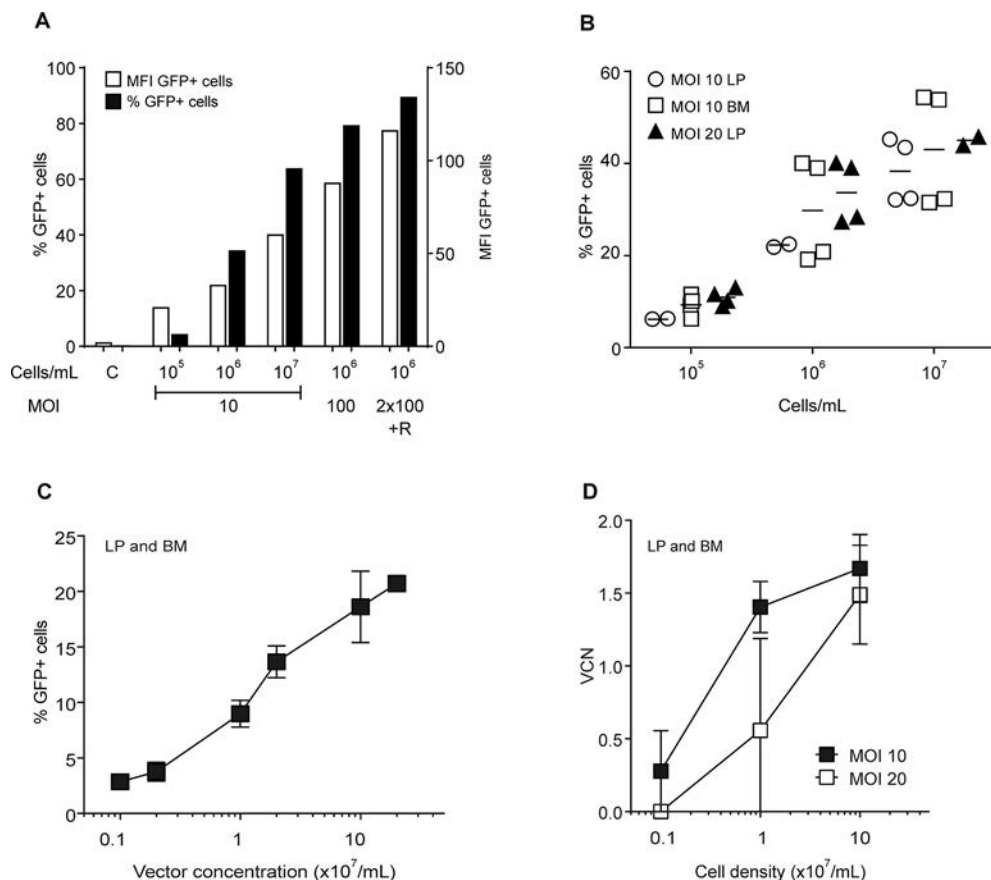
Figure 2. Human CD34+ cells transduced with GLP lentiviral vector lot. (A) CD34+ cells were isolated from buffy coats and cultivated overnight at 4×10^5 cells per mL in StemSpan SFEM medium supplemented with Flt-3L, SCF, IL-3 and IL-6. After 24-hour pre-activation, cell densities were adjusted (10^5–10^7 cells per mL) before transduction at an MOI of 10 or 100. One sample was transduced twice at an MOI of 100 on RetroNectin coated plates. The cells were analyzed 5 days post transduction by flow cytometry. MFI (open bars) and percentage of GFP-modified cells (black bars) are shown. C, control non transduced cells, N = 1 **(B, C)** Human CD34+ cells isolated from bone marrow (BM) or leukapheresis samples (LP) were cultivated in CellGro SCGM medium supplemented with SCF, TPO, IL-3 and Flt-3L at cell densities of 10^5, 10^6 or 10^7 cells per mL (N= 2-7) The cells were transduced with an MOI of 10 or 20 (LP) or 10 (BM). **(D)** After 13 days of culture, transduced CD34+ cells from BM and LP were analysed for the VCN. Flow cytometric analysis and VCN was performed 5-6 days post-transduction (N=2-7).

medium (Fig. 3D and E). The cytokines did not have significant effect on the number of colonies counted.

A similar experiment was performed using human UCB CD34+ cells by comparing STF and TPO conditions, in which the transduction efficiency was comparable (Fig. 3F). StemMACS medium performed slightly better with higher GFP percentage and MFI, and progenitors derived from

3
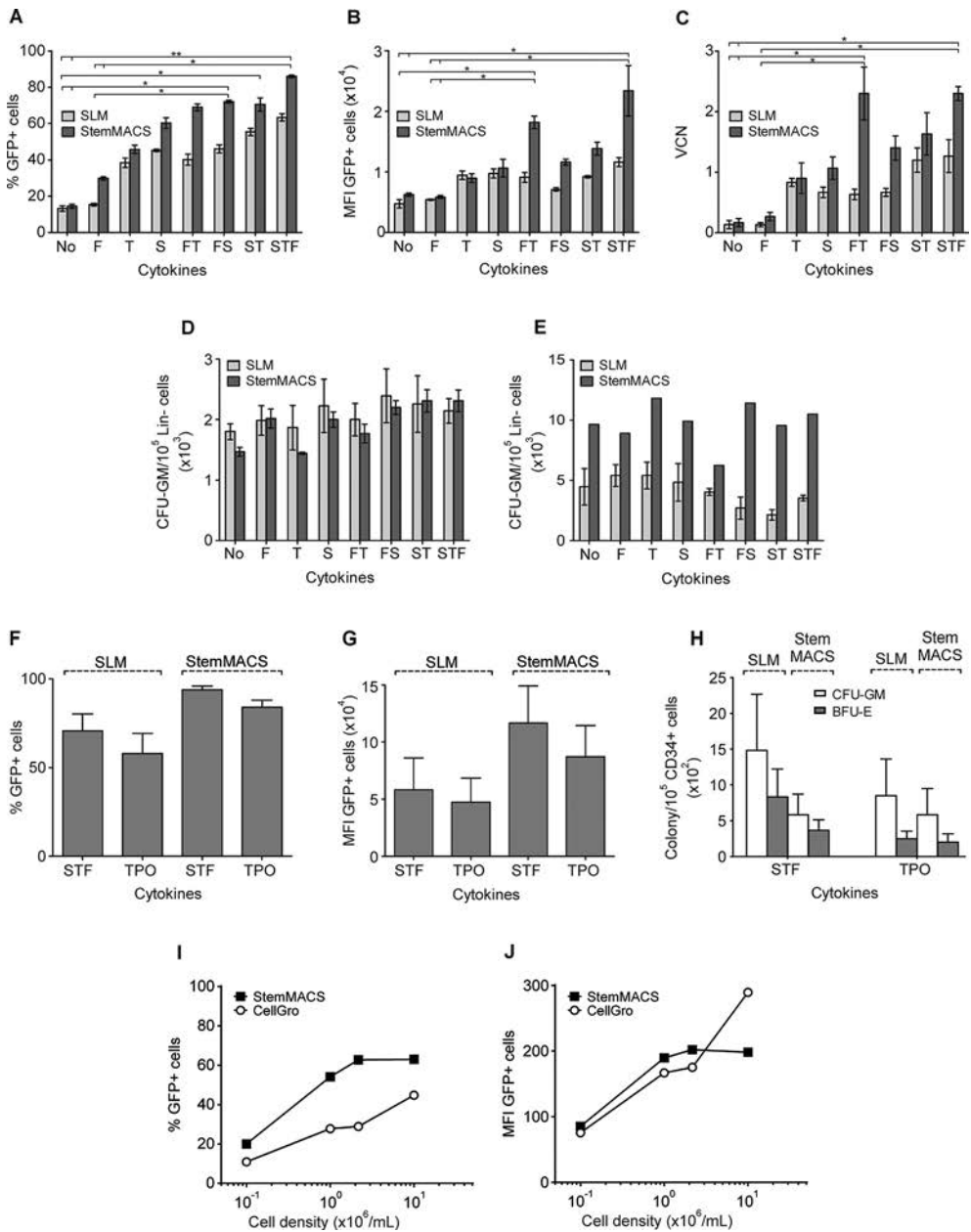
Figure 3. Effect of cytokine combinations on transduction efficiency. Different cytokine combinations determine transduction efficiency of mouse and human HSPCs. SLM or StemMACS HSC Expansion Media XF, human were tested *in vitro* presenting **(A)** GFP percentage, **(B)** mean fluorescence intensity (MFI), and **(C)** vector copy number (VCN) per cell 7 days after transduction at 10^6/ mL, MOI 2. N = 3 experiments. **(D)** Colony forming units- granulocyte monocyte (CFU-GM) of Lin- cells seeded at day 1 and **(E)** 7 days of culture. N = 1-3 experiments. No = no cytokines, F = FLT3-L, T = TPO, S = SCF. **(F)** GFP percentage 7 days after expansion of human UCB CD34+ cells transduced (2×10^6 per mL at an MOI of 10 in SLM or StemMACS media in combination with STF or ▸

▶ TPO, **(G)** the MFI and VCN of SLM cultured cells and **(H)** CFU-GM and burst forming units- erythroid (BFU-E) of CD34+ cells seeded at day 1. N = 3 experiments. **(I, J)** Human CD34$^+$ cells, isolated from apheresis samples, were cultivated in CellGro SCGM medium or StemMACS medium supplemented with SCF, TPO, IL-3 and Flt3-L at the indicated cell densities were transduced with an MOI of 100 at day 1 and analyzed on day 5 for GFP percentage or MFI (N=1). Data represent mean ± SEM. Significant differences were determined by one-way ANOVA on ranks with by post hoc Dunn's test, p<0.05. SLM = standard lab medium.

Table 1. CD45.1 transduced Lin- cells for *in vivo* transplantation.

	GFP+ %	MFI	VCN/cell	Colonies/10^5 cells Seeded day 1
SLM + STF	57.1	10400	0.8	1375
SLM + SCF and TPO	52.9	9239	1.3	1550
SLM + SCF	41.8	7457	0.8	1675
SLM + TPO	24.7	6956	0.6	1375
SLM + No cytokines	6.4	5773	0.1	1025
StemMACS + STF	67.9	11284	2.0	1850
StemMACS + TPO	33.4	8584	0.9	900

The GFP percentage, MFI and VCN/cell were determined at 7 days after transduction.

CD34$^+$ cells seeded at day 1 resulted in similar CFU-GM and BFU-E colony formation (Fig. 3F-H). Comparison with another commercial medium using human CD34$^+$ cells derived from apheresis material (Fig. 3I-J) also supported the observation that StemMACS medium resulted in improved transduction efficiency of human cells.

To investigate whether mouse Lin-cells were able to efficiently reconstitute sublethally irradiated mice, transduced donor Lin- cells were transplanted after overnight transduction in medium containing selected cytokine combinations. Donor cells reconstituted similarly to high levels in all mice as measured in peripheral blood, BM and spleen (Fig. 4A-C). SLM and StemMACS medium with STF resulted in efficient transgene expression in peripheral blood (Fig. 4D-F). This was confirmed in BM and spleen (Fig. 4G-H). Interestingly, TPO alone also resulted in high GFP percentages if StemMACS medium was used, and no cytokines resulted in <5% GFP+ cells, but did not have a significant negative effect on the reconstitution of transplanted cells (Fig. 4A, D-H). The use of the different media did not affect the T, B and myeloid lineage potential to reconstitute, and resulted in similar transduction efficiencies in the hematopoietic lineages, with SCF the least efficient (Fig. I and J).
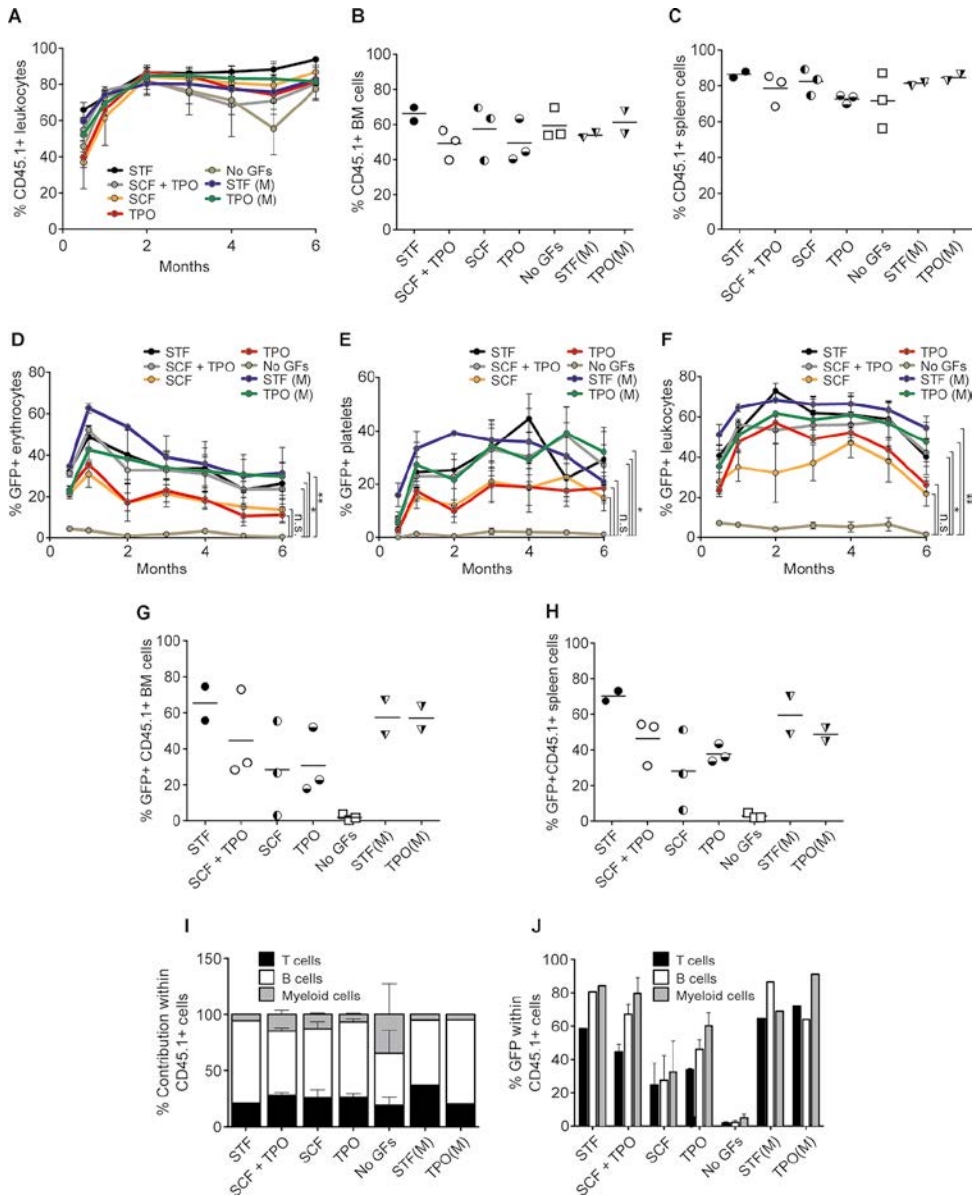
Figure 4. *In vivo* **reconstituted transduced Lin- cells transduced under different cytokine combinations.** Selected cytokine combinations were used to transduce donor mouse Lin- cells at 10^6/mL, MOI 2 in SLM or StemMACS (M) medium, and reconstitution of 1.4×10^5 cells transplanted in recipient mice was monitored for up to 6 months (N = 2-6 mice/ group). The CD45.1 chimerism in **(A)** peripheral blood, (**B**) bone marrow (BM), and **(C)** spleen, and **(D)** the GFP percentage within erythrocytes, **(E)** platelets and **(F)** leukocytes, and **(G)** BM and **(H)** spleen are shown. **(I)** contribution of T (CD3$^+$), B (CD19$^+$) and myeloid cells (CD11b$^+$) distribution in CD45.1 donor peripheral blood and **(J)** GFP percentage in the different leukocyte lineages.. Data represent mean ± SEM. Significant differences were determined at 6 months after transplantation by one-way ANOVA on ranks by Dunn's post hoc test, p<0.05, n.s. not significant.

| DISCUSSION

HSPC clinical gene therapy trials use different transduction protocols.[9-12] These protocols are often derived from older γRV transduction methods, in which two or more transduction rounds are included and 4-5 days of *in vitro* culture is applied.[3, 20] They also often include i) time to pre-stimulate CD34^{+} HSPCs with a cocktail of cytokines, ii) compounds such as protamine sulfate and/or RetroNectin to enhance transduction and iii) the use of high MOIs (MOI 25-200) .[3, 9-11, 14, 20-22] This may have a negative effect on long-term repopulating stem cells, may increase the risk of contamination, and can potentially alter the integration profile, because certain cytokine cocktails strongly promote cell-cycling and dedifferentiation. Protocol developments that result in minimizing the use of costly cytokines may be preferred. Adapting protocols that require a reduced amount of vector particles would be advantageous, since every vector batch has to be validated for quality and is generally laborious to produce. Our aim was to test different HSPC (and vector) densities to enhance transduction efficiency. Increased cell densities resulted in significantly improved transduction of mouse Lin- BM progenitor cells, rhesus macaque CD34^{+} and human derived CD34^{+} HSPCs, so high MOIs are not required. Rhesus macaque CD34^{+} progenitors are relatively difficult to transduce efficiently by HIV-derived lentiviral vectors; hence transduction of these cells is often performed with vectors based on simian immunodeficiency virus (SIV).[23-25] This is caused by HIV-1 replication restriction at an early post-entry step in simian cells, due to the action of inhibitory cellular factors [26], such as in part by the restriction factor tripartite

motif 5α protein (TRIM5α) [27] and binding of the viral capsid to cyclophilin A. [25] This initiated the development of chimeric HIV-1 vectors with SIV components to improve transduction of rhesus cells. [28, 29] These modifications increased transduction of CD34^{+} rhesus macaque BM cells significantly, thereby partially overcoming these barriers. We have demonstrated that by increasing the cell culture density of rhesus CD34^{+} cells during vector exposure, up to 20% of cells could be transduced using low MOIs, and up to 80% with high MOIs (from 0.25 to 2), making *in vivo* experiments with HIV-1 lentiviral vectors in rhesus macaques, without *in vivo* selection, feasible.

Cytokines are required for -RV transduction of HSPCs. However, the use of cytokines for efficient LV transduction may not be that critical. IL-3 has been shown redundant for transduction of human peripheral blood derived CD34^{+} HSPCs.[30] Since IL-3 promotes differentiation of hematopoietic progenitors,[31] this can be easily excluded from clinical gene therapy protocols. Uchida *et al* [30] demonstrated that the use of SCF alone reduced both the ability to engraft as well as the transduction efficiency, in contrast to earlier reports.[32] On our hands, the use of SCF alone did not affect the repopulation of transplanted donor mouse cells (Fig. 4A and I), but did not enhance the transduction efficiency (Fig. 4 D-F, J). In our experiments with SLM medium, adding TPO or SCF alone improved transduction efficiency, similar to an observation in human UCB CD34^{+} cells for SCF without other cytokines.[32] Medium totally lacking in cytokines clearly diminished transduction of short and long

term repopulating cells establishing cytokines are still required for transduction similarly to CD34^{+} UCBs [32] or mouse HSPCs.[32] However, there are also some reports demonstrating that cytokines can be omitted during transduction.[33] The vital role of TPO in the maintenance of HSPCs *ex vivo* and *in vivo* has been previously demonstrated.[34, 35] Our experiments show that TPO alone, added to StemMACS medium, aids transduction of both mouse and human HSPCs *in vitro*, similar to SLM medium containing the cytokines SCF, Flt3-L and TPO.

Amriche *et al* showed that low density lipid receptor (LDL-R) was upregulated by addition of 'early acting cytokines', which was required for binding and reverse transcription of vesicular stomatitis virus G (VSV-G) pseudotyped LVs to result in efficient transduction.[35] Other factors that influence the susceptibility of HPSC transduction that may be modulated by the cytokines additions, for example the cell cycle status at time of transduction[8] or the antiviral proteasome activity able to restrict lentiviral transduction,[36] could have played a role in the observed enhanced transduction efficiency.

Haas *et al* have previously investigated several parameters influencing transduction efficiency of UCB CD34^{+} progenitors by first and second generation LVs. Their observations were that vector concentration, but not MOI, was directly related to transduction efficiency.[37] Those experiments were performed with relatively few cells (1-10 $\times$ 10[4] CD34^{+} UCB cells per condition) and thus by increasing vector concentration at the same time that cell density was increased, transduction efficiency was improved. However, transduction efficiencies were lower than ours presumably due to the relatively low cell densities used (max $\sim 10^5$/mL). We demonstrated that by using higher cell densities and larger number of cells, clinically relevant transduction efficiencies can be reached. Successfully up-scaling these protocols could have significant consequences in terms of amount of vector required per patient, which in turn would enable a future reduction of the LV gene therapy vector batch costs by up to a factor of 10. Few studies explored strategies to enhance LV transduction of mouse and human HSPCs, including the utility or rapamycin[38] and recently, the application of microfluidic transduction system .[39]

Here, we show that cell and vector culture density are critical components to enable efficient transduction of mouse, rhesus and human HSPCs, because these parameters limits the conditions necessary to transduce HSPCs, such as the amount of expensive cytokines or the length of the transduction protocol. Furthermore, we confirm these results with a clinical-grade good-laboratory practice (GLP) vector batch on apheresis derived human CD34^{+} HSPCs. Finally, we demonstrate that by limiting the transduction period to 20 hours with only the addition of TPO, a high level of transduction is observed and that, at the same time, the ability to reconstitute the hematopoietic system in mice is not affected.

In conclusion, we optimized the conditions to efficiently transduce HSPCs. Our approach can be used as a tool to perform preclinical experiments in rhesus macaques. The protocol presented here is valuable for clinical application as it would reduce the amount of vector significantly, limit the time of *ex vivo* culture and increase the number of

patients that can be treated by a single vector batch, as well as reducing the amount of expensive growth factors required to culture the hematopoietic stem cells.

|ACKNOWLEDGMENTS

|CONFLICT-OF-INTEREST DISCLOSURE

CR and IJ are full time employees of Miltenyi Biotec GmbH. CB is full time employee of MolMed S.p.A..

Correspondence: Niek P. van Til, Department of Hematology, Erasmus University Medical Center, Dr. Molewaterplein 50, 3015 GE Rotterdam, the Netherlands; e-mail: N.P.vanTil@umcutrecht.nl

|REFERENCES

1. Hacein-Bey-Abina S, Hauer J, Lim A et al. Efficacy of gene therapy for X-linked severe combined immunodeficiency. N Engl J Med 2010;363:355-364.

2. Gaspar HB, Cooray S, Gilmour KC et al. Long-term persistence of a polyclonal T cell repertoire after gene therapy for X-linked severe combined immunodeficiency. Sci Transl Med 2011;3:97ra79.

3. Aiuti A, Cattaneo F, Galimberti S et al. Gene therapy for immunodeficiency due to adenosine deaminase deficiency. N Engl J Med 2009;360:447-458.

4. van der Loo JC, Swaney WP, Grassman E et al. Critical variables affecting clinical-grade production of the self-inactivating gamma-retroviral vector for the treatment of X-linked severe combined immunodeficiency. Gene Ther 2012;19:872-876.

5. Dull T, Zufferey R, Kelly M et al. A third-generation lentivirus vector with a conditional packaging system. J Virol 1998;72:8463-8471.

6. Zufferey R, Dull T, Mandel RJ et al. Self-inactivating lentivirus vector for safe and efficient in vivo gene delivery. J Virol 1998;72:9873-9880.

7. Zychlinski D, Schambach A, Modlich U et al. Physiological promoters reduce the genotoxic risk of integrating gene vectors. Mol Ther 2008;16:718-725.

8. Sutton RE, Reitsma MJ, Uchida N et al. Transduction of human progenitor hematopoietic stem cells by human immunodeficiency virus type 1-based vectors is cell cycle dependent. J Virol 1999;73:3649-3660.

9. Cartier N, Hacein-Bey-Abina S, Bartholomae CC et al. Hematopoietic stem cell gene therapy with a lentiviral vector in X-linked adrenoleukodystrophy. Science 2009;326:818-823.

10. Cavazzana-Calvo M, Payen E, Negre O et al. Transfusion independence and HMGA2 activation after gene therapy of human beta-thalassaemia. Nature 2010;467:318-322.

11. Biffi A, Montini E, Lorioli L et al. Lentiviral Hematopoietic Stem Cell Gene Therapy Benefits Metachromatic Leukodystrophy. Science 2013.

12. Aiuti A, Biasco L, Scaramuzza S et al. Lentiviral Hematopoietic Stem Cell Gene Therapy in Patients with Wiskott-Aldrich Syndrome. Science 2013.

13. Wognum AW, Visser TP, Peters K et al. Stimulation of mouse bone marrow cells with kit ligand, FLT3 ligand, and thrombopoietin leads to efficient retrovirus-mediated gene transfer to stem cells, whereas interleukin 3 and interleukin 11 reduce transduction of short- and long-term repopulating cells. Hum Gene Ther 2000;11:2129-2141.

14. Boztug K, Schmidt M, Schwarzer A et al. Stem-cell gene therapy for the Wiskott-Aldrich syndrome. N Engl J Med 2010;363:1918-1927.

15. Chuck AS, Clarke MF, Palsson BO. Retroviral infection is limited by Brownian motion. Hum Gene Ther 1996;7:1527-1534.

16. van Til NP, Stok M, Aerts Kaya FS et al. Lentiviral gene therapy of murine hematopoietic stem cells ameliorates the Pompe disease phenotype. Blood 2010;115:5329-5337.

17. Huston MW, van Til NP, Visser TP et al. Correction of murine SCID-X1 by lentiviral gene therapy using a codon-optimized IL2RG gene and minimal pretransplant conditioning. Mol Ther 2011;19:1867-1877.

18. van Til NP, Markusic DM, van der Rijt R et al. Kupffer cells and not liver sinusoidal endothelial cells prevent lentiviral transduction of hepatocytes. Mol Ther 2005;11:26-34.

19. Neelis KJ, Hartong SC, Egeland T et al. The efficacy of single-dose administration of thrombopoietin with coadministration of either granulocyte/macrophage or granulocyte colony-stimulating factor in myelosuppressed rhesus monkeys. Blood 1997;90:2565-2573.

20. Gaspar HB, Parsley KL, Howe S et al. Gene therapy of X-linked severe combined immunodeficiency by use of a pseudotyped gammaretroviral vector. Lancet 2004;364:2181-2187.

3

21. Greene MR, Lockey T, Mehta PK et al. Transduction of human CD34+ repopulating cells with a self-inactivating lentiviral vector for SCID-X1 produced at clinical scale by a stable cell line. Human gene therapy methods 2012;23:297-308.

22. Cavazzana-Calvo M, Hacein-Bey S, de Saint Basile G et al. Gene therapy of human severe combined immunodeficiency (SCID)-X1 disease. Science 2000;288:669-672.

23. Hanawa H, Hematti P, Keyvanfar K et al. Efficient gene transfer into rhesus repopulating hematopoietic stem cells using a simian immunodeficiency virus-based lentiviral vector system. Blood 2004;103:4062-4069.

24. Kim YJ, Kim YS, Larochelle A et al. Sustained high-level polyclonal hematopoietic marking and transgene expression 4 years after autologous transplantation of rhesus macaques with SIV lentiviral vector-transduced CD34+ cells. Blood 2009;113:5434-5443.

25. Tarantal AF, Giannoni F, Lee CC et al. Nonmyeloablative conditioning regimen to increase engraftment of gene-modified hematopoietic stem cells in young rhesus monkeys. Mol Ther 2012;20:1033-1045.

26. Kootstra NA, Munk C, Tonnu N et al. Abrogation of postentry restriction of HIV-1-based lentiviral vector transduction in simian cells. Proc Natl Acad Sci U S A 2003;100:1298-1303.

27. Giblett ER, Anderson JE, Cohen F et al. Adenosine-deaminase deficiency in two patients with severely impaired cellular immunity. Lancet 1972;2:1067-1069.

28. Uchida N, Washington KN, Hayakawa J et al. Development of a human immunodeficiency virus type 1-based lentiviral vector that allows efficient transduction of both human and rhesus blood cells. J Virol 2009;83:9854-9862.

29. Uchida N, Hargrove PW, Lap CJ et al. High-efficiency transduction of rhesus hematopoietic repopulating cells by a modified HIV1-based lentiviral vector. Mol Ther 2012;20:1882-1892.

30. Uchida N, Hsieh MM, Hayakawa J et al. Optimal conditions for lentiviral transduction

of engrafting human CD34+ cells. Gene Ther 2011;18:1078-1086.

31. Nitsche A, Junghahn I, Thulke S et al. Interleukin-3 promotes proliferation and differentiation of human hematopoietic stem cells but reduces their repopulation potential in NOD/SCID mice. Stem Cells 2003;21:236-244.

32. Zielske SP, Gerson SL. Cytokines, including stem cell factor alone, enhance lentiviral transduction in nondividing human LTCIC and NOD/SCID repopulating cells. Mol Ther 2003;7:325-333.

33. Sirven A, Ravet E, Charneau P et al. Enhanced transgene expression in cord blood CD34(+)-derived hematopoietic cells, including developing T cells and NOD/SCID mouse repopulating cells, following transduction with modified trip lentiviral vectors. Mol Ther 2001;3:438-448.

34. Luther-Wyrsch A, Costello E, Thali M et al. Stable transduction with lentiviral vectors and amplification of immature hematopoietic progenitors from cord blood of preterm human fetuses. Hum Gene Ther 2001;12:377-389.

35. Amirache F, Levy C, Costa C et al. Mystery solved: VSV-G-LVs do not allow efficient gene transfer into unstimulated T cells, B cells, and HSCs because they lack the LDL receptor. Blood 2014;123:1422-1424.

36. Santoni de Sio FR, Cascio P, Zingale A et al. Proteasome activity restricts lentiviral gene transfer into hematopoietic stem cells and is down-regulated by cytokines that enhance transduction. Blood 2006;107:4257-4265.

37. Haas DL, Case SS, Crooks GM et al. Critical factors influencing stable transduction of human CD34(+) cells with HIV-1-derived lentiviral vectors. Mol Ther 2000;2:71-80.

38. Wang CX, Sather BD, Wang X et al. Rapamycin relieves lentiviral vector transduction resistance in human and mouse hematopoietic stem cells. Blood 2014;124:913-923.

39. Tran R, Myers DR, Denning G et al. Microfluidic transduction harnesses mass transport principles to enhance gene transfer efficiency. Molecular Therapy 2017.

|SUPPLEMENTARY INFORMATION

Supplementary table S1. Vector copy number cell density transductions.

Cell density (/mL)	Mouse Lin-	Rhesus CD34$^+$	Human CB CD34$^+$
2×10^4	0.13	0.0299	0.085
6×10^4	0.33	0.0014	0.180
1.2×10^5	0.92	0.4600	0.374
2×10^5	1.13	0.0450	0.315
6×10^5	0.99	0.4973	0.857

Average of N=2-3 experiments

Supplementary table S2. Composition of the GLP GFP vector batch.

Physical titer	2,010 (ng p24 Gag/mL)	(2.0 × 10^{10} pp/mL)^A
Functional titer	1.3×10^8 TU/mL	
Infectivity	6.4×10^4 TU/ng p24 Gag	
Infectious/total particles	1:150	
Total residual DNA (Picogreen)	1.01 mg/mL	
LTA residual DNA	5.7×10^3 copies/mL	
Plasmid residual DNA	1.4×10^7 copies/mL	
HCP	135 ng/mL	
Sterility test	negative	
Endotoxin test	< 1.0 EU/mL	

^{A}pp are calculated assuming that 1 ng p24 Gag= 10^7 physical particle (pp)]
TU = transducing unit
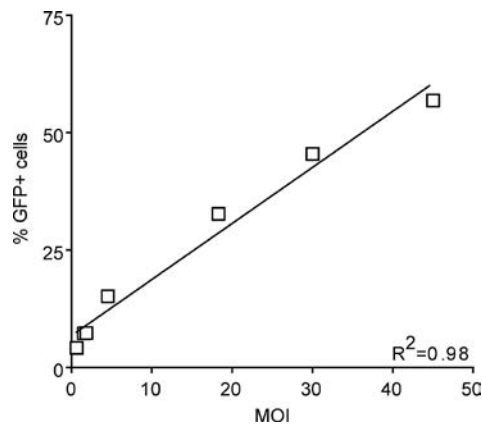
Supplementary figure S1. Multiplicity of infection and cell density. An increase in MOI during transduction of mouse Lin- cells correlates with the percentage of GFP+ cells at a cell density of 5×10^4/mL (N = 1)
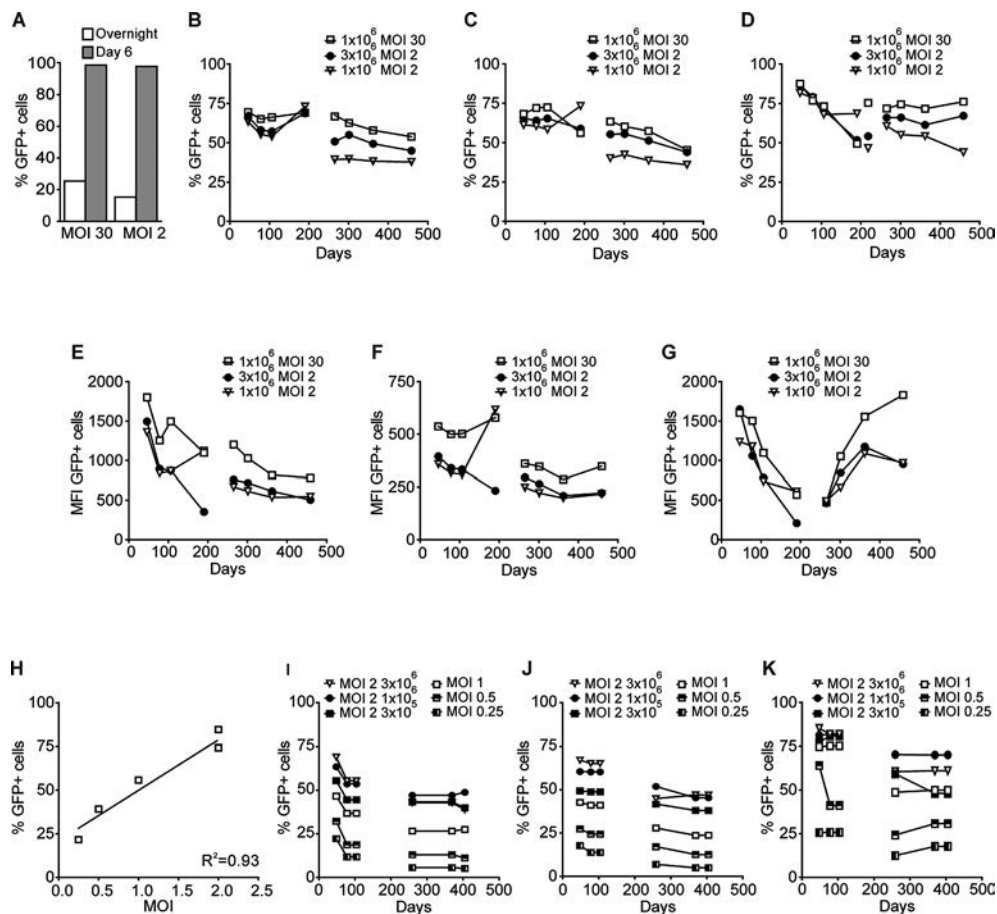
Supplementary figure S2. Long-term reconstitution of transduced cells in mice. (A) Percentage of GFP positive Lin- transduced cells at 1×10^6/mL after overnight and 6 days culture (N=1). Subsequently, different numbers of cells transduced at an MOI 2 or 30 were transplanted in 6 Gy irradiated BALB/c mice. The *in vivo* reconstitution of transduced Lin- cells with GFP positive **(B)** erythrocytes, **(C)** thrombocytes and **(D)** leukocytes is presented including transplantation of ½ femur of primary into secondary recipients at month 7 (n=5-15, and secondary mice n = 10-30 per group). Similarly, the mean fluorescence intensity (MFI) depicted for **(E)** erythrocytes, **(F)** thrombocytes and **(G)** leukocytes. Another experiment titrating down the MOI from 2 to 0.25 at 1.5×10^6/mL and transplanting different cell numbers, the *in vitro* results of **(H)** the percentage of GFP positive cells and *in vivo* reconstitution with secondary transplantations presenting **(I)** erythrocytes, **(J)** thrombocytes and **(K)** leukocytes.

Preclinical efficacy and safety evaluation of hematopoietic stem cell gene therapy in a mouse model of MNGIE

Rana Yadak[1,2], Raquel Cabrera-Pérez[3], Javier Torres-Torronteras3,
Marianna Bugiani[4], Joost C. Haeck[5], Marshall W. Huston1, Elly Bogaerts[6],
Steffi Goffart[7], Edwin H. Jacobs [6], Merel Stok[2,6,8], Lorena Leonardelli[9],
Luca Biasco[9,10,11], Robert M. Verdijk[12], Monique R. Bernsen[5],
George Ruijter[6], Ramon Martí[3], Gerard Wagemaker[*2,13,14],
Niek P. van Til[*2,15], Irenaeus F. M. de Coo[*1]

[1]Department of Neurology, Erasmus University Medical Center, Rotterdam, The Netherlands; [2]Department of Hematology, Erasmus University Medical Center, Rotterdam, The Netherlands; [3]Research Group on Neuromuscular and Mitochondrial Diseases, Vall d'Hebron Institut de Recerca (VHIR), Universitat Autònoma de Barcelona, and Biomedical Network Research Centre on Rare Diseases (CIBERER), Barcelona, Catalonia, Spain; [4]Department of Pathology, VU University Medical Center, Amsterdam, The Netherlands; [5]Department of Radiology & Nuclear Medicine, Erasmus University Medical Center; [6]Department of Clinical Genetics, Erasmus University Medical Center; [7] Department of Biology University of Eastern Finland, Joensuu, Finland; [8] Department of Pediatrics, Erasmus University Medical Center, Rotterdam, The Netherlands; [9]San Raffaele Telethon Institute for Gene Therapy (HSR-TIGET), Milan, Italy; [10]Gene Therapy Program, Dana-Farber/Boston Children's Cancer and Blood Disorders Center, Boston, MA, US; [11]University College of London (UCL), Great Ormond Street Institute of Child Health (ICH), London, UK; [12]Department of Pathology, Erasmus University Medical Center; [13]Hacettepe University, Stem Cell Research and Development Center, Ankara, Turkey; [14]Raisa Gorbacheva Memorial Research Institute for Pediatric Oncology and Hematology, Saint Petersburg, Russia; [15]Laboratory of Translational Immunology, University Medical Center Utrecht, Utrecht, The Netherlands.

(Submitted)
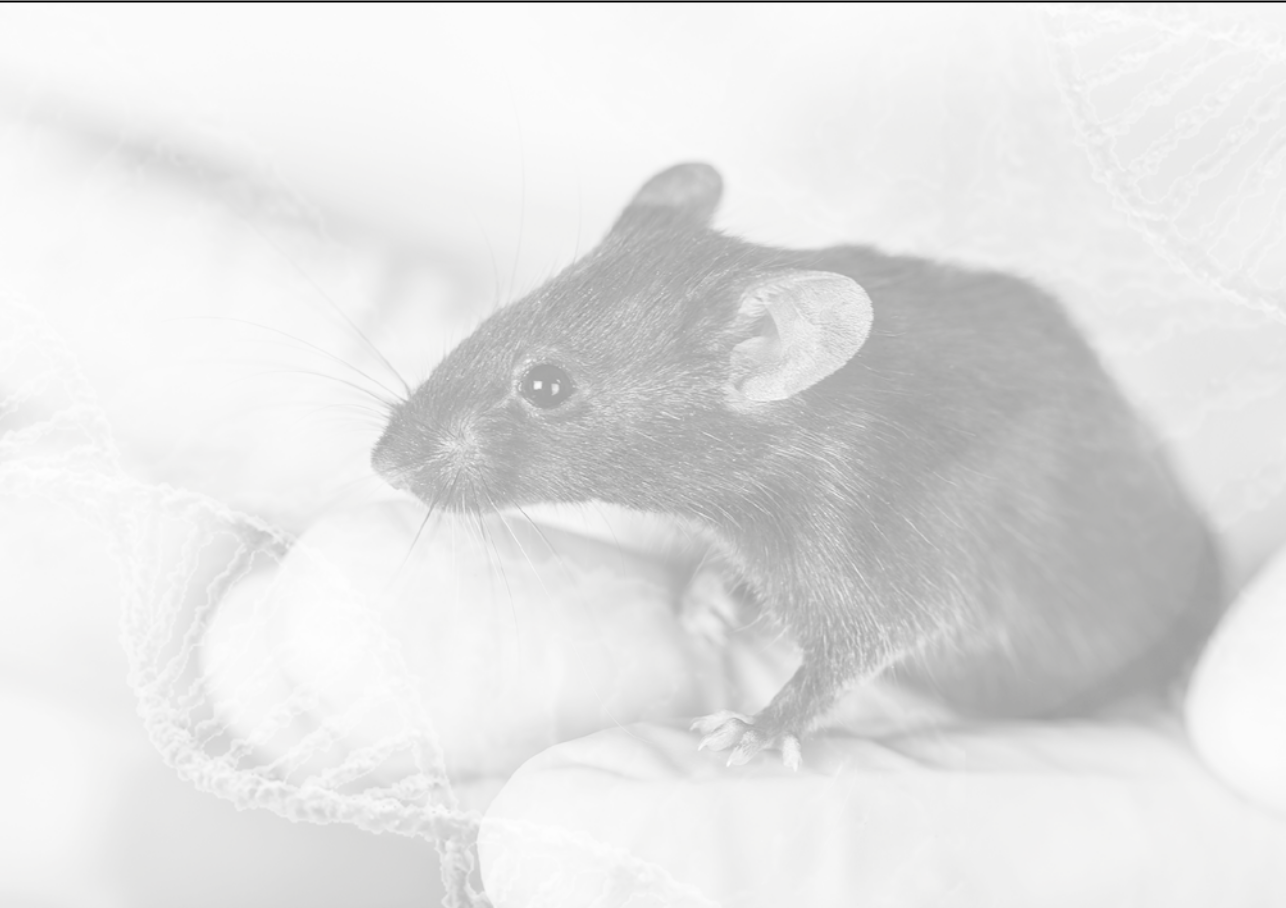
|ABSTRACT

Mitochondrial neurogastrointestinal encephalomyopathy (MNGIE) is an autosomal recessive disorder caused by thymidine phosphorylase (TP) deficiency resulting in systemic accumulation of thymidine (d-Thd) and deoxyuridine (d-Urd) and characterized by early onset neurological and gastrointestinal symptoms. Long-term effective and safe treatment is not available. Allogeneic bone marrow transplantation may improve clinical manifestations, but carries disease and transplant related risks. In this study, lentiviral vector based-hematopoietic stem cell gene therapy (HSCGT) was performed in $Tymp^{-/-}Upp1^{-/-}$ mice with the human phosphoglycerate kinase (PGK) promoter driving TYMP. Supranormal blood TP activity reduced intestinal nucleoside levels significantly at low vector copy number (median, 1.3; range,0.2-3.6). Furthermore, we covered two major issues not addressed before. First, we demonstrate aberrant morphology of brain astrocytes in areas of spongy degeneration, which was reversed by HSCGT. Second, long-term follow-up and vector integration site analysis were performed to assess safety of the therapeutic LV vectors in depth. This report confirms and supplements previous work on the efficacy of HSCGT in reducing the toxic metabolites in $Tymp^{-/-}Upp1^{-/-}$ mice, using a clinically applicable gene transfer vector and a highly efficient gene transfer method, and importantly demonstrates phenotypic correction with a favorable risk profile, warranting further development towards clinical implementation.

INTRODUCTION

Mitochondrial neurogastrointestinal encephalomyopathy (MNGIE) is an autosomal recessive disease caused by mutations in the thymidine phosphorylase gene (*TYMP*)[1], which result in partial or complete deficiency of the enzyme thymidine phosphorylase (TP)[2]. TP deficiency results in systemic accumulation of the substrates d-Thd and d-Urd in plasma and tissues of MNGIE patients[3] and thereby to imbalances in intra-mitochondrial deoxyribonucleoside triphosphates pools (dNTPs), which has been considered to induce somatic mitochondrial DNA alterations in tissues of MNGIE patients[4, 5]. The clinical spectrum of MNGIE ranges from mild symptoms in late-onset cases[6] to early teenage onset with fatal malabsorption and intestinal dysmotility[7]. The typical symptoms include ptosis and ophthalmoplegia, gastrointestinal dysmotility, neuropathy with reduced sensory-motor conduction, as well as central nervous system anomalies[4, 8]. The latter manifest on brain MRI as a unique pattern of progressive symmetrical cerebral (and occasionally cerebellar) hyper-intense signal changes on T2-weighted images[9]. The available treatment options for MNGIE such as peritoneal dialysis, platelets infusion and enzyme replacement therapy fail to achieve persistent clinical improvement[10-12].

As a long-term solution, allogeneic hematopoietic stem cell transplantation (HSCT) has been proposed; however, this is associated with high mortality rates due to disease and transplant related complications[13, 14]. Recently, liver transplantation has emerged as a promising treatment option preferably for patients with pre-existing liver failure; this however requires a matched organ donor and long-term immunosuppression[15]. Autologous hematopoietic stem cell gene therapy (HSCGT) could be beneficial for MNGIE patients as a single intervention with low-dose conditioning and poses no risks of graft rejection or graft- versus host disease. Third generation self-inactivating lentiviral (LV) vectors are currently used successfully in clinical trials for other metabolic disorders[16-18]. The present study supplements and confirms previous reports [19, 20] by using (*i*) a highly efficient transduction method, (*ii*) clinically applicable LV vectors to evaluate the therapeutic efficacy to reverse the biochemical phenotype, and extends these reports by demonstrating (*iii*) therapeutic efficacy of HSGCT in reversing pathological changes, particularly those of the brain, and assessing (*iv*) potential adverse effects such as pheno- and genotoxicity.

RESULTS

LV vectors, experimental design, TP expression and enzyme activity in target cells. Similar to previous studies[19-21], *Tymp^-/-^Upp1^-/-^* mice (referred to here as KO) were used. Unlike in humans, murine UPP1 degrades Thd and d-Urd, therefore *Tymp^-/-^Upp1^-/-^*, rather than Ty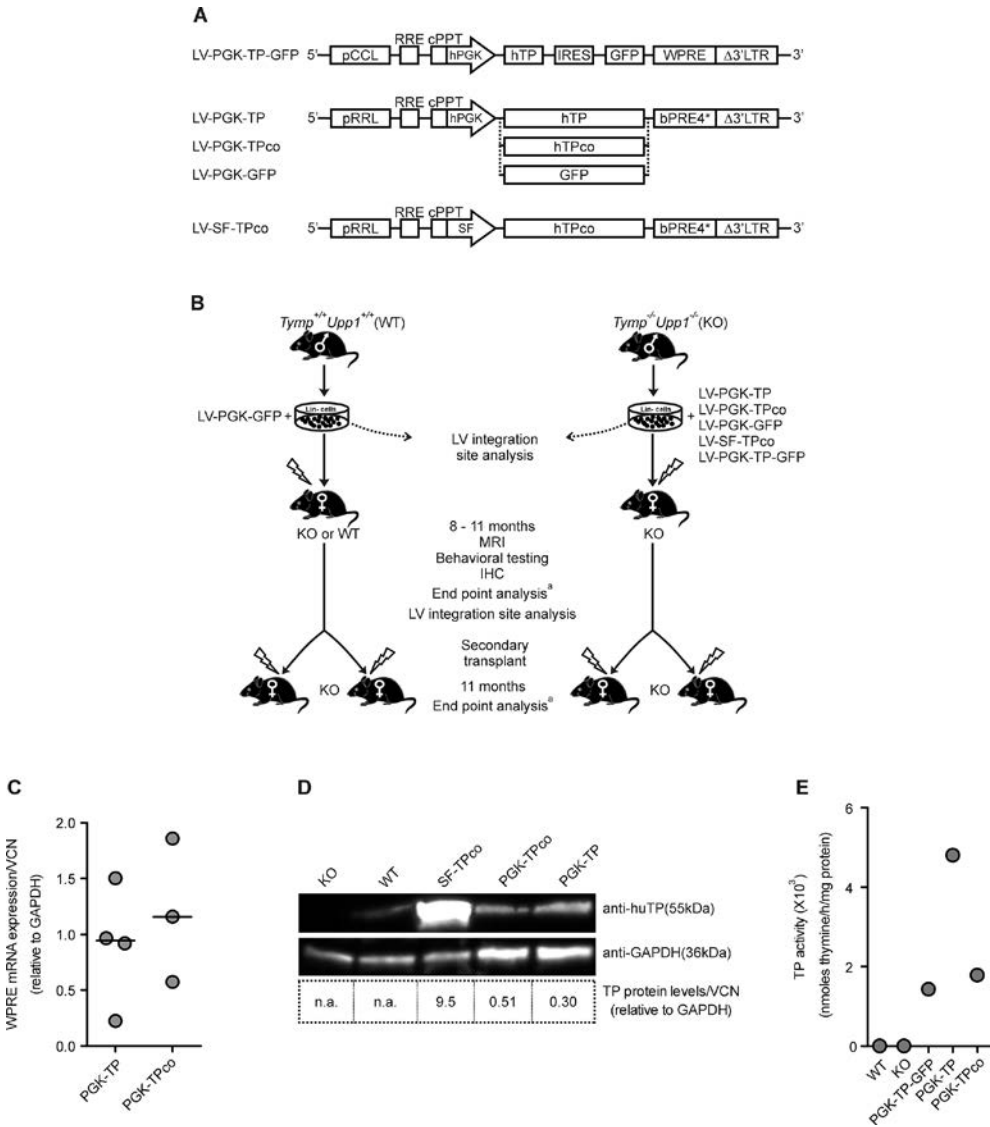mp^-/-^ mice[22], reflect the biochemical phenotype of MNGIE patients. A LV vector containing both TP and GFP sequences (PGK-TP-GFP) was reported previously[19] for biochemical correction in *Tymp^-/-^Upp1^-/-^* mice and is used in this study as a control. In the present study, third generation self-inactivating LVs containing a similar

backbone as currently used in clinical trials for metachromatic leukodystrophy (MLD) [17] and Wiskott-Aldrich syndrome[23] were constructed for expression of TP. The human cellular phosphoglycerate kinase (hPGK) promoter was used to drive expression of the native human TYMP sequence (TP) as well as the re-coded human TYMP sequence (TPco) in the therapeutic vectors, as well as to drive expression of the GFP sequence in the sham control vector (Figure 1A). The rationale for using TPco was to enhance protein production with a minimum number of transduced donor cells and vector copy number, as reported for IL2RG and RAG2 [24, 25]. The strong spleen focus forming (SF) virus promoter, which may contribute to leukemic events by transactivating proto-oncogenes[26], was used to evaluate potential phenotoxicity by excessive overexpression of TYMP and/or genotoxicity rather than an option for potential clinical application (Figure 1A).

Two virus concentrations (multiplicity of infection, MOI) were used for transduction, i.e., MOIs of 3 or10. By transplantation experiments (Figure 1B) the efficiency of the therapeutic LVs (PGK-TP, TPco) were evaluated for (*i*) biochemical correction (MOI 3 or 10) and (*ii*) neurological correction as assessed by brain magnetic resonance imaging (MRI), pathology and behavioral tests (MOI 10). To assess the safety of HSCGT primary recipients were subjected to long-term follow up for potential transgene overexpression-related phenotoxicity (in particular in the SF-TPco treatment group) and LV- related genotoxicity, as well as an integration site analysis of gene modified cells prior to and after engraftment in primary recipient mice

Figure 1. Lentiviral vectors and design of transplantation experiments and TP expression in the target cells. (A) Third-generation self-inactivating LV vectors used in the study and their elements are shown. pCCL and pRRL, LV vectors containing CMV-HIV or RSV-HIV 5' long terminal repeats respectively; RRE, Rev response element; cPPT, central polypurine tract; hPGK, human phosphoglycerate kinase promoter; hTP, native coding sequence of the human *TYMP* cDNA; hTPco, codon-optimized sequence; IRES, internal ribosome entry site; GFP, green fluorescent protein; SF, spleen focus forming virus promoter; WPRE, Woodchuck hepatitis posttranscriptional regulatory element; bPRE4*, adapted form of WPRE[38]. **(B)** Design of HSC transplantation experiments. The hematopoietic stem and progenitor cells (Lin-) from male donor mice were *ex vivo* transduced over night by the LV vector constructs and transplanted into female recipient mice. To determine the integration site profiles, LAM-PCR and integration site analysis were performed on a fraction of the transduced cells *in vitro* and BM cells from transplanted primary mice *in vivo*; see also Figure S3A. To evaluate LV vector-related insertional transformation *in vivo*, Lin- cells from each primary recipient were transplanted into two secondary KO female recipient mice. All transplanted mice received 6Gy total body irradiated 24hr prior to transplantation. All experiments included age matched untreated KO and WT controls. [a] End point analysis: sample collection for biochemical and molecular analysis, flow cytometry analysis. MRI= magnetic resonance imaging, IHC = immunohistochemistry. **(C-E)** TP expression and activity in KO Lin- cells transduced (MOI 10) and cultured *in vitro*. **(C)** qPCR analysis of WPRE mRNA expression normalized to GAPDH levels and corrected for VCN/ cell. The horizontal line represents the median, *n*= 3-4 replicates. **(D)** Western blot of total protein extracts from Lin- cells and their content corrected for VCN/ cell, *n*=1, n.a.= not applicable. Included are also lysates of SF-TPco treated cells confirming the higher TP protein with this promoter. **(E)** TP enzyme activity, *n*=1.

A

LV-PGK-TP-GFP 5'— pCCL — RRE — cPPT — hPGK — hTP — IRES — GFP — WPRE — Δ3'LTR —3'

LV-PGK-TP 5'— pRRL — RRE — cPPT — hPGK — hTP — bPRE4* — Δ3'LTR —3'
LV-PGK-TPco — hTPco —
LV-PGK-GFP — GFP —

LV-SF-TPco 5'— pRRL — RRE — cPPT — SF — hTPco — bPRE4* — Δ3'LTR —3'

B

$Tymp^{+/+}Upp1^{+/+}$ (WT) $Tymp^{-/-}Upp1^{-/-}$ (KO)

LV-PGK-GFP + Lin- cells

LV-PGK-TP
LV-PGK-TPco
LV-PGK-GFP
LV-SF-TPco
LV-PGK-TP-GFP

LV integration site analysis

KO or WT   KO

8 - 11 months
MRI
Behavioral testing
IHC
End point analysis[a]
LV integration site analysis

KO   KO

Secondary transplant

11 months
End point analysis[a]

KO   KO

4

C — WPRE mRNA expression/VCN (relative to GAPDH) — PGK-TP, PGK-TPco

D

KO | WT | SF-TPco | PGK-TPco | PGK-TP

anti-huTP(55kDa)
anti-GAPDH(36kDa)

| n.a. | n.a. | 9.5 | 0.51 | 0.30 | TP protein levels/VCN (relative to GAPDH) |

E — TP activity ($\times 10^3$) (nmoles thymine/h/mg protein) — WT, KO, PGK-TP-GFP, PGK-TP, PGK-TPco

aged 13 months, i.e., 11 months after HSCGT, to estimate the risk of insertional oncogenesis, and finally by secondary transplantation, a useful pre-clinical tool to detect vector induced hematological transformations[26, 27].

Codon optimization of TYMP did not result in improved WPRE mRNA, TP protein levels and TP enzyme activity (Figure 1C-E); therefore the two vectors were used interchangeably and referred to as PGK-TP(co) hereafter.

Biochemical correction and molecular chimerism following *ex vivo* HSCGT

Stable blood TP activity was observed both in the PGK-TP-GFP group as previously reported[20], and in recipients of the therapeutic

LV- PGK-TP(co) (Figure 2A). Lin- cells successfully engrafted both PGK-TP(co) and PGK-GFP recipient KO mice and integrated vector copies were detected (Figure 2B). We next measured TP activity in diseased tissues of our mice. Transduction resulted in increased TP activity to normal levels in brain and small intestine in the PGK- TP(co) treated mice (Figure 2C). As a consequence of the high TP activity, urine and plasma nucleosides were undetectable in almost all recipients of PGK-TP(co) with extensive reduction in brain nucleosides compared to both KO and WT animals (Figure 2D and Figure S1A). Overall, median nucleoside levels were reduced insufficiently at the lower MOI (Figure 2D and Figure S1A), (MOI 3, range, 0.1-0.8 VCN/ cell and percentage chimerism 47 -76 %, n= 5, data not shown). Eleven months after transplantation, recipients of PGK-TP(co) displayed 98% and 57% reduction in median intestinal d-Thd and d-Urd levels, respectively (Figure 2E and Figure S1B). Moreover, HSCGT provided high TP enzyme activity and reduced nucleoside levels in skeletal muscle and liver (Figure S1C). Altogether, although at an MOI 3 significant reduction of nucleosides was observed, full correction of the biochemical phenotype, only occurred at transplantation of 6 Gy irradiated recipients of 5×10^5 MOI 10 transduced cells, particularly in the small intestine , in contrast to the previous study[20].

MRI and rescue of brain white matter damage after HSCGT

Neurological changes are consistently reported in MNGIE patients, and minor changes were reported in old *Tymp*^{-/-}*Upp1*^{-/-} mice aged ≥18 months[22]. To characterize neurological abnormalities at earlier ages and to address the impact of HSCGT as early as at 2 months of age, brain MRI scans and immunohistochemistry (IHC) were performed. In contrast to WT mice, an increase in percentage of fluid content was observed as a hyper-intense signal in the brains of 6 to 12 month aged KO (5 out of 8) (Figure 3A). Increased T2 signals are indicative for fluid accumulation in the white matter surrounding the lateral ventricles, suggesting edema. White matter edema was absent in most treated mice; 8 out of 10 treated mice fell in the same hyper-intense volume range of WT animals (Figure 3B). Brain sections from KO mice stained with mature myelin proteolipid protein (PLP) and myelin basic protein (MBP) revealed the presence of progressive vacuolization in the cerebellar and cerebral white matter structures absent in WT mice. White matter vacuolizations were lined and crossed by thin immunopositive tissue stands, consistent with intramyelinic edema (Figure 3C, D). PLP and MBP-staining revealed disappearance of white matter vacuolization in the cerebellar white matter and corpus callosum of PGK-TP(co) treated group (Figure 3C, D). IHC staining for the astrocyte-specific glial fibrillary acidic protein (GFAP) revealed increased thickness of astrocyte processes abutting the blood vessels in KO mice as young as 2 months, compared with age matched WT mice, which was further increased in 12 months aged KO mice (Figure 3E, F). The thickness of astrocyte perivascular processes in cerebellum, corpus callosum and hippocampus white matter of PGK-TP(co) treated mice were reduced to normal levels (*P*< 0.0001) (Figure 3E, F). In addition, GFAP staining of the cerebellar cortex revealed that Bergmann glia were localized to the molecular layer in KO mice
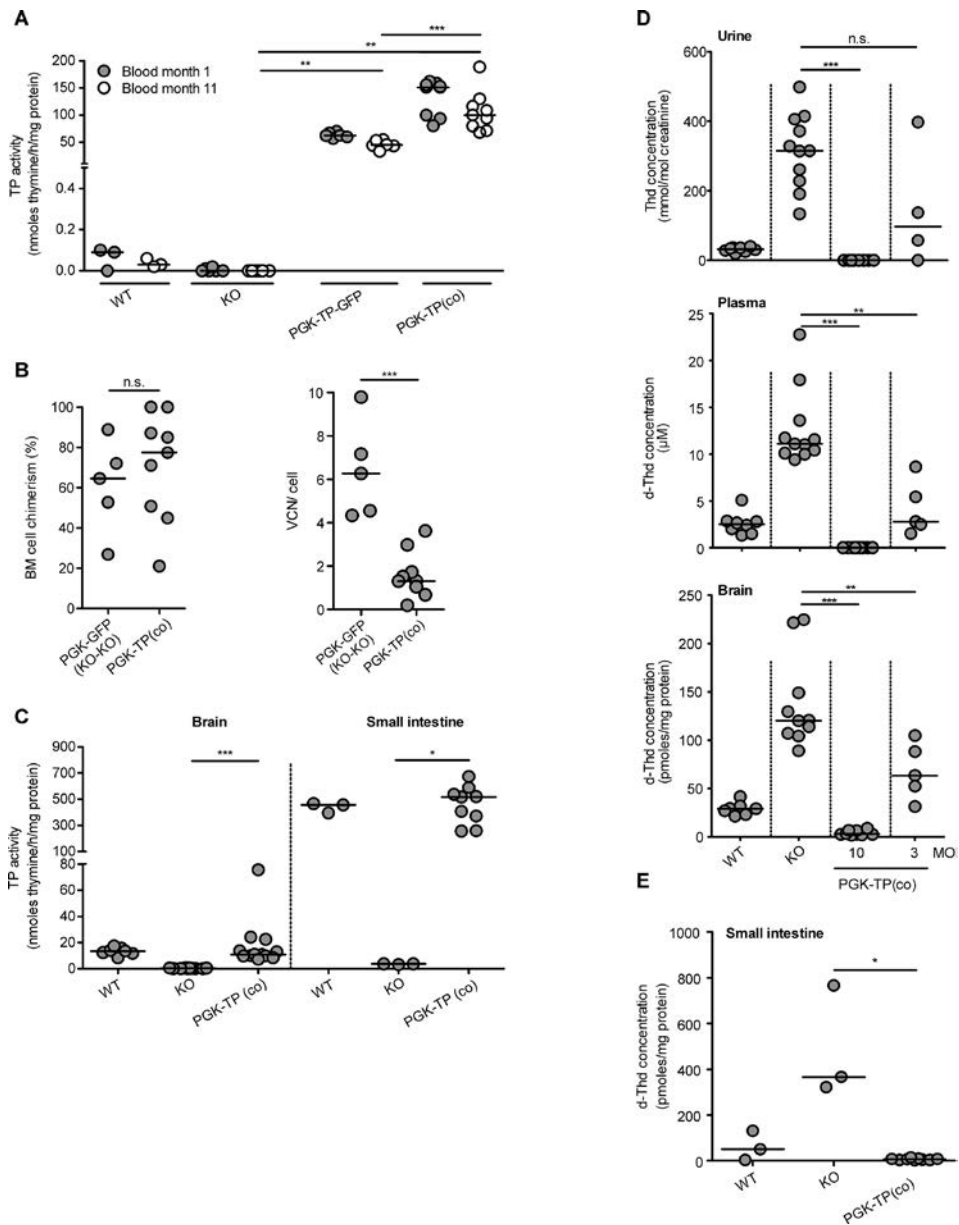
Figure 2. Long-term biochemical correction and molecular chimerism following HSCGT. Lin-cells were transduced with the therapeutic and control LV vectors at MOI 10 and 5×10^5 cells were transplanted into 6 Gy pre-conditioned 2-month-old KO mice. **(A)** TP enzyme activity was measured in blood at months 1 and 11 after transplantation, n=3-9mice/group. **(B)** BM cell chimerism and vector copy number of recipient mice, n=5-9 mice/group. **(C)** Brain and intestine TP activity were measured 11 months after transplantation, n=3-12 mice/group. **(D)** Quantification of Thd in urine, d-Thd in plasma, brain 8-11 months after transplantation (MOI 10, 3), n=4-11 mice /group and **(E)** in intestines 11 months after transplantation, n=3-9 mice /group. The horizontal line represents the median, *P <0.05, **P <0.01 and ***P <0.001, n.s. = not significant.

in contrast to the normal localization in the Purkinje cell layer in WT mice and after treatment (Figure 3G). Altogether, brain MRI and IHC revealed the classical morphological changes in KO mice, however at a younger age and further demonstrated an underlying edema linked to changes of the brain microglia, which are reversed upon HSCGT.

Safety evaluation

Excessive transgene expression-related phenotoxicity and/or genotoxicity caused by LV insertional mutagenesis are potential drawbacks for clinical application of HSCGT. These two issues were not addressed in previous studies [19,20] of HSCGT for MNGIE.

A total of 106 controls and primary recipients of 5×10^5 Lin- cells transduced with therapeutic and GFP LV were monitored for 11 months. Some recipients of PGK-TP or TPco were sacrificed and analyzed prematurely, because of death or high discomfort scores. We have been unable to determine the actual cause of wasting, but importantly, vector positive hematological clonal expansion was not observed (Table 1). At termination, hematopoietic reconstitution between groups was similar, except for a reduction in numbers of spleen CD3+ T-cells in PGK-TP(co) and peripheral blood CD19+ B-cells in SF-TPco treated mice (Figure 4 and Table S1). Nucleosides were not detectable in urine and

Figure 3. Brain magnetic resonance imaging, characterization of brain white matter damage and rescue by HSCGT. Lin- cells were transduced with the therapeutic LV vectors at MOI 10 and $5'10^5$ Lin- cells were transplanted into 6 Gy pre-conditioned 2-month-old KO mice. MRI scans were performed on 2- month-old (young controls) and 6-12-month-old controls and treated mice. **(A)** Representative T2 scans of WT, KO and treated mice. Hyper-intense voxels within the brain (white dotted) were quantified by using a reference ROI (red dotted). **(B)** Results of the quantification of cerebrospinal fluid (CSF) and white matter edema. The data displayed is the percentage of voxels with high signal intensity of the whole brain, *n*= 6-10 mice/group. The horizontal line represents the median. Immunohistochemical staining was performed on brain tissue collected from (young controls) and 12-month-old controls, *n*= 2-3 /group and treated mice 9-10 months after transplantation, *n*= 4 mice. **(C)** Staining for the mature myelin protein proteolipid protein (PLP) of cerebellum of young (left panel and right panels at higher magnification) and old (middle panel) KO and WT female mice shows normal myelin amounts in the cerebellar white matter of a PGK-TP treated mouse. Quantification shows significantly more vacuoles in the cerebellar white matter of KO animals. The horizontal line represents the median, *P<0.05, **P <0.01 and ***P <0.001. **(D)** Staining for the mature myelin protein myelin basic protein (MBP) of the corpus callosum shows myelin pallor in KO compared to WT mice, which is rescued after gene therapy in treated female mice; a section from a recipient of PGK-TPco transduced HSCs is shown. **(E)** Staining for the astrocyte-specific intermediate filament protein glial fibrillary acidic protein (GFAP) shows thicker cellular processes abutting the blood vessels in the cerebellar white matter of KO mice as young as 2 months compared to WT mice. The asterisk indicates the blood vessel lumen. Labeling against GFAP shows thinner perivascular astrocytic processes in the brain of a recipient of PGK-TPco transduced HSCs. **(F)** Thickness of astrocyte processes surrounding blood vessels, *n*≥56 processes/ group. The horizontal line represents the median, ***P<0.0001. **(G)** Stain against the astrocyte-specific intermediate filament protein glial fibrillary acidic protein (GFAP) shows that Bergmann glia (arrows) are located in Purkinje cell layer (PCL) of the cerebellar cortex of WT and a recipient mouse of PGK-TPco transduced HSCs (left and right panels respectively), whereas in KO mice they are mislocalized to the molecular layer (ML) (middle panel), GL; granular layer.

plasma and extremely reduced in the brains of SF-TPco mice as expected due to excessive increase in blood TP activity (Table S2). Although percentage donor chimerism in SF-TPco treated mice was high (Table S2), twelve out of 14 primary recipients were sacrificed prematurely mainly due to severe body weight loss (>15%) observed at death

79
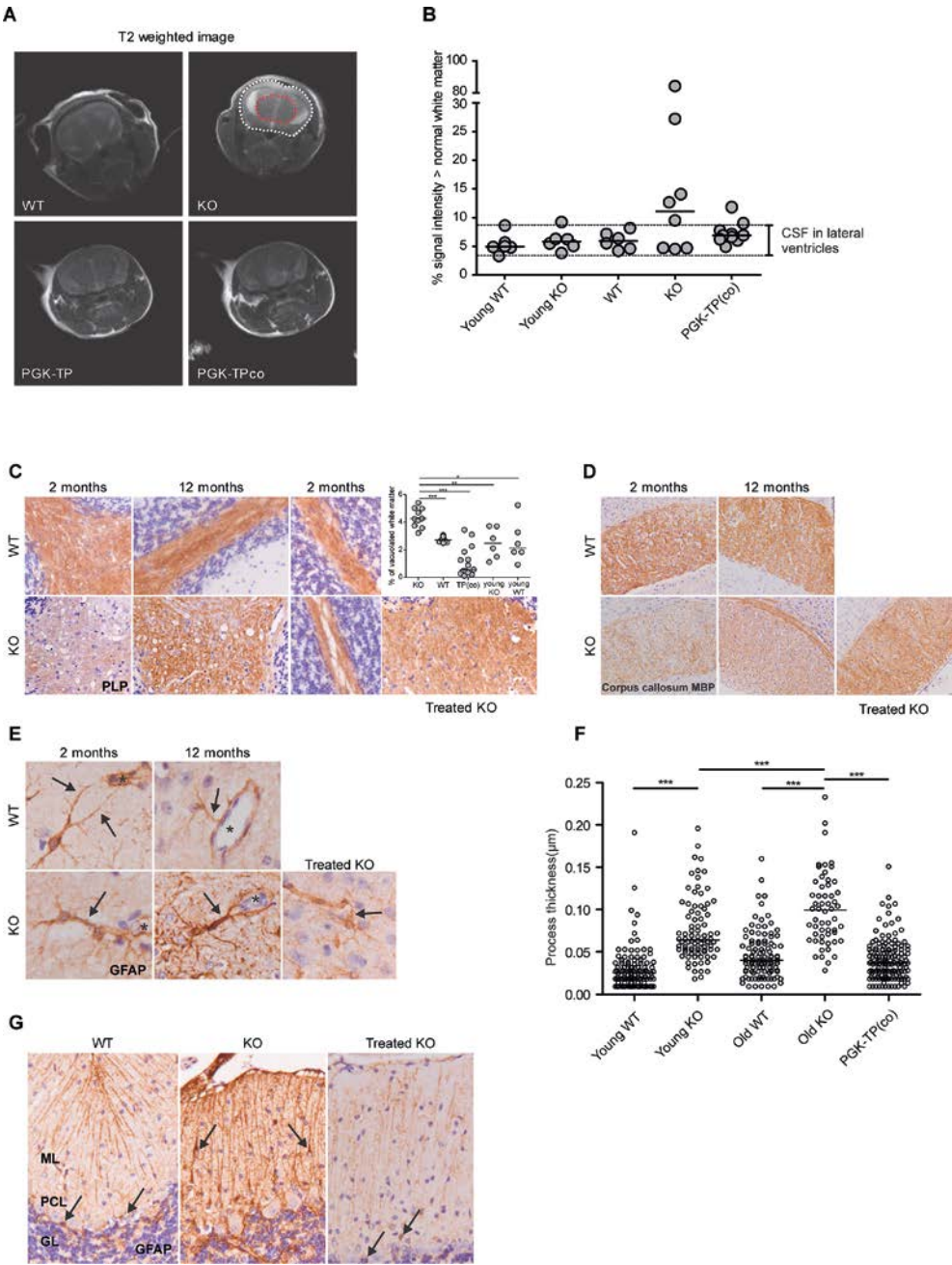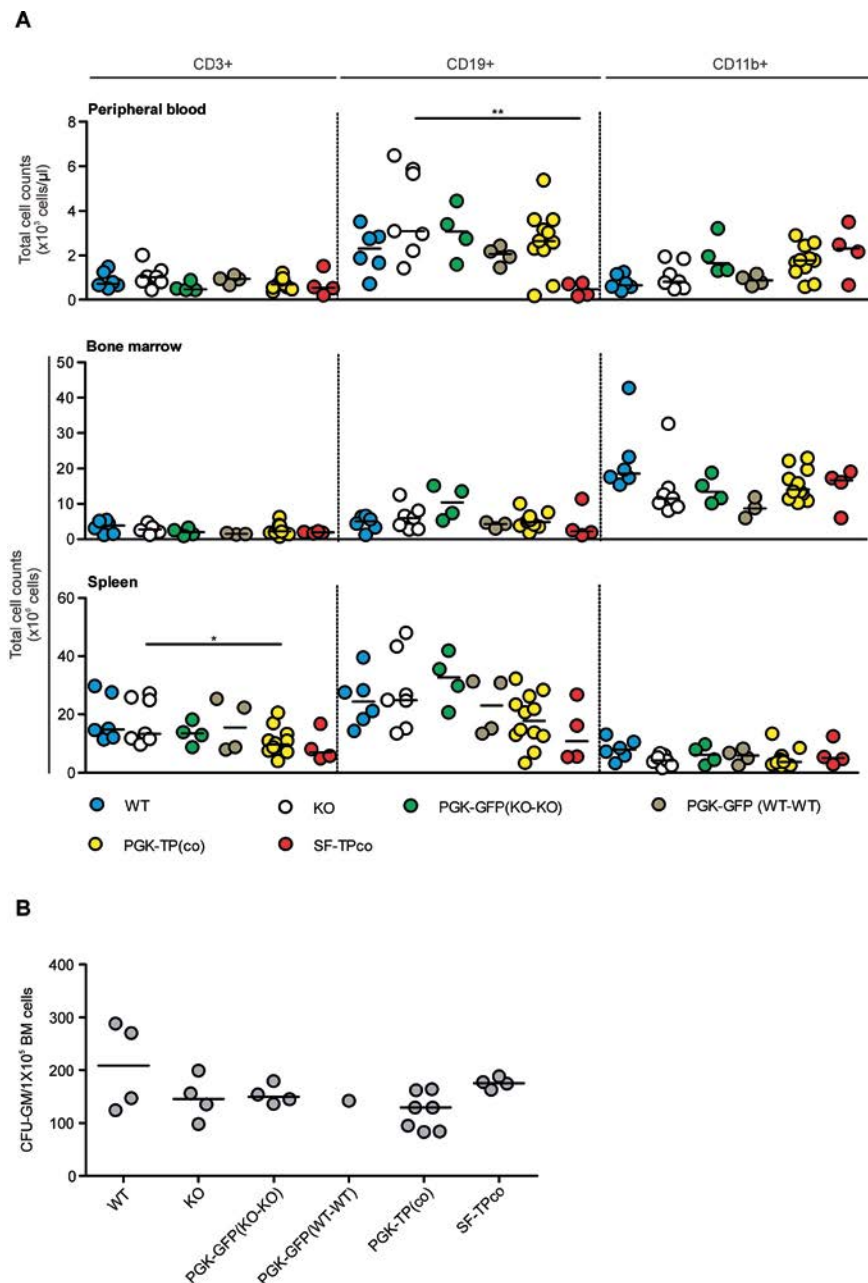
Figure 4. Hematopoietic reconstitution after HSCGT. The following analyses were performed 9-11 months after transplantation of Lin- cells transduced at MOI 10. **(A)** FACS analysis of peripheral blood, bone marrow and spleen cells. Cells were stained with antibodies against CD45.2 and CD3, CD19, CD11b for detection of respectively, T, B and myeloid leukocytes (*n*= 3-12 mice/group), the horizontal line represents the median, *P <0.05, **P<0.01. **(B)** Colony-forming unit assay. BM cells were cultured and granulocyte-monocyte progenitors (CFU-GM) were counted, *n*= 1-6 mice / group. The horizontal line represents the median.

Table 1. Hematological aberrations and clonal expansion of transduced cells were not observed in primary recipient mice.

LV vector	Number of vector-positive hematological aberrations [a]	Number of non-vector-positive hematological aberrations [b]	Number of prematurely dead mice or mice sacrificed with high discomfort scores [c]
WT CTR (n= 13)	0	0	0
KO CTR (n=18)	0	0	1 (macrocephaly)
PGK-GFP [d] (n= 25)	0	0	1 (found dead)
			1 (rectal prolapse)
			1 (passive)
PGK-TP-GFP (n=6)	0	0	0
PGK-TP (n=19)	0	0	1 (plagiocephaly)
			1 (wounds)
			1 (passive)
			1 (epileptic seizure during behavioral test)
			2 (found dead)
			1 (body weight loss) [e]
PGK-TPco (n=11)	0	0	1 (epileptic seizure during behavioral test)
			1 (found dead)
			2 (passive)
SF-TPco (n=14)	0	0	5 (body weight loss)
			1 (kyphosis, body weight loss)
			2 (passive)
			1 (edema)
			1 (found dead)
			2 (kyphosis)

Mice were transplanted with LV transduced 5×10^5 BM Lin- cells (MOI 10) and followed for 11 months after transplantation. CTR, control untreated mice. [a,b] Hematological aberrations and clonal expansion of transduced cells were assessed based on altered FACS phenotypes and/or elevated WBCs, and /or enlarged spleen, thymus or lymph nodes. BM was tested for male donor cells and vector copy number. [c] The right column includes mice that were found dead or mice sacrificed prematurely during the experiment due to high discomfort scores and hematological aberrations could not be identified (details are specified between parenthesis). [d] PGK-GFP group include recipient mice of KO or WT Lin- cells transduced by PGK-GFP. [e] Body weight loss at the time of death >15% over a time span of 1 to 2 months.

(n= 6 out of 12). This increased incidence of weight loss was not observed in PGK-TP or TPco treatment groups (Table 1 and Figure S2). To evaluate genotoxic risk, we analyzed the therapeutic and GFP containing LV vector integration site profiles in mouse Lin-cells in vitro and in BM cells from primary recipient mice (Figure 1B and Figure S3). In total, 7435 unique integration sites (IS) were retrieved by LAM-PCR and sequencing from

4 in vitro samples and 10 transplanted mice (Table 2). A polyclonal integration pattern was observed with 1174 common integration sites (CIS)[28]. In total, 225 IS near oncogenes were identified, accounting for 3.03% of all genes (Table 2). We analyzed the IS patterns for the oncogene frequency between groups classified based on promoter, i.e., PGK vs. SF, or pre-transplantation lineage negative cells vs. bone marrow *in vivo* or transgene GFP vs. TP (co), but no differences were observed (Table 3). To assess genotoxicity further, BM Lin- cells from primary recipients (*n*= 44) were transplanted into 88 secondary

recipients. In both the primary and secondary recipients, we did not observe any vector positive hematological clonal expansion in the therapeutic PGK-TP or PGK-TPco groups (Table S3). In nine recipients of cells LV transduced by PGK-GFP, TP, TPco and SF-TPco vectors altered leukocyte levels and counts revealed hematological aberrations. These cases had very low median VCN/cell (0.03 with range 0.01-0.07) and donor chimerism (0.7% with range 0.2-7.1%, *n*= 8, Table S3) and therefore were classified as non-vector-related. Two PGK-TP-GFP recipients of Lin- cells of a single primary mouse

Table 2. Summary of LV vector integration sites (IS) retrieved by LAM PCR and sequencing

Cell type (donor-recipient)	LV vector	Number of samples	Number of IS	Number of oncogenes	% Oncogenes
In vitro					
Lin- (KO)	PGK-TP	2	3147	102	3.24
Lin- (KO)	SF-TPco	2	2489	74	2.97
In vivo					
BM (WT-WT)	PGK-GFP	2	782	20	2.56
BM (KO-KO)	PGK-TP	5	488	3	0.61
BM (KO-KO)	PGK-TP-IRES-GFP	3	529	26	4.91
	TOTAL	14	7435	225	3.03

Table 3. Summary of LV integration sites (IS) classified based on promoter, cell type and transgene

Group	Number of Samples	Number of IS	Unique genes	Common integration sites (CIS)	Unique oncogenes	Number of Oncogenes	% Oncogenes
All	14	7435	4104	1174	110	226	3.03
PGK only	12	4946	3082	702	87	152	3.07
SF	2	2489	1869	241	52	74	2.97
Lin- (*in vitro*)	4	5636	3408	815	102	177	3.14
BM (*in vivo*)	10	1799	1379	178	35	49	2.72
GFP only	2	782	666	48	17	20	2.56
TP (co)	12	6653	3799	1030	106	206	3.10

developed vector-positive diffuse intermediate to large B220+GFP+ B-cell lymphoma (Table S3) at 9 and 11 months after transplantation. The VCN/ cell and percentage chimerism were 0.86 and 67% in one mouse and 0.76 and 48% in the other mouse. An abundance of abnormally large B cell population of B220+GFP+ cells was observed in BM (Figure S4A) of both mice, i.e., > 80% of total BM cells, (Table S3), spleen and peripheral blood of one mouse. Pathological analysis showed infiltration of malignant B cells in spleen and liver (Figure S4B). The B-cell clone contained a single dominant integration site (IS) in the chromosome 11 gene *Zfp207*. No known oncogenes were found within 500kb of this IS (Figure S4C). Of note; the primary donor mouse had two dominant IS located in the genes *Aplp2* on chromosome 9 and *Csmd3* on chromosome 15, but the *Zfp207* IS was not detected by LAM-PCR. Primer specific PCR amplification confirmed very low presence of this IS in bone marrow and spleen (data not shown). Besides the miscellaneous symptoms observed in therapeutic PGK-TP(co) treated mice, which are not likely to be related to the gene therapy procedure, phenotoxicity was observed in the SF treatment group, i.e. severe weight loss in the majority of the treated cohort. Hematological abnormalities or increased risk of insertional mutagenesis were not observed in the group of mice receiving the therapeutic vectors.

|DISCUSSION

The present study, using a clinically applicable SIN LV vector with a modified WPRE and without GFP and a highly efficient, overnight gene transfer procedure, demonstrates not only full biochemical correction, but, importantly, also complete clearance of intestinal nucleosides and a remarkable phenotype correction in the brain of *Tymp^{-/-}Upp1^{-/-}* mice. Overall, the biochemical correction obtained in blood and tissues reported earlier by using PGK-TP-GFP [20] was confirmed here in a larger cohort of mice by using the therapeutic vectors LV-PGK-TP(co). The additional complete clearance of intestinal nucleosides and remarkable phenotypic correction in the brain demonstrates the feasibility of a curative gene therapy approach for MNGIE patients.

In MNGIE patients, the intestines are severely affected, resulting in cachexia, severe infections and death. The intestine facilitates uptake of nutrients possibly requiring high TP enzyme activities to reduce incoming thymidine levels locally. Of note, intestinal TP activity in WT mice is substantially higher than that in blood and brain tissue (Figure 2A, C), which emphasizes that high TP activity levels in intestine are likely required to normalize nucleosides. In our study, therapeutically relevant transduction efficiencies by PGK-TP(co) (median VCN/ cell= 1.3 (range, 0.2-3.6, Figure 2B) resulted in complete clearance of intestinal nucleosides, in contrast to the earlier study[20] in which d-Thd was significantly reduced in plasma and brain, but not in the intestine. In addition to the high liver and muscle TP activity, this finding of an improved biochemical correction supports our low vector MOI (3, 10 vs.100[20]) and pre-transplant conditioning protocol.

The current experiments, performed with high transduction efficiency and dose,

resulted in supranormal levels of TP activity and in near complete elimination of systemic nucleosides, i.e., below WT levels, indicating that lower enzyme levels should be sufficient to correct the biochemical imbalance. For gene modified and vector dose titration experiments relatively large cohorts of mice are required to demonstrate a dose response relationship. However, whether or not lower cell and LV dose would be efficient is of doubt, since the small intestine requires a high cell dose and an MOI of 10 to normalize TP activity and nucleosides (Figure 2C, E, S1B). The absence of a clear clinical phenotype is a limitation of the only murine disease model of MNGIE, and very few pathological findings have been reported, mainly in *Tymp*^{-/-}*Upp1*^{-/-} mice aged ≥18 months[22]. In the present study, we observed pathological white matter changes in KO animals as early as at 2 months of age and MRI changes at 6 months of age, which resembled findings in the brain of MNGIE patients, i.e., edema without demyelination or gliosis and hyperintense T2-weighted signal changes[8, 29]. Importantly, HSCGT resulted in elevated TP activity restoring brain white matter integrity and reducing edema as evident by MRI and IHC. Another study of MNGIE patients demonstrated that loss of brain TP was associated with loss of blood brain barrier integrity, which resulted in activation of astrocytes[30]. We showed increased astrocytic process thickness in *Tymp*^{-/-}*Upp1*^{-/-} mice, which is limited to the cell processes abutting blood vessels, which argues against reactive astrogliosis and rather suggests swelling of the astrocyte perivascular end-feet. Such a phenotype might be responsible for the observed progressive intramyelinic edema in *Tymp*^{-/-}*Upp1*^{-/-} mice as reported in

other white matter diseases[31] and could be explained by an interference with the normal function of astrocytes in maintaining ion-water homeostasis[32]. The latter finding argues for further research to investigate the molecular mechanisms underlining brain pathophysiology in MNGIE.

We did not demonstrate TP positive hematopoietic cells in the brain, however, previous murine gene therapy studies using AAV2/8 vectors[21] transducing the liver showed reversal of nucleoside imbalance without the local presence of TP in the brain. However, in HSCGT, gene modified monocyte progenitors may migrate to the brain and differentiate into microglia[33]. Since TP is a cytoplasmic protein, we measure this TP activity in the brain (Figure 2C), indicating that transduced microglia might reside in the brain after long-term follow-up. Despite the brain pathology in *Tymp*^{-/-}*Upp1*^{-/-} mice , we could not detect significant differences in several memory and motor function assessments, which involved cerebellum, cortex and hippocampus, between the *Tymp*^{+/+}*Upp1*^{+/+}, *Tymp*^{-/-}*Upp1*^{-/-} and gene therapy treated mice (data not shown). This could be attributed to differences in physiology and life span between mice and man. Other leukodystrophy mouse models, including those for megalencephalic leukoencephalopathy with subcortical cysts similarly lack a clinical phenotype despite the presence of severe pathological abnormalities[31]. Similar to the analysis of MNGIE human brains[30], we did not detect mtDNA depletion, deletions or any changes in mtDNA topology or strand breaks. Although the variation between individual mice is large, *Tymp*^{-/-}*Upp1*^{-/-}and treated mice showed signs of replication stalling in brain tissue (data not shown), which requires further investigation.

Of major concern, as yet unaddressed is the potential transgene or LV- related phenotoxicity or genotoxicity. More experiments are required to elucidate the nature of the toxicity observed in the SF treatment group. We did not observe loss of vector-transduced cells in the hematopoietic compartment, so overexpression has no direct effect on hematopoietic cells. Additionally, the toxicity is not related to the LV vector since LV-PGK-GFP did not show toxicity (Table 1 and Figure S2). Therefore, we assume that the observed toxicity is related to the excessively expressed TP by the strong SF promoter, the increased mortality likely due to complete elimination of d-Thd and/or d-Urd affecting downstream mitochondrial dNTPs. dNTPs pool imbalance triggers cell cycle arrest and apoptosis in vitro in hematopoietic cell lines and yeast variants[34, 35], which, however, needs further investigation in $Tymp^{-/-}Upp1^{-/-}$ mice. Using the therapeutic vectors, oncogenic adverse effects were not observed after a total follow-up in primary and secondary recipient mice of 22 months, demonstrating the safety profile of PGK driven TP expression. A single, possibly insertional, oncogenic event was observed in the PGK-TYMP-IRES-GFP treated mice. Two secondary recipients acquired the same B-cell lymphoma clone with the PGK-TP-GFP vector integrated near the $Zfp207$ gene, which could be traced back to one primary recipient mouse. $Zfp207$ or its human homolog is not reported as a proto-oncogene, but has a role in cell cycle and mitotic nuclear division: in particular, ZFP207 is required for proper chromosome alignment[36] and $Zfp207$ knockdown has been associated with lethal chromosome congression defects in transformed cells[37]. The B-cell lymphoma

contained a lentiviral integration with an early version Woodchuck hepatitis virus PRE element. Although reports have never shown unequivocally that the use of such a PRE element carries additional insertional oncogenic risks, our therapeutic lentiviral vectors contain a mutated element (bPRE4*) to reduce risks further[38]. Since the lymphomas in the secondary transplanted mice were identical, the oncogenic event necessarily occurred in the primary transplanted mouse. The integration near the $Zfp207$ gene might have contributed to the development or expansion of this clone, but it is not excluded that the observed lymphoma is not related to vector integration at all, which would require further investigation of potentially oncogenic mutations.

In summary, the therapeutic PGK-TP(co) vectors provided sufficient expression for biochemical and phenotypic correction without detectable phenotoxicity and a favorable safety profile, similar to the LV vectors currently in clinical trial for other inherited disorders. Nonetheless, excessive TP expression in the LV-SF treatment group, not intended for clinical application, resulted in reduced survival (Table 1), a finding in need of further investigation and underlining the requirement of a moderately strong house-keeping gene promoter such as PGK for clinical application in MNGIE, possibly in combination with low-intensity or non-myeloablative conditioning. It is concluded that the present study warrants further development including cell and vector dose response experiments with a larger cohort of mice, biodistribution studies and assessment in human hematopoietic cells, aiming at clinical implementation of a curative intervention therapy for MNGIE.

4

|MATERIALS AND METHODS

Lentiviral vectors

The self-inactivating transfer vector (SIN) pCCL- hPGK-TP-IRES-GFP-WPRE was described before, and is used in our study as a control[19]. The human *TYMP* sequence from this LV vector, a re-coded *TYMP* sequence (human TPco, GenScript, Piscataway, NJ, USA)[24] with optimized open reading frame (Genscript algorithm) with a consensus Kozak sequence and an additional stop codon, and the green fluorescent protein *GFP* sequence were all cloned into the pRRL-SIN-bPRE4* backbone under the human PGK promoter [38]. Human TPco was also cloned under the SF promoter (Figure 1A). Third-generation packaging plasmids pMDL-g/pRRE, pRSV. REV and envelop plasmid pMD2-VSVg were used[39]. LV vectors were generated by calcium-phosphate precipitation of HEK293T cells[40]. 48 hours after transfection, lentiviral vectors were concentrated by ultracentrifugation at 20, 000 rpm for 2 h at 4°C and the pellets resuspended in PBS. LV vector titration was performed on HeLa cells. After 72 hours, cells were analyzed on an LSR-II flow cytometer and FACS diva software to calculate the titers of a GFP containing batch. Titers of TP, TPco containing vectors were determined by qPCR.

HSC transduction, and primary and secondary transplantation

The generation of *Tymp^{-/-}Upp1^{-/-}* (KO) and *Tymp^{+/+}Upp1^{+/+}* wild type (WT) mice on a C57BL/6J genetic background have been described before[22]. The animals were bred in the Erasmus MC Experimental Animal Center (Rotterdam, The Netherlands). During the experiments, mice were kept in filter top cages, fed with autoclaved water and irradiated chow *ad libitum*. The animal experiments were reviewed and approved by an ethical committee of Erasmus MC, Rotterdam in accordance with legislation in the Netherlands.

Bone marrow cells were harvested aseptically from femurs and tibiae of 4 to 19 week-old male mice by flushing with PBS, followed by lineage depletion (Lin-) according to manufacturer recommendations (BD Biosciences). Lin- cells were cultured overnight in the presence of the LV vector constructs at a multiplicity of infection (MOI) of 10 or 3 in serum-free modified Dulbecco's medium with supplements[41] and stimulated with murine stem cell factor (SCF, 100ng/mL), human FMS-like tyrosine kinase 3 ligand (Flt3-L, 50 ng/mL), murine thrombopoietin (TPO, 20 ng/mL). Subsequently, lin- transduced cells (5×10^5) were injected into the tail vein of 4 to 17 weeks of age recipient KO or WT female mice, subjected to 6 Gy irradiation twenty-four hours prior to transplantation. For the secondary transplantation, similarly each of two 5 to 14 week aged KO female recipients were transplanted with 2×10^5 enriched Lin- cells from viable cryopreserved bone marrow of a single primary recipient mouse (Figure 1B).

Sample collection, analysis and termination of experiments

During the course of experiments, primary and secondary recipient mice were monitored carefully for any signs of discomfort. Body weights and leukocyte phenotypes were measured monthly up to six months post transplantation in some primary recipients. Complete blood cell counts (CBCs)

and leukocyte phenotypes of secondary recipients were monitored three months after transplantation. When applicable, blood and urine samples for biochemical analysis were collected. Mice were removed from experiments if they appeared ill, had severe body weight loss of >15%, had changes in behavior, or for other reasons, for example malocclusion or fight wounds. The following analyses were performed at experimental end point or at death when possible. EDTA peripheral blood and urine samples were collected on ice and stored at -80°C for biochemical analysis. Mice were sacrificed by inhalation of a CO2/O2 mixture and were trans-cordially perfused with PBS. The following was performed: assessment of body weights, physical appearance, presence of abnormality such as pale feet, rectal prolapse, injuries, lumps (tumors, cysts), visual examination of major organs (heart, lung, brain, liver, kidney, gastrointestinal tract, spleen, thymus, lymph nodes), documentation of organomegaly (spleen, thymus, lymph nodes) and processing of samples from lesions and enlarged organs for H&E staining/ IHC. Tissue samples were snap-frozen in liquid nitrogen and stored at -80°C for biochemical analysis. CBCs were measured using automated equipment (scil Vet ABC Hematology Analyzer, Gurnee, IL). Leukocytes, spleen cells and fractions of total bone marrow were used for FACS analysis. In some experiments, bone marrow cells were cultured to assess progenitor cell content by colony assays. Aliquots of bone marrow cells were stored at -80°C for molecular analysis as described below and the remainder of the bone marrow cells was cryopreserved for retransplantation. For testing the risk of insertional oncogenesis, hematological

aberrations were based on abnormal FACS phenotype of at least one of the hematopoietic tissues BM, spleen or peripheral blood and/ or white blood cell counts (WBC) (further analyzed for leukemia in case WBC > 25.0 x 10^3 cells/µl) and /or enlarged spleen, thymus or lymph nodes. The hematological aberration was considered a potential oncogenic clone if both donor cells and VCN were prominent in the recipient's BM sample.

Flow cytometry

Erythrocytes were removed with lysis buffer (0.15M NH4Cl, 0.1M EDTA) and leukocytes, bone marrow and spleen cells were washed with Hank's balanced salt solution (Invitrogen) containing 0.5% (wt/ vol) bovine serum albumin and 0.05% (wt/ vol) sodium azide (HBN) followed by 30 min incubation at 4°C in HBN containing 2% heat-inactivated normal mouse serum and antibodies against CD45.2, CD3, CD19, CD11b , directly conjugated respectively to APC-Cy7, APC, PE, PerCP-Cy5.5; or, against CD8, CD45R/B220, Gr-1, c-Kit or CD4, IgD, CD19, Sca-1 or CD3, IgM, CD11b, directly conjugated respectively to APC, PE or PerCP (Cy5.5) (BD biosciences and Biolegend, UK, London). Cells were washed and measured on a Canto or LSR-II flow cytometer (BD).

Progenitor cell assay

To detect colony forming unit granulocyte monocyte (CFU-GM), 5×10^4 total bone marrow cells in 10% of the total volume were seeded in semisolid methylcellulose 80% of the total volume (MethoCult M3231, Stem cell technology, France) with 10% of the total volume IMDM supplemented with rm-Stem cell factor (100 ng/ml), rm-Interleukin3 (30

ng/ml) and rm-GM-CSF (30 ng/ml) (R&D systems). Cultures were incubated at 37 °C in a humidified atmosphere containing 5% CO_2 and colonies were scored seven days later under an inverted microscope.

Biochemical analysis of TP enzyme activity and nucleoside levels

TP enzyme activity in blood cells, tissue samples and plasma d-Thd and d-Urd levels were measured by liquid chromatography (UPLC-UV), while tissue d-Thd and d-Urd levels were measured by liquid chromatography–mass spectrometry (HPLC-MS) as described before[19, 21]. Urinary Thd and d-Urd were measured by HPLC[42]. Urine samples were thawed to room temperature by incubation at 37C° for 30 min prior to measurement of concentrations. One volume of sample plus 1 volume of internal standard solution was diluted with 1 volume of eluent A (30 μmM ammonium acetate, 1% Methanol, pH 4.80). The samples were incubated at 60 °C for 30 min, followed by centrifugation on filter units at room temperature at 13.000 g for 20 min. 20 μl of filtrates were then injected into HPLC system (Shimadzu, LC20 series with a binary pump and Photodiode array detector), equipped with an Alltima C18 5μ, 250 mm x 4.6 mm column and Alltima C18 5μ guard column. Chromatography was performed as described before[42]. Concentrations were calculated by comparison of the Thd and d-Urd peak areas in samples to the corresponding peak areas of standards using caffeïne as an internal standard to correct for injection volume. Creatinine concentrations of the samples were measured in the same runs.

Q-PCR and western blotting

KO Lin- cells were transduced by PGK-TP, PGK-TPco or SF-TPco (MOI 10) and cultured *in vitro* for seven days. Total RNA was extracted and 1 μg was reverse transcribed into cDNA (RNeasy MicroKit and QuantiTect Reverse Transcription Kit, Qiagen GmbH, Hilden, Germany) following manufacturer's instructions. Genomic DNA isolation from both cultured Lin- cells and bone marrow cells was performed by using NucleoSpin Tissue kits (Bioké, Leiden, The Netherlands) following manufacturer's protocol. RNA and DNA concentration and purity were determined by using Nanodrop (Nano Drop 1000Spectrophotometer). Template cDNA and 100ng template genomic DNA were subject to qPCR by using SYBR Green PCR master mix and the primers described before[26, 43, 44] and summarized in Table S4 (Applied Biosystems, Foster City, CA; Eurogentec, Maastricht, The Netherlands). The PCR reactions were carried out in the ABI7900, Taqman machine and results were analyzed with SDS2.2.2 software (Applied Biosystems). The average vector copy per cell were calculated by comparing the cycle threshold values obtained against a standard curve obtained from mouse 3T3 or Hela cells, and to calculate Y chromosome chimerism a standard curve is obtained from male mice bone marrow samples.

Western blotting was performed by using Novex midi gel system for electrophoresis and blotting (Invitrogen, Carsland, CA) following manual's instructions. Cultured Lin- cells were lysed by sonication, protein concentrations were determined by using BCA protein assay kit (Thermo Fisher) and a total of 15 μg proteins were separated by 4-12% Bis-Tris SDS– PAGE, transferred to nitrocellulose and

PVDF membranes and blotted with primary and secondary antibodies (summarized in Table S5) and finally signals were detected with enhanced chemiluminescent substrates detection kit (Thermo Fisher). Image J software was used to quantify protein levels.

Vector integration sites

In order to identify vector integration sites vector LTR-genome junctions were amplified by LAM-PCR as previously described[45, 46]. Briefly, after linear amplification with biotinylated LTR-specific primers, amplification products were purified using streptavidin magnetic beads. The following steps included complementary strand synthesis, parallel digestion with 3 different restriction enzymes (Tsp509 I, HpyCH4 IV and Aci I), and ligation to a linker cassette. The fragments generated were then amplified by two additional exponential PCR steps. LAM-PCR products were separated by gel electrophoresis on Spreadex high resolution gels (Elchrom Scientific), underwent a fusion PCR for the addition of barcoded adaptors, were pooled into libraries and Illumina sequenced (MiSeq) as previously described[47]. The resulting sequences were processed through a customized informatics pipeline[46], and (Leonardelli *et al.* ASGCT 2016 abstract) which performs cleaning for quality and collisions, mapping and annotating of IS on the mouse Genome (Dec. 2011, GRCm38/mm 10).

mtDNA analysis

Mitochondrial DNA copy number, conformation and integrity were evaluated in total and mitochondrial DNA extracted from tissue samples[48, 49]. Briefly, mtDNA

copy number was determined by Real time-PCR using primers and Taqman probes for mitochondrial and NDUVF1 and the AccuStartII PCR supermix (QuantaBio). The respective primer sequences are summarized in Table S4. To quantify the levels of existing mtDNA strand breaks, mitochondrial DNA and free 3' ends were labeled *in vitro* using radioactive incorporation of dCTP by terminal deoxynucleotide transferase. 0.5 μg of purified mtDNA was incubated with 5 uCi dCTP (3000 Ci/mmol) and 7.5 U TdT in 30 μl 1x TdT buffer at 37°C for 30 min and separated over a 1% TBE/agarose gel containing 0.1 μg/μl ethidium bromide. Equal loading was confirmed by UV visualization, the gel was Southern blotted onto Hybond-XL membrane and the intensity of each lane was quantified by phosphor imaging (Molecular Imager FX, BioRad). The abundance of replication intermediates was visualized using Brewer/Fangman 2D neutral/neutral agarose electrophoresis. MtDNA deletions were detected by long-range PCR as previously described[50] and visualized by Phosporimager.

Magnetic resonance imaging (MRI)

Imaging was performed on a 7.0 T dedicated animal scanner (Discovery MR901, Agilent Technologies/GE Healthcare) using a 4-channel surface receiver coil (Rapid MR International, Ohio, USA) and a 72 mm transmit body coil. Single shot fast spin echo (SSFSE) images were acquired with settings: TR/TE = 1600/8 ms, FOV = 5cm, voxel size 0.2x0.2x1 mm. T2 images were additionally acquired using a fast pin echo sequence for anatomical reference, settings: TR/TE = 2500/25 ms, FOV = 5cm, voxel size 0.2x0.2x1 mm.

Image analysis: The SSFSE is very sensitive for high liquid content and therefore, by using these images, the signal intensity (SI) of voxels with high liquid content is much higher than that of other tissue. This allowed us to determine the fraction of edematic tissue by selecting voxels through thresholding after segmentation of the whole brain. The threshold was determined by quantifying normal tissue values by determining a reference region of interest (ROI) within normal brain tissue. This ROI was manually drawn in a slice of brain without hyper-intense areas. Voxels with SI of 4 standard deviations above the reference ROI SI were considered to have high liquid content (4 sd = 99.9% confidence interval). The analysis was performed using in-house developed software based on MATLAB (MathWorks, Natick, MA, USA).

Immunohistochemistry (IHC)

Mice were euthanized by inhalation of a CO_2/O_2 mixture and transcardially perfused with PBS to remove blood. Brains were extracted and immersion-fixed in 4% paraformaldehyde for 24hr, paraffin-embedded and cut longitudinally to obtain 6 μm-thick sections. Staining was performed as previously described[31]. Antigen retrieval was performed by treatment with 0.01M citrate buffer (pH 6.00) in a steamer, and endogenous peroxidase blocked with 0.3% H_2O_2 in methanol. Sections were blocked in 5% normal goat serum then incubated overnight at 4°C with the primary and secondary antibodies summarized in Table S5. Immunoreactivity was detected with 3-3'-diaminobenzidine as chromogen. Sections were finally counterstained with hematoxylin and visualized under a Leica DM6000B microscope. Omitting the primary antibodies yielded no significant staining. Image series from brain sections stained with H&E or against protein proteolipid protein (PLP) or the glial fibrillary acidic protein (GFAP) were obtained with a ×40 objective. Quantification of vacuoles and astrocytes morphology was performed blind to the genotype using ImageJ. The percentage of cross-sectioned area occupied by vacuoles was quantified in the cerebellar and callosal white matter. The thickness of perivascular astrocytic cell processes at the maximal width was measured.[51]

Statistical analysis

Significance of differences between groups was determined by two-tailed Mann-Whitney *U* test. Data was graphed and analyzed by Graph Pad-Prism5 software (version 5.03).

|CONFLICT OF INTEREST STATEMENT

The authors declare no conflict of interest.

4

|AUTHOR CONTRIBUTIONS

Conceptualization, R.Y., N.P., M.S., I.F.M., G.W.; Investigation, R.Y., R.C., J.T.T., M.B., J.H., E.B., S.G., E.H.J., R.V.; Formal analysis, R.Y., R.C., J.T.T., M.B., N.P., J.H., M.H., E.B., S.G., E.H.J., L.L.; Writing – Original Draft, R.Y.; Writing – Review & Editing, R.Y., N.P. I.F.M. and G.W.; Funding Acquisition, I.F.M, G.W.; Resources, L.B., M.B.,G.R., R.M.; Supervision, N.P., I.F.M.

|REFERENCES

1. Hirano, M., Nishigaki, Y., and Marti, R. (2004). Mitochondrial neurogastrointestinal encephalomyopathy (MNGIE): a disease of two genomes. Neurologist 10, 8-17.

2. Massa, R., Tessa, A., Margollicci, M., Micheli, V., Romigi, A., Tozzi, G., et al. (2009). Late-onset MNGIE without peripheral neuropathy due to incomplete loss of thymidine phosphorylase activity. Neuromuscul Disord 19, 837-840.

3. Valentino, M. L., Marti, R., Tadesse, S., Lopez, L. C., Manes, J. L., Lyzak, J., et al. (2007). Thymidine and deoxyuridine accumulate in tissues of patients with mitochondrial neurogastrointestinal encephalomyopathy (MNGIE). FEBS Lett 581, 3410-3414.

4. Hirano, M., Silvestri, G., Blake, D. M., Lombes, A., Minetti, C., Bonilla, E., et al. (1994). Mitochondrial neurogastrointestinal encephalomyopathy (MNGIE): clinical, biochemical, and genetic features of an autosomal recessive mitochondrial disorder. Neurology 44, 721-727.

5. Gonzalez-Vioque, E., Torres-Torronteras, J., Andreu, A. L., and Marti, R. (2011). Limited dCTP availability accounts for mitochondrial DNA depletion in mitochondrial neurogastrointestinal encephalomyopathy (MNGIE). PLoS Genet 7, e1002035.

6. Marti, R., Verschuuren, J. J., Buchman, A., Hirano, I., Tadesse, S., van Kuilenburg, A. B., et al. (2005). Late-onset MNGIE due to partial loss of thymidine phosphorylase activity. Ann Neurol 58, 649-652.

7. Chapman, T. P., Hadley, G., Fratter, C., Cullen, S. N., Bax, B. E., Bain, M. D., et al. (2014). Unexplained gastrointestinal symptoms: think mitochondrial disease. Dig Liver Dis 46, 1-8.

8. Simon, L. T., Horoupian, D. S., Dorfman, L. J., Marks, M., Herrick, M. K., Wasserstein, P., et al. (1990). Polyneuropathy, ophthalmoplegia, leukoencephalopathy, and intestinal pseudo-obstruction: POLIP syndrome. Ann Neurol 28, 349-360.

9. Morato, L., Bertini, E., Verrigni, D., Ardissone, A., Ruiz, M., Ferrer, I., et al. (2014). Mitochondrial dysfunction in central nervous system white matter disorders. Glia 62, 1878-1894.

10. la Marca, G., Malvagia, S., Casetta, B., Pasquini, E., Pela, I., Hirano, M., et al. (2006). Pre- and post-dialysis quantitative dosage of thymidine in urine and plasma of a MNGIE patient by using HPLC-ESI-MS/MS. J Mass Spectrom 41, 586-592.

11. Lara, M. C., Weiss, B., Illa, I., Madoz, P., Massuet, L., Andreu, A. L., et al. (2006). Infusion of platelets transiently reduces nucleoside overload in MNGIE. Neurology 67, 1461-1463.

12. Bax, B. E., Bain, M. D., Scarpelli, M., Filosto, M., Tonin, P., and Moran, N. (2013). Clinical and biochemical improvements in a patient with MNGIE following enzyme replacement. Neurology 81, 1269-1271.

13. Halter, J. P., Michael, W., Schupbach, M., Mandel, H., Casali, C., Orchard, K., et al. (2015). Allogeneic haematopoietic stem cell transplantation for mitochondrial neurogastrointestinal encephalomyopathy. Brain 138, 2847-2858.

14. Yadak, R., Sillevis Smitt, P., van Gisbergen, M. W., van Til, N. P., and de Coo, I. F. M. (2017). Mitochondrial Neurogastrointestinal Encephalomyopathy Caused by Thymidine Phosphorylase Enzyme Deficiency: From Pathogenesis to Emerging Therapeutic Options. Frontiers in Cellular Neuroscience 11.

15. De Giorgio, R., Pironi, L., Rinaldi, R., Boschetti, E., Caporali, L., Capristo, M., et al. (2016). Liver transplantation for mitochondrial neurogastrointestinal encephalomyopathy. Ann Neurol 80, 448-455.

16. Cartier, N., Hacein-Bey-Abina, S., Bartholomae, C. C., Veres, G., Schmidt, M., Kutschera, I., et al. (2009). Hematopoietic stem cell gene therapy with a lentiviral vector in X-linked adrenoleukodystrophy. Science 326, 818-823.

17. Biffi, A., Montini, E., Lorioli, L., Cesani, M., Fumagalli, F., Plati, T., et al. (2013). Lentiviral hematopoietic stem cell gene therapy benefits metachromatic leukodystrophy. Science 341, 1233158.

18. Wagemaker, G. (2014). Lentiviral hematopoietic stem cell gene therapy in inherited metabolic disorders. Human gene therapy 25, 862-865.

19. Torres-Torronteras, J., Gomez, A., Eixarch, H., Palenzuela, L., Pizzorno, G., Hirano, M., et al. (2011). Hematopoietic gene therapy restores thymidine phosphorylase activity in a cell culture and a murine model of MNGIE. Gene Ther 18, 795-806.

20. Torres-Torronteras, J., Cabrera-Perez, R., Barba, I., Costa, C., de Luna, N., Andreu, A. L., et al. (2016). Long-Term Restoration of Thymidine Phosphorylase Function and Nucleoside Homeostasis Using Hematopoietic Gene Therapy in a Murine Model of Mitochondrial Neurogastrointestinal Encephalomyopathy. Human gene therapy 27, 656-667.

21. Torres-Torronteras, J., Viscomi, C., Cabrera-Perez, R., Camara, Y., Di Meo, I., Barquinero, J., et al. (2014). Gene therapy using a liver-targeted AAV vector restores nucleoside and nucleotide homeostasis in a murine model of MNGIE. Mol Ther 22, 901-907.

22. Lopez, L. C., Akman, H. O., Garcia-Cazorla, A., Dorado, B., Marti, R., Nishino, I., et al. (2009). Unbalanced deoxynucleotide pools cause mitochondrial DNA instability in thymidine phosphorylase-deficient mice. Hum Mol Genet 18, 714-722.

23. Aiuti, A., Biasco, L., Scaramuzza, S., Ferrua, F., Cicalese, M. P., Baricordi, C., et al. (2013). Lentiviral hematopoietic stem cell gene therapy in patients with Wiskott-Aldrich syndrome. Science 341, 1233151.

24. Huston, M. W., van Til, N. P., Visser, T. P., Arshad, S., Brugman, M. H., Cattoglio, C., et al. (2011). Correction of murine SCID-X1 by lentiviral gene therapy using a codon-optimized IL2RG gene and minimal pretransplant conditioning. Mol Ther 19, 1867-1877.

25. van Til, N. P., de Boer, H., Mashamba, N., Wabik, A., Huston, M., Visser, T. P., et al. (2012). Correction of murine Rag2 severe combined immunodeficiency by lentiviral gene therapy using a codon-optimized RAG2 therapeutic transgene. Mol Ther 20, 1968-1980.

26. Modlich, U., Schambach, A., Brugman, M. H., Wicke, D. C., Knoess, S., Li, Z., et al. (2008). Leukemia induction after a single retroviral vector insertion in Evi1 or Prdm16. Leukemia 22, 1519-1528.

27. Zhou, S., Ma, Z., Lu, T., Janke, L., Gray, J. T., and Sorrentino, B. P. (2013). Mouse transplant models for evaluating the oncogenic risk of a self-inactivating XSCID lentiviral vector. PLoS One 8, e62333.

28. Deichmann, A., Brugman, M. H., Bartholomae, C. C., Schwarzwaelder, K., Verstegen, M. M., Howe, S. J., et al. (2011). Insertion sites in engrafted cells cluster within a limited repertoire of genomic areas after gammaretroviral vector gene therapy. Mol Ther 19, 2031-2039.

29. Bardosi, A., Creutzfeldt, W., DiMauro, S., Felgenhauer, K., Friede, R. L., Goebel, H. H., et al. (1987). Myo-, neuro-, gastrointestinal encephalopathy (MNGIE syndrome) due to partial deficiency of cytochrome-c-oxidase. A new mitochondrial multisystem disorder. Acta Neuropathol 74, 248-258.

30. Szigeti, K., Sule, N., Adesina, A. M., Armstrong, D. L., Saifi, G. M., Bonilla, E., et al. (2004). Increased blood-brain barrier permeability with thymidine phosphorylase deficiency. Ann Neurol 56, 881-886.

31. Dubey, M., Bugiani, M., Ridder, M. C., Postma, N. L., Brouwers, E., Polder, E., et al. (2015). Mice with megalencephalic leukoencephalopathy with cysts: a developmental angle. Ann Neurol 77, 114-131.

32. van der Knaap, M. S., Boor, I., and Estevez, R. (2012). Megalencephalic leukoencephalopathy with subcortical cysts: chronic white matter oedema due to a defect in brain ion and water homoeostasis. Lancet Neurol 11, 973-985.

33. Hoogerbrugge, P. M., Suzuki, K., Suzuki, K., Poorthuis, B. J, Kobayashi, T., Wagemaker, G., et al. (1988). Donor-derived cells in the central nervous system of twitcher mice after bone marrow transplantation. Science 239, 1035 - 1038.

34. Oliver, F. J., Collins, M. K., and Lopez-Rivas, A. (1996). dNTP pools imbalance

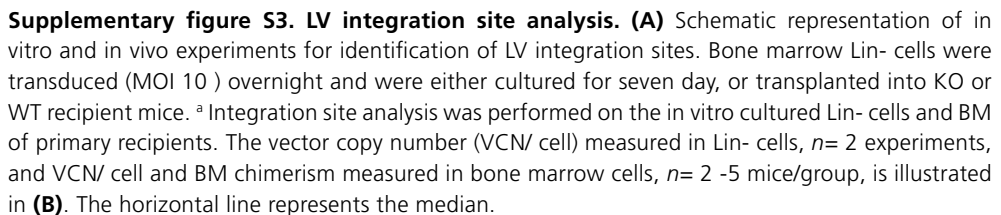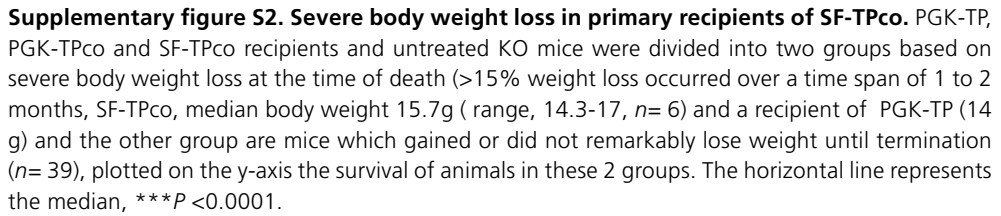**4**

as a signal to initiate apoptosis. Experientia 52, 995-1000.

35. Kumar, D., Viberg, J., Nilsson, A. K., and Chabes, A. (2010). Highly mutagenic and severely imbalanced dNTP pools can escape detection by the S-phase checkpoint. Nucleic Acids Res 38, 3975-3983.

36. Jiang, H., He, X., Wang, S., Jia, J., Wan, Y., Wang, Y., et al. (2014). A microtubule-associated zinc finger protein, BuGZ, regulates mitotic chromosome alignment by ensuring Bub3 stability and kinetochore targeting. Dev Cell 28, 268-281.

37. Toledo, C. M., Herman, J. A., Olsen, J. B., Ding, Y., Corrin, P., Girard, E. J., et al. (2014). BuGZ is required for Bub3 stability, Bub1 kinetochore function, and chromosome alignment. Dev Cell 28, 282-294.

38. Schambach, A., Bohne, J., Baum, C., Hermann, F. G., Egerer, L., von Laer, D., et al. (2006). Woodchuck hepatitis virus post-transcriptional regulatory element deleted from X protein and promoter sequences enhances retroviral vector titer and expression. Gene Ther 13, 641-645.

39. Dull, T., Zufferey, R., Kelly, M., Mandel, R. J., Nguyen, M., Trono, D., et al. (1998). A third-generation lentivirus vector with a conditional packaging system. J Virol 72, 8463-8471.

40. van Til, N. P., Stok, M., Aerts Kaya, F. S., de Waard, M. C., Farahbakhshian, E., Visser, T. P., et al. (2010). Lentiviral gene therapy of murine hematopoietic stem cells ameliorates the Pompe disease phenotype. Blood 115, 5329-5337.

41. Wognum, A. W., Visser, T. P., Peters, K., Bierhuizen, M. F., and Wagemaker, G. (2000). Stimulation of mouse bone marrow cells with kit ligand, FLT3 ligand, and thrombopoietin leads to efficient retrovirus-mediated gene transfer to stem cells, whereas interleukin 3 and interleukin 11 reduce transduction of short- and long-term repopulating cells. Human gene therapy 11, 2129-2141.

42. Van Acker, K. J., Eyskens, F. J., Verkerk, R. M., and Scharpe, S. S. (1993). Urinary excretion of purine and pyrimidine metabolites in the neonate. Pediatr Res 34, 762-766.

43. Huston, M. W., Riegman, A. R., Yadak, R., van Helsdingen, Y., de Boer, H., van Til, N. P., et al. (2014). Pretransplant mobilization with granulocyte colony-stimulating factor improves B-cell reconstitution by lentiviral vector gene therapy in SCID-X1 mice. Human gene therapy 25, 905-914.

44. Farahbakhshian, E., Verstegen, M. M., Visser, T. P., Kheradmandkia, S., Geerts, D., Arshad, S., et al. (2014). Angiopoietin-like protein 3 promotes preservation of stemness during ex vivo expansion of murine hematopoietic stem cells. PLoS One 9, e105642.

45. Schmidt, M., Schwarzwaelder, K., Bartholomae, C., Zaoui, K., Ball, C., Pilz, I., et al. (2007). High-resolution insertion-site analysis by linear amplification-mediated PCR (LAM-PCR). Nat Methods 4, 1051-1057.

46. Biasco, L., Pellin, D., Scala, S., Dionisio, F., Basso-Ricci, L., Leonardelli, L., et al. (2016). In Vivo Tracking of Human Hematopoiesis Reveals Patterns of Clonal Dynamics during Early and Steady-State Reconstitution Phases. Cell Stem Cell 19, 107-119.

47. Biasco, L., Scala, S., Basso Ricci, L., Dionisio, F., Baricordi, C., Calabria, A., et al. (2015). In vivo tracking of T cells in humans unveils decade-long survival and activity of genetically modified T memory stem cells. Sci Transl Med 7, 273ra213.

48. Goffart, S., Cooper, H. M., Tyynismaa, H., Wanrooij, S., Suomalainen, A., and Spelbrink, J. N. (2009). Twinkle mutations associated with autosomal dominant progressive external ophthalmoplegia lead to impaired helicase function and in vivo mtDNA replication stalling. Hum Mol Genet 18, 328-340.

49. Yasukawa, T., Yang, M. Y., Jacobs, H. T., and Holt, I. J. (2005). A bidirectional origin of replication maps to the major noncoding region of human mitochondrial DNA. Mol Cell 18, 651-662.

50. Ylikallio, E., Tyynismaa, H., Tsutsui, H., Ide, T., and Suomalainen, A. (2010). High mitochondrial DNA copy number has detrimental effects in mice. Hum Mol Genet 19, 2695-2705.

51. Bugiani, M., Dubey, M., Breur, M., Postma, N. L., Dekker, M. P., Ter Braak, T., et al. (2017). Megalencephalic leukoencephalopathy with cysts: the Glialcam-null mouse model. Ann Clin Transl Neurol 4, 450-465.

4

|SUPPLEMENTARY INFORMATION
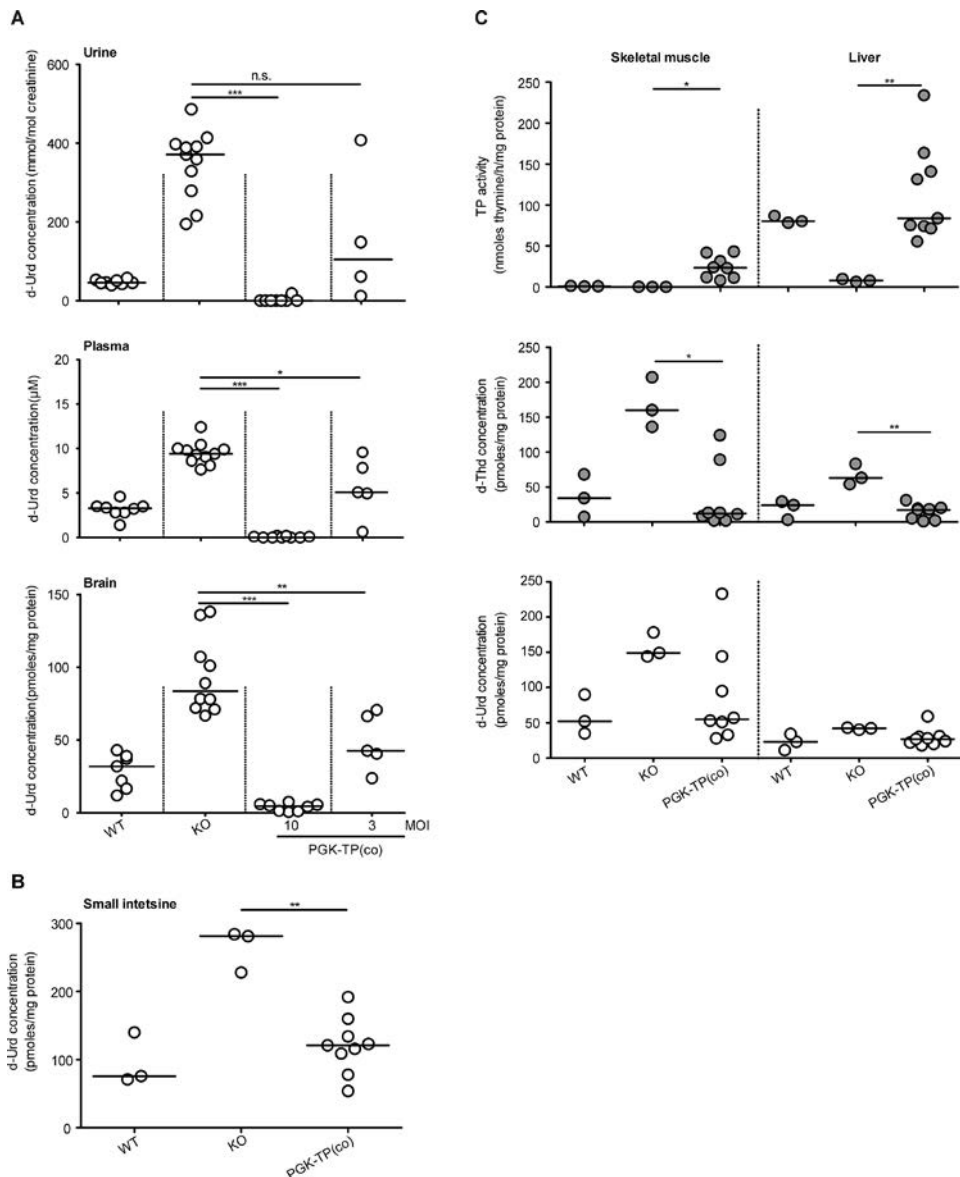
Supplementary figure S1. Biochemical correction in transplanted MNGIE mice. (A) Quantifications of deoxyuridine (d-Urd) in urine, plasma of blood and brain tissues 8-11 months after transplantation of 5×10^5 LV transduced Lin- cells (MOI 10, 3), n= 4-11 mice /group and **(B)** in intestines 11 months after transplantation of $5'10^5$ LV transduced Lin- cells (MOI10), n= 3-9 mice / group.**(C)** Biochemical correction in skeletal muscle and liver tissues 11 months after transplantation of 5×10^5Lin- (MOI 10), n= 3-9 mice /group. The horizontal line represents the median. *P <0.05, **P <0.01 and ***P <0.001, n.s. = not significant.

Supplementary figure S2. Severe body weight loss in primary recipients of SF-TPco. PGK-TP, PGK-TPco and SF-TPco recipients and untreated KO mice were divided into two groups based on severe body weight loss at the time of death (>15% weight loss occurred over a time span of 1 to 2 months, SF-TPco, median body weight 15.7g (range, 14.3-17, *n*= 6) and a recipient of PGK-TP (14 g) and the other group are mice which gained or did not remarkably lose weight until termination (*n*= 39), plotted on the y-axis the survival of animals in these 2 groups. The horizontal line represents the median, ***P <0.0001.

4

Supplementary figure S3. LV integration site analysis. (A) Schematic representation of in vitro and in vivo experiments for identification of LV integration sites. Bone marrow Lin- cells were transduced (MOI 10) overnight and were either cultured for seven day, or transplanted into KO or WT recipient mice. [a] Integration site analysis was performed on the in vitro cultured Lin- cells and BM of primary recipients. The vector copy number (VCN/ cell) measured in Lin- cells, *n*= 2 experiments, and VCN/ cell and BM chimerism measured in bone marrow cells, *n*= 2 -5 mice/group, is illustrated in **(B)**. The horizontal line represents the median.

Supplementary figure S4. Characterization of LV vector positive B-cell lymphoma. (A) FACS blot of BM cells stained for B220+ and demonstration of the size (FSC) and granularity (SSC) of the B220+GFP+ population**. (B)** Histology and immunohistochemistry for large B-cell lymphoma infiltration in liver. H&E and B220 staining (200x) **(C)** Overview of the PGK-TP-GFP insertion into the third intron of *Zfp207* gene as identified by LAM-PCR and sequencing analysis of BM.

Supplementary table S1. Complete blood counts (CBC) of gene therapy treated primary recipient mice and control groups[a]

LV vector	WBC (x10³/µl)	RBC (x10⁶/µl)	HGB (x10⁵)	HCT (x10⁵)	PLT (x10⁹/l)	MCV	MCH	MCHC
KO	6.5	9.8	9.1	0.5	1196	50	0.93	18.4
(n=7)	(2.7-11.4)	(9.3-10.6)	(8.3-9.6)	(0.45-0.52)	(974-1529)	(48-51)	(0.89-0.95)	(17.80-18.90)
WT	4.4	9.1	8.4	0.46	901	50	0.91	18.2
(n=6)	(3-5.7)	(8.5-10.6)	(7.8-9.6)	(0.4-0.5)	(473-1489)	(48-52)	(0.89-0.98)	(17.9-19.1)
PGK-TP	6.2	8.9	8.1	0.46	1277	50	0.93	18.2
(n=5)	(5.2-7.2)	(8-10.2)	(7.6-9.1)	(0.4-0.5)	(931-1705)	(49-52)	(0.88-0.95)	(17.1-19)
PGK-TPco	5.1	7.7	7.2	0.39	861	51.5	0.96	18.3
(n=6)	(3.9-9.3)	(3.4-9.5)	(4-9)	(0.21-0.48)	(240-1531)	(50-63)	(0.90-1.1)	(17.6-18.7)
SF-TPco	4	5	4.8	0.26	1145	52	0.94	18
(n=4)	(1.9-5.4)	(3-9.2)	(3-8.3)	(0.1-0.4)	(773-1198)	(49-54)	(0.9-0.96)	(17.3-18.5)
PGK-GFP	5.8	9.6	8.7	0.48	1086	50	0.90	18
(KO-KO)	(3-7)	(9.4-9.9)	(8.6-9)	(0.46-0.5)	(609-1236)	(48-54)	(0.88-0.92)	(17.2-18.4)
(n=4)								
PGK-GFP	3.7	8.1	7.8	0.41	665	51.5	0.97	18.8
(WT-WT)	(3-4)	(8-9.4)	(7.2-9.2)	(0.41-0.48)	(590-793)	(51-52)	(0.88-0.97)	(17-19)
(n=4)								

[a]WBC: white blood cells; RBC, red blood cells; HGB, hemoglobin; HCT, Hematocrit ;PLT, platelets; MCV, mean cell volume; MCH, mean cell hemoglobin; MCHC, Mean cellular hemoglobin concentration. Data represent median (range)

4

Supplementary table S2. Biochemical and molecular data of LV-SF-TPco treatment group.

Blood TP activity (nmoles thymine/h/mg protein)	Urine Thd (mmol/mol creatinine)	Urnie d-Urd (mmol/mol creatinine)	Plasma d-Thd (µM)	Plasma d-Urd (µM)	Brain TP activity (nmoles thymine/h/mg protein)	Brain d-Thd (pmoles/mg protein)	Brain d-Urd (pmoles/mg protein)	VCN/ cell	BM cell chimerism (%)
406	0	0	0	0.1	240	0.6	1.6	1.8	98
(351-438)	0	0	(0-0.1)	(0-0.1)	(133-501)	(0.2-1.6)	(0.1-3)	(0.3-11)	(75-100)

Quantification of thymidine phosphorylase (TP) enzyme activity, thymidine (d-Thd) and deoxyuridine (d-Urd) 11 months after transplantation of 5×10^5 LV-SF-TPco transduced Lin- cells (MOI 10). Data represent median (range), $n=$ 2- 7 mice.

Supplementary table S3. Incidence of hematological abnormalities in secondary recipients of LV transduced cells

LV vector	Number of donor mice	Number of secondary recipients	VCN/cell [a]	BM cell chimerism (%) [b]	Number of vector-positive hematological aberrations [c]	Number of non-vector-positive hematological aberrations [d]	Number of prematurely dead mice or mice sacrificed with high discomfort scores [e]
PGK-GFP [f]	16	32	0.09 (0.03-0.12)	0.25 (0.16-0.4)	0	1 B220+ B cells (86%)	5 (found dead) 5 (wasting) 1 (malocclusion, wasting)
PGK-TP-GFP	6	12	0.52 (0.21-0.86)	30.4 (3-67.3)	2 B220+GFP+ B-cell lymphoma (83%, 85%)	0	1 (found dead) 3 (wasting)
PGK-TP	6	12	0.22 (0.04-16)	2.8 (0.77-100)	0	1 CD4+CD8+ T cells (52%)	2 (malocclusion, wasting) 1 (wasting)
PGK-TPco	6	12	0.12 (0.01-4.4)	2 (0.10-100)	0	1 B220+ B cell- leukemia (85%, WBC=53×10^3/µl)	1 (reactive pathology/ hepatic steatosis observed at autopsy) 2 (wasting) 1 (passive)
SF-TPco	10	20	0.01 (0.0-0.5)	1 (0.1-47.2)	0	6 B220+ B cell- leukemia (n=1; 64%, WBC = 57×10^3/µl) CD4+CD8+ T cells (n=3; 40%, 68%, 7%) Gr-1+CD11b+ Myeloid cells (n=2; 57%, 35%)	1 (found dead) 2 (wasting) 1 (diarrhea, wasting)

Mice were transplanted with LV transduced 5×10^5 BM Lin- cells (MOI 10 or 12) and followed for 8-11 months after transplantation. Two secondary recipients were transplanted with 2×10^5 BM Lin- cells isolated from one primary recipient mouse. [a, b] Vector copy number per cell (VCN/cell) and bone marrow chimerism of all the secondary recipients in each treatment group are presented as median (range), n=3-16/ group. [c, d] Hematological aberrations and clonal expansion of transduced cells were assessed based on altered FACS phenotypes and/or elevated WBCs (> 25.0 x 10^3 cells/µl= leukemia), and /or enlarged spleen, thymus or lymph nodes of mice with high discomfort scores. The percentage of the abnormal BM phenotypic cells are indicated between parenthesis. The hematological aberration is vector-positive if both donor cells and VCN were prominent in the recipient's BM. [e] The right column includes mice that were found dead or mice sacrificed prematurely during the experiment due to high discomfort scores and hematological aberrations could not be identified (details are specified between parenthesis). [f] PGK-GFP group include recipient mice of KO or WT Lin- cells transduced by PGK-GFP.

4

Supplementary table S4. Primers used in quantitative PCR (qPCR)

Abbreviation	Forward primer (5'>3')	Reverse primer (5'>3')	Employed for
HIV-1 (U3-Psi)	CTGGAAGGGCTAATTCACTC	GGTTTCCCTTTCGCTTTCAG	Detection of integrated viral copies (VCN/cell)
SRY	CATCGGAGGGCTAAAGTGTCAC	TGGCATGTGGGTTCCTGTCC	Detection of male chromosome (Donor cell chimerism)
Mouse GAPDH	ACGGCAAATTCAACGGCACAG	ACACCAGTAGACTCCACGACATAC	Internal control
WPRE	GAGGAGTTGTGGCCCGTTGT	TGACAGGTGGGTGGCAATGCC	WPRE mRNA expression
Mouse mtDNA1978F, 2086R	TGCCTGCCCAGTGACTAAG	GACCCTCGTTTAGCCGTTCA	Quantify mtDNA copynumber
Mouse NDUFV1	ATCCSAGGATCCCACAGAGCT	CCTTTCCAGCAGATGTGGGT	
Mouse mtDNA probe	FAM-TGACCGTGCAAAGGTAGCAT-MGB		
Mouse NDUFV1 probe	VIC-GAGCCTTAGGGAAGAGGCAG-MGB		

Supplementary table S5. Antibodies used in this study

Anti-	Clone	Host organism	Vendor	Dilution	WB*/IHC*
Human TP, 55kDa	P-GF.44C	Mouse	Calbiochem-Merck, GF40	1:250	WB
GAPDH, 36 kDa	6C5	Mouse	Applied Biosystems, AM4300	1:250	WB
Mouse IgG H&L	Polyclonal	Goat	Abcam, Ab97023	1:1000	WB
Mouse PLP	Plpc1	Mouse	AbD Serotec, MCA839G	1:3000	IHC
Mouse MBP	Not specified by vendor	Mouse	Millipore, MAB387	1:50	IHC
Mouse GFAP	Polyclonal	Chicken	Millipore, Ab5541	1:1000	IHC
Mouse B220	RA3.6B2	Rat	Epirus Biopharmaceuticals	1:50	IHC
Mouse IgG	Polyclonal	Goat	Dako, K4000	1:1000	IHC
Rat IgG H&L	Polyclonal	Rabbit	Vector labs, BA-4000	1:150	IHC

*WB, Western blot. *IHC, Immunohistochemistry.

4

Transplantation, gene therapy and intestinal pathology in MNGIE patients and mice

Rana Yadak[1,2], Max V. Boot[3], Niek P. van Til[2,4],
Dominique Cazals-Hatem[5], Armin Finkenstedt[6], Elly Bogaerts[7],
Irenaeus. F. de Coo*[1,8], Marianna Bugiani*[3]

[1]Department of Neurology, Erasmus University Medical Center, Rotterdam, The Netherlands;
[2]Department of Hematology, Erasmus University Medical Center, Rotterdam, The Netherlands;
[3]Department of Pathology, VU University Medical Center, Amsterdam, The Netherlands; [4]Laboratory of
Translational Immunology, University Medical Center Utrecht, Utrecht, The Netherlands; [5]Department
of Pathology, Beaujon Hospital, Paris, France; [6]Department of Medicine I, Medical University of
Innsbruck, Innsbruck, Austria; [7]Department of Clinical Genetics, Erasmus University Medical Center,
Rotterdam, The Netherlands; [8]Department of Clinical Genetics, Maastricht University Medical Center,
Maastricht, The Netherlands

|ABSTRACT

Gastrointestinal complications are the main cause of death in patients with mitochondrial neurogastrointestinal encephalomyopathy (MNGIE). Available treatments often restore biochemical homeostasis, but fail to cure gastrointestinal symptoms. We evaluated small intestine histology of an untreated MNGIE patient and two recipients of hematopoietic stem cells. Additionally, we evaluated the intestinal pathology in a mouse model of MNGIE treated with hematopoietic stem cell gene therapy. Our data confirm that MNGIE presents with muscle atrophy and loss of Cajal cells and CD117/c-kit immunoreactivity in the small intestine. We also show that hematopoietic stem cell transplantation does not benefit human intestinal pathology on short-term.

INTRODUCTION

Mitochondrial neurogastrointestinal encephalomyopathy (MNGIE) is a rare inherited metabolic disorder caused by loss-of-function mutations in the nuclear gene *TYMP* leading to thymidine (Thd) and deoxyuridine (d-Urd) accumulation.[1] Alongside classic neurological signs (external ophtalmoplegia, leukoencephalopathy and sensorimotor peripheral neuropathy), chronic intestinal pseudo-obstruction (CIPO) is reported in almost all MNGIE patients and occurs at onset in 45-67% of cases.[2, 3] Other gastrointestinal symptoms include early satiety, nausea, dysphagia, post-prandial emesis, abdominal pain and/or distention and diarrhea.[4]

Allogeneic hematopoietic stem cell transplantation (HSCT) corrects the biochemical metabolic imbalance as donor-derived leucocytes and platelets are rich in thymidine phosphorylase.[4] It is effective to relieve CIPO in few reported MNGIE cases[5] although malnutrition often persists and most cases rely on nutritional support.[6] Neurogenic and myogenic changes and alterations of the interstitial Cajal cells, the gut pacemakers, were reported in MNGIE patients.[7-10] Restoration of gastrointestinal integrity by available treatments however has not yet been addressed. Also, whether small intestine pathology is recapitulated in the mouse model of MNGIE is not known.[11,12] In this study, we also evaluated the effects of treatment on small intestinal pathology of MNGIE patients and mice.

SUBJECTS AND METHODS

MNGIE patients and controls

Table 1 reports the demographic data of three MNGIE patients and three controls. Patients were diagnosed based on clinical, biochemical, and molecular features.[1] One patient was untreated, two received HSCT. Written informed consent was obtained for all subjects.

MNGIE mice

Tymp$^{-/-}$Upp1$^{-/-}$ (KO) and *Tymp$^{+/+}$Upp1$^{+/+}$* wild type (WT) mice[11] were bred in filter top cages and fed *ad libitum* with autoclaved water and irradiated chow. Animal experiments were approved by the ethical committee of the Erasmus University Medical Center, Rotterdam, in accordance with Dutch legislation. pRRL.PGK.TYMP.bPRE4*.SIN self-inactivating lentiviral transfer plasmid containing the human PGK promoter driving *TYMP* sequence[13], and the third-generation[14] packaging and envelop plasmids were used to generate LV-PGK-TP vector particles, by calcium-phosphate precipitation of HEK293T cells.[15] Titration was performed on HeLa cells and titers determined by quantitative polymerase chain reaction (qPCR). Donor KO male bone marrow lineage-depleted (Lin-) cells (BD Biosciences) were transduced overnight with the lentiviral vector at a multiplicity of infection 10 in serum-free modified Dulbecco's medium with supplements,[16] conditioned with murine stem cell factor, human Flt3-L, and murine thrombopoietin. Five to 10-week-old recipient KO female mice received 6Gy total body irradiation 24 hours prior to tail vein injection of 0.5×10^6 Lin-transduced cells. Bone marrow genomic DNA (Bioké, Leiden, The Netherlands) was used as template for qPCR using primers and SYBR

Table 1. Clinical and molecular data of MNGIE patients and controls

Patient	MNGIE-1	MNGIE-2[20]	MNGIE-3	Control-1	Control-2	Control-3
Age of onset	18 y	23 y	10 y	NA	NA	NA
Age at diagnosis	19 y	32 y	17 y	41 y	46 y	28 y
GI symptoms	Diarrhea, vomiting, weight loss, abdominal pain, liver steatosis	Diarrhea, weight loss, liver steatosis	Diarrhea, weight loss, abdominal pain	NA	NA	NA
Extra-GI symptoms	Ptosis, peripheral neuropathy, neurogenic bladder, leukoencephalopathy, lactic acidosis, hypertriglyceridemia	External ophtalmoplegia, peripheral neuropathy, leukoencephalopathy	Retinopathy, peripheral neuropathy, leukoencephalopathy	NA	NA	NA
Diagnosis	TP deficiency	Urinary d-Urd, c.866A>C in TYMP	c.866A>C in TYMP	Pancreatitis	IOPN	GIST
Treatment of MNGIE (age)	- None	Allogeneic HSCT (34 y)	Allogeneic HSCT (17 y)	-	-	-
Follow-up	Alive (6 y)	Multi-organ failure; died 18 days after treatment	GVHD, sepsis; died 6 months after treatment	NA	NA	NA

GI, gastrointestinal. NA, not available. TP, thymidine phosphorylase enzyme. d-Urd, deoxyuridine. TYMP, thymidine phosphorylase. IOPN, intra-ductal oncocytic papillary neoplasm. GIST, gastrointestinal stromal tumor. HSCT, hematopoietic stem cell transplantation. GVHD, graft-versus-host disease.

Green PCR master mix (Applied Biosystems, Foster City, CA; Eurogentec, Maastricht, The Netherlands). PCR reactions were carried out in the ABI7900, Taqman machine, and analysis performed with SDS2.2.2 software (Applied Biosystems). The Cycle threshold values were compared against a standard curve obtained from mouse 3T3 to calculate average vector copy per cell, or from male mice bone marrow to calculate Y chromosome chimerism.

High performance liquid chromatography (Shimadzu, LC20 series with a binary pump and Photodiode array detector)[17] equipped with an Alltima C18 5μ, 250 mm x 4.6 mm column and Alltima C18 5μ guard column was used to measure urinary Thd and d-Urd.

Pathological analysis

Formalin-fixed paraffin-embedded 5-μm-thick small intestine tissue sections were routinely stained for Hematoxylin-Eosin and Phosphotungstic acid-hematoxylin and immunostained as described[18] against smooth muscle actin (SMA, Dako, 1:200), CD117/c-kit (Dako, 1:50), calretinin (Dako, 1:200), CD3 (Dako, 1:250), CD8 (Dako, 1:50) and glial fibrillary acidic protein (GFAP, Dako, 1:300). Immunoreactivity was detected using 3,3'-Diaminobenzidin or Liquid Permanent Red as chromogen. Pictures were taken with a Leica DM3000 microscope. Muscle thickness was measured on transversally cut intestinal sections (N=40 for mice, N$\geq$25 for humans). Quantification of muscle wall thickness and ganglion cell density was performed blind to the genotype with ImageJ.

Statistical analysis

Data were analyzed with Graph Pad-Prism5 (version 5.03). Significance of differences between groups was determined by two-tailed Mann-Whitney *U* test (P<0.05).

|RESULTS

Small intestine pathology in MNGIE patients

Microscopic analysis (Fig 1) revealed a preserved layer composition of the small intestine in all MNGIE patients with no villous atrophy or significant inflammation. In MNGIE patients, however, the external layer of the tunica muscularis propria was fibrotic and thinner than in controls, suggesting muscle atrophy. The submucosal plexus appeared normal. In the myenteric plexus, no significant loss or morphologic abnormalities of ganglion cells and enteric glial cells were observed. Cajal cells, however, identified by CD117/c-kit immunoreactivity, were completely lost in all MNGIE patients.

Small intestine pathology in MNGIE mice

We investigated small intestine histopathology in MNGIE mice using 2 (young) and 12-month-old animals (old) to also check for signs of progression (Fig 2). Hematoxylin-Eosin staining revealed significant atrophy of the tunica muscularis propria and loss of myenteric ganglion cells in old KO compared to young *Tymp*^{-/-}*Upp1*^{-/-} and old WT mice. Unfortunately, CD117/c-kit immunostaining was unsuccessful.

We then assessed the effects of treatment on the MNGIE phenotype (Fig 2). Following hematopoietic stem cell gene therapy (HCSGT), vector copies number

5

per cell, engraftment levels and urinary nucleosides concentrations indicated efficient hematological reconstitution and biochemical correction. Histopathology showed recovery of tunica muscularis propria thickness in old treated mice compared to $Tymp^{-/-}Upp1^{-/-}$ mice; however, no significant changes were observed in the number of myenteric ganglion cells.
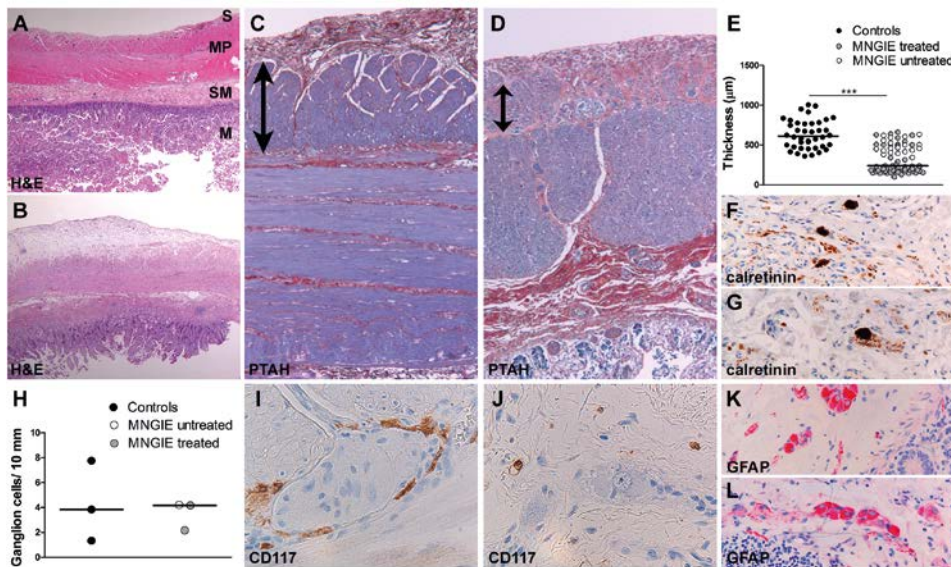

Figure 1. Small intestinal histopathology in MNGIE patients. (A, B) Hematoxylin-Eosin (H&E) stains of the small intestine of control subjects (A) and MNGIE patients (B) show normally layered organization of the wall in both groups (M: tunica mucosa; S: tunica submucosa; MP: tunica muscularis propria; S: tunica serosa). (C, D) Compared to controls (C), phosphotungstic acid-hematoxylin (PTAH) stains of MNGIE small intestines (D) show thinning of the external layer of the tunica muscularis propria (blue, arrows). (E) Quantification demonstrates muscle wall atrophy in the three MNGIE patients compared to two controls. One control was omitted because the tunica muscularis was incompletely present. (F, G) Immunostain against calretinin shows presence of ganglion cells in the submucosal Meissner plexus of controls (F) and MNGIE patients (G). (H) Quantification of myenteric ganglion cells shows similar cell density in MNGIE patients and controls. (I, J) Immunostain against CD117 shows normal presence of interstitial Cajal cells around grouped myenteric ganglion cells in controls (I), whereas Cajal cells are completely depleted in MNGIE patients (J). Small immunopositive cells in J are mast cells. (K, L) Immunostain against the glial fibrillary acidic protein (GFAP) shows normal immunoreactivity in myenteric ganglion and enteric glia cells in MNGIE (L) as in controls (K). In both graphs bars denote the median. Original magnifications (A, B): 12.5x; (C, D): 25x; (I, J): 400x; (K, L): 200x. ***$P<0.001$.
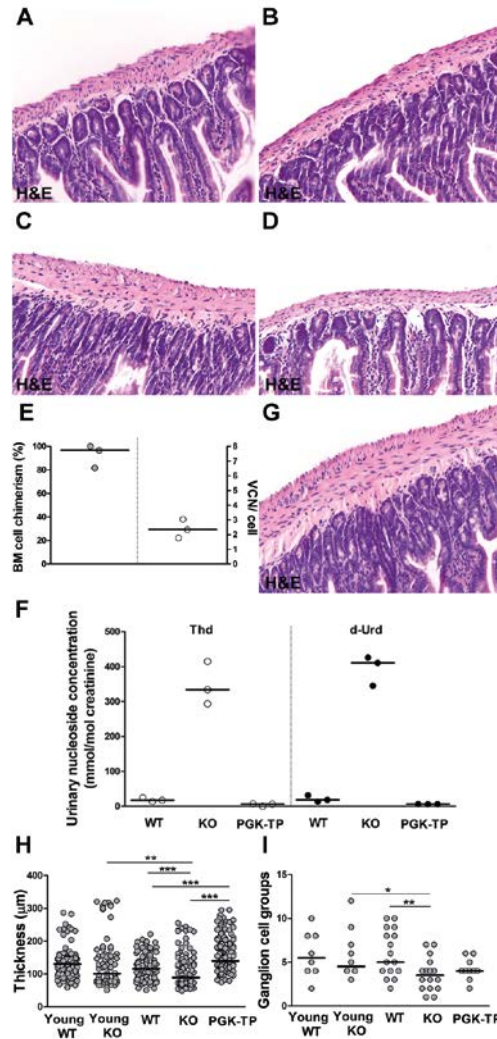
Figure 2. Small intestinal histopathology in MNGIE mice. (A, B) Hematoxylin-Eosin (H&E) stains of the small intestine of young (2-month-old) control mice (A) and age-matched *Tymp⁻ᐟ⁻Upp1⁻ᐟ⁻* mutants (B) show normally layered organization of the intestinal wall in both groups. (C, D) H&E stains of the small intestine show normal thickness of the tunica muscularis propria in old (12-month-old) control mice (C), whereas in age-matched *Tymp⁻ᐟ⁻Upp1⁻ᐟ⁻* mutants (D) the muscle wall is atrophic. (E) Bone marrow cell chimerism and vector copy number in recipients of 0.5×10⁶ Lin- cells transduced by LV-PGK-TP (MOI10) (*n*=3 mice). (F) Quantification of Thd and d-Urd in urine of untreated controls and age-matched recipients 6 and 11 months after transplantation (*n*=3 mice). (G) H&E stain of the small intestine shows recovery of normal thickness of the tunica muscularis propria in old (12-month-old) *Tymp⁻ᐟ⁻Upp1⁻ᐟ⁻* mice 10 months after treatment. (H) Quantification confirms atrophy of the muscle wall in 12-month-old *Tymp⁻ᐟ⁻Upp1⁻ᐟ⁻* mice compared to wild-type age-matched controls. Treatment is associated with normal thickness of the tunica muscularis propria. (I) Quantification of the number of myenteric ganglion cell groups per tissue section shows progressive loss of ganglion cells in *Tymp⁻ᐟ⁻Upp1⁻ᐟ⁻* mice, without effect of the treatment. *N*=2-4 mice/group; in all graphs lines represent the median; *$P<0.05$, **$P<0.01$, ***$P<0.001$. Original magnification (A-D and G): 200x.

| DISCUSSION

MNGIE is associated with gastrointestinal symptoms, including CIPO[2,3]. Limited understanding of the pathological and molecular mechanisms underlying gastrointestinal complications in MNGIE stems from limited availability of patient tissue and models[11] that accurately recapitulate the human gastrointestinal pathology. Our study confirms the morphological changes in human MNGIE small intestine, including atrophy and fibrosis of the external layer of the tunica muscularis propria.[8] The selective involvement of this layer has been attributed to physiologically very low mitochondrial DNA amounts making this compartment selectively vulnerable to disease.[8] Muscle wall atrophy was more pronounced in transplanted patients, possibly due to additional HSCT-related stress. We also found complete loss of interstitial Cajal cells and networks in patients' small intestine. Cajal cells play roles in orchestration of normal gastrointestinal motility and in dysmotility disorders.[19] One study previously described similar findings in a MNGIE patient.[9] Altogether, these findings suggest that Cajal cell loss is a cellular substrate of human MNGIE gastrointestinal pathology.

We used $Tymp^{-/-}Upp1^{-/-}$ mice, a model of MNGIE, to investigate whether it recapitulates the human gastrointestinal pathology. In mutant mice, histopathology revealed atrophy of the tunica muscularis propria as in MNGIE patients and, in addition, loss of myenteric ganglion cells. These features were more prominent in old $Tymp^{-/-}Upp1^{-/-}$ compared to young animals. In $Tymp^{-/-}Upp1^{-/-}$ mice, we did not see presence of Cajal cell on routine Hematoxylin-Eosin stained sections. Unfortunately, CD117/c-kit immunostaining of mouse small intestine was unsuccessful, so that we cannot conclude on Cajal cells absence in $Tymp^{-/-}Upp1^{-/-}$ mice. However, taking our patient and mouse data together, we can suppose a sequence of pathological events leading to MNGIE small intestinal disease, including loss of interstitial Cajal cells and their networks followed by atrophy of the tunica muscularis propria and eventually loss of myenteric ganglion cells[9]. The observed loss of myenteric ganglion cells in the mice, but not in patients' small intestine may be attributed to inter-species differences and the construct of the MNGIE mouse model being knock-out for both disease-related enzymes. Our study describes, for the first time, the small intestinal pathology in MNGIE patients treated with HSCT. Although the study is limited by the small patient number and relatively short time lapse between treatment and demise, HSCT did not significantly change the trend to intestinal muscle wall atrophy and complete loss of Cajal cells in treated compared to the untreated patient. This suggests that MNGIE small intestinal pathology may not be recovered upon HSCT, which could explain the repeatedly reported insufficient improvement of gastrointestinal symptoms in MNGIE patients after treatment.[5]

The HSCT procedure carries a high mortality rate[5]. Recently, HSCGT has been explored in $Tymp^{-/-}Upp1^{-/-}$ mice, providing higher enzymatic levels compared to HSCT and abating the risk of graft-versus-host disease.[12] Due to intrinsic limitations of the mouse model, i.e. lack of an apparent clinical phenotype, only biochemical

correction was shown after HSCGT. Moreover, the pathological changes in the intestine of *Tymp*^{-/-}*Upp1*^{-/-} mice were never evaluated.[12] Here, we show that the transplanted gene modified cells engrafted well in recipient mice, leading to clearance of systemic nucleosides. The observed atrophy of the tunica muscularis propria was recovered upon HSCGT, whereas the degree of myenteric ganglion cell loss remained unchanged. Similarly as for MNGIE patients, recovery of ganglion cells may take longer than our follow-up of the mice.

Alternatively, the possibility that MNGIE permanently affects ganglion cells, including their precursors, cannot be excluded.

In conclusion, our data suggest that allogeneic HSCT may be insufficient to correct gastrointestinal pathology completely, especially at later stages of MNGIE. As interstitial Cajal cells and their networks play a key role in development of gastrointestinal dysmotility, alternative therapeutic approaches taking absence of these cells into account could be required.

|AUTHOR CONTRIBUTIONS

|CONFLICTS OF INTEREST

None.

|ACKNOWLEDGMENTS

5

|REFERENCES

1. Hirano M, Silvestri G, Blake DM, et al. Mitochondrial neurogastrointestinal encephalomyopathy (MNGIE): clinical, biochemical, and genetic features of an autosomal recessive mitochondrial disorder. Neurology. 1994;44:721-7.

2. Munoz MT, Solis Herruzo JA. [Chronic intestinal pseudo-obstruction] Pseudo-obstruccion intestinal cronica. Rev Esp Enferm Dig. 2007;99:100-11.

3. Kapur RP. Pathology of Intestinal Motor Disorders in Children. Surg Pathol Clin. 2010;3:711-41.

4. Yadak R, Sillevis Smitt P, van Gisbergen MW, van Til NP, de Coo IF. Mitochondrial Neurogastrointestinal Encephalomyopathy Caused by Thymidine Phosphorylase Enzyme Deficiency: From Pathogenesis to Emerging Therapeutic Options. Front Cell Neurosci. 2017;11:31.

5. Halter JP, Michael W, Schupbach M, et al. Allogeneic haematopoietic stem cell transplantation for mitochondrial neurogastrointestinal encephalomyopathy. Brain. 2015;138:2847-58.

6. Filosto M, Scarpelli M, Tonin P, et al. Course and management of allogeneic stem cell transplantation in patients with mitochondrial neurogastrointestinal encephalomyopathy. J Neurol. 2012;259:2699-706.

7. Perez-Atayde AR, Fox V, Teitelbaum JE, et al. Mitochondrial neurogastrointestinal encephalomyopathy: diagnosis by rectal biopsy. Am J Surg Pathol. 1998;22:1141-7.

8. Giordano C, Sebastiani M, De Giorgio R, et al. Gastrointestinal dysmotility in mitochondrial neurogastrointestinal encephalomyopathy is caused by mitochondrial DNA depletion. Am J Pathol. 2008;173:1120-8.

9. Zimmer V, Feiden W, Becker G, et al. Absence of the interstitial cell of Cajal network in mitochondrial neurogastrointestinal encephalomyopathy. Neurogastroenterol Motil. 2009;21:627-31.

10. Perez-Atayde AR. Diagnosis of mitochondrial neurogastrointestinal encephalopathy disease in gastrointestinal biopsies. Hum Pathol. 2013;44:1440-6.

11. Lopez LC, Akman HO, Garcia-Cazorla A, et al. Unbalanced deoxynucleotide pools cause mitochondrial DNA instability in thymidine phosphorylase-deficient mice. Hum Mol Genet. 2009;18:714-22.

12. Torres-Torronteras J, Cabrera-Perez R, Barba I, et al. Long-Term Restoration of Thymidine Phosphorylase Function and Nucleoside Homeostasis Using Hematopoietic Gene Therapy in a Murine Model of Mitochondrial Neurogastrointestinal Encephalomyopathy. Hum Gene Ther. 2016;27:656-67.

13. Torres-Torronteras J, Gomez A, Eixarch H, et al. Hematopoietic gene therapy restores thymidine phosphorylase activity in a cell culture and a murine model of MNGIE. Gene Ther. 2011;18:795-806.

14. Dull T, Zufferey R, Kelly M, et al. A third-generation lentivirus vector with a conditional packaging system. J Virol. 1998;72:8463-71.

15. van Til NP, Stok M, Aerts Kaya FS, et al. Lentiviral gene therapy of murine hematopoietic stem cells ameliorates the Pompe disease phenotype. Blood. 2010;115:5329-37.

16. Wognum AW, Visser TP, Peters K, Bierhuizen MF, Wagemaker G. Stimulation of mouse bone marrow cells with kit ligand, FLT3 ligand, and thrombopoietin leads to efficient retrovirus-mediated gene transfer to stem cells, whereas interleukin 3 and interleukin 11 reduce transduction of short- and long-term repopulating cells. Hum Gene Ther. 2000;11:2129-41.

17. Van Acker KJ, Eyskens FJ, Verkerk RM, Scharpe SS. Urinary excretion of purine and pyrimidine metabolites in the neonate. Pediatr Res. 1993;34:762-6.

18. Dubey M, Bugiani M, Ridder MC, et al. Mice with megalencephalic leukoencephalopathy with cysts: a developmental angle. Ann Neurol. 2015;77:114-31.

19. De Giorgio R, Sarnelli G, Corinaldesi R, Stanghellini V. Advances in our understanding

of the pathology of chronic intestinal pseudo-obstruction. Gut. 2004;53:1549-52.

20. Finkenstedt A, Schranz M, Bosch S, et al. MNGIE Syndrome: Liver Cirrhosis Should Be Ruled Out Prior to Bone Marrow Transplantation. JIMD Rep. 2013;10:41-4.

Hematopoietic stem cell lentiviral integration profiles are stable across multiple species, disease phenotypes and hematopoietic cell types

6

Marshall W. Huston[1, 2], Sebastiaan Horsman[3], Ali Nowrouzi[4,5],
Guus van der Velden[1], Amir. K.Varkouhi[1,6], Yuedan Li[1,7],
Rana Yadak[1,2], Merel Stok[1,8], Fatima Aerts Kaya[1,9],
Elnaz Farahbakhshian[1], Irenaeus F. de Coo[2], Andrew Stubs[3],
Manfred Schmidt[5], Christof von Kalle[5], Peter van der Spek[3],
Gerard Wagemaker*[1,9] and Niek P. van Til*[1,10]

[1]Department of Hematology, Erasmus University Medical Center, Rotterdam, the Netherlands, [2]Current affiliation: Department of Neurology, Erasmus University Medical Center, Rotterdam, the Netherlands, [3]Department of Bioinformatics, Erasmus University Medical Center, Rotterdam, the Netherlands, [4]Department of Translational Oncology, National Center for Tumor Diseases and German Cancer Research Center (DKFZ), Heidelberg, Germany, [5]Current affiliation: Division of Translational RadioOncology, National Center for Tumor Diseases and German Cancer Research Center (DKFZ), Heidelberg, Germany, [6]Current affiliation: Department of Ophthalmology and Visual Sciences, University of Alberta, Edmonton, Canada, [7]Current affiliation: Department of Radiology, Leiden University Medical Center, Leiden, the Netherlands, [8]Current affiliation: Department of Pediatrics, Department of Clinical Genetics, Center for Lysosomal and Metabolic Diseases, Erasmus University Medical Center, Rotterdam, the Netherlands, [9]Current affiliation: Stem Cell Research and Development Center, Hacettepe University, Ankara, Turkey, [10]Current affiliation: Laboratory of Tumor Immunology, University Medical Center Utrecht, Utrecht, the Netherlands

(To be submitted)

GGACCGCTGTGCGCGAACCCTGAACCCTACGGTCCCGACCCGCGGGCGAGGCCGGGTACCTG
TCCGGAGCAAGCGGGCGAGGGCAGCGCCCTAAGCAGGTACGGGCGGGGCTCAAGTCGCGAGG
CGGGAGGCAGACACGGACGAGGGCGACACAGACACGGGACCGAGGGGCGGACACCGGAGAGA
AGGGGTCGGGACAGGAGCACGTGGCTCAGACACCGACGCCGGGAGGCCGCAGACCCCGGACG
ATCCCCGCAGGCCCGGAGCGATGGCAGCCTTGATGACCCCGGGAACCGGGGCCCCACCCGCG
CTTCTCCGGGGAAGGGAGCCAGGGACTTCCCGACCCTTCGCCAGAGCCCAAGCAGCTCCGG.
CGCATGAAGCGAGACGGAGGCCGCCTGAGCGAAGCGGACATCAGGGCTTCGTGGCCGCTGT
GGAGCGCGCAGGCGCACAGATCGGTGCGTGGGGAGGGTTGGGCGTTCCTGACCCCGACTGG
CCCGAGAGACTTTGGGTCCCTGGGGGTGCGACGGTGCCCCACTACCAGCACCGGCCCCAGGG
CGCTGTGGGCTGCCACCCTCACGCGTACCCCCACATACCAGGGGCCATGCTGATGGCCATCC
GGCATGGATCTGGAGGAGACCTCGGTGCTGACCCAGGCCCTGGCTCAGTCGGGACAGCAGCT
CAGAGGCCTGGCGCCAGCAGCTTGTGGACAAGCATTCCACAGGGGGTGTGGGTGACAAGGTC
CCGAGCTCCGCCCTCCAGGCGGCCCCACCCGCCTGCCGTCCTGGGGCGCCGCCGCCCCGCCG
GGACCGCTGTGCGCGAACCCTGAACCCTACGGTCCCGACCCGCGGGCGAGGCCGGGTACCT
TCCGGAGCAAGCGGGCGAGGGCAGCGCCCTAAGCAGGTACGGGCGGGGCTCAAGTCGCGAG

|ABSTRACT

The potential of ex vivo hematopoietic stem cell (HSC) gene therapy to treat monogenic inherited disorders has been convincingly demonstrated in clinical trials. These trials also underlined the inherent genotoxic risks of gammaretroviral vectors and the possible contribution of the disease background. To acquire more insight on lentiviral integration patterns, human, rhesus and murine hematopoietic stem cell progenitors were transduced and expanded *in vitro*. Gene corrected murine progenitor cells were subsequently transplanted into severe combined immunodeficiency, Pompe disease, mitochondrial neurogastrointestinal encephalomyopathy or healthy mice. Vector-genome fusion sequences were pooled into an over 12,000 lentiviral integration sites (LVIS) database. The results demonstrated consistent integration profiles among the three species studied, and neither promoter choice nor transgene significantly influenced the integration pattern *in vivo*. LVIS flanking oncogenes occurred at a frequency consistent with random distribution. Importantly, the spleen focus forming virus promoter vectors did not differ in integration pattern from those with cellular promoters. Genes near the detected LVIS found *in vitro* and *in vivo* were involved in different overrepresented functional pathways, suggesting that either the long-term repopulating HSC differ in integration pattern from actively proliferating progenitors or a negative selection of certain integration sites occurred during hematopoietic reconstitution *in vivo*.

|INTRODUCTION

Clinical hematopoietic stem cell gene therapy trials implemented since 2000 have successfully reversed the disease phenotype in a number of patients with life-threatening inherited diseases, but also underlined the risks associated with genomic integration of the viral vectors used. Trials for X-linked severe combined immunodeficiency (SCID-X1)[1, 2], adenosine deaminase deficiency (ADA-SCID)[3, 4], X-linked chronic granulomatous disease (CGD)[5], Wiskott-Aldrich syndrome (WAS)[6, 7], β-thalassemia[8], X-linked adrenoleukodystrophy[9] and metachromatic leukodystrophy[10] all reported that the majority of patients obtained a clear clinical benefit to their disease phenotype. However, in the SCID-X1 trials five patients (out of 20 treated) developed acute clonal T cell lymphoproliferative disorders caused by the insertional activation of proto-oncogenes *LMO2* or *CCND2*[11, 12]. Four of these patients were successfully treated with chemotherapy without compromising the effectiveness of their gene therapy treatment, while the fifth patient succumbed in spite of treatment. Two CGD patients treated with gene therapy developed myelodysplasia due to insertional activation of the proto-oncogene *MDS1-EVI1*, with one patient undergoing allogeneic hematopoietic stem cell transplantation and the other dying of sepsis[13]. Seven out of ten patients in the WAS gammaretroviral clinical trial developed acute lymphocytic leukemia similar to that seen in the SCID-X1 trials[6, 14].

These vector-associated adverse events, which had been observed in experimental settings only at a very low frequency prior to the SCID clinical trials, resulted in several studies on the mechanisms of viral vector integration and oncogenic transformation in hematopoietic cells. Retroviral vector integration into hematopoietic cells is semi-random, with the viral subtype, long terminal repeats (LTRs), promoter, transgene and number of integrations per cell all potentially having an influence on either the site of integration or the genotoxic potential of the gene therapy regimen. It has been clearly demonstrated that gammaretroviral vectors have a bias towards targeting enhancers and promoter regions[15, 16], whereas lentiviral vectors show a preference for integrating into active genes[17, 18]. Transcriptionally active LTRs and strong viral enhancer/promoter regions have been shown to substantially increase the risk of oncogenesis[19, 20], while self-inactivating LTR vectors and well insulated or weaker promoters potentially confer a reduced genotoxic risk. Despite the prodigious amount of research that has been performed on retroviral vectors[21-23], many of their mechanisms for cell targeting and integration are still poorly understood.

In the course of developing new therapeutic lentiviral vectors for immune deficiencies such as SCID-X1[24], recombination activating gene 1 and 2 (RAG)-SCID[25, 26], lysosomal storage disorder Pompe disease[27] and mitochondrial neurogastrointestinal encephalomyopathy (MNGIE)[28], we have tested a wide range of expression cassettes differing with respect to their selected promoters and transgenes, all incorporated in the same third generation self-inactivating lentiviral vector backbone. Hematopoietic stem and progenitor cells (HSC) were extracted from diseased mice, transduced and transplanted for long-term follow up. Lentiviral vector integration sites

6

(LVIS) were generated by linear amplification mediated PCR (LAM-PCR)[29] and high throughput sequencing. LVIS were collected from a variety of tissues, including lineage negative (Lin-) bone marrow cells pre-transplantation and bone marrow, spleen, and thymus after transplant. Additional lentiviral integrations were generated *in vitro* by transduction of HSC derived from mouse bone marrow, rhesus bone marrow or human umbilical cord blood. In total, 12,236 unique LVIS were annotated from murine experiments, including 4434 *in vitro* and 7802 *in vivo* integrations. Experiments in human and rhesus HSC produced an additional 714 and 914 *in vitro* LVIS, respectively.

These integrations, generated using the same transduction protocol in a single laboratory, provided the opportunity to perform a comparative analysis of lentiviral integration profiles across disease phenotypes, hematopoietic cell types, and transgenes. Here we have performed an in-depth analysis of oncogene prevalence, common integration site frequency, the tendency of LVIS to be located near a TSS or near/within a Refseq gene, Ingenuity Pathways Analysis and HSC gene expression levels to determine if any integration profile characteristics is over- or underrepresented in certain sample sets, thereby generating further insight into the integration profile of lentiviral vectors.

|RESULTS

Generation of an in silico dataset for comparison

In silico datasets composed of 10,000, 3000, 1000, 500 or 300 randomly generated integrations in the mouse genome were generated, using random chromosome and nucleotide position and weighted by the size of the chromosome. Using this method, random chromosomal integration would produce a consistent integration profile in datasets of 500 or more integrations (data not shown). For comparison with the experimentally-produced LVIS, a random dataset of 1000 integrations was chosen since similar in size to most of the experimental datasets analyzed.

Integration site profiles of cultured mouse, rhesus and human HPSC

Wild type Lin- mouse bone marrow (BM) cells, CD34+ cells derived from rhesus bone marrow and CD34+ human umbilical cord blood cells were cultured overnight with

the pRRL.PPT.[SF or PGK].GFP.bPRE4*. SIN lentiviral vector[30, 31], at an MOI of 1-3 in order to determine as to whether lentiviral integration site preferences had a species-specific component. A total of 8 murine samples, 10 rhesus samples and 4 human samples were analyzed, yielding 1025, 914 and 714 unique integration sites, respectively. The percentage of LVIS within 10kb of a gene TSS (Table 1) ranged from 14.7% of mapped LVIS for the human samples up to 20.3% for the murine samples and the frequency of integrations within a gene or less than 10kb from a 5'or 3' gene terminus ranged from 69.6% (rhesus) to 73.4% (human). The number of hot spots, termed common integration sites (CIS) scaled with the total number of LVIS analyzed: a list of 3rd order or higher CIS for each dataset can be found in Supplemental Table 1. One 3rd order CIS oncogene (*Mef2c*) was found in the mouse Lin- dataset. The frequency of LVIS found near proto-

Table 1. LVIS recovered from cultured hematopoietic stem and progenitor cells.

	human[a]	rhesus[b]	mouse[c]	*Il2rg*[d]	*Rag1*[d]	*Rag2*[d]	*Gaa*[d]	In silico
Total LVIS	714	914	1025	1043	148	402	188	1000
unique genes	642	802	892	893	141	373	181	859
LVIS within 10kb of TSS[f]	105	142	208	176	25	78	36	141
LVIS within 10kb of gene	524	636	731	730	123	311	124	362
intronic LVIS	460	545	628	640	111	273	101	298
unique oncogenes	16	19	23	25	6	8	5	23
total oncogenes	20	23	32	31	7	10	5	28
percent oncogenes	2.8%	2.5%	3.1%	3.0%	4.7%	2.5%	2.7%	2.8%
percent w/in 10kb of TSS[f]	14.7%	15.5%	20.3%	16.9%	16.9%	19.4%	19.1%	14.1%
percent w/in 10kb of gene	73.4%	69.6%	71.3%	70.0%	83.1%	77.4%	66.0%	36.2%

[a] CD34+ cells derived from umbilical cord blood
[b] CD34+ bone marrow cells
[c] Lin- bone marrow cells from wild type BALB/c mice
[d] Lin- bone marrow cells from knockout mice
[e] 1000 randomly-generated murine genome integrations
[f] transcription start site (TSS)

6

oncogenes (as defined by the Retrovirus and transposon Tagged Cancer Gene Database) in the rhesus, human and mouse datasets was 2.5%, 2.8% and 3.1%, respectively, which is similar to the 2.8% frequency found in the *in silico* dataset. For each dataset, the Ingenuity Pathways analysis was applied to the genes within 10kb of an LVIS, and the top 20 results, measured by p-value, listed in the Disease and Functions analysis were compared. All three species as well as the *in silico* dataset had Cancer and Tissue Morphology among the top 20 pathways (Supplemental Table 2). The top functional pathway for the murine Lin- samples was Cancer, with 46.4% of mapped genes linked to this pathway (Supplemental Figure 1).

Lin- bone marrow cells derived from murine models for SCID-X1 (*Il2rg*^{-/-}), RAG1 SCID (*Rag1* [-/-]), RAG2 SCID (*Rag2* [-/-]), and Pompe disease (*Gaa*^{-/-}), as well as wild type BALB/c mice were cultured overnight with therapeutic lentiviral vectors containing the human version of the appropriate transgene or GFP as a control. The cells were subsequently cultured for 10-14 days without viral vectors before DNA was purified for LAM-PCR and LVIS analysis (Table 1). The frequency of oncogenes was lowest in the *Rag2* samples (2.5%) and highest in the *Rag1* samples (4.7%), although the difference in oncogene frequency between these groups was not significant (p=0.176). The percentage of LVIS within

10kb of a gene TSS or within 10kb of a gene appeared to be similar for all mouse disease phenotypes analyzed.

The *Il2rg*^{-/-} Lin- dataset had 1043 LVIS and thus the frequency of CIS could be directly compared to the wild type mouse Lin- dataset (1025 LVIS). The frequency of integrations flanking a TSS, gene, or oncogene were very similar for the two datasets, with a slightly higher frequency of LVIS within 10kb of a gene in the wild type group. The *Il2rg*^{-/-} data contained no CIS oncogenes out of 54 CIS, whereas the wild type group had one 3rd order CIS oncogene (*Mef2c*) and a pair of second order CIS oncogenes (*Akap13* and *Ghr*) out of 70 total CIS; however, this difference in CIS oncogene prevalence was statistically not significant (p=0.261).

Comparison of integration profiles between murine *in vitro* and *in vivo* samples

Lin- bone marrow cells derived from *Il2rg*^{-/-}, *Rag1*^{-/-}, *Rag2*^{-/-}, *Gaa*^{-/-} and *Tymp*^{-/-} *Upp*^{-/-} mice were cultured overnight with therapeutic vectors or a GFP control vector and subsequently transplanted into the appropriate mouse disease phenotype. Other wild type mice were transplanted with wild type Lin- cells after overnight transduction with a GFP control vector. Transgene expression was driven by the spleen focus forming virus (SF), ubiquitous promoter elements phosphoglycerate kinase (PGK) and ubiquitous chromatin opening element (UCOE), or cellular promoters including the RAG1 promoter (RAG1p), the TCR Vβ6.7 gene promoter (TCRVβp), and the γ chain promoter (γcPr). Genomic DNA was purified from cultured Lin- cells and from bone

marrow, spleen, and thymus tissue collected 6-12 months after transplantation. Subsequent LAM-PCR and sequencing of vector-genome fusion sequences yielded over 2,000,000 raw sequencing reads, which were annotated into 10,608 unique LVIS suitable for analysis.

Investigation of common integration sites (CIS) in murine *in vitro* and *in vivo* samples

Comparing the individual lists of CIS for the various *in vivo* and *in vitro* datasets revealed a number of CIS genes of 3rd order or higher found in multiple datasets (Supplemental Table 3a), including proto-oncogene *Mef2c*. In total, 11 oncogenes were found out of 264 total CIS of 3rd order or higher (4.2% frequency of CIS oncogenes, listed in Supplemental Table 3b).

Pooling all *in vivo* LVIS (consisting of integrations recovered from spleen, BM and thymus, 7802 total LVIS) resulted in the expected expansion of the number of CIS found, with 522 CIS genes of 3rd order or higher being returned. Similarly, the pooled murine *in vitro* LVIS (consisting of 2806 total LVIS recovered from cultured Lin- cells) contained 80 CIS of 3rd order or higher. 72% (58 out of 80) of the Lin- CIS genes were also present as CIS genes in the integrations derived from murine cell types (Figure 1). Three of the top five ranking CIS genes were the same for both sample sets (Figure 2): a 139kb region on chromosome 11 near *Sfi1* (10th order *in vivo* and 20th order *in vitro*), a 130kb region on chromosome 5 near *Uba6* (6th order and 21st order) and a 181kb region on chromosome 14 flanking *Ngly1* (7th and 12th order). Another high-ranking CIS found in both datasets was a 185kb region on chromosome 1, covering
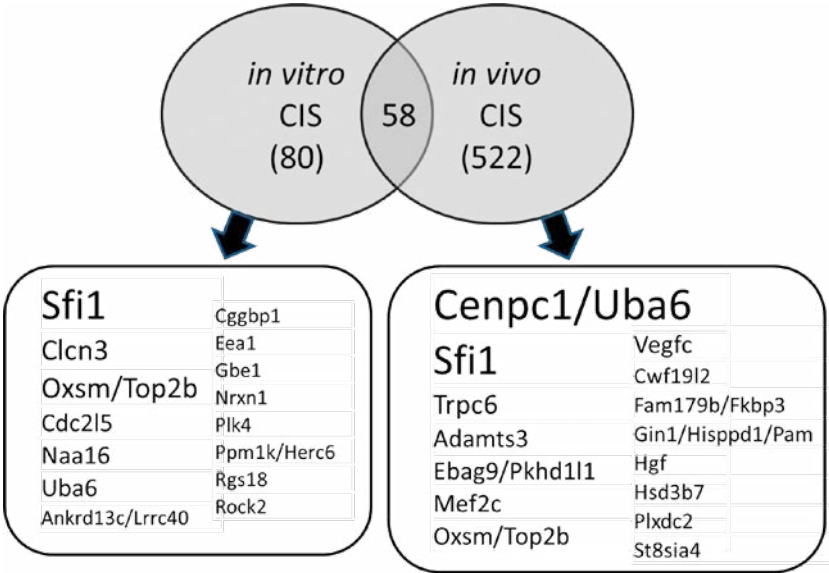
Figure 1. Common integration sites (CIS) of 3rd order or higher in murine *in vitro* vs *in vivo* datasets. CIS of 3rd order or higher are reported in the overlapping ovals, with 58 shared CIS genes. Word clouds below the ovals correspond to the relative frequency of each named gene in the CIS pool (only the top 15most prevalent CIS genes in each dataset are shown).

6

most of gene *Rgs18* (5th order and 10th order). In general, these high ranking CIS were well distributed between vectors, promoters and transgenes and were not associated with any specific murine phenotype (Figure 2).

Whereas no overall enrichment of oncogenes was seen (frequency of LVIS flanking oncogenes was 3.0% and 3.6% for the *in vitro* and *in vivo* datasets, respectively), the *in vivo* data had proportionally more oncogenes present in high ranking CIS compared to the *in vitro* data. The frequency of oncogenes in the upper 25% of CIS (corresponding to 4th order or higher *in vivo* and 3rd order or higher *in vitro*) was more prominent in the *in vivo* dataset (5.9%, compared to 3.8% for the *in vitro* dataset), although also this difference was not statistically significant (p= 0.589). Two

oncogenes are present in these high ranking CIS in both datasets: *Lnpep* and *Mef2c*.

The only tissue analyzed for all mouse phenotypes was BM, so it was chosen as the focus of further analysis (Table 2a). The percentage of the LVIS in BM flanking proto-oncogenes in the various disease phenotypes ranged from 2.3% (Pompe dataset) to 4.1% (wild type dataset), although these differences were not significant. CIS of 3rd order or greater for these datasets can be found in Supplemental Table 4, and the list of CIS oncogenes of 3rd order or higher can be found in Supplemental Table 5. Notably, the percentage of LVIS within 10kb of a gene was significantly lower for wild type mice using GFP vectors (59.3%) than in any of the disease phenotypes (67.1% to 71.1%, p<0.001 for all disease phenotypes
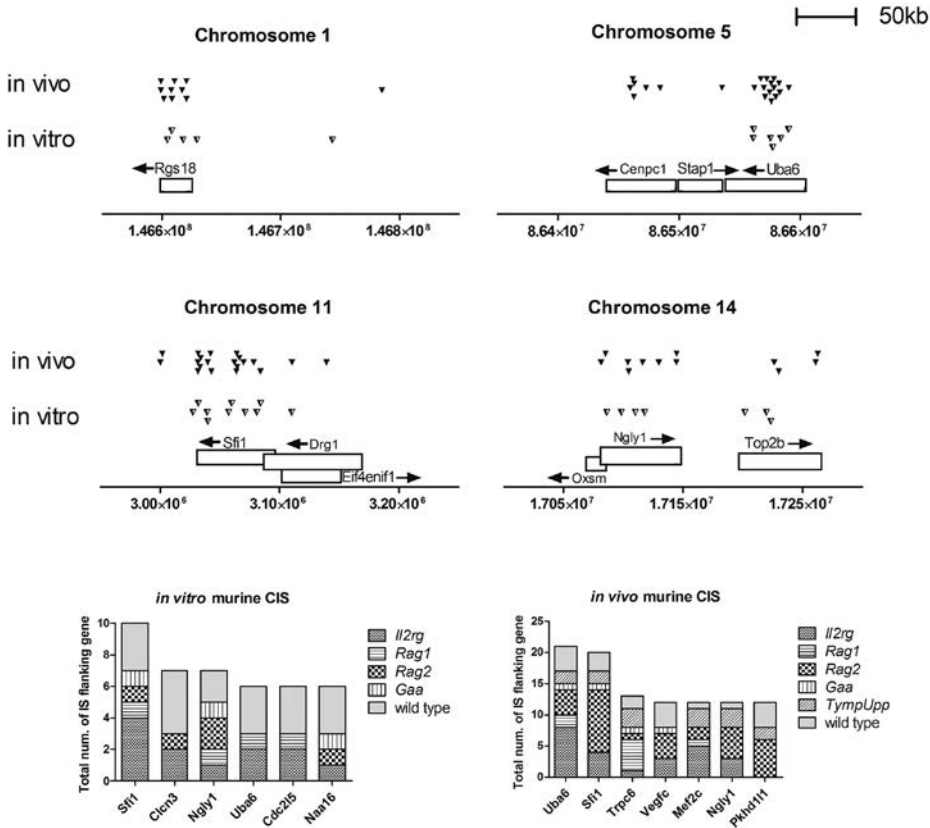
Figure 2. Map of high ranking murine CIS found in both *in vitro* and *in vivo* samples. Top: mouse chromosomal regions containing a high frequency of LV integrations *in vivo* and *in vitro* are illustrated. Each marker (triangle) represents a single integration site. Bottom: distribution of LVIS among murine phenotypes for each of the highest-level CIS found in the *in vitro* and *in vivo* datasets.

compared to the wild type group). Separating the disease phenotypes into GFP vector LVIS and therapeutic vector LVIS (Table 2b) did not significantly alter the LVIS profile, except that the Pompe therapeutic vector subset had significantly fewer LVIS within 10kb of a gene than the GFP vector subset (P = 0.04).

In order to determine as to whether *in vivo* selection of clones in the BM during or after engraftment skewed the integration profile, the LVIS of cultured Lin- and BM samples for each of the four mutant mouse strains

were compared (Table 2a). The percentages of LVIS within 10kb of a gene TSS and within 10kb of a gene end were significantly lower in LVIS recovered from wild type BM samples than in LVIS recovered from wild type Lin- samples (p <0.0001), but this difference was not seen in the disease models. Significant differences were not observed between Lin- and BM samples in the frequency of oncogenes (group averages of oncogene frequency were 3.2% and 3.4%, respectively). The integration profiles in spleen and thymus

Table 2a. LVIS recovered from Lin- and BM cells in murine disease models and WT

	Il2rg	Rag1	Rag2	Gaa	TympUpp	WT	
total LVIS	1043	148	402	188	ND	1025	
unique genes	893	141	373	181	ND	892	
percent oncogenes	3.0%	4.7%	2.5%	2.7%	ND	3.1%	Lin-
percent w/in 10kb of TSS	16.9%	16.9%	19.4%	19.1%	ND	20.3%	
percent w/in 10kb of gene	70.0%	83.1%	77.4%	66.0%	ND	71.3%	
total LVIS	1372	515	491	574	1075	1402	
unique genes	1032	448	446	502	885	981	
percent oncogenes	3.2%	3.9%	2.9%	2.3%	3.9%	4.1%	BM
percent w/in 10kb of TSS	14.1%	21.4%	17.7%	19.9%	15.2%	10.7%	
percent w/in 10kb of gene	67.1%	69.7%	68.8%	68.4%	71.1%	59.3%	

Table 2b. BM LVIS stratified by transgene

	GFP transgene				
	Il2rg	Rag1	Rag2	Gaa	TympUpp
total LVIS	647	31	36	364	511
unique genes	542	26	35	321	461
percent oncogenes	4.1%	0.0%	0.0%	2.2%	3.9%
percent w/in 10kb of TSS	14.0%	12.9%	13.9%	20.6%	15.3%
percent w/in 10kb of gene	67.1%	74.2%	66.7%	71.4%	70.1%

	Therapeutic transgene				
	Il2rg	Rag1	Rag2	Gaa	TympUpp
total LVIS	725	484	455	210	564
unique genes	607	423	413	196	479
percent oncogenes	2.5%	4.1%	3.1%	2.4%	3.9%
percent w/in 10kb of TSS	14.0%	21.9%	18.0%	18.1%	15.1%
percent w/in 10kb of gene	66.8%	69.4%	69.0%	62.9%	72.2%

Table 2c. Spleen and thymus LVIS stratified by transgene

	GFP transgene			Therapeutic transgene		
	Il2rg	Rag1	Rag2	Il2rg	Rag1	Rag2
total LVIS	306	81	125	52	810	1357
unique genes	188	60	115	31	602	1080
percent oncogenes	2.9%	0.0%	2.4%	3.8%	4.4%	4.5%
percent w/in 10kb of TSS	20.9%	17.3%	13.6%	21.2%	21.7%	19.9%
percent w/in 10kb of gene	68.3%	64.2%	70.4%	78.8%	72.3%	73.0%

6

were compared to BM in the same manner (Table 2c; the non-SCID phenotypes did not have sufficient integrations for comparative analysis). Significant differences between these tissues were not found when comparing the frequency of LVIS near genes, gene TSS or oncogenes.

LVIS association to cellular gene expression levels

Genes flanking LVIS were referenced against an expression level binning database generated via an Affymetrix mouse 430 2.0 gene array. Briefly, cDNA derived from mouse Lin- Sca-1+cKit+ (LSK) cells after 2 days of stimulation with growth factors was measured on this whole genome array, and the resulting gene expression values were sorted into five equally sized bins based on expression level. Genes flanking an LVIS in the Lin- and BM datasets were referenced against this database and sorted into the appropriate bin. The resulting binning chart (Supplemental Figure 2) confirms that lentiviral vectors prefer to integrate near or into active genes in HSC. A similar expression pattern was seen in genes flanking *in vitro* LVIS (top) and *in vivo* (bottom) integrations, suggesting that LVIS near highly expressed genes undergo minimal selective pressure. However, the top 10 overrepresented functions and diseases based Ingenuity Pathways analysis that appear for Lin- and BM datasets markedly differed (Figure 3). The BM datasets showed a high frequency of Cancer, Hematopoiesis, Cell to Cell Signaling and Interaction and Cellular Development in their top 10 (these diseases/functions were found in 4 out of 5 Lin- datasets). Conversely, the Lin- datasets had a high frequency of Small Molecule

Biochemistry, Cell Cycle, and Cell Death and Survival (each found in 4 out of 5 BM datasets). Hematological System Development and Function was frequently found in the top 10 of both groups: in all 5 BM datasets and in 4 out of 5 Lin- datasets.

Comparison of integration profiles: GFP vs therapeutic transgenes

To determine as to whether insertion of a therapeutic transgene results in a selective advantage and LVIS bias after engraftment, the integration profiles of BM samples from diseased mice treated with therapeutic vectors were compared with those of mice treated with GFP control vectors (Table 2b). Significant difference in the frequency of LVIS near genes, TSS or oncogenes were not seen between the *GFP* and the therapeutic gene datasets. Ingenuity Pathways Analysis revealed that 6 out of the top 10 Ingenuity Functions and Diseases, and 13 of the top 20, were shared between the *GFP* and *IL2RG* groups (Figure 4).

Comparison of integration profiles: SF vs eukaryotic promoter elements

The murine integrations analyzed here include some studies using vectors containing the SF promoter element in order to maximize expression of the therapeutic transgene, as well as SF-GFP control vectors. The SF promoter has been implicated in the onset of oncogenic transformation in hematopoietic cells[19]. The *in vivo* integrations collected from murine disease models were stratified for SF vs non-SF promoters (i.e., PGK, RAG1p, TCRβp, UCOE and γcPr) to assess possible skewing vector integration profiles *in vivo*. A total of 3396 SF vector integrations from BM, spleen
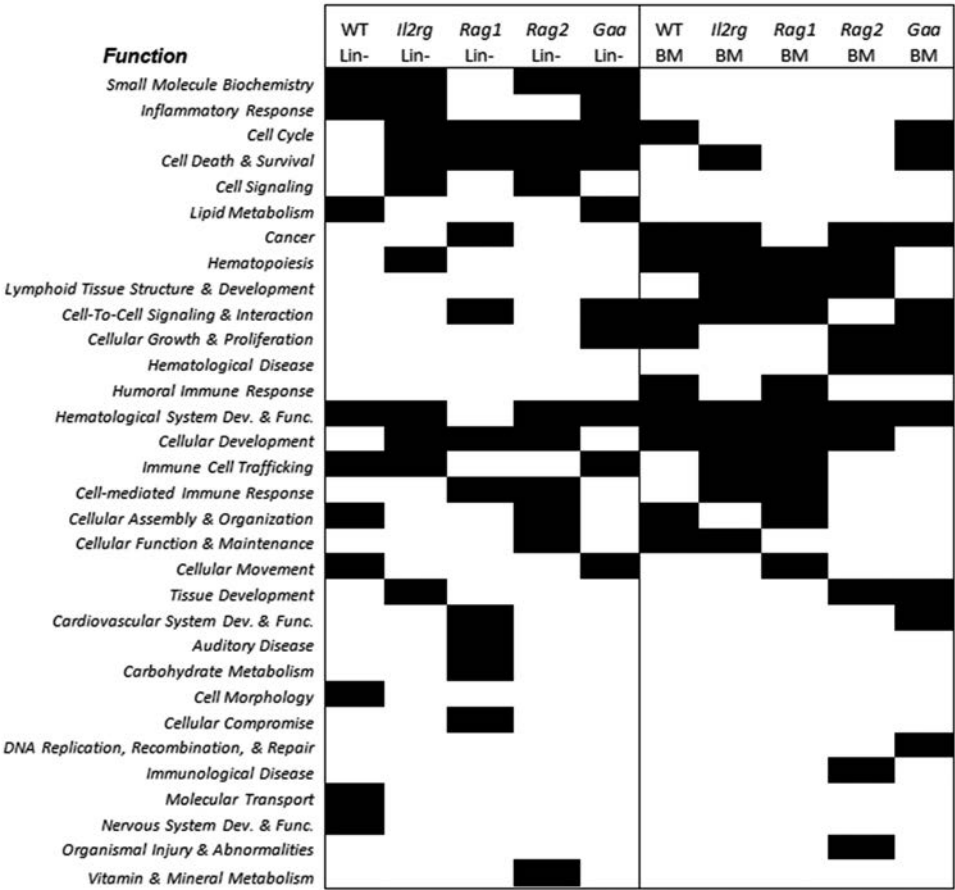
Figure 3. Top 10 ranked IPA Diseases and Functions for murine Lin- and BM datasets. This matrix shows the top 10 highest significance (based on p-value) Ingenuity Diseases and Functions for the LVIS genes in wild type (WT) and mouse disease models. The LVIS genes were stratified by integrations recovered from *in vitro* (Lin- cells, left half of the figure) and *in vivo* (bone marrow, right half of figure) samples.

or thymus were compared to 3058 non-SF vector LVIS (Table 3a). The frequency of LVIS flanking oncogenes for the two datasets was 3.5% and 3.6% respectively and did not differ significantly (p=0.904). Six of the top 10 IPA diseases and functions were shared between the SF and eukaryotic promoter integrations (Table 3b). Further stratifying the *in vivo* LVIS pool by promoter (SF vs eukaryotic promoters) and transgene (GFP vs therapeutic

gene) resulted in no significant differences between the 4 resulting data subsets (Table 3a). Stratifying only the BM integrations by promoter returned the same non-significant results (data not shown).

Analysis of LVIS found in leukemic SCID mice

Experimental mice (primary and secondary transplants) were monitored for adverse

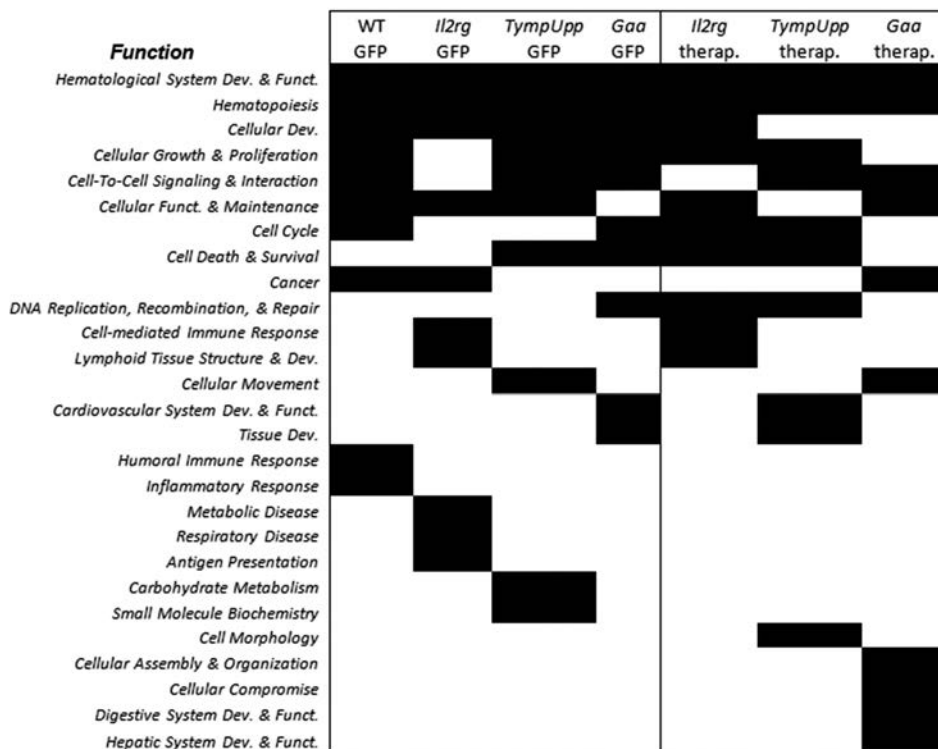| Function	WT GFP	Il2rg GFP	TympUpp GFP	Gaa GFP	Il2rg therap.	TympUpp therap.	Gaa therap.
Hematological System Dev. & Funct.							
Hematopoiesis							
Cellular Dev.							
Cellular Growth & Proliferation							
Cell-To-Cell Signaling & Interaction							
Cellular Funct. & Maintenance							
Cell Cycle							
Cell Death & Survival							
Cancer							
DNA Replication, Recombination, & Repair							
Cell-mediated Immune Response							
Lymphoid Tissue Structure & Dev.							
Cellular Movement							
Cardiovascular System Dev. & Funct.							
Tissue Dev.							
Humoral Immune Response							
Inflammatory Response							
Metabolic Disease							
Respiratory Disease							
Antigen Presentation							
Carbohydrate Metabolism							
Small Molecule Biochemistry							
Cell Morphology							
Cellular Assembly & Organization							
Cellular Compromise							
Digestive System Dev. & Funct.							
Hepatic System Dev. & Funct.							

Figure 4. Top Ingenuity Functional Pathways linked to *in vivo* samples containing GFP or therapeutic transgenes. Matrix shows the top 10 highest significance (based on p-value) Ingenuity Diseases and Functions for LVIS recovered from bone marrow in wild type (WT) and mouse disease models. The BM LVIS genes were further stratified by integrations from GFP control vectors (left panel) or therapeutic vectors (right panel).

Table 3a. Integration profiles of *in vivo* LVIS stratified by promoter (SF viral promoter vs. eukaryotic promoters) and transgene

	SF	euk.	SF-GFP	euk.-GFP	SF-therap.	euk.-therap.
total LVIS	3396	3058	456	1586	2940	1472
percent oncogenes	3.5%	3.6%	1.8%	3.7%	3.7%	3.5%
percent w/in 10kb of TSS	19.0%	16.8%	19.7%	15.6%	18.8%	17.9%
percent w/in 10kb of gene	70.3%	69.3%	70.0%	68.4%	70.4%	70.2%

events. In the course of LV gene therapy treatment of *Il2rg*^{-/-} mice, 18 cases of malignant hematopoietic clonal expansion were confirmed (Table 4 and Supplemental Table 6), including 8 in mice treated with *IL2RG* vectors (out of 117 primary mice, a 6.8% adverse event rate), 7 in mice treated with GFP vectors or vectors containing no transgene (out of 95 mice, 7.4%) and 3 in mice given untransduced wild type Lin- cells (out

Table 3b. Top 10 Ingenuity Pathways Analysis functions and diseases for *in vivo* LVIS, stratified by promoter (SF viral promoter vs. eukaryotic promoters)

SF promoter		eukaryotic promoters	
Category	**p-value**	**Category**	**p-value**
Cellular Growth and Proliferation	5.06E-04	Cell Cycle	1.21E-05
Organismal Survival	5.93E-04	DNA Replication, Recombination, and Repair	1.21E-05
Cell Death and Survival	7.05E-04	Cancer	1.82E-05
Gene Expression	8.50E-04	Cellular Development	8.30E-05
Hematological System Development and Function	1.08E-03	Hematological System Development and Function	8.30E-05
Hematopoiesis	1.08E-03	Hematopoiesis	8.30E-05
Tissue Morphology	1.08E-03	Lymphoid Tissue Structure and Development	8.30E-05
Cell Cycle	1.25E-03	Cellular Growth and Proliferation	9.82E-05
DNA Replication, Recombination, and Repair	1.25E-03	Cell-mediated Immune Response	1.13E-04
Cancer	1.79E-03	Cellular Function and Maintenance	1.13E-04

6

of 27 mice, 11.1%). 15 out of the 18 events were T-cell derived, including 13 CD4+CD8+ leukemia's, and 2 single positives for CD4 and CD8. The remaining malignancies consisted of one B220+CD19+, one CD11b+ and one Sca-1+ leukemia. All but one of these malignancies were donor-derived, as determined by PCR through Y chromosome chimerism levels. A clear correlation between leukemiagenesis and promoter or transgene was not observed; mice transplanted with untransduced wild-type control cells had the highest leukemic frequency. BM and spleen DNA from these mice was analyzed via LAM-PCR to determine if certain integrations were dominant, i.e. consisted of 50% or more of the LVIS pool, which is often associated with dominant leukemic clones. Integrations found in the leukemic mice were excluded from the LVIS datasets to avoid skewing that data and increasing the prevalence of certain oncogenes in the larger analysis.

LAM-PCR analysis of these BM of these mice revealed dominant LVIS flanking or in the introns of oncogenes (*Mef2c*, *Mll3*, *Ccnd2*, *Pax5*, and *Aspscr1*), transcriptional repressor genes (*Pum2* and *Kctd1*) and proposed tumor suppressor genes (*Pyhin1* and *Shprh*). It is possible that some of these integrations may have played a role in tumorigenesis in these animals, although no direct relation between any IS and a leukemic event were confirmed. Other mice with leukemia contained no prominent LVIS were found within 500kb of any known proto-oncogene or tumor-related genes.

Three leukemias were observed in control *Il2rg*-/- mice transplanted with untransduced wild type BALB/c Lin- cells, including the sole recipient-derived malignancy with two in primary transplants and one in a secondary transplant. The primary leukemias were CD8+ (donor derived) and CD4+CD8+ (recipient

Table 4. Overview of leukemia phenotypes seen in *Il2rg^-/-* mice during Lin- cell transplantation and gene therapy experiments

ID	transplant type	LV vector	donor cells	TBI dose	onset of illness (weeks)	PB WBC count	malignancy phenotype	% phenotype in BM	Y-chimerism (BM)
1	2°	PGK.coIL2RG	Il2rg--	6 Gy	66	67.8	CD4CD8	89	86%
2	2°	PGK.GFP	BALB/c	6 Gy	44	3.2	CD4CD8	79	87%
3	2°	PGK.GFP	BALB/c	6 Gy	68	4.5	CD4CD8	44	71%
4	2°	PGK.GFP	BALB/c	6 Gy	68	2.5	CD4CD8	37	71%
5	2°	PGK.GFP	BALB/c	6 Gy	52	20.5	CD4CD8	64	70%
6	1°	SF.coIL2RG	Il2rg--	0 Gy*	27	258	CD4CD8	60.9	59%
7	1°	SF.Il2RG	Il2rg--	6 Gy	21	243	Sca-1	93	95%
8	1°	SF.Il2RG	Il2rg--	6 Gy	25	80	CD4CD8	87	62%
9	1°	SF.empty	BALB/c	6 Gy	35	153	CD11b	96	72%
10	1°	SF.empty	Il2rg--	6 Gy	22	137	CD4CD8	82	75%
11	1°	γcPR.coIL2RG	Il2rg--	2 Gy	30	29.8	CD4CD8	57	95%
12	1°	γcPR.coIL2RG	Il2rg--	2 Gy	33	1.7	CD4CD8	92	57%
13	1°	γcPR.coIL2RG	Il2rg--	2 Gy	28	65.9	CD4	86	63%
14	1°	γcPR.coIL2RG	Il2rg--	2 Gy	28	71	CD4CD8	94	82%
15	1°	γcPR.GFP	BALB/c	2 Gy	35	28.8	CD4CD8	83	88%
16	2°	none	BALB/c	6 Gy	67	16.8	CD19	96	95%
17	1°	none	BALB/c	2 Gy	27	2.9	CD8	84	97%
18	1°	none	BALB/c	2 Gy	27	16.5	CD4CD8	75	12%

* this mouse was given G-CSF mobilization in lieu of TBI
1° = primary transplant
2° = secondary transplant
TBI = total body irradiation
PB = peripheral blood
WBC = white blood cell
SF.empty = control vector, no transgene

derived), and the secondary leukemia had a donor-derived, B220+CD19+ phenotype.

Four CD4+CD8+GFP+ leukemias were found in mice treated with *LV.PGK.GFP*, all in the secondary transplants of a single experiment. This experiment involved an alternate transplantation protocol: a very low number of transduced wild type Lin- cells (3000 to 300 cells per mouse) were expanded *in vitro* for seven days, then the expanded cells were transplanted into 6 Gy conditioned *Il2rg-/-* recipients. Three of the leukemias shared an integration site on chromosome 5 in intron 1-2 of gene *Phtf2* (putative homeodomain transcription factor 2), suggesting that the pre-leukemic clone originated in the primary cell pool prior to transplantation. No known oncogenes were found within 500kb of these LVIS.

|DISCUSSION

Lentiviral vectors are a viable alternative to gammaretroviral vectors for clinical gene therapy trials, offering a distinct integration pattern which favors integrations in or near active genes rather than near gene transcription start sites and have no propensity to integrate near oncogenes. Previous studies conducted with gammaretroviral and lentiviral vectors demonstrated that transcriptionally active LTRs, such as those used in the initial SCID-X1 clinical trials, are major determinants of genotoxicity[19]. The same studies suggested that lentiviral vectors require a 10-fold higher viral load to trigger leukemogenesis than gammaretroviral vectors, likely due to gammaretroviruses' preference to integrate into the promoter regions of active genes and into genes involved in cell growth and cancer[15].

Although many groups are investigating lentiviral gene therapy vectors for treatment of inherited diseases, assessing lentiviral integration patterns is complicated by differences in vector design, transduction protocols and integration site annotation methodology, which induce variability and complicate direct comparison of lentiviral integration profiles derived from different sources. To enable large-scale comparison of lentiviral integration profiles under a wide range of physiological settings, we pooled the total LVIS annotations from our *in vitro* and *in vivo* experiments performed in the same lab. Nearly 14,000 lentiviral integration sites have been annotated and analyzed, including murine LVIS collected *in vitro* and *in vivo* from immune deficiencies, a lysosomal storage disorder, a mitochondrial disorder and wild type mice, and LVIS from transduced human and rhesus CD34+ cells. By stratifying the pooled LVIS based on various parameters, we can observe which vector features, such as promoter and transgene, may act as selective forces on gene therapy-treated HSC after transplantation and engraftment in the bone marrow.

Comparison of LVIS generated *in vitro* in mouse, rhesus and human hematopoietic stem and progenitor cells confirms that the vector's integration preferences are not species specific. The percentage of LVIS within 10kb of a gene TSS ranged from 14.7% of mapped LVIS for the human samples up to 20.3% for the murine samples, a range consistent with previous observations of LV vectors in human HPSC and lower than the percentage reported

for gammaretroviral vectors (29.3%)[32]. The expected LV integration bias into gene regions[17] was observed, with the percentage of LVIS within a gene or less than 10kb distant ranging from 69.6% (rhesus) to 73.4% (human). Significant differences were not found between the three species when comparing the frequency of LVIS near genes, gene TSS, or oncogenes. The three species also had a similar profile of Ingenuity Functional Pathways, with all three having an overrepresentation of genes involved in cancer and tissue morphology.

It has been hypothesized that viral integrations which improve the relative fitness of transduced hematopoietic progenitor cells in the competitive environment of the bone marrow niche or thymus will give those cells a competitive advantage. If this is the case, integration sites near proto-oncogenes or genes involved in cell proliferation, would more likely be found *in vivo*. The study described here compared pre-transplant Lin- samples to samples collected from bone marrow, spleen and thymus 6 months or longer post-transplantation and revealed similar frequencies in LVIS flanking an oncogene. The expression profiles of genes flanking LVIS in Lin- and BM samples were similar, with highly expressed genes being favored. The relative frequency of LVIS within 10kb of a gene was lower in transplanted cells than in Lin- cells for all phenotypes except the *Gaa*^{-/-} mice. The reduction in LVIS near or in genes may result from some of the integrations disrupting gene function and reducing the viability of the transduced cells, an effect which would not be seen in Lin- cells cultured for only a week. There is also evidence that suggests post-transplant site selection. Ingenuity Pathways analysis

of the genes flanking LVIS shows several pathways more prevalent in BM samples than in Lin- samples (Figure 3), including Cancer, Hematopoiesis, and Lymphoid Tissue Structure and Development. The nature of these overrepresented pathways suggests that selection for integrations flanking cellular expansion genes could take place *in vivo*. It is also possible that there is no selection *in vivo*, but that the differences found are due to the differences in cycling state at transduction: the integration profiles of the Lin- cells analyzed here represent integrations in cycling hematopoietic progenitors as well as HSC, whereas the profile observed *in vivo* is exclusively derived from long-term repopulating stem cells and their progeny, which are not cycling at the start of overnight transduction.

The frequency of common integration sites (CIS) varied based on the size of the dataset analyzed, but in all cases was 3-to 4-fold higher than the expected frequency of CIS in datasets of comparable size based on mathematical models of random integration or on *in silico* data [33]. This further emphasizes that lentiviral integration patterns are only semi-random and that LV integration hot spots are prevalent in murine HSC. A majority of the CIS genes identified in the Lin- samples were also CIS genes in the post-transplant samples, indicating that these genes are located in areas of frequent lentiviral integrations. Two hot spots in particular, located in ~140kb spans in genes *Sfi1* and *Uba6*, were found frequently across multiple cell types, vectors and disease phenotypes (Figure 2). *Sfi1*, one of the most commonly found LVIS genes in both the *in vitro* and *in vivo* data, is involved in hematopoietic differentiation and has been noted previously as a lentiviral integration

hot spot in both murine Lin- BM cells[34, 35] and hepatocytes[36]. *Uba6* is an ubiquitin-activating gene, and LV integrations near this gene have been reported before in a tumor-prone mouse model[34]. To the best of our knowledge, LV integration hot spots found on chromosomes 1 and 14 have not been previously associated with viral integration.

Two CIS oncogenes were found in both the *in vitro* and *in vivo* murine integrations: *Mef2c* on chromosome 13, and *Lnpep* on chromosome 17. Both of these oncogenes were high-order CIS *in vivo* (12th order and 9th order, respectively). An integration near *Mef2c* was also found in a *Il2rg*^{-/-} mouse transduced with a *LV.SF.IL2RG* vector which had an unusual *Sca-1*^{+} leukemic phenotype. *Mef2c* is a CIS for gammaretroviral vectors[37, 38], which suggests a role in hematopoietic development. Additionally, this gene has been previously identified as a possible contributor to T-ALL in humans[38].

The Lin- data had one additional CIS oncogene, *Akap13*, which was not a CIS in the transplanted tissues (only 2 integrations were found flanking this gene *in vivo*). There were 47 CIS oncogenes in the transplanted cells that were not present as CIS in the Lin- cells, including an 8th order CIS in the *Mds1* and *Evi1* complex locus (MECOM), an integration site commonly found in transduced mouse hematopoietic progenitors[39]. Overall, the frequency of CIS oncogenes was somewhat lower for the Lin- than the transplanted LVIS (3.3% vs 3.9%), although not significantly (p=0.738).

Comparing the LVIS profiles of therapeutic vectors to GFP control vectors revealed no evidence of integration site skewing in the frequency of integrations flanking gene TSS or oncogenes and did not affect the overrepresented Ingenuity Functional Pathways (Figure 4). Stratifying the LVIS profiles of mouse disease models by promoter and comparing vectors where transgene expression is driven by the SF viral promoter versus vectors using a eukaryotic promoter also showed no significant differences in the function of flanking genes or the frequency of nearby oncogenes. These findings indicate that the promoter and transgene incorporated by lentiviral vectors has little or no effect on LV integration profiles.

Following the initial reports of leukemias in SCID-X1 gene therapy trials[11, 12], the MFG Moloney-gammaretrovirus derived vector used in these trials was implicated as having a role in oncogenesis. The case against viral enhancer/promoters was made due to the strength of activation of nearby genes and its possible influence on the integration site profile [18, 20]. *In vitro* immortalisation assays seemed to confirm the higher genotoxic risks of viral promoters, such as the SF promoter, compared to weaker eukaryotic promoters [20, 40].

In our experiments with SIN lentiviral vector gene therapy for murine SCID-X1, the choice of promoter seemed to have no effect on the rate of leukemogenesis. Mice treated with the SF promoter had a leukemia rate of 6%, similar to the rates seen in eukaryotic promoters PGK (9%) and γcPr (6%), while the highest leukemia rate (11 %) was observed in recipients of untransduced wild-type cells. While it is feasible that the additional risks associated with the SF vector *in vitro* are reduced *in vivo* due to regulation of the bone marrow niche, it is also possible that our mouse model assay, with its limited number of mice per group, is not sufficiently sensitive to detect differences in the oncogenic potential

6

of the various promoters. However, the more likely explanation involves leukemogenesis due to the *Il2rg*^{-/-} phenotype independent of vector integrations. Il2rg^{-/-} mice are known to be prone to leukemia development[41], particularly after HSC transplantation. The large majority (15 out of 18) of the observed leukemia's occurred in the T cell lineages. This was highly significant and suggests that the T cell lineages are especially prone to oncogenesis in this setting. It is noteworthy that all 5 leukemias seen in the human SCID-X1 gene therapy trials were T-ALL, as were 6 out of 7 leukaemias seen in the trial for Wiskott-Aldrich syndrome (WAS)[14]: both WAS and SCID-X1 are T[-] immunodeficiencies. Similarly, the two adverse events seen in the chronic granulomatous disease (CGD) clinical trial were myelodysplasias[13]. It is possible that corrected hematopoietic progenitor cells belonging to the deficient cell type are subjected to additional proliferative stress and therefore more susceptible to transformative events, particularly when this stress is combined with disruptive viral integrations near key oncogenes.

Overall, these data suggest that lentiviral integration profiles are stable across species and in mice with a wide range of phenotypes, and that LV vector HSC gene therapy has a low risk of integrating vectors near oncogenes similar to that found in *in silico* and random integration datasets.

| MATERIALS AND METHODS

Animals

Wild-type BALB/c or C57BL/6, and C57BL-6-*Rag1*[-/-26], BALB/c-*Rag2*[-/-25], BALB/c-*Il2rg*[-/-24], FVB/N-*Gaa*[-/-42] and C57BL/6-*Tymp*^{-/-}/*Upp*^{-/-} (MNGIE) mice were used for gene therapy studies as previously described. Purpose bred rhesus monkeys (*Macaca mulatta*) aged 2 to 3 years were housed in stainless steel cages, preferably in small peer groups and provided with normal daylight rhythm, conditioned to 20°C with a relative humidity of 70%. All mice and rhesus monkeys were bred in the Experimental Animal Center of Erasmus MC. Housing, experiments and all other conditions were approved by the institutional Animal Ethical Committee of Erasmus MC in accordance with legislation in the Netherlands.

Lentiviral vectors

The third generation self-inactivating (SIN) HIV-1 lentiviral vector (LV) pRRL.PPT. SF.GFP.bPRE4*.SIN[30, 31] backbone was used and derivatives were constructed using as previously described[24-27].

Therapeutic promoter cassettes were divided in virus promoter (spleen focus forming virus; SF), ubiquitous promoters (UP) and cellular restricted promoters (CP). UP included the house keeping promoter phosphoglycerate kinase (PGK), and a ubiquitous chromatin opening element (UCOE)[43]. The CP used were the human RAG1 promoter (RAG1p), the TCR Vβ6.7 gene promoter (TCRVβp), and the γ chain promoter (γcPr)[26, 44]. The CP promoters were made by PCR amplification of human genomic DNA.

The *SF.GFP* construct was used for *in vitro* transduction of murine, rhesus and human HSC and *in vivo* studies in wild type BALB/c mice. The full list of lentiviral vector constructs used for *in vivo* murine experiments and the disease backgrounds can be found in

Supplemental Table 7. Several therapeutic genes were subjected to codon optimization of transgene cDNA (nomenclature "co") to improve transcription and translation[45]. Codon optimization was performed by GeneOptimizer® software (GeneArt AG, Regensburg, Germany) or OptimumGene™ - Codon Optimization (Genscript, USA).

Transduction of human, rhesus and mouse hematopoietic progenitors

Lin- cells from male mice were purified by lineage depletion (Lin-) (BD Biosciences, Santa Clara, CA). Rhesus CD34+ HSC were obtained from freshly collected or cryopreserved humeral bone marrow aspirants followed by positive selection for the CD34 antigen. Human CD34+ HSC were obtained from freshly collected or cryopreserved umbilical cord blood followed by positive selection for the CD34 antigen. All cells were cultured in serum free modified Dulbecco's medium with supplements as described [46] and growth factors murine stem cell factor (mSCF) 100 ng/mL, human FMS-like tyrosine kinase 3-ligand (hFlt3-L) 50ng/ml and murine thrombopoietin (mTPO) 10ng/ml for murine cells. Human SCF was used for human and rhesus cells, and human TPO and rhesus TPO was used for species specific cells at similar concentrations as for murine cells. All hematopoietic cells were transduced overnight at various cell densities. Vector dose varied based on the experiment, with a range 0.2 to 5.9 vector copies per Lin- cell, as measured by qPCR. Subsequently, cells were cultured for 5-9 days before harvesting Lin- samples, ormurine cells cultured overnight and subsequently injected in a range of 1×10^6 to 1×10^4 Lin- cells into the tail vein of 6 Gy or 2 Gy irradiated female recipients. Mice were followed for six to twelve months and subsequently DNA was purified from bone marrow, spleen and thymus.

LAM-PCR and integration site analysis workflow

High-resolution insertion-site analysis by linear amplification–mediated PCR (LAM-PCR) of vector-genome border regions was performed as previously described [29]. Restriction enzymes Tsp509I or MseI were used with the lentiviral (HIV) primer set. LAM-PCR products were pooled and sequenced at GATC Biotech (Konstanz, Germany) and subsequently annotated. Briefly, viral sequences were trimmed and the remaining genomic sequences aligned to the appropriate genome via BLAST using previously described parameters for to distinguish bona-fide integration sites[7], with the following exceptions: MAVRIC[47] was used as the annotation software with the following parameters: no repeat masking, minimum sequence length = 20 bp, minimum BLAST e-value = 0.01, max distance from integration site to look for genes = 100kb. Sequences were aligned to the murine genome via BLAST (v.37) and nearby genes identified using Ensembl version 59. Sequences with a sequence count <2 were excluded from further analysis. Each LVIS was annotated with a single, nearest Refseq gene, which was subsequently used for downstream analysis. Genes nearest to an integration site were flagged as proto-oncogenes based on a list of 528 mouse common integration site genes from the Retrovirus and transposon Tagged Cancer Gene Database. Common integration sites (CIS) were determined based on established methods[48].

6

Statistics

P values for comparisons of the frequency of oncogenes, LVIS near TSS, and LVIS within 10kb of a gene were calculated using the Chi-square test or Fisher's Exact test (2-sided), with Bonferroni's correction used to adjust the threshold p value (α) where applicable. P-values for overrepresented functional pathways calculated automatically using Ingenuity's software (Fisher's Exact test) and adjusted for multiple comparison analysis using Bonferroni's correction (calculated on the basis of 75 functional groups for each analysis).

|ACKNOWLEDGEMENTS

|REFERENCES

1. Gaspar, HB, Cooray, S, Gilmour, KC, Parsley, KL, Adams, S, Howe, SJ, et al. (2011). Long-term persistence of a polyclonal T cell repertoire after gene therapy for X-linked severe combined immunodeficiency. Sci Transl Med 3: 97ra79.

2. Hacein-Bey-Abina, S, Hauer, J, Lim, A, Picard, C, Wang, GP, Berry, CC, et al. (2010). Efficacy of gene therapy for X-linked severe combined immunodeficiency. N Engl J Med 363: 355-364.

3. Aiuti, A, Cattaneo, F, Galimberti, S, Benninghoff, U, Cassani, B, Callegaro, L, et al. (2009). Gene therapy for immunodeficiency due to adenosine deaminase deficiency. N Engl J Med 360: 447-458.

4. Gaspar, HB, Cooray, S, Gilmour, KC, Parsley, KL, Zhang, F, Adams, S, et al. (2011). Hematopoietic stem cell gene therapy for adenosine deaminase-deficient severe combined immunodeficiency leads to long-term immunological recovery and metabolic correction. Sci Transl Med 3: 97ra80.

5. Ott, MG, Schmidt, M, Schwarzwaelder, K, Stein, S, Siler, U, Koehl, U, et al. (2006). Correction of X-linked chronic granulomatous disease by gene therapy, augmented by insertional activation of MDS1-EVI1, PRDM16 or SETBP1. Nat Med 12: 401-409.

6. Boztug, K, Schmidt, M, Schwarzer, A, Banerjee, PP, Diez, IA, Dewey, RA, et al. (2010). Stem-cell gene therapy for the Wiskott-Aldrich syndrome. N Engl J Med 363: 1918-1927.

7. Aiuti, A, Biasco, L, Scaramuzza, S, Ferrua, F, Cicalese, MP, Baricordi, C, et al. (2013). Lentiviral Hematopoietic Stem Cell Gene Therapy in Patients with Wiskott-Aldrich Syndrome. Science 341.

8. Cavazzana-Calvo, M, Payen, E, Negre, O, Wang, G, Hehir, K, Fusil, F, et al. (2010). Transfusion independence and HMGA2 activation after gene therapy of human beta-thalassaemia. Nature 467: 318-322.

9. Cartier, N, Hacein-Bey-Abina, S, Bartholomae, CC, Bougneres, P, Schmidt, M, Kalle, CV, et al. (2012). Lentiviral hematopoietic cell gene therapy for X-linked adrenoleukodystrophy. Methods Enzymol 507: 187-198.

10. Biffi, A, Montini, E, Lorioli, L, Cesani, M, Fumagalli, F, Plati, T, et al. (2013). Lentiviral Hematopoietic Stem Cell Gene Therapy Benefits Metachromatic Leukodystrophy. Science.

11. Hacein-Bey-Abina, S, Garrigue, A, Wang, GP, Soulier, J, Lim, A, Morillon, E, et al. (2008). Insertional oncogenesis in 4 patients after retrovirus-mediated gene therapy of SCID-X1. J Clin Invest 118: 3132-3142.

12. Howe, SJ, Mansour, MR, Schwarzwaelder, K, Bartholomae, C, Hubank, M, Kempski, H, et al. (2008). Insertional mutagenesis combined with acquired somatic mutations causes leukemogenesis following gene therapy of SCID-X1 patients. J Clin Invest 118: 3143-3150.

13. Stein, S, Ott, MG, Schultze-Strasser, S, Jauch, A, Burwinkel, B, Kinner, A, et al. (2010). Genomic instability and myelodysplasia with monosomy 7 consequent to EVI1 activation after gene therapy for chronic granulomatous disease. Nat Med 16: 198-204.

14. Braun, CJ, Boztug, K, Paruzynski, A, Witzel, M, Schwarzer, A, Rothe, M, et al. (2014). Gene therapy for Wiskott-Aldrich syndrome--long-term efficacy and genotoxicity. Sci Transl Med 6: 227ra233.

15. Schwarzwaelder, K, Howe, SJ, Schmidt, M, Brugman, MH, Deichmann, A, Glimm, H, et al. (2007). Gammaretrovirus-mediated correction of SCID-X1 is associated with skewed vector integration site distribution in vivo. J Clin Invest 117: 2241-2249.

16. LaFave, MC, Varshney, GK, Gildea, DE, Wolfsberg, TG, Baxevanis, AD, and Burgess, SM (2014). MLV integration site selection is driven by strong enhancers and active promoters. Nucleic Acids Res 42: 4257-4269.

17. Schroder, AR, Shinn, P, Chen, H, Berry, C, Ecker, JR, and Bushman, F (2002). HIV-1 integration in the human genome favors active genes and local hotspots. Cell 110: 521-529.

18. Montini, E, Cesana, D, Schmidt, M, Sanvito, F, Ponzoni, M, Bartholomae, C, et al. (2006).

Hematopoietic stem cell gene transfer in a tumor-prone mouse model uncovers low genotoxicity of lentiviral vector integration. Nat Biotechnol 24: 687-696.

19. Montini, E, Cesana, D, Schmidt, M, Sanvito, F, Bartholomae, CC, Ranzani, M, et al. (2009). The genotoxic potential of retroviral vectors is strongly modulated by vector design and integration site selection in a mouse model of HSC gene therapy. J Clin Invest 119: 964-975.

20. Modlich, U, Bohne, J, Schmidt, M, von Kalle, C, Knoss, S, Schambach, A, et al. (2006). Cell-culture assays reveal the importance of retroviral vector design for insertional genotoxicity. Blood 108: 2545-2553.

21. Cavazza, A, Moiani, A, and Mavilio, F (2013). Mechanisms of retroviral integration and mutagenesis. Hum Gene Ther 24: 119-131.

22. De Ravin, SS, Su, L, Theobald, N, Choi, U, Macpherson, JL, Poidinger, M, et al. (2014). Enhancers are major targets for murine leukemia virus vector integration. J Virol 88: 4504-4513.

23. Ciuffi, A, and Bushman, FD (2006). Retroviral DNA integration: HIV and the role of LEDGF/p75. Trends Genet 22: 388-395.

24. Huston, MW, van Til, NP, Visser, TP, Arshad, S, Brugman, MH, Cattoglio, C, et al. (2011). Correction of murine SCID-X1 by lentiviral gene therapy using a codon-optimized IL2RG gene and minimal pretransplant conditioning. Mol Ther 19: 1867-1877.

25. van Til, NP, de Boer, H, Mashamba, N, Wabik, A, Huston, M, Visser, TP, et al. (2012). Correction of murine Rag2 severe combined immunodeficiency by lentiviral gene therapy using a codon-optimized RAG2 therapeutic transgene. Mol Ther 20: 1968-1980.

26. van Til, NP, Sarwari, R, Visser, TP, Hauer, J, Lagresle-Peyrou, C, van der Velden, G, et al. (2014). Recombination-activating gene 1 (Rag1)-deficient mice with severe combined immunodeficiency treated with lentiviral gene therapy demonstrate autoimmune Omenn-like syndrome. J Allergy Clin Immunol 133: 1116-1123.

27. van Til, NP, Stok, M, Aerts Kaya, FS, de Waard, MC, Farahbakhshian, E, Visser, TP, et al. (2010). Lentiviral gene therapy of murine hematopoietic stem cells ameliorates the Pompe disease phenotype. Blood 115: 5329-5337.

28. Nishino, I, Spinazzola, A, and Hirano, M (2001). MNGIE: from nuclear DNA to mitochondrial DNA. Neuromuscul Disord 11: 7-10.

29. Schmidt, M, Schwarzwaelder, K, Bartholomae, C, Zaoui, K, Ball, C, Pilz, I, et al. (2007). High-resolution insertion-site analysis by linear amplification-mediated PCR (LAM-PCR). Nat Methods 4: 1051-1057.

30. Follenzi, A, and Naldini, L (2002). Generation of HIV-1 derived lentiviral vectors. Methods Enzymol 346: 454-465.

31. Follenzi, A, and Naldini, L (2002). HIV-based vectors. Preparation and use. Methods Mol Med 69: 259-274.

32. Cattoglio, C, Facchini, G, Sartori, D, Antonelli, A, Miccio, A, Cassani, B, et al. (2007). Hot spots of retroviral integration in human CD34+ hematopoietic cells. Blood 110: 1770-1778.

33. Candotti, F, Shaw, KL, Muul, L, Carbonaro, D, Sokolic, R, Choi, C, et al. (2012). Gene therapy for adenosine deaminase-deficient severe combined immune deficiency: clinical comparison of retroviral vectors and treatment plans. Blood 120: 3635-3646.

34. Cesana, D, Ranzani, M, Volpin, M, Bartholomae, C, Duros, C, Artus, A, et al. (2014). Uncovering and dissecting the genotoxicity of self-inactivating lentiviral vectors in vivo. Mol Ther 22: 774-785.

35. Maetzig, T, Brugman, MH, Bartels, S, Heinz, N, Kustikova, OS, Modlich, U, et al. (2011). Polyclonal fluctuation of lentiviral vector-transduced and expanded murine hematopoietic stem cells. Blood 117: 3053-3064.

36. Rittelmeyer, I, Rothe, M, Brugman, MH, Iken, M, Schambach, A, Manns, MP, et al. (2013). Hepatic lentiviral gene transfer is associated with clonal selection, but not with tumor formation in serially transplanted rodents. Hepatology 58: 397-408.

37. Bosticardo, M, Ghosh, A, Du, Y, Jenkins, NA, Copeland, NG, and Candotti, F (2009). Self-inactivating retroviral vector-mediated

gene transfer induces oncogene activation and immortalization of primary murine bone marrow cells. Mol Ther 17: 1910-1918.

38. Dave, UP, Akagi, K, Tripathi, R, Cleveland, SM, Thompson, MA, Yi, M, et al. (2009). Murine leukemias with retroviral insertions at Lmo2 are predictive of the leukemias induced in SCID-X1 patients following retroviral gene therapy. PLoS Genet 5: e1000491.

39. Modlich, U, Navarro, S, Zychlinski, D, Maetzig, T, Knoess, S, Brugman, MH, et al. (2009). Insertional transformation of hematopoietic cells by self-inactivating lentiviral and gammaretroviral vectors. Mol Ther 17: 1919-1928.

40. Zychlinski, D, Schambach, A, Modlich, U, Maetzig, T, Meyer, J, Grassman, E, et al. (2008). Physiological promoters reduce the genotoxic risk of integrating gene vectors. Mol Ther 16: 718-725.

41. Shou, Y, Ma, Z, Lu, T, and Sorrentino, BP (2006). Unique risk factors for insertional mutagenesis in a mouse model of XSCID gene therapy. Proc Natl Acad Sci U S A 103: 11730-11735.

42. Bijvoet, AG, van de Kamp, EH, Kroos, MA, Ding, JH, Yang, BZ, Visser, P, et al. (1998). Generalized glycogen storage and cardiomegaly in a knockout mouse model of Pompe disease. Hum Mol Genet 7: 53-62.

43. Zhang, F, Thornhill, SI, Howe, SJ, Ulaganathan, M, Schambach, A, Sinclair, J, et al. (2007). Lentiviral vectors containing an enhancer-less ubiquitously acting chromatin opening element (UCOE) provide highly reproducible and stable transgene expression in hematopoietic cells. Blood 110: 1448-1457.

44. Markiewicz, S, Bosselut, R, Le Deist, F, de Villartay, JP, Hivroz, C, Ghysdael, J, et al. (1996). Tissue-specific activity of the gammac chain gene promoter depends upon an Ets binding site and is regulated by GA-binding protein. J Biol Chem 271: 14849-14855.

45. Pike-Overzet, K, Rodijk, M, Ng, YY, Baert, MR, Lagresle-Peyrou, C, Schambach, A, et al. (2011). Correction of murine Rag1 deficiency by self-inactivating lentiviral vector-mediated gene transfer. Leukemia 25: 1471-1483.

46. Neelis, KJ, Hartong, SC, Egeland, T, Thomas, GR, Eaton, DL, and Wagemaker, G (1997). The efficacy of single-dose administration of thrombopoietin with coadministration of either granulocyte/macrophage or granulocyte colony-stimulating factor in myelosuppressed rhesus monkeys. Blood 90: 2565-2573.

47. Huston, MW, Brugman, MH, Horsman, S, Stubbs, A, van der Spek, P, and Wagemaker, G (2012). Comprehensive Investigation of Parameter Choice in Viral Integration Site Analysis and Its Effects on the Gene Annotations Produced. Hum Gene Ther.

48. Deichmann, A, Brugman, MH, Bartholomae, CC, Schwarzwaelder, K, Verstegen, MM, Howe, SJ, et al. (2011). Insertion sites in engrafted cells cluster within a limited repertoire of genomic areas after gammaretroviral vector gene therapy. Mol Ther 19: 2031-2039.

6

|SUPPLEMENTARY INFORMATION
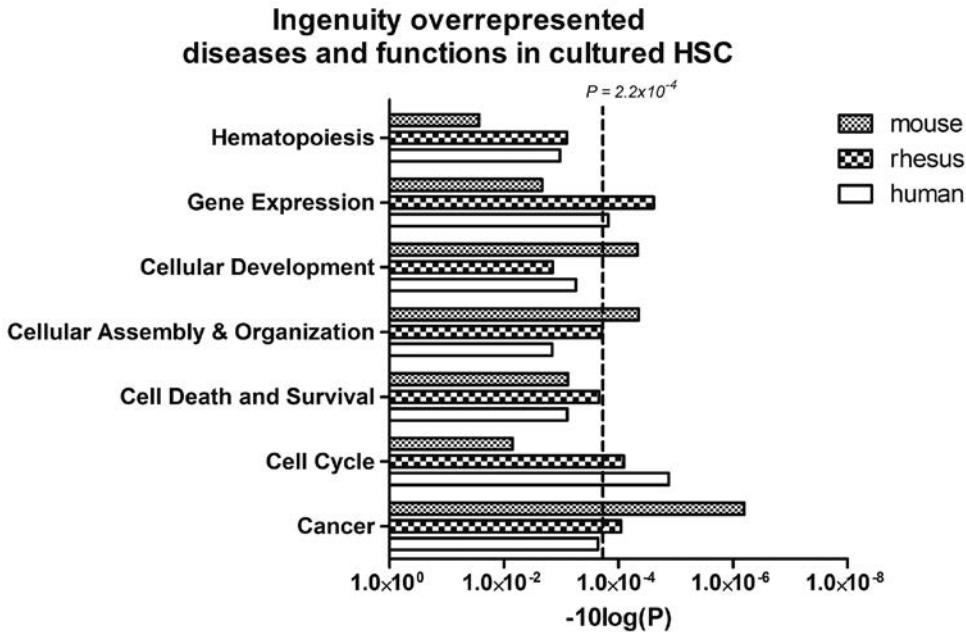
Supplementary figure 1. Ingenuity Functional Pathways analysis of HSC integration sites.
Overrepresented Ingenuity functional pathways for genes flanking integration sites in hematopoietic stem and progenitor cells (HPSC) purified from murine, rhesus and human sources transduced with GFP lentiviral vectors. Significance is shown on y-axis as –log10 P value. The base significance threshold of P < 0.05 was adjusted for multiple comparisons using the Bonferroni correction to reach a new threshold of P < 0.00022 (75 functional classes and 3 cell types = 225 function comparisons).
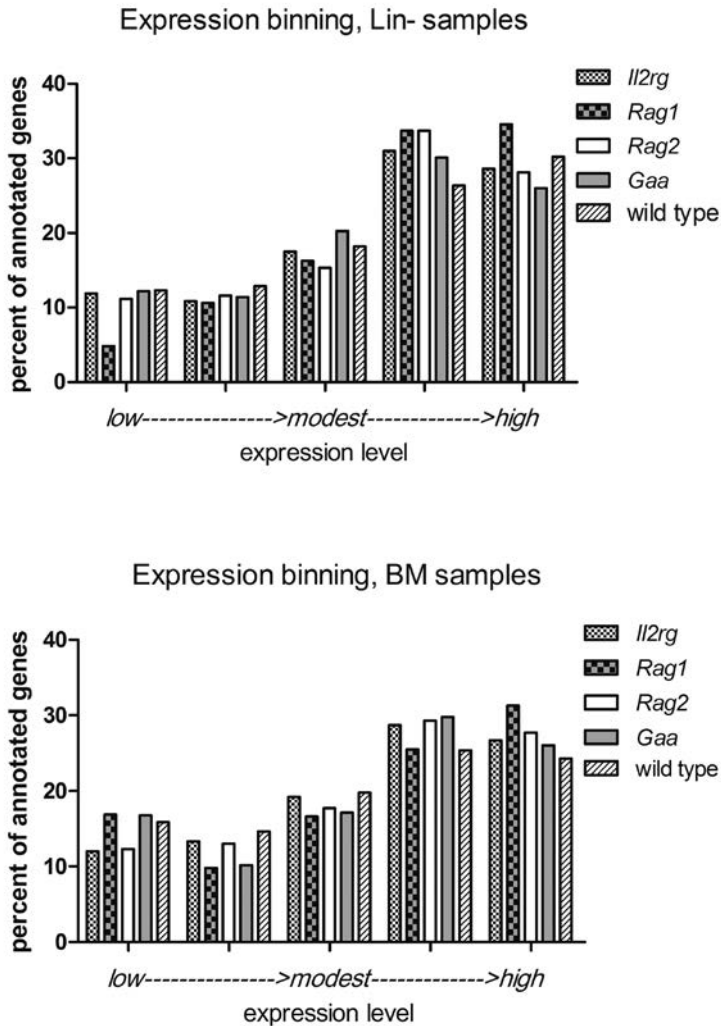
Supplementary figure 2. Gene expression binning data. Gene expression values of Lin- Sca-1+ c-Kit+ cells after two days of stimulation, as measured on an Affymetix mouse 430 2.0 array, were sorted into 5 equally-sized bins based on their relative expression levels. The genes nearest to an integration site in one of the lineage negative (Lin-) or bone marrow (BM) datasets are used to generate a histogram based on this binning profile. Highly expressed genes are much more likely to contain nearby integrations in both the Lin- and BM samples.

Supplementary table 1. CIS of 3rd order or higher in cultured hematopoietic stem/progenitor cells

species	CIS order	Chrom- osome	Loci	Genes
mouse	4	8	63392605;63405611;63437922;63453218	2700029M09Rik;Clcn3
mouse	3	1	99612093;99640538;99649662	D1Ertd622e;Gin1
mouse	3	1	179046612;179054779;179082714	Akt3
mouse	3	5	86575222;86577004;86583707	Uba6
mouse	3	6	8681945;8699661;8707816	Ica1
mouse	3	6	65022182;65032843;65058002	Smarcad1;Hpgds
mouse	3	9	92153249;92154125;92190992	Plscr1;1700057G04Rik
mouse	3	10	66642587;66650208;66660333	Reep3
mouse	3	13	83673980;83674833;83688671	Mef2c*
mouse	3	13	89998176;90012865;90043437	Gm4117
rhesus	4	2	1954335;1959596;1993923;2030622	LOC719197
rhesus	3	6	128127211;128129891;128133390	RAPGEF6
rhesus	3	8	17822238;17829654;17859303	PCM1
rhesus	3	8	87646981;87665223;87665361	LRRCC1
rhesus	3	18	47431494;47461444;47461626	MBD2
human	3	4	80874986;80876679;80877724	ANTXR2

*RTCGD listed proto-oncogene.

Supplementary table 2. Ingenuity pathways analysis of overrepresented diseases and functions in cultured HSC transduced with lentiviral vectors

Top 20 disease or biological function	found in
Cancer	all
Tissue Morphology	all
Gene Expression	H, R, S
Cardiovascular System Development & Function	H, M, S
Organismal Development	H, M, S
Cellular Development	H, M, S
Cell Death & Survival	H, R, S
Cellular Movement	M, R, S
Cellular Assembly & Organization	M, R, S
Cell Morphology	M, R, S

H=human, M=murine, R=rhesus, S=*in silico* datasets

Supplementary table 3a. CIS found in multiple murine datasets (3rd order or higher)

CIS gene	Chromosome	CIS order	Range of loci	Dataset
Uba6	5	6	86569855-86582241	Il2rg *in vivo*
		3	86567296-86590346	Rag2 *in vivo*
		3	86575222-86583707	WT *in vitro*
		3	86562050-86583025	WT *in vivo*
Gtdc1	2	4	44703455-44758157	Rag2 *in vivo*
		3	44742547-44776921	UppTP *in vivo*
		3	44550627-44550702	Rag1 *in vivo*
Mef2c	13	5	83640034-83757178	Il2rg *in vivo*
		3	83673980-83688671	WT *in vitro*
Plxdc2	2	4	16422537-16484631	Il2rg *in vivo*
		3	16402704-16428376	Rag2 *in vivo*
Mrps9	1	3	42912652-42929105	Il2rg *in vivo*
		3	42923559-42931481	Il2rg *in vitro*
Ube3a	7	3	66528779-66562531	Il2rg *in vivo*
		3	66524455-66547103	Rag2 *in vivo*
Pcdh9	14	3	94187748-94187763	Il2rg *in vivo*
		3	94196123-94197963	Rag1 *in vivo*
Gin1	1	3	99612093-99649662	WT *in vitro*
		3	99661378-99661493	Rag1 *in vivo*
Samsn1	16	3	75892377-75911575	Rag2 *in vivo*
		3	75945565-75945918	Rag1 *in vivo*
Sfi1	11	10	3031603-3110289	Rag2 *in vivo*
		4	3039287-3110058	Il2rg *in vitro*
Cntnap2	6	3	45043093-45065563	Rag2 *in vivo*
		3	45228340-45256599	WT *in vivo*
Slc4a7	14	5	15548060-15598104	WT *in vivo*
		3	15470107-15470296	Rag2 *in vivo*

6

Supplementary table 3b. CIS oncogenes found in mouse datasets (3rd order or higher)

CIS oncogene	CIS order	Chromosome	Loci	dataset
Arid1a	4	4	133273225-133273420	Rag1 *in vivo*
Cdk6	3	5	3375849-3381855	Rag1 *in vivo*
Coro1a	3	7	133862044-133863162	Rag1 *in vivo*
Gimap7	4	6	48659062-48679534	Rag1 *in vivo*
Ikzf1	3	11	11604680-11624778	Rag1 *in vivo*
Lnpep	3	17	17750933-17764326	WT *in vivo*
Lrmp	3	6	145076099-145076149	Rag2 *in vivo*
Mef2c	5;3	11	83640034-83757178	Il2rg *in vivo*; WT *in vitro*
Plag1	8	4	3858379-3862732	WT *in vivo*
Sdccag8	4	1	178831743-178832157	Il2rg *in vivo*
Zfp608	3	18	55122201-55123377	Rag2 *in vivo*

Supplementary Table 4. all CIS of 3rd order or higher in murine phenotype BM samples

phenotype	CIS order	chromosome	genes	loci
Il2rg	6	5	Uba6	86569855-86582241
	5	5	Hgf	16095587-16294275
	5	5	Adamts3	90216928-90284089
	4	3	Mecom	30117285-30119266
	4	12	Coch; Strn3	52693480-52762846
	3	1	Mrps9	42912652-42929105
	3	1	Hisppd1	99630458-99661078
	3	1	Pam	99908290-99908664
	3	4	Smc2	52459854-52487919
	3	7	Ube3a	66528779-66562531
	3	11	Sfi1	3031770-3078236
	3	11	Polr2a	69550965-69551453
	3	12	4930579E17Rik	37623133-37669935
	3	13	Mef2c	83640034-83681077
	3	14	Elf1	79940798-79941001
	3	17	Gm17251	33891546-33892143
	3	18	Smad7	75574839-75574919
	3	18	Socs6	89049399-89050188
	3	19	Btaf1	37025311-37035490
	3	19	Hells	39020441-39034829
	3	X	Alg13; Trpc5	140762892-140788621
TympUpp	4	13	Lyst; Gng4	13744606-13790854
	3	1	Kcnj13	89281135-89281173
	3	2	Gtdc1	44742547-44776921
	3	8	Pcm1	42357497-42390158
	3	9	Cwf19l2; Gucy1a2	3428516-3477478
	3	10	Ascc3	50320516-50359114
	3	11	Scgb3a1	49496481-49503060
	3	12	Fut8	78429053-78467732
	3	X	Diap2	126677649-126719423
Rag1	3	4	Arid1a	133273234-133273420
	3	14	Gcap14	37721390-37729164
	3	14	Dnajc3	119414191-119414225
	3	17	Zfp760	21825425-21869361
	3	17	Nfkbil1; Bat1a	35368970-35385457
	3	17	Pja2	64672665-64673226
wild type	8	4	Plag1	3858379-3862732
	6	7	Uba2	34930305-35091597
	5	14	Slc4a7	15548060-15598104
	4	1	Trip12	84739858-84766670
	4	8	Vegfc	55188886-55262672
	4	13	Nqo2; Ripk1; Bphl	34082481-34155957
	4	17	Fshr	89494826-89573458

6

Supplementary Table 4. (continued)

phenotype	CIS order	chromosome	genes	loci
	4	18	Ap3s1	46919714-46942581
	3	1	Cdc73	145537654-145545756
	3	2	Immp1l	105761317-105761521
	3	5	Cpeb2	43735180-43759290
	3	5	Uba6	86562050-86583025
	3	6	Cntnap2	45228340-45256599
	3	17	Lnpep	17750933-17764326
	3	17	A930001N09Rik	26872812-26876216
	3	18	Tmx3	90689757-90706582

Supplementary table 5. CIS oncogenes found in murine *in vitro* and *in vivo* LVIS datasets

phenotype	oncogene	CIS order	chromosome	loci
Il2rg *in vivo*	Mef2c	5	13	83640034-83757178
Il2rg *in vivo*	Sdccag8	4	1	178831743-178832157
murine *in vitro*	Mef2c	3	13	83673980-83688671
Rag1 *in vivo*	Arid1a	4	4	133273225-133273420
Rag1 *in vivo*	Gimap7	4	6	48659062-48679534
Rag1 *in vivo*	Cdk6	3	5	3375849-3381855
Rag1 *in vivo*	Coro1a	3	7	133862044-133863162
Rag1 *in vivo*	Ikzf1	3	11	11604680-11624778
Rag2 *in vivo*	Lrmp	3	6	145076099-145076149
Rag2 *in vivo*	Zfp608	3	18	55122201-55123377
WT *in vivo*	Plag1	8	4	3858379-3862732
WT *in vivo*	Lnpep	3	17	17750933-17764326

Supplementary table 6. details of LVIS found in *Il2rg^-/-* leukemias

ID #	vector	integrations per BM cell	% clonal dominance	chrom-osome	LVIS locus	flanking gene	distance from IS to gene 5' end
1	PGK. colL2RG	1.1	99	11	120421360	Arl16	92.6 kb US
						Gm17586	73.7 kb US
						Npb	48.4 kb US
						Anapc11	38.4 kb US
						Gm11789	28.4 kb US
						Fam195b	10.5 kb US
						Ppp1r27	9.0 kb US
						P4hb	13.1 kb DS
						Arhgdia	21.4 kb DS
						Gcgr	29.3 kb DS
						Alyref	38.2 kb DS
						Pcyt2	57.8 kb DS
						Sirt7	65.1 kb DS
						Slc25a10	68.2 kb DS
						Mafg	73.4 kb DS
						Mrpl12	75.4 kb DS
						Pycr1	83.6 kb DS
						Myadml2	88.0 kb DS
						Hgs	92.4 kb DS
2	PGK.GFP	2.4	92	5	20378460	Tmem60	9.6 kb US
						Phtf2	9.4 kb DS
3	PGK.GFP	3.8	37	5	20378460	Tmem60	9.5 kb US
						Phtf2	9.4 kb DS
			31	11	69550965	Mpdu1	74.9 kb US
						Cd68	71.4 kb US
						Eif4a1	65.1 kb US
						Senp3	55.5 kb US
						Tnfsf13	51.8 kb US
						BC096441	41.4 kb US
						Zbtb4	28.4 kb US
						Polr2a	21.1 kb DS
						Amac1	24.4 kb DS
						2010012P19Rik	55.3 kb DS
						Chrnb1	58.4 kb DS
						Fgf11	64.3 kb DS
						Tmem102	68.1 kb DS
						Mir1934	74.4 kb DS
						4933402P03Rik	80.9 kb DS
						Sox15	82.1 kb DS
						Spem1	84.6 kb DS
			24	5	90217670	Adamts3	94.7kb DS

6

Supplementary table 6. (continued)

ID #	vector	integrations per BM cell	% clonal dominance	chrom-osome	LVIS locus	flanking gene	distance from IS to gene 5' end
4	PGK.GFP	2.6	80	19	27937685	Rfx3	10.5 kb US
			19	4	111458245	Spata6	65.7 kb DS
5	PGK.GFP	3.1	92	5	20378460	Tmem60	9.5 kb US
						Phtf2	9.4 kb DS
6	SF.coIL2RG	1.1	97	12	8728063	Sdc1	50.0kb US
						Pum2	47.1kb DS
7	SF.IL2RG	2.2	72	13	83644300	Mef2c*	1.1 kb DS
			10	3	75428013	Pdcd10	67.4 kb US
						Serpini1	66.5 kb DS
8	SF.IL2RG	2.8	52	5	24812154	Galntl5	124.8 kb DS
						Galnt11	83.4 kb DS
						Mll3*	192.3 kb DS
			22	2	108962025	Mettl15	158.9 kb DS
			18	10	12297464	Utrn	291.6 kb DS
9	SF.poly	2.9	69	16	8632961	Pmm2	4.7 kb US
						Tmem186	4.6 kb DS
						Carhsp1	39.1 kb DS
			30	3	29899713	Mecom	547kb DS
10	SF.poly	0	n/a	n/a	n/a	n/a	n/a
11	cPR.coIL2RG	1.4	61	X	154308268	Klhl34	51.9 kb DS
			13	12	107028782	Papola	10.3 kb DS
						Ak7	84.6 kb DS
			10	6	127152223	9630033F20Rik	92.7 kb US
						Ccnd2*	51.2 kb US
						9330179D12Rik	52.8 kb DS
12	cPR.coIL2RG	1.6	68	2	32444912	Mir1954	63.2 kb US
						Eng	57.5 kb US
						Ak1	32.7 kb US
						St6galnac6	10.6 kb US
						St6galnac4	2 kb DS
						Pip5kl1	14.3 kb DS
						Dpm2	18.2 kb DS
						Fam102a	53.8 kb DS
						Fpgs	114.7 kb DS
			22	11	43946382	Il12b	267.2 kb DS
13	γcPR.coIL2RG	1.8	99	18	15379080	Kctd1	69 kb US
14	γcPR.coIL2RG	1.7	58	4	44798766	Pax5*	74.5 kb US
						Gm12463	32.8 kb US
						Zcchc7	30 kb DS
			33	10	9576597	Stxbp5	
15	γcPR.GFP	0.8	99	16	6884479	Rbfox1	75 kb DS

* known proto oncogene; # tumor suppressor gene

Supplemental table 7. list of LV vectors used in each murine phenotype

Phenotype	Vector
Il2rg	PGK-GFP
	PGK-IL2RGco
	SF-IL2RG
	SF-IL2RGco
	γcPr-GFP
	γcPr-IL2RGco
TympUpp	PGK-GFP
	PGK-TYMP
	PGK-TYMPco
	SF-TYMPco
Gaa	PGK-GAAco
	SF-GAAco
	SF-GFP
Rag1	RAG1p-RAG1co
	SF-GFP
	SF-RAG1co
	TCRβp-RAG1co
	γcPr-RAG1co
Rag2	SF-RAG2co
	UCOE-GFP
	UCOE-RAG2co
BALB/c	PGK-GFP
	SF-GFP

6

General discussion

7

LENTIVIRAL VECTOR GENE TRANSFER INTO HEMATOPOIETIC STEM CELLS

Hematopoietic stem cell gene therapy (HSCGT) has been successfully used in clinical trials for a wide range of inherited hematological, metabolic, and immune deficiency disorders.[1] Recently, the first *ex vivo* HSCGT drug (Strimvelis) was approved for marketing in Europe for the treatment of adenosine deaminase severe combined immunodeficiency (ADA-SCID). The product is made of autologous hematopoietic stem cells (HSCs) transduced with a gammaretroviral (γ-RV) vector containing ADA, therefore an excellent personalized treatment of ADA-SCID patients for whom a matched donor is lacking. Due to the highly proliferative capacity of hematopoietic stem and progenitor cells (HSPCs), RVs have been employed in HSC gene transfer protocols for their capacity to integrate into the host's genomic DNA and propagate transgene expression into progenitors and mature cells. Pre-clinical studies resulted in sufficient proof of concept [2,3] to move towards clinical trials for primary immunodeficiencies using γ-RV vectors. These trials showed the efficacy of this gene therapy approach demonstrating phenotypic correction and clinical improvements following the restoration of the cellular, and in some, also the humoral immunity.[4,5] However, a large proportion of the X-linked SCID and Wiskott Aldrich γ-RV trials reported hematological malignancies related to the upregulation of proto-oncogenes close to the vector insertion sites.[6-11] Therefore, efforts were directed towards the development of third generation self-inactivating (SIN) lentiviral

(LV) vectors as an alternative vector system for reducing the risk of insertional oncogenesis.[12]

Another advantage of using LV vectors is that the proliferation of HSPCs during gene transfer is not a requirement, in contrast to γ-RV vectors.[13] The current protocols using RV (both γ-RV and LV) employ two rounds of transduction, high vector doses (MOI 100), and relatively high concentrations of multiple cytokines.[14,15] These conditions, however, could affect the efficacy and safety outcomes of HSCGT, by increasing the risk of insertional mutagenesis of the genes involved in cell-cycling and by compromising the long-term repopulation capacity of gene modified HSCs. Our findings show efficient gene transfer into HSPCs during a short transduction time by increasing the target cell density with a proportional increase of LV particles. Addition of thrombopoietin (TPO) alone was sufficient in maintaining the *in vivo* repopulation capacity and ensuring efficient transduction at the same time. Our evaluation of human HSPCs was limited to *in vitro* assessments, and further experiments might be required to estimate the efficacy of prolonged gene marking and repopulation capacity through transplantation into the humanized mouse model.[16] Additionally, of interest is the application of this protocol in mouse models of human diseases to evaluate the contribution towards phenotypic correction; performance of the transductions in microfluid-based transduction system, wherein the probability of infection is increased;[17] and combination with prostaglandin E2 stimulation leading

7

to effective LV transduction of HSCs during short culture time (less than 38hrs).[18]

These advancements at generating a clinically viable and feasible protocol for LV transduction of HSPCs could be combined with strategies to enhance the expansion of gene modified HSPCs. *Ex vivo* expansion would support the maintenance of the (stemness) of the gene modified HSPCs, enable selection of HSPCs with integrated LV vector copies and transgene expression prior to transplantation, and the evaluation of LV-integration site profiles. In that regard, biomolecules such as neurotrophic factors represent novel candidates for enhancing the expansion and survival of HSPCs, [19] while the pyrimidoindole derivative UM171 was recently successfully employed for the *ex vivo* expansion of LV transduced human mobilized peripheral blood HSCs with long term repopulation capacity.[18] The therapeutic outcomes can be further enhanced by the integration of approaches aiming at improving the homing and engraftment of gene modified HSPCs. These strategies include inhibition of CD26[20] peptidase that negatively affects the levels of the chemokine stromal cell-derived factor 1 (SDF-1) and priming of HSCs with prostaglandin E2 prior to transplantation.[18,21,22]

HSCGT: an efficient and safe treatment for MNGIE?

Allogeneic HSCT for treatment of MNGIE is associated with a high mortality rate and the therapeutic outcomes are transient and limited.[23,24] As a result of the encouraging therapeutic outcomes and incremental improvements related to LV vector design, HSCGT holds promise as a safe and effective treatment for multiple life-threatening diseases, including MNGIE.

Development of a LV vector-mediated HSCGT protocol for the treatment of MNGIE would require *(i)* a clinically relevant mouse model, *(ii)* a clinically applicable LV vector, *(iii)* assessment of therapeutic outcomes, beyond correction of the biochemical phenotype, and *(iv)* assessment and minimizing the risks related to pre-transplant conditioning, transgene expression and LV vectors.

The studies performed in this thesis address these points, but clinical translation requires additional studies to provide HSCGT as a cure for MNGIE patients.

(i) The generation of $Tymp^{-/-}Upp1^{-/-}$ mice was instrumental to enhance the development of alternative treatments to cure MNGIE patients.[25] $Tymp^{-/-}Upp1^{-/-}$ mice exhibit a biochemical phenotype similar to MNGIE patients (elevated dThd and dUrd), however, only ≥18 month old mice demonstrate mild neurological phenotypes. The lack of other relevant similarities to MNGIE such as alterations of mitochondrial DNA (mtDNA) and pronounced motor dysfunctions, limits the evaluation of the therapeutic outcomes beyond the biochemical phenotype.[26-28] To enforce these phenotypes the nutritional diet can be changed, consisting of increased dThd and dUrd amounts, but mice still need to be maintained for very long periods (up to 24 months).[29] These limitations challenged the suitability of $Tymp^{-/-}Upp1^{-/-}$ mice to model MNGIE. We therefore carefully characterized the brain and intestinal phenotypes at an earlier age to evaluate HSCGT efficacy. First, we carefully examined the neurological aspects of $Tymp^{-/-}Upp1^{-/-}$ mice which confirmed the previously reported white matter changes

in brain MRI and histology,[25] but at an earlier age, and additionally demonstrated an abnormal phenotype of brain astrocytes. Further experiments are required to elucidate the nature of the cellular and molecular changes observed in brain astrocytes morphology and the altered mtDNA replication, and how that relates to unbalanced nucleosides levels. In this regard, experiments to evaluate ion-water homeostasis are relevant. Specifically, we observed an increase in the thickness of the astrocytes processes in $Tymp^{-/-}Upp1^{-/-}$ mice. This is similar to megalencephalic leukoencephalopathy with cysts (MLC) mice models ($Mlc1$-null and $Glialcam$-null mice). These studies provide evidence that defective astrocytic fluid volume regulation underlies the pathomechanism of MLC. [30,31] Future studies could be performed to investigate the status of volume regulated anion channel (VRAC) currents and regulated volume decrease in astrocytes of $Tymp^{-/-}Upp1^{-/-}$ mice. Additionally, we report abnormalities in the myogenic and neurogenic compartments of the intestine of $Tymp^{-/-}Upp1^{-/-}$ mice. However the mice did not develop profound cachexia, unlike MNGIE patients, perhaps due to ad $libitum$ feeding, or that the mice are double knock out for two genes unlike in MNGIE patients, or the physiological differences between mice and man. Nonetheless, the intestinal pathology of $Tymp^{-/-}Upp1^{-/-}$ mice occurs at an early age and is similar to the pathology in MNGIE patients. Therefore, testing potential treatments in the mouse model may still predict the therapeutic response in MNGIE patients.

(ii) Our results indicate that the developed therapeutic LV vectors (PGK-TP(co) could efficiently correct MNGIE phenotypes with the following minor modifications: **(a)** The physiological promoter (hPGK) led to lower levels of TP expression which were sufficient for phenotypic correction, without the increased risk of transactivation of nearby oncogenes as compared with the strong promoter of the spleen focus forming virus (SF); **(b)** at low VCN/cell (median ≤ 2.3, MOI 10); and **(c)** at moderate levels of engraftments (median, 77 %, PGK-TP(co)). Altogether, these results indicate that the therapeutic LV-PGK-TP and TPco vectors mediate efficient correction, thereby abrogating the necessity for further enhancement of the vector performance. Although codon optimization of $TYMP$ did not enhance $TYMP$ transcription or protein levels, unlike in the case of other disease models,[32,33] other algorithms might be investigated to still improve protein production per VCN.

In order to control transgene expression, enhance the biodistribution of- and improve the reconstitution of- transduced hematopoietic cells, numerous modifications could be implemented. Cell specific targeted transgene expression could be achieved through the incorporation of cell specific promoters or enhancers such as GP1BA, ITGA2B, and PF4 megakaryocyte-specific gene promoters [34] to selectively drive moderate levels of $TYMP$ expression in platelets, a rich source of TP in healthy people. Tropism of LV vectors can be altered through modifications of LV envelopes to target long-term repopulating stem cells, or the expression restricted to certain cell types via miRNA de-targeting (reviewed in Goyvaerts C, *et al.* 2013).[35] This would allow for strong and prolonged expression levels in target stem cells, without the toxicity on nontarget cells. Alternatively, targeted gene editing of HSCs

7

with artificial endonucleases such as Zinc-Finger Nucleases (ZFNs), Transcription Activator Like Effector Nucleases (TALENs) and Clustered Regularly Interspaced Short Palindromic Repeats/ CRISPR-associated (CRISPR/Cas) could reduce the risk of insertional oncogenesis through the direct integration into pre-determined genomic loci. In this regard, protocols are developed for efficient gene targeting of HSCs by using ZFN, augmented with adapted culture conditions.[22] The delayed culture timing prior to gene targeting and the presence of StemRegenin 1 and prostagandin E2 to preserve stemness permitted for efficient targeted integration in human HSCs with long term repopulation in immunodeficient mice. The functionality of this approach was proven by targeted integration of the corrective cDNA into *IL2RG* in HSCs from a SCID-X1 patient. 3-11% GFP+ were detected in the BM CD34+ subpopulations isolated from the patient after targeting for *IL2RG* correction. For MNGIE, probably higher efficiency are required, since *TYMP* gene corrected cells, in contrast with *IL2RG* corrected cells, might not confer a selective advantage.

In contrast to ZFNs, TALENS targeting the same site of CCR5 were reported to have a reduced off-target activity.[36] TALENs were successfully used for targeting the human β-globin locus; i.e. correction of the pathological mutations in iPSCs from patients of β-thalassemia[37] and sickle cell anemia,[38] to express normal b-globin in the differentiated hematopoietic progenitors and erythroblast. This is probably also feasible for correction of *TYMP* as well.

The CRISPR/Cas9 system can be used for efficient gene editing of primary murine and human HSPCs,[39] or patient-derived induced pluripotent stem cells (iPSCs). In this approach, CRISPR/Cas9 is applied for correction of the disease underlying mutation in patient-derived iPSCs, which are differentiated afterwards to, for instance, hematopoietic progenitor cells, for transplantation in patients. The majority of lysosomal storage diseases are candidate targets for treatment with this approach, because of the monogenic mutations and the ability of gene corrected cells to excrete the deficient enzyme.[40] These advancements and progress towards clinical trials (e.g. treatment of HIV infection[1], and mucopolysaccharidosis I and II[2]) render therapeutic gene editing an attractive treatment option, feasible for application in MNGIE patients as well. However, several limitations need to be considered prior to the clinical application of iPSCs. These include the large-scale manufacturing steps such as the genetic re-programming and *in vitro* expansion, increased incidence of deletions or changes in DNA copy number and thereby tumorigenesis, which is also underlined by the use of integrating viruses and oncogenes, and risks of immune response or graft rejection. Furthermore, translation of gene editing strategies into clinical settings requires further enhancements of the delivery, efficiency and specificity of the gene correction machinery. First, *in vivo* gene editing is usually performed with AAV,[41] which imposes challenges including off-target editing related to the constitutively expressed nucleases, and immunity against

https://clinicaltrials.gov/ (2017) [1](NCT01252641), [2] (NCT02702115, NCT03041324)

certain serotypes. On the other hand, for *ex vivo* gene targeting of HSCs, transient expression of the nuclease is sufficient and can be achieved through electroporation or non-integrating LV vectors.[22,39] In order to avoid excessive expression of nucleases and off-target editing integrating LV vectors are not preferred. Second, the efficiency of targeted gene correction could be enhanced by modulation of double strand break pathways, which are dependent on the target cell cycle. Modulation of *ex vivo* cell culture conditions could be useful to control the cell cycle.[22]

In addition, several approaches can be applied in order to achieve above normal *TYMP* expression levels (as discussed in ***iii***) including the targeted integration of an expression cassette with a strong promoter in a pre-selected safe harbor such as AAVS1, or fusion of the open reading frame of TYMP with the mRNA of a highly expressed endogenous gene such as CD45 in HSPCs. As in the case for the treatment of hemophilia B, *in vivo* genome editing by using ZFNs and AAV2/6 was successfully used for the insertion of a therapeutic copy of human factor 9 into the albumin locus in liver hepatocytes, leading to the production of therapeutic levels of human factor 9 (>1% of normal) in mice and non-human primates.[42]

Finally, off-target gene editing and constitutively expressed nucleases could result in undesired alterations of cancer-related genes or lead to loss of function, therefore the specificity of CRISPR/Cas9 targeting can be enhanced by selection of the nucleases used,[43] or by using truncated guide RNA, guide RNA extension, Cas9 nickases, RNA-guided FokI–dCas9 nucleases, or engineered Cas9. [44]

(iii) Above-normal TP activity was required for restoration of neurological and intestinal phenotypes and was achieved with LV-PGK-TP(co) at a moderate LV dose (MOI 10). This is similar to findings in other metabolic disorders, where above-normal expression of the therapeutic enzyme led to correction of disease phenotypes which are otherwise not responsive to traditional HSCT. This includes the amelioration of neurological phenotypes in mucopolysaccharidose II [45] and globoid cell leukodystrophy mice[46] (reviewed in Biffi A, *et al*. 2017).[47] Only the highest dose used in our studies in *Tymp$^{-/-}$Upp1$^{-/-}$* mice, an MOI of 10, resulted in above-normal levels of TP activity in blood (range, 68-188 nmol/h/mg protein), was just sufficient at normalizing intestinal TP activity and rescued the pathology after HSCGT, while HSCT in MNGIE patients did not rescue the intestinal pathology despite biochemical correction as demonstrated in **Chapters 4 and 5** and by Halter *et al*. (range, 262-1285 nmol/h/mg protein).[23] Graft versus host disease or graft rejection following allogeneic HSCT, timing of treatment (HSCGT was administered at the same age when the intestinal pathology was minor, versus MNGIE patients who are usually treated at a late stage of the disease), or interspecies differences could also explain the contrasting responses of human and mice to treatments.

In contrast to using LV-mediated HSCGT, above-normal TP levels in blood were not achieved through AAV2/8-mediated liver directed gene therapy in *Tymp$^{-/-}$Upp1$^{-/-}$* mice, even with high vector dose (>2×10^{11} vg/kg). Importantly, nucleoside accumulation was not reduced in the intestine of these mice.[27] AAV gene therapy for MNGIE is an attractive treatment option because it does not require

7

pre-conditioning or a suitable HSCs donor. However, compared with clinical trials for hemophilia B, in which a small proportion of transduced hepatocytes is sufficient to convert a severe patient into a moderate phenotype, it is speculated that an effective treatment for MNGIE would require an improved expression cassette, targeted expression in affected organs or a higher AAV vector dose. A higher dose increases the risk of eliciting immunity towards the viral capsid and liver toxicity. The pros and cons of AAV- and LV-based gene therapy approaches are discussed in more detail in **Chapter 2**.

In addition to the above-normal TP levels, the timing of treatment is critical for the resolution of the intestinal phenotypes. HSCGT was administered prior to detectable pathological appearance (at 2 months of age), whereas MNGIE patients receive HSCT usually when symptomatic (i.e. after development of a clinical phenotype). To that end, early diagnosis through genetic screening of newborns is critical. Nonetheless, vector and transplanted gene modified cell dose escalation experiments involving a large group of mice is required to establish the minimal dose sufficient for phenotypic correction and without cellular or molecular toxicity before translation into a clinical protocol for treatment of MNGIE patients.

Moreover, albeit correction of the biochemical, neurological, and intestinal phenotypes we were unable to evaluate the contribution of HSCGT to recovery of apparent clinical phenotypes such as motor function and cachexia, due to their absence in the $Tymp^{-/-}Upp1^{-/-}$ mice. $Tymp^{-/-}Upp1^{-/-}$ mice fed with a diet consisting of dThd and dUrd in order to induce the clinical phenotypes [29] could be used to assess the effects of HSCGT

on recovery of apparent phenotypes such as motor dysfunction. *(iv)* Adverse events could occur that are related to toxicity of the pre-transplant conditioning, transgene over expression or immunity against the transgene product, or genotoxicity of integrated LV vectors. In this thesis, we addressed these points in relation to HSCGT for MNGIE. Prior to HSCT, a relatively mild conditioning consisting of busulfan and fludarabine or in combination with anti T cell antibodies, is usually applied. [23] However, an alternative mild conditioning could be preferred for treatment of MNGIE patients who are usually in a very poor condition. Novel non-cytoreductive conditioning approaches have been successful in preclinical studies, including the administration of HSC mobilizing cytokines such as human granulocyte colony stimulating factor,[48] or antagonists of endogenous HSC markers such as anti c-kit [49] or anti CD45.[50] Our results show that following sub-lethal total body irradiation of $Tymp^{-/-}Upp1^{-/-}$ mice, moderate levels of engraftment were sufficient for disease correction. Therefore, application of the novel non-cytoreductive pre-transplant conditioning may be adequate to achieve sufficient levels of donor cell chimerism for disease correction, and avoid toxicity and further deterioration of mtDNA, in particular when combined with the advancements of gene transfer protocols and the *ex vivo* expansion. In order to assess any potential phenotoxicity related to *TYMP* over expression, further in depth experiments are required. In this regard, it is important to evaluate if HSCGT sufficiently restores the depleted dCTP levels and investigate any potential negative effects of TP over expression on dNTPs pool homeostasis,

mtDNA replication, cell cycle arrest, and apoptosis.[51,52]

The results of this thesis indicate that HSCGT for MNGIE can be performed with low risks of *in vivo* mutagenesis or integration nearby oncogenes. Follow up of primary and secondary recipients of LV-PGK-TP(co) for 22 months revealed no detectable hematological abnormalities and the LAM-PCR demonstrated benign vector integration patterns. No differences in the frequency of integration near oncogenes were observed between the control and gene therapy treated groups, or classified based on the promoter (PGK vs. SF) or transgene (therapeutic vs. GFP) used and were also similar to those obtained for different inherited diseases such as in *Il2rg*^{-/-} and *Gaa*^{-/-} mice. Two secondary recipients in the PGK-TP-GFP treatment group developed B cell lymphoma; the clone contained a single dominant integration site in gene *Zfp207*. *Zfp207* is required for proper chromosome alignment[53] and therefore, interruption by for instance, a LV insertion could have augmented oncogenesis. This requires further experiments to elucidate the role of *Zfp 207* as a potential tumor related gene. For example, DNA and RNA sequencing can be performed

in order to profile altered signaling pathways or changes in the mitotic checkpoint protein Budding Uninhibited by Benzimidazoles 3 (BUB3), the main target for *Zfp207*, as well as functional studies that entitle knockdown of *Zfp207 in vitro* or *ex vivo* to determine the effect on cycling HSCs, and to determine its role in the contribution of oncogenesis.

In conclusion, LV vector-mediated HSCGT for MNGIE patients is a feasible treatment option which can successfully reverse the biochemical, neurological, and intestinal phenotypes in *Tymp*^{-/-} *Upp1*^{-/-} mice without apparent toxicity. Clinical application of HSCGT for the treatment of MNGIE patients would require further experiments to assess the minimal LV dose for the correction of clinical phenotypes such as motor function or cachexia, and additional evaluation of potential toxicity related to *TYMP* over expression. Future advancements could involve strategies to direct and control transgene expression in target cells, and strategies for improving the HSCGT procedure such as enhanced LV transduction of HSPCs and *ex vivo* expansion and selection of gene modified cells prior to transplantation, in addition to the application of non-cytoreductive preconditioning.

7

|REFERENCES

1. Naldini L. Gene therapy returns to centre stage. Nature. 2015;526:351-360.

2. Lo M, Bloom ML, Imada K, et al. Restoration of lymphoid populations in a murine model of X-linked severe combined immunodeficiency by a gene-therapy approach. Blood. 1999;94:3027-3036.

3. Soudais C, Shiho T, Sharara LI, et al. Stable and functional lymphoid reconstitution of common cytokine receptor gamma chain deficient mice by retroviral-mediated gene transfer. Blood. 2000;95:3071-3077.

4. Cavazzana-Calvo M, Hacein-Bey S, de Saint Basile G, et al. Gene therapy of human severe combined immunodeficiency (SCID)-X1 disease. Science. 2000;288:669-672.

5. Gaspar HB, Parsley KL, Howe S, et al. Gene therapy of X-linked severe combined immunodeficiency by use of a pseudotyped gammaretroviral vector. Lancet. 2004;364:2181-2187.

6. Hacein-Bey-Abina S, von Kalle C, Schmidt M, et al. A serious adverse event after successful gene therapy for X-linked severe combined immunodeficiency. N Engl J Med. 2003;348:255-256.

7. Hacein-Bey-Abina S, Von Kalle C, Schmidt M, et al. LMO2-associated clonal T cell proliferation in two patients after gene therapy for SCID-X1. Science. 2003;302:415-419.

8. Hacein-Bey-Abina S, Garrigue A, Wang GP, et al. Insertional oncogenesis in 4 patients after retrovirus-mediated gene therapy of SCID-X1. J Clin Invest. 2008;118:3132-3142.

9. Howe SJ, Mansour MR, Schwarzwaelder K, et al. Insertional mutagenesis combined with acquired somatic mutations causes leukemogenesis following gene therapy of SCID-X1 patients. J Clin Invest. 2008;118:3143-3150.

10. Braun CJ, Boztug K, Paruzynski A, et al. Gene therapy for Wiskott-Aldrich syndrome--long-term efficacy and genotoxicity. Sci Transl Med. 2014;6:227ra233.

11. Stein S, Ott MG, Schultze-Strasser S, et al. Genomic instability and myelodysplasia with monosomy 7 consequent to EVI1 activation after gene therapy for chronic granulomatous disease. Nat Med. 2010;16:198-204.

12. Cattoglio C, Facchini G, Sartori D, et al. Hot spots of retroviral integration in human CD34+ hematopoietic cells. Blood. 2007;110:1770-1778.

13. Naldini L, Blomer U, Gallay P, et al. In vivo gene delivery and stable transduction of nondividing cells by a lentiviral vector. Science. 1996;272:263-267.

14. Biffi A, Montini E, Lorioli L, et al. Lentiviral hematopoietic stem cell gene therapy benefits metachromatic leukodystrophy. Science. 2013;341:1233158.

15. Aiuti A, Biasco L, Scaramuzza S, et al. Lentiviral hematopoietic stem cell gene therapy in patients with Wiskott-Aldrich syndrome. Science. 2013;341:1233151.

16. Cosgun KN, Rahmig S, Mende N, et al. Kit regulates HSC engraftment across the human-mouse species barrier. Cell Stem Cell. 2014;15:227-238.

17. Tran R, Myers DR, Denning G, et al. Microfluidic Transduction Harnesses Mass Transport Principles to Enhance Gene Transfer Efficiency. Molecular Therapy.

18. Zonari E, Desantis G, Petrillo C, et al. Efficient Ex Vivo Engineering and Expansion of Highly Purified Human Hematopoietic Stem and Progenitor Cell Populations for Gene Therapy. Stem Cell Reports. 2017;8:977-990.

19. Fonseca-Pereira D, Arroz-Madeira S, Rodrigues-Campos M, et al. The neurotrophic factor receptor RET drives haematopoietic stem cell survival and function. Nature. 2014;514:98-101.

20. Campbell TB, Hangoc G, Liu Y, Pollok K, Broxmeyer HE. Inhibition of CD26 in human cord blood CD34+ cells enhances their engraftment of nonobese diabetic/severe combined immunodeficiency mice. Stem Cells Dev. 2007;16:347-354.

21. Cutler C, Multani P, Robbins D, et al. Prostaglandin-modulated umbilical cord blood hematopoietic stem cell transplantation. Blood. 2013;122:3074-3081.

22. Genovese P, Schiroli G, Escobar G, et al. Targeted genome editing in human repopulating haematopoietic stem cells. Nature. 2014;510:235-240.

23. Halter JP, Michael W, Schupbach M, et al. Allogeneic haematopoietic stem cell transplantation for mitochondrial neurogastrointestinal encephalomyopathy. Brain. 2015;138:2847-2858.

24. Baker MK, Schutte CM, Ranchhod N, Brittain D, van Rensburg JE. Transient clinical improvement of a mitochondrial neurogastrointestinal encephalomyopathy-like syndrome after allogeneic haematopoietic stem cell transplantation. BMJ Case Rep. 2017;2017.

25. Lopez LC, Akman HO, Garcia-Cazorla A, et al. Unbalanced deoxynucleotide pools cause mitochondrial DNA instability in thymidine phosphorylase-deficient mice. Hum Mol Genet. 2009;18:714-722.

26. Torres-Torronteras J, Cabrera-Perez R, Barba I, et al. Long-Term Restoration of Thymidine Phosphorylase Function and Nucleoside Homeostasis Using Hematopoietic Gene Therapy in a Murine Model of Mitochondrial Neurogastrointestinal Encephalomyopathy. Hum Gene Ther. 2016;27:656-667.

27. Torres-Torronteras J, Viscomi C, Cabrera-Perez R, et al. Gene therapy using a liver-targeted AAV vector restores nucleoside and nucleotide homeostasis in a murine model of MNGIE. Mol Ther. 2014;22:901-907.

28. Camara Y, Gonzalez-Vioque E, Scarpelli M, et al. Administration of deoxyribonucleosides or inhibition of their catabolism as a pharmacological approach for mitochondrial DNA depletion syndrome. Hum Mol Genet. 2014;23:2459-2467.

29. Garcia-Diaz B, Garone C, Barca E, et al. Deoxynucleoside stress exacerbates the phenotype of a mouse model of mitochondrial neurogastrointestinal encephalopathy. Brain. 2014;137:1337-1349.

30. Dubey M, Bugiani M, Ridder MC, et al. Mice with megalencephalic leukoencephalopathy with cysts: a developmental angle. Ann Neurol. 2015;77:114-131.

31. Bugiani M, Dubey M, Breur M, et al. Megalencephalic leukoencephalopathy with cysts: the Glialcam-null mouse model. Ann Clin Transl Neurol. 2017;4:450-465.

32. Huston MW, van Til NP, Visser TP, et al. Correction of murine SCID-X1 by lentiviral gene therapy using a codon-optimized IL2RG gene and minimal pretransplant conditioning. Mol Ther. 2011;19:1867-1877.

33. van Til NP, de Boer H, Mashamba N, et al. Correction of murine Rag2 severe combined immunodeficiency by lentiviral gene therapy using a codon-optimized RAG2 therapeutic transgene. Mol Ther. 2012;20:1968-1980.

34. Wilcox DA. Megakaryocyte- and megakaryocyte precursor-related gene therapies. Blood. 2016;127:1260-1268.

35. Goyvaerts C, Liechtenstein T, Bricogne C, Escors D, Breckpot K. Targeted Lentiviral Vectors: Current Applications and Future Potential. In: Molina FM, ed. Gene Therapy - Tools and Potential Applications. Rijeka: InTech; 2013:Ch. 14.

36. Mussolino C, Morbitzer R, Lutge F, Dannemann N, Lahaye T, Cathomen T. A novel TALE nuclease scaffold enables high genome editing activity in combination with low toxicity. Nucleic Acids Res. 2011;39:9283-9293.

37. Ma N, Liao B, Zhang H, et al. Transcription activator-like effector nuclease (TALEN)-mediated gene correction in integration-free beta-thalassemia induced pluripotent stem cells. J Biol Chem. 2013;288:34671-34679.

38. Ramalingam S, Annaluru N, Kandavelou K, Chandrasegaran S. TALEN-mediated generation and genetic correction of disease-specific human induced pluripotent stem cells. Curr Gene Ther. 2014;14:461-472.

39. Gundry MC, Brunetti L, Lin A, et al. Highly Efficient Genome Editing of Murine and

7

Human Hematopoietic Progenitor Cells by CRISPR/Cas9. Cell Rep. 2016;17:1453-1461.

40. Christensen C, Choy F. A Prospective Treatment Option for Lysosomal Storage Diseases: CRISPR/Cas9 Gene Editing Technology for Mutation Correction in Induced Pluripotent Stem Cells. Diseases. 2017;5:6.

41. Yin H, Kauffman KJ, Anderson DG. Delivery technologies for genome editing. Nat Rev Drug Discov. 2017;16:387-399.

42. Wechsler T, Meyer KE, Spratt SK, et al. ZFN-Mediated Gene Targeting at the Albumin Locus in Liver Results in Therapeutic Levels of Human FIX in Mice and Non-Human Primates. Blood. 2015;126:200-200.

43. Tsai SQ, Zheng Z, Nguyen NT, et al. GUIDE-seq enables genome-wide profiling of off-target cleavage by CRISPR-Cas nucleases. Nat Biotechnol. 2015;33:187-197.

44. Tsai SQ, Joung JK. Defining and improving the genome-wide specificities of CRISPR-Cas9 nucleases. Nat Rev Genet. 2016;17:300-312.

45. Wakabayashi T, Shimada Y, Akiyama K, et al. Hematopoietic Stem Cell Gene Therapy Corrects Neuropathic Phenotype in Murine Model of Mucopolysaccharidosis Type II. Hum Gene Ther. 2015;26:357-366.

46. Gentner B, Visigalli I, Hiramatsu H, et al. Identification of hematopoietic stem cell-specific miRNAs enables gene therapy of globoid cell leukodystrophy. Sci Transl Med. 2010;2:58ra84.

47. Biffi A. Hematopoietic Stem Cell Gene Therapy for Storage Disease: Current and New Indications. Mol Ther. 2017;25:1155-1162.

48. Huston MW, Riegman AR, Yadak R, et al. Pretransplant mobilization with granulocyte colony-stimulating factor improves B-cell reconstitution by lentiviral vector gene therapy in SCID-X1 mice. Hum Gene Ther. 2014;25:905-914.

49. Xue X, Pech NK, Shelley WC, Srour EF, Yoder MC, Dinauer MC. Antibody targeting KIT as pretransplantation conditioning in immunocompetent mice. Blood. 2010;116:5419-5422.

50. Palchaudhuri R, Saez B, Hoggatt J, et al. Non-genotoxic conditioning for hematopoietic stem cell transplantation using a hematopoietic-cell-specific internalizing immunotoxin. Nat Biotechnol. 2016;34:738-745.

51. Oliver FJ, Collins MK, Lopez-Rivas A. dNTP pools imbalance as a signal to initiate apoptosis. Experientia. 1996;52:995-1000.

52. Kumar D, Viberg J, Nilsson AK, Chabes A. Highly mutagenic and severely imbalanced dNTP pools can escape detection by the S-phase checkpoint. Nucleic Acids Res. 2010;38:3975-3983.

53. Jiang H, He X, Wang S, et al. A microtubule-associated zinc finger protein, BuGZ, regulates mitotic chromosome alignment by ensuring Bub3 stability and kinetochore targeting. Dev Cell. 2014;28:268-281.

Appendix

Summary
Samenvatting
Arabic summary (ملخص)
List of terms and abbreviations
PhD portfolio
List of publications
Curriculum vitae
Acknowledgements

| SUMMARY

Hematopoietic stem cell gene therapy (HSCGT) is an attractive treatment option for a wide range of disorders. The initial clinical trials for X- linked severe combined immunodeficiency (SCID-X1) and ADA-SCID applied γ-RV vectors successfully, but hematological malignancies occurred in SCID-X1 due to vector integration and transactivation of nearby oncogenes. Therefore, efforts were directed towards finding alternative viral vector systems leading, eventually, to the development of the new 3rd generation self-inactivating (SIN) lentiviral (LV) vectors with enhanced efficiency and benign integration profiles.

Mitochondrial neurogastrointestinal encephalomyopathy (MNGIE) is currently treated with allogeneic hematopoietic stem cell transplantation (allogeneic HSCT). Allogeneic HSCT successfully reverses the biochemical phenotype. However, HSCT is associated with high mortality rates, requires the availability of matched donor hematopoietic stem and progenitor cells (HSPCs) while knowledge about the long term therapeutic outcome is limited. LV-mediated HSCGT uses autologous cells, may require lower pre-conditioning regimens and is expected to provide long-term systemic disease correction as discussed in **Chapter 2**.

In **Chapter 3**, we optimized the *ex vivo* culture conditions of LV vector mediated gene transfer into HSPCs to achieve efficient gene marking within a short transduction time period, with a minimal number of integrated vector copies, and minimal cytokine additions. The results indicate the feasibility to improve gene transfer by increasing the density of mouse, rhesus, or human HSPCs target cells. Additionally, overnight transduction of mouse and human HSPCs in stem cell medium with addition of thrombopoietin (TPO) only enhanced transduction sufficiently for *in vivo* purposes. The addition of the growth factors SCF, TPO, Flt3-L at relatively low concentrations provided the most efficient gene transfer (> 60% GFP marking) while maintaining progenitor and stem cells repopulation capacity. Altogether, these findings open intriguing possibilities for overcoming the limitations of the current gene transfer protocols: an enhanced efficiency and improved safety of gene correction, minimal *ex vivo* manipulation during a short culture period, and the added economic value of using small amounts of clinical grade lentiviral vectors and cytokines.

Chapters 4 and 5 focus on the evaluation of the efficiency and safety of LV vector-mediated HSCGT as a treatment for MNGIE in *Tymp$^{-/-}$Upp1$^{-/-}$* mice. Therapeutically applicable SIN LV vectors were used containing the physiological human phosphoglycerate kinase (hPGK) promoter for ubiquitous expression of native or codon optimized human TYMP cDNA (PGK-TP or PGK-TPco, respectively). LV-SF-TPco bearing the strong spleen focus forming virus (SF) promoter was used for safety evaluation to highly express TP, and to assess potential genotoxicity. The results in **Chapter 4** demonstrated persistent TP activity and clearance of nucleosides in the brain of treated *Tymp$^{-/-}$Upp1$^{-/-}$* mice at relatively low vector copy numbers (PGK-TP(co): MOI 10, range; 0.2-3.6 VCN/cell). Here, we showed that this resulted also in reversal of the phenotypic alterations apparent in brain astrocytes of

A

Tymp$^{-/-}$Upp1$^{-/-}$ mice, as well as reduction of white matter edema demonstrated by brain MRI and immunohistological analysis. Long term follow up of recipients of HSCGT revealed no side effects from the procedure: *(i)* Graft failure or toxicity related to sub-lethal total body irradiation was not observed. *(ii)* Survival curves of mice in the PGK-TP(co) treatment groups did not differ significantly from controls. *(iii)* LV- related insertional mutagenesis or hematopoietic transformation were not observed after a total of 22 months follow up of primary and secondary recipients of HSCs transduced by therapeutic LV vectors PGK-TP(co). *(iv)* LAM-PCR and sequencing demonstrated a polyclonal integration pattern and no bias towards integration near or selection of proto-oncogenes.

Gastrointestinal manifestations are prominent and the main cause of death among MNGIE patients. In **Chapter 5** we examined the pathology of the small intestine of MNGIE patients and *Tymp$^{-/-}$Upp1$^{-/-}$* mice and the impact of allogeneic HSCT or gene therapy, respectively. Our findings confirmed the previously reported atrophy of the muscularis propria and absence of interstitial cells of Cajal in MNGIE patients. HSCT did not resolve these pathological characteristics in the short period studied post transplantation. This might explain the repeatedly reported persistent gastrointestinal manifestations after treatment. In contrast, HSCGT rescued the atrophic muscularis propria of the small intestine in treated *Tymp$^{-/-}$Upp1$^{-/-}$* mice 10 months after treatment. This suggests that the myogenic changes can be reversed when gene therapy

is provided early in life. Finally, in **Chapter 6**: we further evaluated in depth the LV vectors integration profiles in gene modified human, rhesus or murine HSCs cultured *in vitro*, and *in vivo* after transplantation in disease models of SCID, Pompe, MNGIE and healthy mice. The integration patterns were similar in all species studied, and were not skewed based on the type of promoter (SF versus PGK, RAG1p, TCRβp, UCOE and γcPr), or transgene used (*GFP* versus *Il2rg, Rag1*, *Rag* 2, *Gaa* and *Tymp*).

In conclusion, the results presented in this thesis demonstrate efficient and persistent correction of the biochemical phenotype in affected organs of *Tymp$^{-/-}$Upp1$^{-/-}$* mice, brain neurological phenotypes (white matter edema and astrocytes morphology), and intestinal myopathy (atrophy of the muscularis propria), at relatively low LV-PGK-TP(co) vector copy number per cell and without obvious vector or disease related phenotoxicity or genotoxicity. Due to the lack of some of the major neurological or gastrointestinal clinical phenotypes in *Tymp$^{-/-}$Upp1$^{-/-}$* mice (such as motor dysfunction or cachexia) we should be cautious in translating our findings from mice to MNGIE patients. Nonetheless, it is recommended to perform more studies before clinical application, including evaluating HSCGT in more clinically relevant models that mimic human MNGIE disease (e.g. *Tymp$^{-/-}$Upp1$^{-/-}$* mice fed with a diet to enforce the phenotypes), dosing of LV vector and transplanted gene modified cells, and more thorough assessment of vector biodistribution and safety studies addressing potential phenotoxicity and genotoxicity in depth.

|SAMENVATTING (DUTCH SUMMARY)

Hematopoietische stamcelgentherapie (HSCGT) is een aantrekkelijke behandelingsoptie voor een breed scala van aandoeningen. Bij de eerste klinische studies naar X-linked ernstig gecombineerde immunodeficiëntie (SCID-X1) en adenosine deaminase (ADA)-SCID heeft men γ-RV vectoren met succes toegepast, maar bij SCID-X1 ontstonden hematologische maligniteiten als gevolg van vectorintegratie en transactivatie van nabije oncogenen. Daarom werd gezocht naar alternatieve virale vectorsystemen. Dit leidde uiteindelijk tot de ontwikkeling van de nieuwe, derde generatie zelf-inactiverende (SIN) lentivirale (LV) vectoren met verbeterde efficiëntie en goedaardige integratieprofielen.

Mitochondriële neurogastrointestinale encefalomyopathie (MNGIE) wordt momenteel behandeld met allogene hematopoietische stamceltransplantatie (allogene HSCT). Deze therapie leidt tot reversie van het biochemische fenotype, maar is geassocieerd met hoge sterftecijfers. Verder dienen matchted donor hematopoietische stam- en voorlopercellen (HSPCs) beschikbaar te zijn, en er is nog weinig bekend over de uitkomst op de lange termijn. LV-gemedieerde HSCGT maakt gebruik van autologe cellen, kan mogelijk toe met lagere pre-conditioneringsregimes en kan naar verwachting systemische ziekte op termijn corrigeren, zoals besproken in **Hoofdstuk 2**.

In **Hoofdstuk 3** optimaliseerden we de *ex vivo* kweekomstandigheden van LV-vector gemedieerde genoverdracht in hematopoietische stam en voorloper cellen (HSVC's). Het doel hiervan was om efficiënte transductie te bereiken binnen een korte

incubatietijd, met een minimaal aantal geïntegreerde vectorkopieën en minimale cytokine toevoegingen. De resultaten geven aan dat het haalbaar is de genoverdracht te verbeteren door het verhogen van de dichtheid van muizen-, rhesus- of humane HSVC-cellen. Ook zagen we dat de overnacht transductie van muis- en humane HSVC's in stamcelmedium waaraan alleen trombopoëtine (TPO) was toegevoegd als cytokine, significant verbeterde transductie opleverde voor *in vivo* doeleinden. Toevoeging van relatief lage concentraties van de groeifactoren SCF, TPO, Flt3-L gaf de meest efficiënte genoverdracht (60% GFP-markering) met behoud van de mogelijkheid tot repopulatie van voorloper- en stamcellen. Alles bij elkaar genomen bieden deze bevindingen mogelijkheden om de beperkingen van de huidige genoverdrachtprotocollen te verbeteren door een verhoogde efficiëntie en minder veiligheidsrisico's m.b.t. insertionele mutagenese, met minimale *ex vivo* manipulatie gedurende een korte kweekperiode en de toegevoegde commerciële waarde van het gebruik van kleine hoeveelheden klinische lentivirale vectoren en cytokines.

In de **Hoofdstukken 4 en 5** lag de nadruk op de evaluatie van de efficiëntie en veiligheid van LV vector-gemedieerde hematopoietische stam en voorloper cel gentherapie (HSVGT) als een behandeling voor MNGIE in *Tymp^{-/-} Upp1^{-/-} muizen*. Hierbij werden therapeutisch toepasbare SIN LV-vectoren gebruikt met de fysiologische humane fosfoglyceraatkinase (hPGK) promotor om algemene expressie van oorspronkelijk- of codon-geoptimaliseerd humaan TYMP cDNA te bewerkstelligen (respectievelijk PGK-TP of PGK-TPco).

A

Voor evaluatie van de veiligheid werd de LV-SF-TPco gebruikt met de sterke milt-focusvormende viruspromotor waarbij een hoge TP-expressie wordt verkregen om de mogelijke genotoxiciteit te beoordelen. De resultaten in **Hoofdstuk 4** wezen op persisterende TP-activiteit en klaring van nucleosiden in de hersenen van behandelde $Tymp^{-/-}$ $Upp1^{-/-}$ muizen bij relatief lage aantallen vector-kopieën (PGK-TP(co): MOI 10, bereik, 0,2-3,6 VCN /cel). Dit resulteerde niet alleen in de correctie van de fenotypische veranderingen die te zien waren in de hersenastrocyten van $Tymp^{-/-}$ $Upp1^{-/-}$ muizen, maar ook in vermindering van oedeem in de witte stof, zoals aangetoond met hersen-MRI en immunohistochemie. Bij de lange termijn follow-up van de van behandelde HSCGT muizen zijn geen nadelige bijwerkingen van de procedure gezien: *(i)* Falen van donormateriaal of toxiciteit door de subletale bestraling van het gehele lichaam zijn niet waargenomen. *(ii)* De overlevingscurven van de muizen in de PGK-TP(co) behandelingsgroepen waren statistisch niet significant verschillend van de overlevingscurven van de controledieren. *(iii)* LV-gerelateerde insertiemutagenese of hematopoietische transformatie werden niet waargenomen na in totaal 22 maanden follow-up van de primaire en secundaire ontvangers van door therapeutische LV-vectoren (PGK-TP(co)) getransduceerde HSC's. *(iv)* LAM-PCR en sequencing lieten een polyclonaal integratiepatroon zien zonder bias naar integratie in de nabijheid van of in proto-oncogenen.

Gastrointestinale aandoeningen komen veel voor en zijn de belangrijkste doodsoorzaak bij MNGIE-patiënten. In **Hoofdstuk 5** hebben we onderzoek gedaan naar de pathologie van de dunne darm van MNGIE-patiënten en $Tymp^{-/-}$ $Upp1^{-/-}$ muizen en de effecten van respectievelijk allogene HSCT of gentherapie. Onze bevindingen bevestigden de al eerder gerapporteerde atrofie van de muscularis propria en afwezigheid van interstitiële cellen van Cajal bij MNGIE-patiënten. HSCT liet geen effect zien in de korte tijd tot enkele maanden na transplantatie. Dit kan de herhaaldelijk gemelde aanhoudende gastrointestinale klachten na de behandeling verklaren. Daarentegen herstelde HSCGT de atrofische muscularis propria van de dunne darm in behandelde $Tymp^{-/-}$ $Upp1^{-/-}$ muizen 10 maanden na de behandeling. Dit suggereert dat de myogene veranderingen omgekeerd kunnen worden wanneer gentherapie vroeg in het leven wordt gegeven. Tenslotte, **Hoofdstuk 6** betreft een diepgaandere evaluatie van de LV vector integratieprofielen in gen-gemodificeerde humane, rhesus of muizen HSVC's, gekweekt *in vitro* en *in vivo* na transplantatie in ziektemodellen van SCID, Pompe, MNGIE en in gezonde muizen. De integratiepatronen waren vergelijkbaar in alle onderzochte species en niet afhankelijk van het type promotor (SF versus PGK, RAG1p, TCRβp, UCOE en γcPr) of het gebruikte transgen (*GFP* versus *IL2RG*, *RAG-1*, *Rag 2*, *Gaa* en *Tymp*).

Concluderend blijkt uit de resultaten in dit proefschrift een effectieve en aanhoudende correctie van het biochemische fenotype in aangedane organen van $Tymp^{-/-}$ $Upp1^{-/-}$ muizen, hersen- fenotypes (witte stof oedeem en astrocyten morfologie) en intestinale myopathie (atrofie van de muscularis propria), bij een relatief aantal LV-PGK-TP(co) vector copien per cel en zonder duidelijke vector- of ziekte gerelateerde fenotoxiciteit of genotoxiciteit. Door het ontbreken van enkele

belangrijke neurologische of gastrointestinale klinische fenotypes in *Tymp^-/- Upp1^-/-* muizen (zoals motor dysfunctie of magerzucht) moeten we terughoudend zijn bij het vertalen van onze bevindingen bij de muizen naar MNGIE-patiënten. Het is aan te bevelen meer onderzoek te doen voordat dit klinisch kan worden toegepast. Zoals het evalueren van HSCGT in meer klinisch relevante modellen van humane MNGIE-muizen (bijvoorbeeld *Tymp^-/- Upp1^-/-* muizen die dieetvoeding krijgen om de fenotypen te forceren), de dosering van LV vector en getransplanteerde gen-gemodificeerde cellen, en verdere diepgaande evaluatie van de biodistributie van vectors alsmede grondiger veiligheidsstudies naar de mogelijke fenotoxiciteit en genotoxiciteit.

A

سلامة زيادة تركيز بروتين فوسفوريليز ثايميدين (TP)، ولتقييم مدى إمكانية وجود سمية ورائية. تشير النتائج الواردة في **الفصل الرابع** إلى وجود نشاط متواصل لبروتين TP واختفاء النيوكليوسيدات في دماغ الفئران *Tymp⁻/⁻Upp1⁻/⁻* التي خضعت للمعالجة، وذلك بعدد نسخ منخفضة نسبياً VCN ٣٫٦−٠٫٢، المدى: ((MOI 10 :PGK-TP(co)) لكل خلية). هنا، قمنا بإظهار كيف أن هذا تسبب أيضاً في عكس التغيرات المظهرية التي حصلت في الخلايا النجمية (astrocytes) لدماغ الفئران من فئة *Tymp⁻/⁻Upp1⁻/⁻* التي خضعت للمعالجة، كما أنها تسببت في تقليل وذمة المادة البيضاء (white matter edema) التي ظهرت في صورة الرنين المغناطيسي (MRI) التي أجريت للدماغ وتحاليل الكيمياء الهيستولوجية المناعية (immunohistological analysis). أظهرت المتابعة طويلة الأمد بعد تلقي العلاج الجيني للخلايا الجذعية الدموية (HSCGT) عدم وجود أي أعـراض جانبية للعملية: (أ) لم يتم ملاحظة فشل الزراعة أو أي تسمم ناتج عن تعرض الجسم لأشعة سينية شبه قاتلة. (ب) لم تختلف منحنيات البقاء على قيد الحياة بشكل ملحوظ عند الفئران التي تمت معالجتها باستخدام PGK−TP(co) عن المدى الطبيعي. (ج) لم يتم ملاحظة أي طفرات إدراجية أو تغيرات في مكونات الدم مرتبطة بالفيروسات البطيئة (LV) بعد مدة وصلت إلى ٢٢ شهراً من المتابعة للمستقبلين الأوليين والثانويين للخلايا الجذعية التي تم تحويلها باستخدام الفايروس البطيء العلاجي PGK-TP(co). (د) أظهرت تحاليل LAM-PCR وتحليلات التسلسل وجود نمط اندماج متعدد النسائل من دون أي انحياز نحو حدوث اندماج بالقرب من أو في أي تجمع لطليعة الجين الورمي.

تعد مظاهر الألم في الجهاز الهضمي سائدة وتعد السبب الرئيسي للوفاة لدى المرضى المصابين بمرض منجي (MNGIE). في **الفصل الخامس** قمنا بفحص وتحليل الأمراض الظاهرة في الأمعاء الدقيقة لدى المرضى المصابين بمرض منجي (MNGIE) ولدى الفئران من

فئة *Tymp⁻/⁻Upp1⁻/⁻*، إضافة إلى دراسة أثر زراعة نخاع العظم بالخلايا الجذعية (allogeneic HSCT) أو العلاج الجيني (gene therapy)، على التوالي. أكدت النتائج التي توصلنا إليها الادعاءات السابقة بحدوث ضمور في العضلة الخصوصة (atrophy of the muscularis propria) وعدم وجود أي خلايا خلالية من نوع كاجال (Cajal) لدى المصابين بمرض منجي (MNGIE). لم يتسبب العلاج بالخلايا الجذعية (HSCT) في حل هذه الخصائص المرضية خلال الفترة القصيرة التي تم دراستها بعد إجراء عملية الزراعة. يمكن لهذه النتيجة أن تفسر التغييرات الظاهرة في الجهاز الهضمي التي يتم الإبلاغ عنها بشكل متكرر لدى المرضى بعد تلقي العلاج. وعلى عكس ذلك، فإن العلاج الجيني للخلايا الجذعية الدموية (HSCGT) تسبب في تقليل ضمور العضلات المخصوصة في الأمعاء الدقيقة لدى الفئران من فئة *Tymp⁻/⁻Upp1⁻/⁻* بعد ١٠ أشهر من تلقي العلاج. قد تشير هذه النتائج إلى أن يمكن عكس التغيرات الناشئة من العضل في حال تم إعطاء العلاج الجيني في مرحلة مبكرة من الحياة. وأخيراً، في **الفصل السادس**، قمنا بإجراء تقييمات أكثر عمقاً لمكونات الدم مرتبطة بالفيروسات البطيئة (LV) لدى الكائنات التي طبقت عليها تعديلات جينية من البشر، أو القردة الصغيرة، أو الخلايا الجذعية المكونة للدم من الفئران مستنبتة في البيئة المخبرية وفي الوسط الحيوي بعد عملية الزراعة في الفئران المصابة بمرض العوز المناعي المكتسب الشديد (SCID)، داء اختزان الغلايكوجين النمط الثاني (Pompe)، ومرض منجي (MNGIE)، إضافة إلى فئران سليمة. كانت أنماط الاندماج متشابهة لدى جميع الأصناف التي تم دراستها، ولم يظهر أي اختلاف بناءاً على نوع المحفز المستخدم (SF, PGK, RAG1p, TCRβp, UCOE, γcPr)، أو الجين المستخدم (GFP, Il2rg, Rag1, Rag 2, Gaa, Tymp).

في الختام، فإن النتائج الواردة في هذه الرسالة تظهر تصحيح فعال ومستمر للنمط الظاهري البيوكيميائي في الأعضـاء المصابة للفئران من فئة *Tymp⁻/⁻Upp1⁻/⁻*،

ملخص (Arabic summary)|

يعد العلاج الجيني بالخلايا الجذعية (HSCGT) خيار علاجي مغر للعديد من الاضطرابات المرضية. أظهرت نتائج التجارب السريرية الأولية لمرضى داء نقص المناعة المشترك الشديد (SCID-X1) و (ADA-SCID) بأنها تتوافق بنجاح مع النواقل الفايروسية القهرية من نوع جاما (γ-RV vectors)، إلا أن الأورام الدموية الخبيثة حصلت في حالة نقص المناعة المشترك الشديد (SCID-X1) بسبب اندماج الفايروسات القهرية وعملية التفعيل النسخي للجينات المسرطنة المجاورة. وعليه، تم تركيز الجهود نحو إيجاد أنظمة فايروسية بديلة أدت، في نهاية المطاف، إلى تطوير الجيل الثالث من الفايروسات البطيئة (LV) ذات التعطيل التلقائي (SIN) ذات الكفاءة العالية والتي تتمتع بفاعلية محسنة وبروفايلات إندماج حميدة.

في الوقت الحالي، يتم علاج مرض منجي (MNGIE) عن طريق زراعـة نـخـاع الـعـظـم بـالـخـلايـا الـجـذعـيـة (allogeneic HSCT). تنجح عملية زراعة نخاع العظم بالخلايا الجذعية بعكس النمط الظاهري البيوكيميائي. إلا أن عمليات زراعة نخاع العظم بالخلايا الجذعية ترتبط بنسب وفيات عالية، وهي تتطلب وجود متبرع تتطابق خلاياه الجذعية وخلاياه السلفية (HSPCs) مع المريض، كما أن المعرفة بالنتائج العلاجية طويلة الأمد محدودة. يتم خلال العلاج الجيني للخلايا الجذعية الدموية (HSCGT) باستخدام الفايروسات البطيئة استخدام الـخـلايـا ذاتـيـة المنشأ، وقد تحتاج هذه العلاجات إلى متطلبات وإجراءات أقل للمريض ما قبل زراعة نخاع العظم ومن المتوقع أن تعطي تصحيح مرضى طويل الأمل، كما هو موضح في **الفصل الثاني.**

في **الفصل الثالث**، قمنا بتهيئة بيئة خارجية (*ex vivo* culture conditions) مثالية لعمليات نقل الجينات من خلال الفايروسات البطيئة إلى الخلايا الجذعية والسلفية المكونة للدم (HSPCs) لضمان كفاءة نقل الجينات خلال فترة تنبيت قصيرة، وباستخدام أقل عدد ممكن من النواقل

الفايروسية، والحد الأدنى من إضافات السيتوكينات. تشير النتائج إلى فاعلية تحسين نقل الجينات من خلال زيادة كثافة الخلايا الجذعية و السلفية المكونة للدم المستهدفة المستخلصة من الفئران، أو القرد الصغير، أو الانسان. عـلاوة على ذلك، فإن عملية نقل الجينات التي تتم بين ليلة وضحاها للخلايا الجذعية والسلفية المكونة للدم لدى الفئران والإنسان في مستنبت الخلايا الجذعية مع إضافة ثرومبوبويتين (TPO) فقط تسببت في تحسين نقل المادة الوراثية لأغراض الدراسة في البيئة الداخلية (*in vivo*). إن إضافة عوامل النمو SCF، و TPO، و Flt3-L بتركيزات منخفضة نسبياً تسببت في نقل الجينات بالكفاءة الأكثر (بنسبة تفوق الـ 60% على مؤشر GFP)، مع الحفاظ على قدرة إعادة إنتاج الخلايا الجذعية والخلايا السلفية. في الإجمال، تساعد هذه النتائج في فتح احتمالات مثيرة للاهتمام لتخطي القيود التي تنتج عن بروتوكولات نقل الجينات الحالية: كفاءة أعلى وتحسين في مدى سلامة التصحيح الجيني، إضافة إلى الحد الأدنى من التعديلات على البيئة الخارجية خلال فترة تنبيت قصيرة، والقيمة الاقتصادية المضافة التي نحصل عليها عند استخدام كميات صغيرة من الفايروسات البطيئة والسيتوكينات.

يتم التركيز في **الفصل الرابع والفصل الخامس** على تقييم مدى كفاءة ودرجة أمـان الفايروسات البطيئة في العلاج الجيني للخلايا الجذعية الدموية (LV vector-mediated HSCGT) كعلاج لمرض منجي (MNGIE) عند تطبيقها على الفئران من فئة *Upp1-/-Tymp-/-*. تم استخدام الفايروسات البطيئة (LV) ذات التعطيل التلقائي (SIN)، وقابلة للتطبيق علاجياً، والتي تحتوي على محفز كيناز الفُسفوغليسِرات الفسيولوجي الموجود في الإنسان (hPGK promoter) من أجل التعبير عن human TYMP cDNA الأصلي (PGK-TP) أو المعدل (PGK-TPco). تم استخدام الفايروسات البطيئة LV–SF–TPco، والتي تحمل محفزي (SF) لتقييم مدى

والأنماط الظاهرية لخلايا الدماغ العصبية (وذمة المادة البيضاء والخلايا النجمية)، والاعتلال العضلي في الأمعاء (ضمور العضلة المخصوصة) وذلك من خلال عدد قليل نسبياً لنسخ عامل LV-PGK-TP(co) لكل خلية، من دون حصول أي تسمم جيني أو تغير مظهري ظاهر. وبسبب وجود نقص في عدد من أهم الأنماط الشكلية العصبية أو الخاصة بالجهاز الهضمي لدى الفئران من فئة *Tymp⁻/⁻Upp1⁻/⁻* (مثل الاختلال في الوظائف الحركية أو الدنف (متلازمة الهزال))، فإنه يتوجب علينا أن نكون حذرين عند ترجمة النتائج التي توصلنا إليها عند دراسة الفئران وتطبيقها على المرضى المصابين بمرض منجي (MNGIE). بالرغم من ذلك، فإننا ننصح بإجراء دراسات

إضافية قبل القيام بالتطبيق السريري، على أن تشمل تلك الدراسات تقييم مدى فاعلية العلاج الجيني للخلايا الجذعية الدموية (HSCGT) في بيئة سريرية أكثر ملائمة تحاكي جسد الإنسان المصاب بمرض منجي (MNGIE) (مثل فئران من فئة *Tymp⁻/⁻Upp1⁻/⁻* خاضعة لنظام غذائي يحفز الأنماط الظاهرية)، وجرعة معامل الفايروسات البطيئة (LV) والخلايا المزروعة المعدلة جينياً، إضافة إلى إجراء تقييمات أكثر عمقاً للتوزيع البيولوجي للفيروسات، إضافة إلى دراسات أكثر عمقاً تتطرق لإمكانية حدوث تسمم جيني (phenotoxicity) أو تغير مظهري ظاهر (genotoxicity).

|LIST OF TERMS AND ABBREVIATIONS

AAV	adeno-associated virus
ADA-SCID	adenosine deaminase-severe combined immunodeficiency
ANT-1	adenine nucleotide translocase type 1
BBB	blood brain barrier
BFU-E	burst forming unit-erythroid
BM	bone marrow
CD	cluster of differentiation
cDNA	complimentary DNA
CFU-GM	colony forming unit- granulocyte monocyte
CGD	chronic granulomatous disease
CIPO	chronic intestinal pseudo obstruction
CIS	common integration sites
CNT	concentrative nucleoside transporter
CPEO	chronic progressive external ophthalmoplegia
cPPT	central polypurine tract
CRISPR/Cas	clustered regularly interspaced short palindromic repeats/ CRISPR-associated
dCTP	Deoxycytidinetriphosphate
dTTP	deoxythymidine triphosphate
DNA	deoxyribonucleic acid
dNTP	deoxyribonucleoside triphosphates
dThd	thymidine
dUrd	deoxyuridine
ECGF1	platelet-derived endothelial cell growth factor
EE-TP	erythrocyte encapsulated TP
ENT	equilibrative nucleosides transport
ERT	enzyme replacement therapy
FIX	coagulation factor IX
FACS	fluorescence activated cell sorting

Flt3-L	FMS-like tyrosine kinase 3-ligand
G-CSF	granulocyte colony stimulating factor
GFAP	glial fibrillary acidic protein
GFP	green fluorescent protein
γ-RV	gammaretrovirus
GVHD	graft versus host disease
Gy	Gray (irradiation dose unit)
H&E	hematoxylin-Eosin
HIV	human immunodeficiency virus
HLA	human leukocyte antigen
hPGK	human phosphoglycerate kinase
HSCs	hematopoietic stem cells
HSCT	hematopoietic stem cell transplantation
HSCGT	hematopoietic stem cell gene therapy
HSPCs	hematopoietic stem and progenitor cells
iPSCs	induced pluripotent stem cells
IRES	internal ribosome entry site
LAM-PCR	linear amplification mediated PCR
LHON	Leber's hereditary optic neuropathy
Lin-	lineage negative
LV	lentivirus
LVIS	lentiviral integration sites
MBP	myelin basic protein
MDS	mitochondrial DNA depletion syndrome
MNGIE	mitochondrial neurogastrointestinal encephalomyopathy
MOI	multiplicity of infection
mRNA	messenger RNA

A

mtDNA	mitochondrial DNA	**SF**	spleen focus forming virus
NT	nucleoside transporter	**SIN-LV**	self-inactivating LV
OLT	orthotopic liver transplantation	**TALENs**	transcription activator-like effector nucleases
PCR	polymerase chain reaction		
PEO	progressive external ophthalmoplegia	**TP**	thymidine phosphorylase enzyme
PLP	proteolipid protein	**TPO**	thrombopoietin
PTAH	phosphotungstic acid-hematoxylin	**TYMP**	thymidine phosphorylase gene
qPCR	quantitative PCR	**TYMPco**	codon optimized TYMP gene
RAG -SCID	recombination activating gene 1 and 2 severe combined immunodeficiency	**UCB**	umbilical cord blood
		VCN	vector copy number
		VRAC	volume regulated anion channel
RNA	ribonucleic acid	**WAS**	Wiskott-Aldrich Syndrome
RRE	Rev response element	**WPRE**	woodchuck hepatitis posttranscriptional regulatory element
SCF	stem cell factor		
SCID- X1	X-linked severe combined immunodeficiency	**ZFNs**	zinc-finger nucleases

|PHD PORTFOLIO

Name PhD student: Rana Yadak
Erasmus MC Department: Neurology
Research School: Molecular Medicine (MolMed)
PhD period: Sept. 2011- Dec. 2017
Promoter: Prof.dr. P.A.E. Sillevis Smitt
Supervisors: Dr. N.P. van Til and Dr. I.F.M. de Coo

	Year	Workload (ECTS)
1- PhD training		
General courses		
Laboratory animal science	2012	3
Basic Human Genetics	2013	0.5
Basic Introduction Course on SPSS	2013	1
Research management for PhD students	2014	1
Research integrity	2015	0.3
Biomedical scientific English writing	2016	2
Specific courses		
5B irradiation protection course	2015	1.4
Seminars and workshops		
Annual MolMed day (2x)	2012-2013	0.6
NCBI & other open source software	2014	1
Toxicology of gene-modified hematopoietic cells- Hannover Medical school	2014	0.6
Photoshop and Illustrator CS 6 workshop	2014	0.3
Presentations		
NVGCT- Lunteren (3x)	2014-2016	3
NVKN- Alkmaar	2014	1
ESHG- Milan	2014	1
YMF and Euromit- Tampere	2014	1
CELL- PID- Ankara	2014	1
The XXIInd Annual ESGCT congress- The Hague	2014	1
ASGCT 18th annual meeting - New Orleans	2015	1
11th EPNS- Vienna	2015	1
International MNGIE consortium meeting- Innsbruk	2016	1
Posters		
Spierziektecongres- Veldhoven (2x)	2014-2015	0.6
Euromit- Tampere	2014	0.3
ICNC- Amsterdam	2016	0.3
National conferences		
NVGCT- Lunteren (3x)	2014-2016	1.7
International conferences		
PERSIST annual EU-project meeting – Leukerbad	2012	1.1

A

PhD Portfolio (continued)

	Year	Workload (ECTS)
CELL- PID annual EU-project meeting- Stresa (2x)	2012-2013	2.3
ESHG- Milan	2014	1.1
YMF and Euromit- Tampere	2014	1.7
CELL- PID- Ankara	2014	0.6
The XXIInd Annual ESGCT congress- The Hague	2014	1.1
ASGCT 18th annual meeting - New Orleans 11th	2015	1.1
EPNS- Vienna	2015	1.1
International MNGIE consortium meeting- Innsbruk	2016	0.3
ICNC- Amsterdam	2016	0.3

2-Teaching

Supervising a student during her master's thesis	2013	38

3-Others

Research visits

Dept. of Immunology, Weizmann Institute of Science (4 months)	2012	
Dept. of Pathology, VUMC- Amsterdam (3 months)	2015,2017	
Lab of Neuromuscular and Mitochondrial Disorders, Vall d'Hebron research Institute- Barcelona (3 weeks)	2015	

Travel grants

Tebu Bio researchers travel grant to attend ESHG in Milan	2014	
Meritorious abstract travel award to attend the ASGCT 18th annual meeting in New Orleans	2015	

Volunteer activity

The XXIInd Annual ESGCT congress-The Hague	2014	

|LIST OF PUBLICATIONS

Yadak R, Sillevis Smitt P, van Gisbergen MW, van Til NP, de Coo IF. Mitochondrial Neurogastrointestinal Encephalomyopathy Caused by Thymidine Phosphorylase Enzyme Deficiency: From Pathogenesis to Emerging Therapeutic Options. Front Cell Neurosci. 2017;11:31.

Van Gisbergen MW, Voets AM, Starmans MH, de Coo IF, **Yadak R**, Hoffmann RF, et al. How do changes in the mtDNA and mitochondrial dysfunction influence cancer and cancer therapy? Challenges, opportunities and models. Mutat Res Rev Mutat Res. 2015;764:16-30.

Huston MW, Riegman AR, **Yadak R**, van Helsdingen Y, de Boer H, van Til NP, et al. Pretransplant mobilization with granulocyte colony-stimulating factor improves B-cell reconstitution by lentiviral vector gene therapy in SCID-X1 mice. Hum Gene Ther. 2014;25(10):905-14.

Khurana S, Melacarne A, **Yadak R**, Schouteden S, Notelaers T, Pistoni M, et al. SMAD signaling regulates CXCL12 expression in the bone marrow niche, affecting homing and mobilization of hematopoietic progenitors. Stem Cells. 2014;32(11):3012-22.

Yadak R, Cabrera-Pérez R, Torres-Torronteras J, Bugiani M, Haeck J, Huston MW, et al. Preclinical efficacy and safety evaluation of hematopoietic stem cell gene therapy in a mouse model of MNGIE. *(Submitted)*.

Yadak R, Boot M, van Til NP, Cazals-Hatem D, Finkenstedt A, Bogaerts E, et al. Transplantation, gene therapy and intestinal pathology in MNGIE patients and mice. *(Submitted)*.

Van Til NP *, **Yadak R***, Buffa V, Huston MW, Aerts-Kaya F, van Helsdingen Y, et al. Development of a highly efficient lentiviral gene transfer protocol for hematopoietic stem cells. *(To be submitted)*.
*The authors contributed equally

Huston MW, Horsman S, Nowrouzi A, van der Velden G, Varkouhi A, Li Y, **Yadak R**, et al. Hematopoietic stem cell lentiviral integration profiles are stable across multiple species, disease phenotypes and hematopoietic cell types. *(To be submitted)*.

A

|CURRICULUM VITAE

Name   Rana Mahmoud AbdulRaheem Yadak
Date of birth   23 March 1986
Place of birth   Nablus, the West Bank, Palestine
E-mail   Rana.yadak@gmail.com

Positions
2011-2016   PhD position: Dept. of Hematology and Dept. of Neurology, Erasmus University Medical Center, Rotterdam, the Netherlands

Education
2011-2017   PhD candidate, Biomedical Sciences, Dept. of Hematology and Dept. of Neurology, Erasmus University Medical Center, Rotterdam, the Netherlands
                    Thesis: *'Lentiviral Hematopoietic Stem Cell Gene Therapy for MNGIE'*
                    Promotion date: 19 December 2017
2009-2011   MSc, Biomedical Sciences (Cell and Gene Therapy), Faculty of Medicine and Pharmacy, Vrije Universiteit Brussel, Brussels, Belgium,
                    Thesis*: 'Role of BMP signaling in regulating SDF-1α expression in murine bone marrow derived stromal cells'*
2004-2008   BSc in Medical Laboratory Sciences, Faculty of Science,
                    An-Najah National University, Nablus, Palestine

|ACKNOWLEDGEMENTS

easy. **Jeroen**, I enjoyed working together on the isolation of mtDNA. Our brain storming sessions on MNGIE, in particular the lymphoma and the AAV gene therapy projects, which we could not pursue, were greatly appreciated. **Kees**, **Lidia** and **Jacqueline**, you allowed me to perform experiments in your lab and provided valuable assistance and guidance during the mtDNA isolation. I enjoyed working in a group with you all, and **Kees**, I appreciate our discussions at the Romit and beyond. Thank you all.

To my former colleagues at the Hematology department, dear **Trui,** I learned a lot from you, I am forever indebted to your wisdom and kindness; **Leonie** and **Qiushi**, I find it expressive what Qiushi wrote, 'it is the mutual support we have given to each other that have helped us go thus far in our PhDs' and personal lives, and Qiushi, I am proud of us, we made it through our PhDs. I very much enjoyed having you around in the ML-I, -II, bacteria lab, the big lab, the animal house. Particularly, your presence was immensely supportive at the end of our localization at the Hematology dept. , as well as our discussions how to face challenges. Your PhD thesis confirmed to me that it takes more than hard work and dedication to achieve an exceptional PhD thesis, thanks to your supervisors and team members who supported your thesis and projects. To my student **Valentina**, you did great with your master's thesis. I was proud watching you learning, discussing your experiments and the results. To **Elnaz**, **Fatima**, **Yvette**, **Guus** and **Gwen**, I appreciate your assistance, valuable instructions and feedback. To **Merel**, thanks for your contribution in the beginning of MNGIE

project, and for saying "no" to me, thus I am better trained to deal with genotyping and experimental matters besides solving the problems independently. To **Noemi, Joyce, Davine**, **Amiet**, **Roberto**, **Adrian**, **Ferry**, and **Jasper**, I enjoyed the occasional talks and social activities. Thanks to **Eric Bindels** and **Elwin** for the technical assistance.

Department of Molecular Genetics, thank you for hosting me during the last part of my PhD. Particularly, I would like to thank **Prof. Roland Kanaar, Prof. Jan Hoeijmakers,** and **Dr. Pier Mastroberardino** for giving me the opportunity to finish my experiments and for valuable advice on many occasions. **Peter**, **Wilbert**, **Joris**, **Renata**, **Serena**, **Sander**, **Yvette**, **Yvonne**, **Silvia**, **Nicole**, **Maria**, **Soraya**, **Sabine**, **Shirley**, **Meneka, Danny, Jasperina** and the staff of the Molecular Genetics dept., I am grateful for the intellectual and technical support whenever I needed it, the very useful discussions, and the wonderful and uplifting social events.

To Diana, Akos, Chiara, Aida, Chang, Ines, Marjolein and Hester, I cannot thank you enough for everything you have done for me in the past two years. I am indebted to you all for our stimulating scientific and personal discussions, the lovely gatherings for international food, multiple celebrations, the wonderful meetings at Worm and hiking in Theux and Spa. Thank you, your support helped me get through my tough journey. **Diana, Akos, Chiara**, words cannot express how thankful and grateful I am for your caring and support until the last day of my PhD. To **Rajendra**, म मेरो यात्रामा तपाईको अनन्त समर्थनको लागी अनिवार्य छु, हाम्रो यात्रा र

नेपाल को त्यो यात्रा, र कोरल इरा संग सहयोग. **Hugo** and **Tina**, I will always remember our wonderful hike in the Ardennes and look forward to having similar trips soon. **Martha** and **Rui, Amany, Ali, Thabet, Nael, David, Kfir, Juliet and Ludo, Patrick,** and **Jorrit**, thank you all very much for your intellectual and emotional support.

To my fellow **PhD students**, all the best in finalizing your theses, and just remember what the great philosopher Nietzsche said, *"what does not kill you, makes you stronger."*

I also dedicate this work to all **the patients** who might eventually benefit directly or indirectly from the findings outlined in this thesis.

Palestine, I owe you so much for becoming who I am now due to the difficult times we experienced during the second Intifada. The braveness and stubbornness in going to school under siege prepared me to face the challenges I encountered during my PhD.
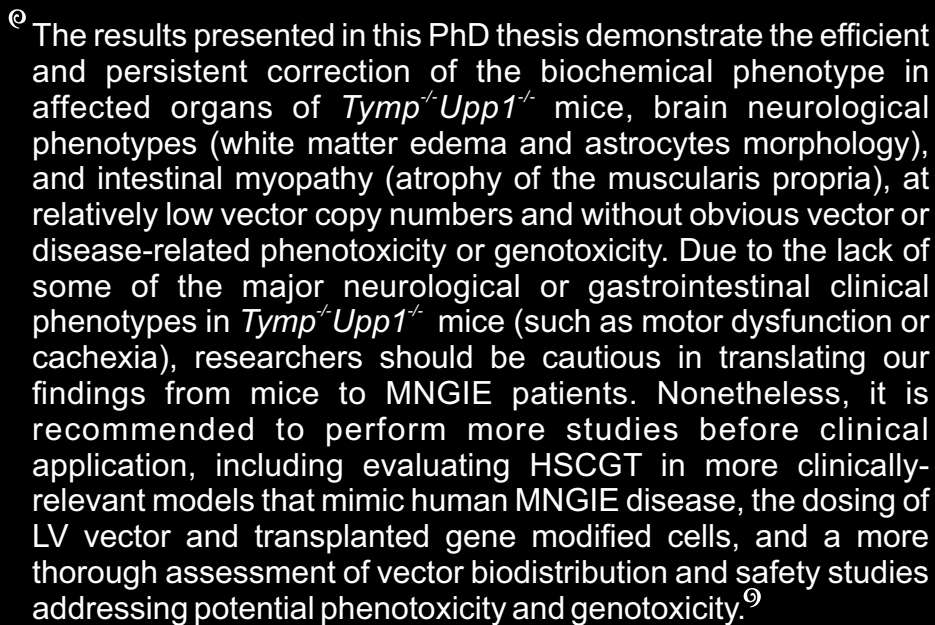
Dr. Riad Amer and **Mr. Nader Asfour**, I very much appreciate our insightful scientific discussions and your support to advance in my career.

To **Nour**, we both are at different places yet always by each other's side, thanks for being there for me. **Reem**, **Abud**, **Dr. Mohammad** and his **family**, **grandmother**, **aunts** and **uncle**s and their **families**, thank you very much for your kindness and prayers.

Last but not least, my beloved parents. To **father**, you encouraged me to pursue higher education, and your support was immeasurable. You gave me the opportunity to spread my wings and fly. Thank you, forever. My beloved **mother**, I cannot express my gratitude for your kindness and concern; your voice and the coffee in the early mornings gave me warmth and the strength to continue till the end of the day. To you, I am forever grateful.

Rana

P.S. There's more to publishing scientific papers than good science or advancing our career as scientists. Behind every word and between every line lies the curiosity, dedication, and sacrifice of the PhD students who helped bring it to fruition. This journey, filled with both tears and laughter, is what makes for a rewarding experience in publishing scientific work.

A

The results presented in this PhD thesis demonstrate the efficient and persistent correction of the biochemical phenotype in affected organs of *Tymp⁻ᐟ⁻Upp1⁻ᐟ⁻* mice, brain neurological phenotypes (white matter edema and astrocytes morphology), and intestinal myopathy (atrophy of the muscularis propria), at relatively low vector copy numbers and without obvious vector or disease-related phenotoxicity or genotoxicity. Due to the lack of some of the major neurological or gastrointestinal clinical phenotypes in *Tymp⁻ᐟ⁻Upp1⁻ᐟ⁻* mice (such as motor dysfunction or cachexia), researchers should be cautious in translating our findings from mice to MNGIE patients. Nonetheless, it is recommended to perform more studies before clinical application, including evaluating HSCGT in more clinically-relevant models that mimic human MNGIE disease, the dosing of LV vector and transplanted gene modified cells, and a more thorough assessment of vector biodistribution and safety studies addressing potential phenotoxicity and genotoxicity.